Characterisation of anergic B cells in a new mouse model with altered B cell receptor signalling

LINGLING ZHANG

A thesis submitted to

The University of Birmingham

for the degree of

Doctor of Philosophy

INSTITUTE OF IMMUNOLOGY AND IMMUNOTHERAPY

COLLEGE OF MEDICAL AND DENTAL SCIENCE

UNIVERSITY OF BIRMINGHAM

MAY 2019

UNIVERSITYOF
BIRMINGHAM

University of Birmingham Research Archive

e-theses repository

Abstract

While the B cell antigen receptor (BCR) membrane IgM (mIgM) transmits signals via Igα/β, the cytoplasmic tail of mIgG is able to transmit signals directly. We have generated mice where the IgG1 cytoplasmic signalling tail was added to the C-terminus of IgM (IgMg1 mouse). During B cell development, IgMg1 B cells experience stronger negative selection resulting in tonic BCR signal transduction being repressed and reduced mIgM expression. BCR stimulation of immature and mature IgMg1 B cells results in reduced signalling. This shows that IgMg1 B cells leave the bone marrow as anergic cells.

IgMg1 B cells respond less efficiently to thymus-independent antigens. They do, however, respond well to the thymus-dependent antigen. The anergic pattern of IgMg1 B cells is maintained throughout the GC response and even after they become IgG switched memory B cells (MBCs). These effects may contribute to a delay in the shift of antigen-specificity of GC B cells.

These results are in line with recent studies showing that anergic B cells are licensed to participate in Germinal Centre (GC) reactions, where they can undergo clonal redemption. We conclude that IgMg1 mice are a new model to study anergy in B cells with a complete repertoire of BCR-specificities.

Acknowledgements

Firstly, I would like to express my most sincere thanks and respect to Professor Kai-Michael Toellner for his supervision and guidance for the past three years. He always discusses with me patiently and shows respect to different opinions. With his patience and expertise in science, he has taught me a lot in scientific research and scientific writing.

Thanks must be expressed to Dr. Juan Carlos Yam-Puc, who is involved into this project and has helped me a lot with the experiments, given me useful advices and encouragement.

I would like to thank Dr. Yang Zhang and Dr. Laura Garcia-Ibanez for their greatest help when I first come to this city. They have helped me develop basic lab work skills, such as flow cytometry, ELISA, cryosection, immunofluorescence, and be there to support me when I was not that confident at the beginning. I have to address my sincere appreciation to all the lab-mates who helped me with the proofreading of the thesis. Mike, Juan Carlos, Yang, Cameron, I know how tough the job is, thank you very much for all the help. I am also grateful to the present and past members of Toellner group.

I am indebted to Dr. David Withers for the useful discussion, support and supervision he provided for the past three years. I wish to extend my thanks to all people in 4th floor of IBR, especially Dr. Sky Ng, for the helpful discussions, for providing technical support and guidance. Thanks to BMSU staff and their assistance, they are always being helpful. Special thanks must be addressed to Dr. Abid Karim for all his kind help and professional guidance in screening auto-immune slides.

Juan Carlos, Noni, Marisol, Yang, Cameron, thank you for your company, chatting with you during lunch is the most relaxed and enjoyable time every day at work.

Finally, I would like to express my utmost gratitude to my husband and families for their years of love and support.

Abbreviations

7-AAD	7-amino-actinomycin D	EdU	5-ethynyl-2′-deoxyuridine
AF	Alexa Fluor	ELISA	Enzyme-linked immunosorbent analysis
AID	Activation-induce cytidine deaminase	FITC	Fluorescein isothiocyanate
AP	Alkaline phosphatase	FACs	Fluorescence-activated cell sorting
APC	Allophycocyanin // Antigen-presenting cell	FCS	Foetal calf sera
B cell	Bursa of Fabricius cell	FDC	Follicular dendritic cell
BAFF	B cell activating factor	FRC	Fibroblastic reticular cell
Bcl-6	B cell lymphoma protein 6	GAG	Glycosaminoglycan
BCR	B cell receptor	GC	Germinal centre
BEC	Blood endothelial cell	GFP	Green fluorescent protein
BLyS	B-lymphocyte stimulator	GPCR	G protein–coupled receptor
BLNK	B-cell linker	HEL	Hen Egg Lysozyme
BM	Bone marrow	HEV	High endothelial venule
bp	Base pairs	HSC	Hematopoietic stem cell
b.p.	*Bordetella pertussis*	ITAM	Immunoreceptor tyrosine-based activation motif
BrdU	Bromodeoxyuridine	IFN	Interferon
BSA	Bovine serum albumin	Ig	Immunoglobulin
Btk	Bruton's tyrosine kinase	IL	Interleukin
BV	Brilliant Violet	i.p.	Intraperitoneal
CCL19	Chemokine C-C motif ligand 19	i.v.	Intravenous
CCL21	Chemokine C-C motif ligand 21	kDa	Kilo Dalton
CCR7	C-C chemokine receptor 7	KO ko	Knock-out
CD	Cluster of differentiation	LEC	Lymphatic endothelial cell
CGG	Chicken gamma globulin	LPS	Lipopolysaccharide
CLP	Common lymphoid precursor	LZ	Light zone
CSR	Class-switch recombination	LN	Lymph node
CXCL12	C-X-C motif chemokine 12	MAPK	Mitogen-activated protein kinase
CXCL13	C-X-C motif chemokine 13	MBC	Memory B cell
CXCR4	C-X-C chemokine receptor type 4	MFI	Median fluorescence intensity
CXCR5	C-X-C chemokine receptor type 5	MHC	Major histocompatibility complex
DC	Dendritic cell		
DZ	Dark zone		

NF-κB	Nuclear factor kappa-light-chain-enhancer of activated B cells		Tfh	T follicular helper cell
N-FAT	Nuclear factor of activation T cells		TI	T cell independent
			TD	T cell dependent
NP	4-Hydroxy-3-nitrophenyl acetyl		TM	Transmembrane
PALS	Periarteriolar lymphoid sheath			
Pax5	Paired box protein 5			
PB	Plasmablast			
PBS	Phosphate buffer saline			
PBMC	Peripheral blood mononuclear cell			
PC	Plasma cell			
PE	Phycoerythrin			
PI-3K	Phosphoinositide-3-kinase			
PI(3,4,5)P$_3$	Phosphatidylinositol 3,4,5-triphosphate			
PLCγ2	Phospholipase C-gamma 2			
pLN	Popliteal lymph node			
PMS	Plasma sheet			
PTK	Protein tyrosine kinase			
QM	Quasi monoclonal			
RGS	Regulator of G protein signalling			
RT-PCR	Real-time polymerase chain reaction			
SA	Streptavidin			
SAP	SLAM-associated protein			
s.c.	Subcutaneous			
SCS	Subcapsular sinus			
SFK	Src-family kinase			
SH2	Src-homology 2			
SHM	Somatic hypermutation			
SLO	Secondary lymphoid organ			
SRBC	Sheep red blood cell			
Syk	Spleen tyrosine kinase			
TBM	Tangible body macrophage			

Table of Contents

List of figures and tables

Chapter 1 . Introduction

1.1 General introduction of B cells

Adaptive immunity is a highly evolved system which can specifically distinguish tiny differences between different "foreign invaders", and also differences between "foreign" and "self". This ability is driven by T and B lymphocytes in the immune system. During B cell development, gene segments encoding for B-cell receptor (BCR) variable region undergo a process called random re-arrangement. This random arrangement not only brings uniqueness of BCR expressed on each B cell, but also allows for the generation of a highly diverse BCR repertoire, which potentially enables our immune system to respond specifically to any foreign antigen.

Antibody secretion is the most well-known and widely studied function of B cells. An antibody is the secreted form of a BCR, comprised of two regions; the variable antigen recognition and constant structural regions. After recognition and binding to foreign antigen, antibodies can inhibit virus infection through a process called neutralization, which then follows with agglutination. Also, they can help to destroy bacteria with the help of phagocytic cells through a process called opsonisation. Opsonisation is not working on its own, by activating the complement system through coating pathogens, antibodies can promote the lysis and ingestion of these pathogens. Recent studies have shown that antibody could regulate BCR signalling by ligating

with Fc receptors and thus affecting B cell development and differentiation (Nguyen, Klasener et al. 2017).

Besides antibody secretion, B cells, especially plasma cells, have also been reported to have immune regulatory roles (Mauri and Bosma 2012, Fillatreau 2015, Kranich and Krautler 2016) and the role of B cells as antigen-presenting cells (APCs) has long been overlooked (Lassila, Vainio et al. 1988). However, a recent study has shown that B cells are as capable as dendritic cells to present certain viral antigens (Hong, Zhang et al. 2018). By presenting auto-peptides and activating T cells, this ability makes B cells capable of breaking immune tolerance and inducing auto-immune responses (Chan and Shlomchik 1998, Giles, Kashgarian et al. 2015). Memory B cells are antigen-experienced activated B cells which have long-term life span, and are able to reactivate an immune response immediately at the second time of exposure to a related antigen (Moran, Nguyen et al. 2018). (Decision events in the Germinal Centre: the role of ACKR4, LAURA GARCIA-IBANEZ, published thesis, 2016)

One important transitional microstructure during T-cell dependent (T-D) immune response is the germinal centre (GC), where somatic hypermutation (SHMs) takes place. BCR on GC B cells are selected and modified, so that they respond with higher affinity to foreign antigen. GC B cells can further differentiate into plasma cells or memory B cells.

The characteristics discussed above are mainly based on observations on conventional B cells, termed B2 cells, such as follicular B cells and marginal zone B cells. However, there is another B cell population called B1 cells. B1 cells are CD21$^{low/-}$ CD23$^{low/-}$ innate-like cells, with a relatively limited BCR repertoire. They are mainly generated in the fetal developmental stage and can self-renew once development has progressed past this stage. They are the producers of natural IgM, without the need for co-stimulatory help from T helper cells (Baumgarth 2016).

Despite having advanced knowledge of B cell biology, we are yet to truly understand the diversity of the mature B cell pool in healthy individuals, and the regulations that these B cells experience during development and after activation.

1.2 Structure of secondary lymphoid organs

The secondary lymphoid organs consist of spleen, lymph nodes, Peyer's patches and some other isolated lymphoid follicle structures. This study mainly focuses on spleen and lymph nodes. Each has distinct structure and function in the immune system.

1.2.1 Lymph node

Lymph nodes (LNs) are distributed all around the body along lymphatic vessels. Their locations are aimed at rapidly mounting immune response towards captured foreign antigens. On the midsagittal section of a lymph node, along the direction of lymphatic fluid, the afferent lymphatic vessel is on the top and connected with the capsule of

lymph node. The entire internal structure of the lymph node is enclosed within the capsule. Below the capsule, there is a lymphoid fluid filled sinus, called the sub-capsular sinus. Beyond the sub-capsular sinus, B cell follicles sit side by side, with interfollicular cortex filling the space between them. T cells are also sitting in the interfollicular areas and localised below B cell follicles, forming a relatively large T zone. At the bottom of lymphoid lobule is the medullary area, comprised of medullary cords separated by medullary sinuses. The whole structure ends with efferent lymphatic vessels (Fig. 1.1) (Willard-Mack 2006).

Antigens can travel to LNs via lymph vessels. It has been reported that antigen entry from lymph vessels is very rapid and can only take a few minutes (Gerner, Casey et al. 2017). B cells and LN resident DCs efficiently capture those antigens and mount an immune response (Mempel, Henrickson et al. 2004, Batista and Harwood 2009). Antigen-bearing B cells are activated and migrate to T-B border, where they are in close contact with activated T cells to receive co-stimulation signalling (Reif, Ekland et al. 2002). After fate decision at this stage, a small fraction of antigen-specific activated B cells differentiate into germinal centre (GC) precursor B cells. These cells then migrate back to the B cell follicle and go through clonal divisions to form a distinct micro-anatomical structure called the germinal centre (MacLennan 1994).
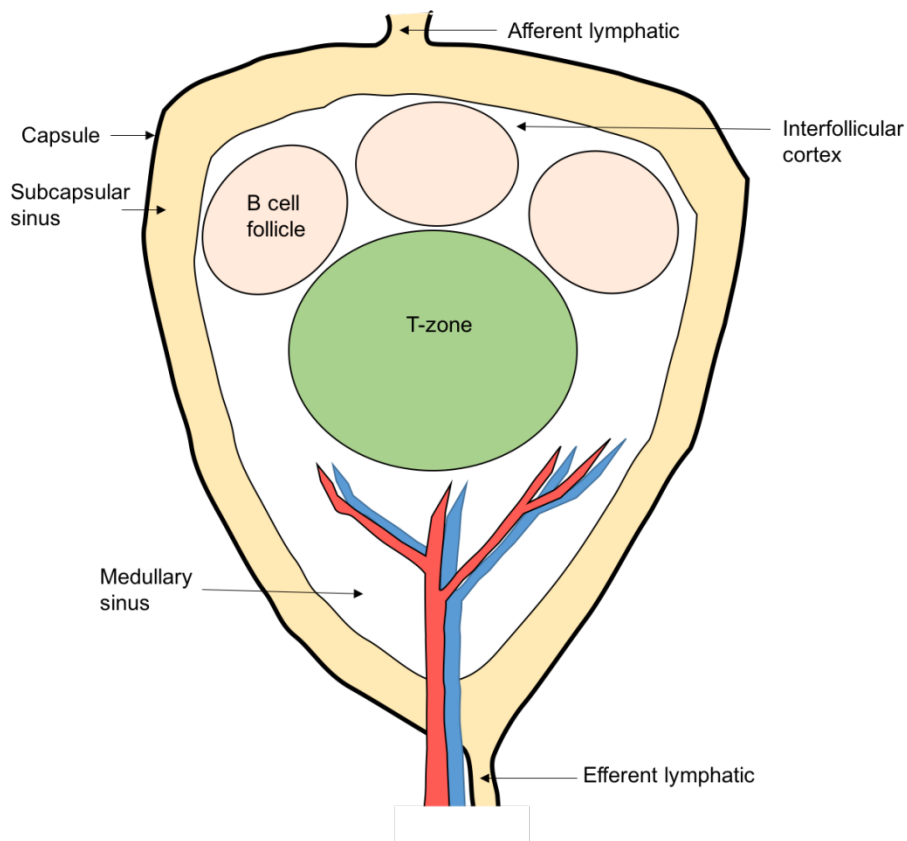
Figure 1.1: The structure of lymph node.

The whole structure is enclosed in the capsule, and is connected to the lymph system by the afferent and efferent lymphatic vessels (top and bottom, respectively). Similar to the structure of white pulp in the spleen, the lymphoid lobule contains an extended T-zone and several B cell follicles. The artery and vein spread out to form a network proximal to the T-zone, which is called medullary area. Within this area, there are medullary sinuses and cords. Cited and modified from Willard-Mack (Willard-Mack 2006)

1.2.2 Spleen

The spleen is a unique secondary lymphoid organ, distinct from lymph nodes which mainly function to mount immune responses toward foreign antigens. The spleen also functions to host the peripheral maturation of B cells. Structurally, the spleen spreads along the tree of afferent splenic artery. At the end of small arterial branches, there are well-organised lymphoid regions, which are called the white pulp of the spleen. The white pulp is further divided into the T-cell zone, also known as the periarteriolar lymphoid sheath (PALS), and B cell follicles. The structure of white pulp resembles the structure of lymph nodes, where one or more B cell follicles sit among T cells (Fig. 1.2). B cell follicles contain recirculating follicular B cells and host transitional B cells to complete their maturation (Loder, Mutschler et al. 1999). Different from lymph nodes, in each island of lymphoid region within the spleen, there is a central arteriole in the middle of each T zone. The central arteriole is also connected to the marginal sinus, another unique structure within the white pulp of the spleen (Steiniger, Ruttinger et al. 2003). The marginal sinus is a transit area, where cells and foreign antigens exiting the central arteriole first come to this area before further migration to B cell follicles (Cyster and Goodnow 1995). The marginal zone contains a large amount of resident B cells, called marginal zone B cells (MZ B cells), which are the front-line defenders against blood-borne pathogens (Zandvoort and Timens 2002). MZ B cells have been reported to shuffle between B cell follicles and the marginal zone area to transport captured antigens (Cinamon, Matloubian et al. 2004, Arnon, Horton et al. 2013).
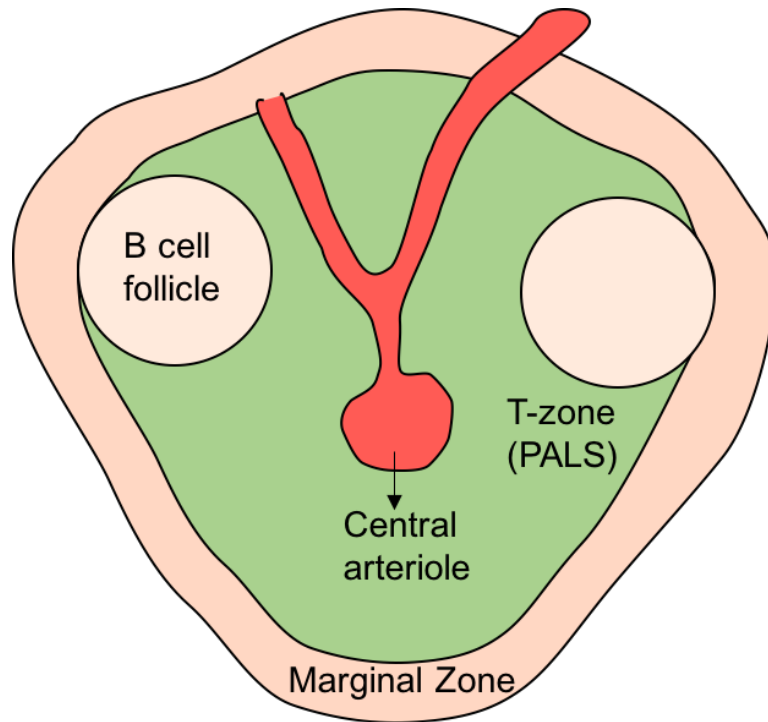
Figure 1.2: The structure of white pulp in mouse.

T cells form the periarteriolar lymphoid sheath (PALS) around the central arteriole. B cell follicles are localised at the border of T-zone. The marginal zone area forms the border of white pulp, and it is directly connected with central arteriole. Cited and modified from Mebius *et al.* (Mebius and Kraal 2005).

Surrounding the white pulp, the collecting veins and the venous system form the red pulp of the spleen (Fig. 1.3) (Mebius and Kraal 2005). When arterial branches end in the cords of red pulp, the blood contains a large fraction of old erythrocytes, which not only gives the red pulp the "red" colour, but highlights the spleen's function to filter blood and recycle iron (MacDonald, Ragan et al. 1987, Knutson and Wessling-Resnick 2003, Mebius and Kraal 2005).
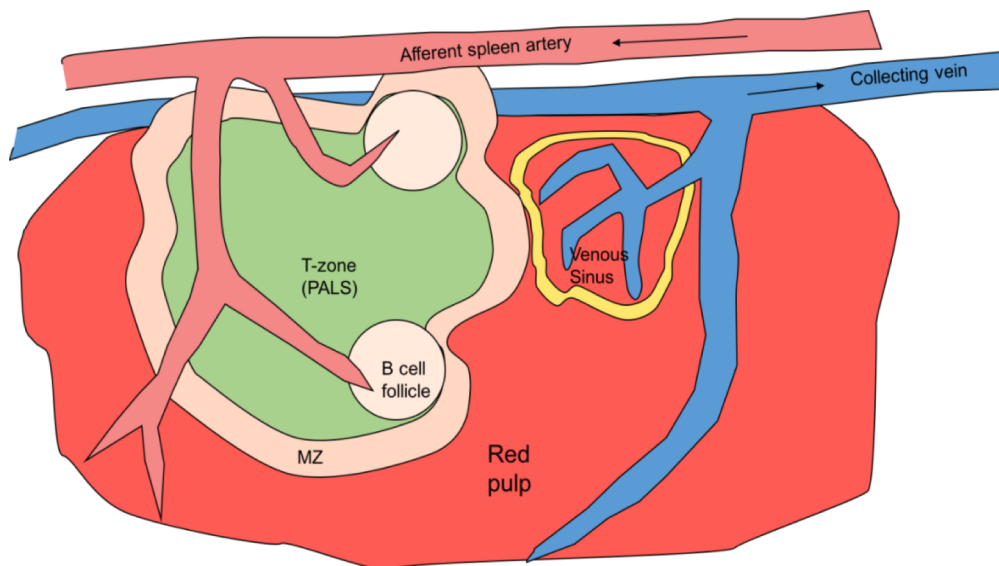
Figure 1.3: The schematic structure of spleen in mouse.

The white pulp is formed at the end of afferent splenic arterioles branches. This structure consists of T-zone (also known as PALS, green), B cell follicles (white) and marginal zone around T zone and B cell follicles (purple). Surrounding the white pulp is the red pulp, this structure spreads along the collecting vein and is comprised of the venous sinus and sinus cords, lined by discontinuous epithelial cells. Cited and modified from Mebius *et al.* (Mebius and Kraal 2005).

The highly organised structure of white pulp is dynamically regulated by chemokine receptors and chemokines. Follicular stromal cells, such as follicular dendritic cells (FDCs) and marginal zone reticular cells, both highly express CXCL13 (Forster, Mattis et al. 1996, Cyster, Ansel et al. 2000, Katakai, Suto et al. 2008). The high concentration of CXCL13 in B cell follicles attracts CXCR5 expressing B cells by chemotaxis into follicles. While stromal cells within the T zone highly express CCL19 and CCL21, which forms a chemokine gradient from the T zone to outer regions. T cells and DCs, with higher CCR7 expression on their surface are sensitive to this gradient and chemotaxis to locate in T zone (Forster, Schubel et al. 1999, Okada and Cyster 2007, Forster, Schubel et al. 2016). CCR7 is also expressed on naïve mature B cells, although normally at lower level compared to T cells. After cognate antigen recognition and activation, B cells up-regulate CCR7 expression and chemotaxis through the CCL19/CCL21 gradient (Okada, Ngo et al. 2002, Phujomjai, Somdee et al. 2016). Newly generated plasmablasts or plasma cells migrate to the border of white/red pulp through chemotaxis, forming plasma clusters in the red pulp (MacLennan, Toellner et al. 2003). This delicate location ensures antigen-specific antibodies produced by these plasma cells rapidly enter into the blood stream for effective function.

1.3 Two types of immune responses

According to the different nature of antigens, B cell responses have been generally divided into two different classes: T cell dependent immune responses (T-D response)

and T cell independent response (T-I response). These are classified not only according to the nature of antigens, but also the B cell populations recruited and the different processes undergone during the responses.

1.3.1 T-I immune response

T-I immune responses are induced by antigens which can directly activate B cells to function through Toll-like receptors (TLRs) or BCRs, without the requirement for T cell co-stimulation help. Depending on the nature of antigens and their different distinct cognate receptors, T-I immune responses have been further divided into type I and type II (Mosier, Mond et al. 1977, de Vinuesa, Cook et al. 2000).

Type I antigens are mitogenic stimuli which activate poly-clonal B cells via TLRs regardless of the specificity of BCRs. Typical Type I antigens are lipopeptides, lipopolysaccharide (LPS), CpG, poly-IC, some viral-coating particles and pathogenic nucleic acids (Bekeredjian-Ding and Jego 2009). These antigens mainly induce the production of extra-follicular plasma cells (Martin, Oliver et al. 2001), without the need for co-stimulatory help from T cells. And this process usually occurs faster than T-D immune response.

Type II antigens are polysaccharide antigens which are present in the capsules of pathogenic bacteria or viruses (Garcia de Vinuesa, O'Leary et al. 1999). These highly repetitive structures activate B cells through surface BCRs and are dependent on the

signal transmitted through Bruton's tyrosine kinase (Btk) (Amsbaugh, Hansen et al. 1972). Still, the main B cell product from a TI-2 immune response is extra-follicular plasma cells. These antigens are able to elicit strong and long-term primary antibody responses (Garcia de Vinuesa, O'Leary et al. 1999). Germinal centres have been reported to be rapidly induced and of short duration in TI-2 immune responses. Different from germinal centres in T-D immune responses, only very low levels of somatic mutations and class switching have been observed in TI GC B cells. T cells are thought to be dispensable for the activation of B cells and initiation of TI GC responses (Lentz and Manser 2001). Besides plasma cells and GC B cells, studies have shown that TI-2 antigens can induce the generation of memory B cells and elicit antigen-specific recall response (Obukhanych and Nussenzweig 2006).

Labour is divided between different B cell populations for different immune responses. Along with B1 cells, MZ B cells have been reported to be the dominant B cell population in the early T-I immune response (Martin, Oliver et al. 2001). MZ B cells respond through the generation of plasma cells and produce large amounts of IgM as the first wave of defence.

1.3.2 T-D immune response

In T-D immune responses, the full activation of antigen-specific B cells for functional terminal differentiation requires the presence of co-stimulation signals from T cells (Feldmann and Easten 1971). Compared with T-I antigens, T-D antigens are normally proteins which have relatively complicated structures (Stein 1992). The recognition of these antigens through BCRs is strictly in compliance with BCR specificity. Antigens are captured and processed by APCs, such as DCs and B cells. The processed antigens need to be presented by Major Histocompatibility Class II (MHCII) molecules on the surface of APCs to initiate the activation of T cells (MacLennan, Gulbranson-Judge et al. 1997). In T-D immune responses, only after having received the initial activation signal from the BCR and followed by the co-stimulation signalling from T cells, can B cells be fully activated (Van den Eertwegh, Noelle et al. 1993). The close contact of T and B cells happens at the T-B border in secondary lymphoid organs (Garside, Ingulli et al. 1998). Guided by surface chemokine receptors, activated B cells move from B cell follicle to the T-B border, where activated T cells also move towards. During this close T-B interaction, T cell receptors (TCRs) on the T cell surface recognize cognate MHCII-peptide complex presented by activated B cells. Then, activated T cells deliver co-stimulation signals such as CD40L or cytokines to fully activate B cells (Hollenbaugh, Grosmaire et al. 1992, Lane, Brocker et al. 1993). Adhesion molecules such as LFA-1 and ICAM-1 have also been reported to be involved in this process for the stable formation of T-B contact (Noelle and Snow 1990, Armitage, Macduff et al. 1993).

The dominant B cell population responding to T-D antigens is follicular B cells (Fo B cells). One hallmark feature of the T-D immune response is the formation of germinal centres, where affinity maturation takes place (MacLennan 1994). The early products from T-D immune response are GC-independent plasma cells and memory B cells. After the maturation of GCs, plasma and memory B cells are the outputs of GCs, and these are normally class-switched and contain hyper-mutations on their BCRs (MacLennan 1994, Toellner, Gulbranson-Judge et al. 1996, Methot and Di Noia 2017).

1.3.3 Hapten: (4-hydroxy-3-nitrophenyl)acetyl

C57BL/6 mice consistently produce anti-(4-hydroxy-3-nitrophenyl)acetyl (NP) antibodies (Imanishi and Makela 1974). VDJ sequences encoding for this in-frame IgH gene rearrangement were cloned and BCR knockin mouse models were constructed (Reth, Hammerling et al. 1978, Bartlett, Kohan et al. 1979, Cascalho, Ma et al. 1996, Sonoda, Pewzner-Jung et al. 1997). These mouse models are widely used to help us reveal fundamental knowledge of B cell biology. NP-specific cells can be followed by flow cytometry and histology to study both T-I and T-D immune responses. Antibody maturation toward NP can be followed by ELISA. Key mutations on canonical VDJ regions during affinity maturation toward NP are identified. These together make NP the most widely used hapten in B cell research field. After conjugated with Ficoll, the synthetic polymer sucrose with high molecular weight, the product – NP-Ficoll can serve as a T-independent type II antigen (Inman 1975). When NP conjugated with chicken gamma globulin (CGG), the product – NP-

CGG can recruit B cells into T-D immune responses (Azuma, Sakato et al. 1987). In this study, we mainly used these hapten-conjugates to study T-I and T-D immune responses.

1.4 B cell fate decisions after activation

The first step to activate B cells is their engagement with antigens. This engagement is normally BCR dependent, like TI-2 and T-D immune responses, or *in vivo* TI-1 immune response (Garcia De Vinuesa, Gulbranson-Judge et al. 1999). Follicular B cells have no direct access to blood-borne antigens. Opsonized antigens are transported by marginal zone B cells from marginal zone to follicles (Arnon, Horton et al. 2013). As the major population of re-circulating B cells, Fo B cells circulate between secondary lymphoid organs through blood and lymph (Nieuwenhuis and Ford 1976), where they can directly contact antigens and then selectively migrate to the spleen (Liu, Zhang et al. 1991, Toellner, Gulbranson-Judge et al. 1996). Unlike Fo B cells, MZ B cells do not recirculate. Located close to the marginal sinus, they are well-positioned within secondary lymphoid tissue to directly contact blood-borne antigens. In addition, they can also retrieve intact bacterial antigen from blood-borne immature DCs (Balazs, Martin et al. 2002).

1.4.1 The generation of plasma cells

One major source of plasma cells generated is the extra-follicular response. In the spleen, after activation by T-I antigens, both B1 and MZ B cells are directly activated and differentiate into plasmablasts or plasma cells in the extra-follicular foci of spleen (Martin, Oliver et al. 2001). During T-D immune response, after stable contact with primed-T cells, activated B cells develop into GC precursor B cells, MBCs or plasmablasts. These plasmablasts reside in the extra-follicular foci of spleen or medullary cords of LN to generate PCs (MacLennan, Toellner et al. 2003).

An alternative pathway for plasma cell generation is the germinal centre response (see chapter 1.4.2). Germinal centres are sites where antigen-specific activated B cells undergo affinity maturation (Klein and Dalla-Favera 2008, Zhang, Garcia-Ibanez et al. 2016). As a transient B cell population, GC B cells ultimately differentiate into PCs or MBCs and output from GCs to exert immune functions. Unlike PCs generated during the extra-follicular response, GC-dependent PCs are normally class switched and have relatively high affinity toward the specific antigens (Shlomchik and Weisel 2012).

1.4.2 Germinal centres and GC B cells

As transient micro-anatomical structures, GCs are normally observed during T-D immune responses within secondary lymphoid organs, such as the spleen and LNs (Klein and Dalla-Favera 2008, Gabriel and Michel 2012, De Silva and Klein 2015). GCs start with a small number of antigen-activated B cells that become destined to differentiate into GC B cells at the T-B border. GC founder B cells migrate back into

B cell follicles to seed the GC response (MacLennan, Liu et al. 1990, De Silva and

Klein 2015). They undergo clonal expansion to form the initial GCs. The timing of

the presence of GCs varies, depending on different antigens and routes of

immunisation, from several days to weeks (Jacob, Kassir et al. 1991, MacLennan

1994). When visualized in conventional histology, a well-formed GC can be divided

into two compartments: Dark Zone (DZ) and Light Zone (LZ) (Fig. 1.4). The DZ is

close to the T-zone, consists almost exclusively of highly proliferative GC B cells,

which give them a "dark" appearance in conventional histology. While the LZ is

proximal to the sub-capsular sinus in LNs, contains spreading FDCs networks, $CD4^+$

follicular T help (Tfh) cells and B cells interspersed among them (Victora and

Nussenzweig 2012, Zhang, Garcia-Ibanez et al. 2016).
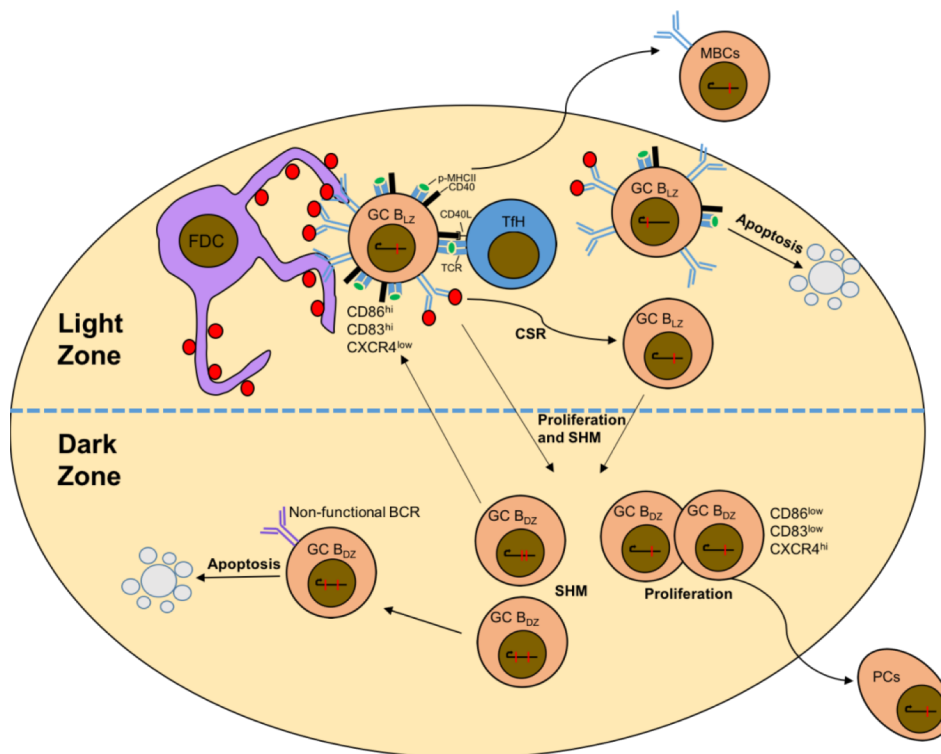
Figure 1.4: Schematic structure of a germinal centre.

This structure has been divided into two parts: light zone (LZ) and dark zone (DZ). The LZ is composed of B cells, T cells and DCs, while DZ mainly consists of B cells. GC B cells are selected and triggered to proliferate in LZ and the majority of them migrate to DZ to complete their cell cycle and go through SHM. Cite and modified from De Silva *et al* (De Silva and Klein 2015).

Different cell distributions in LZ and DZ endow different functions to these two compartments. DZ is the place where clonal expansion and somatic hyper-mutation occur (Kepler and Perelson 1993, Oprea and Perelson 1997). Both *AID* and error-prone DNA polymerase η are highly expressed in DZ GC B cells (Victora and Nussenzweig 2012, McHeyzer-Williams, Milpied et al. 2015). During this stage, immunoglobulin genes in GC B cells have been subject to a high rate of mutation.

Original BCRs are replaced with newly mutated ones before B cells re-enter into LZ for further selection. B cells bearing damaging mutated BCRs are induced into rapid death (Stewart, Radtke et al. 2018). DZ is the place for B cell clonal proliferation, with the majority of mitotic GC B cells concentrate in this area (Victora, Schwickert et al. 2010). LZ has been generally accepted as the place for GC B cell selections. It is less compact and contains diverse cell populations, such as FDCs, Tfh and B cells (Mesin, Ersching et al. 2016). FDCs in LZ mainly display antigens on their surface and provide a platform for BCR dependent antigen-driven selection (Zhang, Meyer-Hermann et al. 2013). Besides BCR affinity, limited help signalling from Tfh cells has been reported to be another LZ selection point in GC response (Meyer-Hermann, Maini et al. 2006, Gitlin, Shulman et al. 2014, Gitlin, Mayer et al. 2015).

LZ and DZ GC B cells are less different than previously expect, they can hardly be distinguished by size and morphology (Allen, Okada et al. 2007, Hauser, Junt et al. 2007, Schwickert, Lindquist et al. 2007). Both of them are larger than unstimulated Fo B cells (Victora, Schwickert et al. 2010). Currently markers to distinguish these two populations by flow cytometry are identified. CXCL12 expression is enriched in DZ micro-environment (Bannard, Horton et al. 2013). Before re-entry into DZ, LZ GC B cells up-regulate CXCR4 expression to enable chemotaxis to DZ area (Allen, Ansel et al. 2004, Victora, Schwickert et al. 2010). Thus, surface markers CXCR4 and CD86 (or CD83) have been suggested to be used for identifying these two sub-populations, with CXCR4 highly expressed on DZ GC B cells, while CD86 (CD83)

expressed at higher level on LZ GC B cells (Allen, Okada et al. 2007, Schwickert, Lindquist et al. 2007, Victora, Schwickert et al. 2010).

GC B cells fate decisions happen during GC response. LZ GC B cells can either re-enter the DZ, or generate output as GC-derived plasma cells and GC-derived MBCs. Plasma cells have been observed to leave GC through GC-T zone interface (Zhang, Tech et al. 2018), while MBCs leave the GC by migration towards the sub-capsular sinus (Moran, Nguyen et al. 2018). (Decision events in the Germinal Centre: the role of ACKR4, LAURA GARCIA-IBANEZ, published thesis, 2016)

1.4.3 The generation of memory B cells

Over the years, MBCs have been defined as antigen specific, Ig class switched, non-plasma and non-GC B cells. Despite the fact that the existence of non-switched IgM$^+$ MBCs and non-mutated MBCs has long been known (Takahashi, Ohta et al. 2001, Dogan, Bertocci et al. 2009). Recently, several subpopulations of MBCs have been defined, which has led to a broadening of the definition of MBCs to be the population of cells which are resting, antigen-experienced and long-lived derived from the initial stimulus (Shlomchik and Weisel 2012). The maintenance of their long-term survival is antigen and T cell independent (Yefenof, Sanders et al. 1986, Maruyama, Lam et al. 2000, Gagro, Toellner et al. 2003, Good, Avery et al. 2009), but, require B-lymphocyte stimulator (BLyS/BAFF/TNFSF13B) (Scholz, Crowley et al. 2008). When re-challenged with the same antigen, MBCs can be activated more easily and

rapidly by either differentiating into plasma cells or re-entry into GCs (Kurosaki, Kometani et al. 2015, Moran, Nguyen et al. 2018).

The fate decisions of memory B cells also occur at two stages. During early T-B interactions at the T-B border, a proportion of antigen-activated B cells would commit to the MBC fate. These MBCs are called GC independent memory B cells, and they can be isotype switched, but typically harbour very few mutations on their BCRs (Kurosaki, Kometani et al. 2015). The mechanism of fate decision at this stage remains unclear. Studies have shown that B cells with higher affinity are more prone to differentiate into plasma cells on T-B border (Paus, Phan et al. 2006), indicating B cells with lower affinity BCRs possibly would differentiate into MBCs. The second MBC generation pathway is GC dependent, supported by isotype switching and immunoglobulin hyper mutation observed in part of MBCs (McHeyzer-Williams and McHeyzer-Williams 2005). MBC fate decision in GCs is not fully understood either. According to a recent study, GC B cells with lower BCR affinity have higher expression of *Bach2*, which leads to the commitment of MBC fate (Shinnakasu, Inoue et al. 2016).

1.5 B cell development

1.5.1 B cell development pathway

In the fetus, B cells are primarily generated in the liver. However, in proceeding developmental stages, especially in adult, B cells are mostly produced in the bone marrow (BM) and mature in the spleen (Fig. 1.5). B cells are derived from multipotent hematopoietic stem cells (HSCs). The first descendants of HSCs are multipotent progenitor cells (MPPs). This cell population has the potentiality to give rise to all lymphocyte lineages. Signalling from FLT3, a receptor on MMP surface, drives the differentiation of MMPs into common lymphoid precursor cells (CLPs) (Adolfsson, Borge et al. 2001). CLPs are the direct precursor cells of B lymphocytes linage, as well as T lymphocytes and innate lymphoid cells (ILCs). The expression of B-lineage-specific transcription factor E2A, combined with induction of early B-cell factor (EBF) together promote ILCs to differentiate into pro-B cells (Lin, Jhunjhunwala et al. 2010). Pro-B cells are the first cell population to express B cell linage surface marker B220 (CD45). Sufficient expression of transcription factor Pax5 is necessary for pro-B cells to further mature into pre-B cells and to immature B cell stage (Nutt, Heavey et al. 1999).

Germline heavy chain V-D-J segments begin random re-arrangement during pro-B cell stage. The re-arranged μ chain, together with two surrogate light chains can be transiently expressed on the surface of pre-B cells (Karasuyama, Rolink et al. 1996). Light chain encoding segments start to re-arrange at the late stage of pre-B cells and

complete at immature B cell stage. This allows for the expression of mature IgM BCRs on the membrane of immature B cells.

Around a quarter of immature B cells mature in BM from T2 cells directly into Fo B cells (Cariappa, Chase et al. 2007, Lindsley, Thomas et al. 2007). The majority of immature B cells emigrate from the BM to the periphery for further maturation. Shortly after emerging from BM, immature B cells become transitional 1 (T1) B cells and migrate to B cell follicles in secondary lymphoid organs to complete final maturation (Pillai and Cariappa 2009). T1 B cells mature into T2 B cells. Depending on their tonic BCR signalling strength, T2 B cells then differentiate into MZ B cells and Fo B cells (Pillai, Cariappa et al. 2005). However, recently it was shown that MZ B cells can directly differentiate from T1 B cells (Hammad, Vanderkerken et al. 2017). The existence of a third transitional B cells (T3 B cells) is described, they are AA4.1$^+$CD23$^+$IgM^{low} (Allman, Lindsley et al. 2001), an immature B cell population with typical follicular B cells surface markers. T3 B cells have been suggested to be the reservoir of physiological anergic B cells (Merrell, Benschop et al. 2006).

MZ B cells and Fo B cells are named after their locations. MZ B cells are located at the marginal zone area around the B cell follicle, characterised by a low level of IgD and high level of CD21 expression on their cell surface membrane (Stein, Bonk et al. 1980). Fo B cells are seated at the follicular region adjacent to T zone and is the dominate B cell population in the periphery, expressing high levels of IgM, IgD and CD23.

	CLPs cell	Pro-B cell	Pre-B cell	Immature B cell	Trans B cell	Mature B cell
H-chain genes	Germline	V-D-J rearranging	V-D-J rearranged	V-D-J rearranged	V-D-J rearranged	V-D-J rearranged
L-chain genes	Germline	Germline	Germline	V-J rearranged	V-J rearranged	V-J rearranged
Surface Ig	Absent	Absent	Pre-BCR transiently expressed	IgM constantly expressed	IgD started to express since T1	IgM IgD constantly expressed

Bone marrow | Spleen

Figure 1.5: B cell and B cell receptor development.

B cell development is accomplished in a two-stage process. The differentiation of hematopoietic stem cells (HSCs) to immature B cells takes place in bone marrow. Immature B cells then migrate from bone marrow to periphery, mainly in spleen, to complete B cell maturation. B cell receptors develop along with B cells, during bone marrow stage, and only IgM is expressed on the cell surface of B cells. The expression of IgD begins from transitional B cell stage in the spleen and on all mature B cells surface. Cited and modified from Janeway's Immunobiology 9th Edition (Murphy and Weaver 2017).

1.5.2 B cell receptor development

The B cell receptor simultaneously matures and plays decisive roles during B cell development (Fig. 1.5). BCRs are membrane-bound immunoglobulins, with two identical heavy chains and two identical light chains. They also contain trans-membrane and cytoplasmic regions to help them anchor to B cell surface membrane. Both heavy and light chains can be further divided into two parts; the variable region and the constant region. The variable region is the product of random re-arrangement of V-D-J segments of the Ig heavy chain encoding region, or V-J segments in the light chain encoding region. This re-arrangement brings diversity to BCRs. Further P nucleotide insertions (palindromic) by recombination activation genes (Rags) and non-templated nucleotides (N regions) insertions by terminal deoxynucleotidyl transferase (TdT) add to this diversity (Sobacchi, Marrella et al. 2006). The wide spectrum of BCR repertoire enables B cells to specifically recognise any potential foreign antigens. After re-arrangement, the gene combination encoding for the variable region and the unique footprint of the V-D-J junction area in CDR3 is a unique sequence identity in each B cell and can be used to identify B cell clones.

The re-arrangement of heavy chain D-J genes starts firstly in the CLPs, and normally finishes at early pro-B cells. Next is V-DJ rearrangement, which also takes place in the pro-B cell stage. After VDJ re-arrangement, the first heavy chain − μ chain, combined with surrogate light chain can be assembled to express pre-BCRs transiently expressed on the surface of pre-B cells (Karasuyama, Rolink et al. 1996).

The signalling capability of the pre-BCR complex is tested during this stage, and only the pre-BCRs which can transduce effective down-stream signalling would be selected to survive for further differentiation (Karasuyama, Rolink et al. 1994). This is the positive selection during B cell development. Positively selected pre-B cells go through light chain V-J re-arrangement, and generate the first mature IgM BCR and display this on the cell-surface membrane of immature B cells. Auto-reactivity of BCRs will be checked during immature B cell stage. Only B cells with no or weak self-binding are allowed for further peripheral maturation (Meffre and Wardemann 2008, Pelanda and Torres 2012). Once entered into the periphery, immature B cells develop into transitional B cells and their BCRs are tested further for auto-reactivity during T1 stage (Meffre and Wardemann 2008). Cells permitted for further maturation become mature B cells and express IgD on their cell surface membrane as well. IgM and IgD co-expressed on the same B cell share the same antigen specificity, as they are generated by alternative mRNA splicing using the same variable region genes for both (Enders, Short et al. 2014).

According to the different structures of their heavy chains, BCRs have been divided into five classes or isotypes; IgM, IgD, IgG, IgE and IgA (Bengten, Wilson et al. 2000). Each class of BCRs can be further divided into subclasses, according to the subtle difference of their heavy chains as well, such as IgG1, IgG2a under IgG. Naïve B cells only express IgM and IgD, with marginal zone B cells expressing much lower levels of IgD than follicular B cells. Activated B cells can go through a process called class switch recombination, after which they start to express the other isotypes

(Chaudhuri and Alt 2004). This thesis will mainly focus on IgM and IgG1 and their downstream signalling. Downstream signalling events will be further reviewed in Chapter 3.

1.5.3 Negative selection during B cell development

The diversity of BCR repertoire comes from random re-arrangement, but, so does auto-reactivity. Thus, our immune system employs negative selection during B cell development to detect these self-reactive cells, and either eliminate or modify them to avoid potential risks. This elimination or inactivation of self-reactive immature B cells in BM is called central tolerance. The mature IgM BCR is expressed on the outer cell membrane of B cells at immature B cell stage. Unlike pre-BCR, the mature BCR has fully re-arranged light and heavy chains, providing each BCR with unique antigen specificity. The first negative selection happened during the stage during BM development (Pelanda and Torres 2012). According to recent studies, immature B cells are tested by self-antigens displayed in the micro-environment of BM. If surface BCRs strongly bind to self-antigen, the corresponding B cell is induced to enter apoptosis (Brink and Phan 2018). Alternatively, their Ig light chain genes can go through several rounds of re-arrangement which may reduce self-reactivity of the newly formed BCRs and rescue these cells, a process called light chain editing (Prak, Trounstine et al. 1994, Prak and Weigert 1995). BCRs with medium to weak self-

binding can survive through this primary negative selection, however, they will be induced into a non- or low-responsive state of anergy (Brink and Phan 2018).

B cell central tolerance induction is not perfect. In some cases, self-reactive B cells can be permitted to enter into the periphery, such as self-reactive B cells which are specific for tissue limited antigens, which has been called clonal ignorance (Goodnow 1992). Thus, to enable their further development in the periphery, B cells have to be selected again based on the strength of self-reactivity. Peripheral tolerance takes place in transitional 1 stage, immediately after immature B cells enter into periphery (Jacobi and Diamond 2005). B cells strongly reacting with self-antigens displayed at this stage are eliminated immediately. If this binding is medium to weak, B cells can be induced to become anergic B cells.

Self-reactive B cells that survive both central and peripheral negative selection enter the mature B cell pool as anergic B cells.

1.6 B cell anergy

1.6.1 General introduction of anergic B cells

The functional silence of self-antigen specific B cells in Hen Egg Lysozyme (HEL) specific B cell receptor (BCR) transgenic mouse model was first described by Goodnow *et al* (Goodnow, Crosbie et al. 1988). The general concept of B cell anergy

has been developed based on this and related mouse models (Glynne, Ghandour et al. 2000, Burnett, Langley et al. 2018).

B cell anergy is defined by the absent or reduced activated downstream signalling in B cells after activation through B cell receptors only (Goodnow, Crosbie et al. 1988). Contrary to what would be expected, 75% of the immature B cells to some degree display self-binding ability (Wardemann, Yurasov et al. 2003), and anergic B cells have been estimated to account for as much as 20-30% of peripheral mature B cells pool (Grandien, Fucs et al. 1994, Wardemann, Yurasov et al. 2003). Healthy individuals silence these auto-reactive B cells, which are probably involved in the sudden breakout of auto-immune disease in some individuals (Wardemann, Yurasov et al. 2003, Smith, Packard et al. 2015). In homo sapiens, the use of heavy chain V_H4-34 has been reported to lead to self-binding, and cannot be rescued by light chain editing (Pugh-Bernard, Silverman et al. 2001). Despite this, there are still 0.5% of total serum antibodies containing the V_H4-34 heavy chain within normal healthy individuals (Stevenson, Smith et al. 1989). These observations inevitably lead to one question: why does our immune system not eliminate these potentially auto-reactive B cells in the first place? Currently clonal redemption is the most widely accepted explanation, and was well-supported by experiments from Goodnow's Lab (Sabouri, Schofield et al. 2014, Burnett, Langley et al. 2018). According to this theory, anergy is there to prevent the generation of holes in the primary B cell repertoire, as many pathogens adopt molecular mimicry to mimic self-antigens to evade immune surveillance (Pinschewer, Perez et al. 2004, Scherer, Zwick et al. 2007, Gristick, von

Boehmer et al. 2016). Despite being silenced through negative selections during tolerance induction, anergic B cells are allowed to be recruited into responses to self-crossreactive pathogens by entering GCs. During GC reactions, these recruited anergic B cells would be redeemed through mutating away from self-reactivity and accumulating affinity to foreign antigens (Sabouri, Schofield et al. 2014, Burnett, Langley et al. 2018). More detailed information on this topic will be reviewed in chapter 4.

1.6.2 Characteristics of anergic B cells

The most recognised and the defining feature of anergic B cells is impaired or absent down-stream BCR signalling. BCR signalling is usually measured by calcium mobilisation and phosphorylation of SYK, Igα and Igß, after stimulation through BCRs. In most of the anergic mouse models, there are no or reduced calcium mobilisation and reduced phosphorylated SYK, Igα and Igß (Erikson, Radic et al. 1991, Goodnow, Brink et al. 1991, Benschop, Aviszus et al. 2001). The maintenance of this non-responding or low-responding state after activation through BCRs requires constant self-antigen occupancy (Gauld, Benschop et al. 2005). The weak constant stimulation from self-antigen can result in higher intracellular calcium mobilization and higher tonic phosphorylation levels, as observed in some anergic models (Goodnow, Brink et al. 1991, Benschop, Aviszus et al. 2001, Culton, O'Conner et al. 2006). This constant surface BCR and auto-antigen interaction are regarded to be the cause for down-regulation of surface IgM as well. Studies have shown that this down-

regulation is due to post-translational modification rather than reduced mRNA expression levels (Glynne, Ghandour et al. 2000). The lower surface IgM expression on B cells has been observed in most of the anergic models and is used to define anergic B cells in humans (Erikson, Radic et al. 1991, Goodnow, Brink et al. 1991, Benschop, Aviszus et al. 2001, Borrero and Clarke 2002, Duty, Szodoray et al. 2009).

Additional characteristics of anergic B cells can be observed in some but not all anergic models. Following adoptive transfer of HEL-specific anergic B cells into WT mice, Cyster *et al.* have found that these anergic B cells are excluded from entry into B cell follicles, but are instead unusually localised to the T-B border (Cyster, Hartley et al. 1994). These B cells express higher levels of CCR7 on their surfaces and are more sensitive to the CCL19/CCL21 chemokine gradient, indicating a hyper-activated basal state (Cyster, Hartley et al. 1994). This exclusion of follicle entry has been observed in some models (Mandik-Nayak, Bui et al. 1997, Noorchashm, Bui et al. 1999), however, in other models, anergic B cells can localise to follicles normally (Noorchashm, Bui et al. 1999, Borrero and Clarke 2002). Besides altered localisation to unusual anatomical sites, anergic B cells can also experience developmental blockade. In some models, studies have shown a remarkably biased cell differentiation into T3 B cells in periphery (Goodnow, Crosbie et al. 1989, Merrell, Benschop et al. 2006). T3 cells have been regarded to be the pool of natural anergic B cells (Merrell, Benschop et al. 2006). In addition to the transitional stage, the immature B cell stage is another critical auto-reactivity check point, and in some

models B cells have been shown to be blocked at the immature stage (Erikson, Radic et al. 1991, Nguyen, Mandik et al. 1997).

It has been reported that anergic B cells normally have a shortened life span (Fulcher and Basten 1994, Mandik-Nayak, Seo et al. 2000). And this phenomenon has been observed in some of anergic mouse models, however, an almost equal number of mouse models also show that the life-span of anergic B cells is normal (Rojas, Hulbert et al. 2001, Cambier, Gauld et al. 2007). According to current studies, the decreased life-span of anergic B cells is not due to their intrinsic defect (Cyster, Hartley et al. 1994), but because they are less competitive to occupy the limited survival niche than non-anergic B cells (Cyster, Hartley et al. 1994, Cyster and Goodnow 1995, Mackay, Schneider et al. 2003).

Overall, the phenotypes of anergic B cells vary among different anergic models. The diversity of these anergic phenotypes can be partly explained by BCR self-antigen recognition characteristics, such as affinity for that self-antigen and sites of encountering the antigen (Erikson, Radic et al. 1991, Santulli-Marotto, Retter et al. 1998, Benschop, Aviszus et al. 2001, Rojas, Hulbert et al. 2001, Cambier, Gauld et al. 2007). It seems that BCR/ligand binding strength and subsequent BCR downstream signalling still play a decisive role on the phenotypic outcome of anergic B cells.

These studies have shed light on B cell anergy and helped to reveal the break of tolerance of anergic B cells in auto-immune diseases. However, the questions of how

are these anergic B cells regulated in healthy individuals to avoid autoimmunity and why does our immune system preserve such a large proportion of these silenced auto-reactive B cells in the periphery, still wait to be answered.

1.7 B cell receptor signalling and B cell fate decision

1.7.1 B cell receptor signalling

B cell receptor signalling starts with the engagement of a BCR with cognate antigen. For years, observations on initiation of BCR signalling have been interpreted as the cross-linking of BCRs (Metzger 1992, Minguet, Dopfer et al. 2010). However, BCR segregation model promoted by Reth *et al.* have shown that BCRs are intrinsically prone to form oligomers on resting B cells, and the initiation of BCR signalling requires the segregation of these oligomers to form clustered monomers (Yang and Reth 2010).

Possessing short cytoplasmic regions, mIgM and mIgD expressed on naïve B cell surface merely transduce a BCR-antigen binding event into signal that can be propagated. They achieve this by signalling through their non-covalently associated co-receptors: CD79a (Igα) and CD79b (Igß) (Campbell and Cambier 1990, Hombach, Tsubata et al. 1990). These two co-receptors have short extracellular regions, but have extended cytoplasmic tails containing immunoreceptor tyrosine-based activation motifs (ITAMs) (Yao, Flaswinkel et al. 1995). The ligation of the BCR with cognate

antigen leads to the phosphorylation of ITAMs in CD79a and CD79b (Gold, Matsuuchi et al. 1991). Following the phosphorylation of ITAMs, Src-family kinase (SFK), such as LYN in B cells, binds to this phosphorylation site through Src-homology 2 (SH2) and upregulates its kinase activity to further phosphorylate ITAMs (Johnson, Pleiman et al. 1995). SYK then binds to dual phosphorylated ITAMs through its SH2 domain. This binding leads to SYK phosphorylation and activation (Kurosaki, Johnson et al. 1995, Rowley, Burkhardt et al. 1995). Activated SYK can then phosphorylate the adaptor protein B-cell linker (BLNK, SLP-65) (Kabak, Skaggs et al. 2002).

Activated phospho-BLNK serves as a platform to recruit a group of proteins for the propagation of multiple down-stream pathways. Among them are: Bruton's tyrosine kinase (Btk), Phospholipase C-gamma 2(PLCγ2) and Vav-1 (Fu, Turck et al. 1998). Btk phosphorylates its closely contacted PLCγ2, which then cleaves phosphoinositide PI(4,5)P2 to generate second messengers IP_3 and DAG (Ransom, Harris et al. 1986). Additionally, activated LYN phosphorylates the cytoplasmic tail of CD19, creating a binding site for phosphoinositide-3-kinase (PI-3K). PI-3K phosphorylate $PI(4,5)P_2$ to generate another critical second messenger Phosphatidylinositol 3,4,5-triphosphate $(PI(3,4,5)P_3)$.

Through binding to IP_3 receptor, IP_3 leads to both release of intracellular Ca^{2+} and the influx of extracellular Ca^{2+} (Hogan, Lewis et al. 2010). Ca^{2+} is required for the activation and translocation of nuclear factors such as nuclear factor kappa B (NF-κB)

and nuclear factor of activation T cells (N-FAT) (Su, Guo et al. 2002). DAG signals through binding to Ras guanyl nucleotide-releasing protein (RasGRP) and the protein kinase C family, such as PKCβ in B cells, to regulate the mitogen-activated protein kinase (MAPK) family (Guo, Su et al. 2004, Roose, Mollenauer et al. 2007). The downstream branched distal signals together drive the biological events, including; cell activation, proliferation, differentiation and antigen-presentation.

1.7.2 B cell receptor signalling and B cell development

B cell receptor signalling has been generally divided into ligand-induced signalling and tonic signalling. Both pre-BCR and BCR tonic signalling, at least at minimally sufficient levels, are transduced by Igα and Igß, without the need for BCR co-expression (Bannish, Fuentes-Panana et al. 2001, Fuentes-Panana, Bannish et al. 2005). Studies have shown that BCR signalling and its strength play important roles and can affect B cell fate decisions during B cell maturation (Niiro and Clark 2002, Monroe 2006, Pillai and Cariappa 2009). At pre-B cell stage, only B cells with functional tonic signalling through pre-BCR can survive for further development. During immature B cell stage, the affinity of BCR toward self-antigens influences the fate of B cells. Immature B cells with strong self-binding are deleted or go through light-chain editing. The ones with intermediate to weak self-binding are induced into anergic state. A similar check point which still depends on the affinity of BCR toward self-antigen happens in transitional stage, inducing peripheral tolerance.

The fate decisions of peripheral MZ and Fo B cells depend in part on BCR signalling strength. During peripheral MZ B cell differentiation, BCR signalling has been reported to be critical for Taok3 activation and subsequent membrane expression of ADAM10. ADAM10 then cleaves Notch2 and CD23, which leads to the final commitment to MZ B cell fate (Gibb, El Shikh et al. 2010, Hammad, Vanderkerken et al. 2017). Genetically manipulated mice with altered BCR signalling have shown that lower BCR signalling favours MZ B cell fate, and transitional B cells with higher BCR signalling strength are prone to differentiate into Fo B cells (Cariappa, Tang et al. 2001, Samardzic, Marinkovic et al. 2002). However, a recent study showed that lacking secreted IgM leads to increased BCR signalling and enhanced MZ B cell differentiation (Tsiantoulas, Kiss et al. 2017). Despite BCR signalling strength and its role in mature B cell fate commitment remaining open for debate, these studies suggest that mature B cell fate decisions are tightly connected with BCR signalling strength.

Besides tonic BCR signalling, ligand-binding BCR signalling strength has also been suggested to be involved in MZ or Fo fate commitment decisions. Studies have shown that silenced or non-silenced self-reactive B cells are retained in the mature Fo B cell compartment (Wardemann, Yurasov et al. 2003, Zikherman, Parameswaran et al. 2012), indicating that self-ligand binding BCR signalling possibly promotes Fo B cell fate.

Among these studies, one very useful transgenic reporter mouse is the Nur77-GFP reporter mouse. This is a BAC vector transgenic mouse in which the expression of GFP is under control of the regulatory region of the Nur77 coding gene *Nr4a1* (Zikherman, Parameswaran et al. 2012). Nur77 is an inducible orphan nuclear receptor. Its expression is rapidly up-regulated after receptor-antigen ligation in both T and B cells (Winoto and Littman 2002). In this transgenic or related mouse models, the expression of GFP is immediately induced after TCR or BCR activation, which enables us to visualise signalling strength and pattern in T and B cells (Zikherman, Parameswaran et al. 2012, Noviski, Mueller et al. 2018).

1.7.3 B cell receptor signalling and B cell fate decision during GC response

For years, we have known that the GC is where antigen-specific B cells achieve affinity maturation. This directed evolution towards higher affinity to a specific epitope is not a random process but is based on complicated selection within GCs. As mentioned earlier, immunoglobulin hyper-mutation occurs in the GC DZ, however, selection takes place in LZ. As the evolution of high affinity B cell clones requires the stepwise accumulation of many mutations, GC B cells need to cycle between the LZ and DZ.

Currently there are two models to explain the selection mechanisms. The first is the "T cell centric" model. In this model, BCR affinity and signalling can be converted to

T-B interaction strength, and LZ GC B cells which receive stronger T cell co-stimulation enter the DZ faster and undergo more cell cycles in DZ. This model has been conceived in different studies using different techniques (Batista and Neuberger 2000, Allen, Okada et al. 2007, Schwickert, Victora et al. 2011, Gitlin, Mayer et al. 2015). However, it has only helped us to understand regulation of GC B cells from LZ to DZ.

Antibody-feedback is another model to explain LZ selection. According to this model, competition of GC B cells with different BCR affinities for the unlimited amounts of antigen displayed on FDC surfaces is achieved by a competition of B cells with antibody covering antigen epitopes on immune complexes presented by FDC (Zhang, Meyer-Hermann et al. 2013). Antigen – antibody binding kinetics would only allow higher affinity BCR variants to outcompete antibody covering the antigen and allow only higher affinity B cell variants to access, phagocytose, and present antigen to Tfh cells. This model can explain how an adequate continuously rising affinity selection threshold is achieved during the GC response, as antibody on immune complexes on FDC is continuously replaced by antibody variants produced by GC-derived plasma cells of ever increasing affinity. This generates adequate directional selection pressure leading to slow directional evolution towards rising affinity (Zhang, Garcia-Ibanez et al. 2016).

A further hypothetical model is the BCR signalling based selection model. This model is not mutually exclusive with the T cell selection model. In fact, it laid the foundation

for T cell selection model. Studies have shown that B cells with higher affinity can better capture antigens and present increased p-MHCII complex to gain more T cell help (Gitlin, Shulman et al. 2014, Gitlin, Mayer et al. 2015), indicating an indirect effect of BCR affinity and signalling on GC B cell selection.

BCR signalling has been reported to be repressed during the GC response (Khalil, Cambier et al. 2012) and GC B cells appear unresponsive after BCR stimulation by antigen in solution (Victora, Schwickert et al. 2010). However, a recent study has shown that BCR signalling in GC B cells can be effectively activated by antigens coated on immobilized plasma sheets (PMSs), suggesting the way of activating BCRs can be different in naïve and GC B cells (Nowosad, Spillane et al. 2016). Despite overall repressed BCR signalling in GC B cells, researchers have observed a small proportion of GC B cells which highly express GFP in *Nur77*-GFP reporter mice, with activated BCR signalling. These cells are mainly localised in the LZ of the GC, displaying a genetic pattern thought to be related with positive selection (Mueller, Matloubian et al. 2015). Recently, Luo *et al.* directly prove that BCR signalling is indispensable for retaining GC B cells in GC LZ (Luo, Weisel et al. 2018). Together, these observations indicate that BCR signalling can be directly involved in LZ selection during GC response.

Except for the gain or loss function which BCR signalling plays during LZ selection, more insights come from fate decisions of different class-switched GC B cells. These B cells have different cytoplasmic regions and theoretically transduce varied down-

stream signalling. IgE[+] GC B cells, for example, are disfavoured during the GC response, and they mainly reside in the DZ and are likely to go through apoptosis (Yang, Sullivan et al. 2012, He, Meyer-Hermann et al. 2013). Although there is no direct evidence to show signalling differences in IgE[+] and other isotype switched GC B cells, the only difference between them is the BCRs.

Very recently, a study showed that GC B cells with damaging immunoglobulin mutations failed to enter into LZ, indicating BCR-dependent signalling is required for DZ GC B cells to re-enter LZ and complete the GC cycle (Stewart, Radtke et al. 2018).

Differences in BCR signalling and B cell activation in the GC can not only be derived from BCR/antigen binding affinity, but it can be intrinsically variable due to the activation state of B cells. While non-self-reactive normal naive B cells have been well studied, there is less information how changed signalling in anergic B cells affects their activation and selection during GC reactions. Chapter 4 in this study will focus on this topic.

1.8 General aims of this thesis

B cell receptor signalling strength plays a vital role in fate decisions during B cell development and B cell activation. Previous studies have shown that, compared to IgM, IgG1 or the addition of IgG1 cytoplasmic region to IgM is able to transduce hyper-activate BCR signalling. If there is a minimum BCR signalling threshold

needed to activate B cells, then, hypothetically, these hyper-activate B cells would get activated by lower-immunogenic antigens, unable to trigger activation in normal B cells. With this in mind, the IgMg1 mouse model was constructed. In this mouse, the IgG1 cytoplasmic region was inserted downstream of extracellular and transmembrane regions of IgM, preserving the complete germ-line VDJ repertoire. The general aim of this thesis is to characterise B cell development and differentiation in this newly constructed IgMg1 mouse model.

Chapter 3 tests the hypothesis that hyperactive signalling of IgMg1 B cell receptors affects B cell development. B cell development and BCR signalling strength was followed in bone marrow and secondary lymphoid tissue in IgMg1 mice.

Unexpectedly, chapter 3 shows that, rather than being hyper-activated, B cells produced in IgMg1 mice are anergic. Chapter 4 therefore tests how changed BCR signalling in anergic B cells affects the B cell response to T-I and T-D antigens, with a special focus on dynamic changes during the GC reaction.

Chapter 2 . Material and methods

2.1 Mice

Mice were bred and maintained under specific pathogen-free conditions at the Biomedical Services Unit, University of Birmingham, UK. All animal experiments were approved by the institutional ethics committee and the Home Office UK (Project license: PEAE5FA92). Mice were aged 6 - 10 weeks. For ageing experiment, mice were aged beyond 27 weeks.

2.1.1 C57BL6 and C57BL/6-Ly5.1 (BoyJ) WT mice

C57BL/6N WT mice were bred and maintained at the Biomedical Services Unit, University of Birmingham, UK. B cells in these mice express allotype marker CD45.2. C57BL/6-Ly5.1 (BoyJ) WT mice were purchased from Charles River and maintained at the Biomedical Services Unit, University of Birmingham, UK. B cells in these mice express allotype marker CD45.1.

2.1.2 IgMg1 mice

IgMg1 mice were generated by our collaborator MedImmune. A vector containing genome sequence encoding IgM heavy chain constant region M1 and M2 with cytoplasmic tail extension of IgG1 cDNA, as well as inverted terminal repeats (ITRs) flanked neomycin cDNA was microinjected into embryonic stem (ES) cells. The 75 bp sequence coding for the 25 C-terminal amino acids of the IgG1 cytoplasmic region was inserted into the genome of C57BL6/N ES cells through homologous recombination. Positively recombined ES cells were selected by G418 (Geneticin)

and screened by PCR. PCR primers: Fwd: 5'- tgcaggtgaaatggatcttctcctc -3'; Rev: 5' – aaccagagtgctatccattgg – 3'. The selection cassette containing an ITR flanked neomycin gene was deleted by PiggyBac transposase mediated excision. Positively selected ES cells were then injected into blastocysts to generate high percentage chimeras. Chimeric founder mice were bred to generate homozygous IgMg1 mice.

2.1.3 IgMg1 Nur77 mice

Nur77-GFPCre B6-820 mouse (MGI ID: 5007644) was a kind gift from Professor Graham Anderson (University of Birmingham). It was generated by embryo microinjection of a BAC vector containing *Nr4a1* locus, 60 kb sequence flanking each side of *Nr4a1* locus as well as an eGFP-Cre fusion protein cDNA sequence. The selected founder mice were then bred with C57BL/6NCr mice (Moran, Holzapfel et al. 2011). Nur77-GFPCre B6-820 mice were backcrossed onto IgMg1 homozygous mice. Mice were genotyped to be homozygous for the IgMg1 insertion site and positive for GFP by real time PCR (Transnetyx).

2.1.4 Ha/Hb heterozygous

IgMg1 or C57BL/6N WT mice were crossed with BALB/c mice. F1 hybrid mice were used for experiments. As IgMg1 are C57BL/6N background and therefore express Ig heavy chain IgH[b], whereas BALB/C mice allotype IgH[a]. Due to allelic exclusion B cells from F1 hybrid mice express either IgH[a] (IgMwt), or IgH[b] (IgMg1).

2.2 Construction of BM chimeras

8 weeks old recipient C57BL/6 WT mice were purchased from Charles River. One week before irradiation, mice were treated with Baytril (Bayer) by adding this to drinking. Mice were irradiated with 5.5 Gy in the morning and 5.5 Gy in the afternoon.

Immediately after the secondary irradiation, equal amounts of 2.5×10^6 BM cells from C57BL/6N CD45.2$^+$ WT mice and C57BL/6-Ly5.1 CD45.1$^+$ mice (IgMwt/IgMwt WT chimera controls) or from IgMg1 CD45.2$^+$ mice and C57BL/6-Ly5.1 CD45.1$^+$ mice (IgMg1/IgMwt chimera experimental group) were transferred into irradiated recipients. Each mouse received 5×10^6 BM cells in total. Body weights of mice were recorded daily, before and after irradiation. Mice were culled if their body weight dropped 20% from their weight before irradiation.

Recipient Mice were kept for hematopoietic reconstitution for 6-8 weeks, in the presence of Baytril for the first 2 weeks after cell transfer. After this, mice were immunised with NP-CGG in the foot as described in section 2.4.1. Popliteal LNs were collected to analyse the immune responses after 8 days of immunisation. BM and spleens were harvested to follow B cell development in BM chimeric mice.

2.3 Flow cytometry

2.3.1 Staining for surface markers

Spleens were harvested and cut into two parts. The larger parts of spleens were frozen immediately on dry ice for immunofluorescence histology. The smaller pieces were macerated in complete RPMI-1640 culture medium (Table I). Both the weight of complete spleens and weight of the smaller pieces were recorded for later cell counting. Lymph nodes were torn apart by needles firstly and then macerated in complete RPMI-1640 culture medium. Femur and tibia bones were the source of BM cells in our experiments. The two ends of the bones were cut off and then were flushed with complete RPMI-1640 culture medium.

All cell suspensions were filtered through 70 um cell strainer (Thermo Fisher Scientific) to generate single cell suspensions. Samples were then spun down at 150 g, 4 ˚C for 4 mins. After centrifugation, supernatants were discarded and cell pellets were re-suspended with complete RPMI-1640 culture medium again. Aliquots from each sample were added to V-shape 96-well microtitre plates (ThermoFisher) for staining.

Before incubation with antibody cocktails, anti-CD16/32 antibody was added to block Fc gamma receptors (20 min, 4 ˚C). In standard surface staining, all antibodies were diluted in FACS buffer (Table II). After blocking, surface antibody cocktail (Table IV)

was added and incubated at 4 ˚C for 20 min. Then cells were washed twice at 150 g, 4 ˚C for 4 mins with FACS buffer before analysis.

5 µl counting beads (Spherontech, Inc) were added to the samples, mixed thoroughly before loading the samples to a flow cytometer (BD LSRFortessa Analyzer, BD Biosciences, with BD FACSDiva). Results were exported and analysed by FlowJo v.9 or 10 (FlowJo LLC, TreeStar). Percentages from threshold/rectangular gates and mean fluorescent intensity (MFI) of gated populations were analysed and exported for calculations. To calculate Nur77$^+$ B cells, Overton % Positive was used (Overton 1988).

2.3.2 Staining for active Caspase3$^+$ apoptotic cells

Cell suspensions from different tissues were generated as described above. Intracellular active Caspase3 (aCaspase3) staining was carried out after surface staining.

When surface staining was finished, cells were washed once and then fixed in 100 µl Fixation and Permeabilisation buffer (Foxp3 Transcription Factor Staining Buffer Kits, eBiosciences) at 4 ˚C for 30 min. Then, cells were spun down still in the 96-well plate at 150 g, 4 ˚C for 4 mins and re-suspended in 200 µl 1X Wash Buffer (eBiosciences) at 4 ˚C for 30 min. Cells were then washed with FACS buffer and stained with rabbit anti-mouse aCaspase3 antibody (BD biosciences). Secondary

antibody swine anti-rabbit biotin (DAKO) was added and followed by streptavidin PE-Cy7 (eBiosciences).

2.3.3 EdU proliferation assay

5-Ethynyl-2'-deoxyuridine (EdU), a thymidine analogue, was dissolved in PBS at the concentration of 2 mg/ml as stock and preserved at -20 ˚C. Mice were i.p. injected with 200 μg EdU in 200 μl PBS, 2 hours before dissection. EdU incorporation was detected using the Click-it EdU flow cytometry kit (Life Technologies).

Nuclear EdU incorporation staining was carried out after surface staining (except antibodies with RPE, PE-tandem, or Qdot conjugates). After surface staining, cells were washed with PBS-1%BSA and fixed with click-it fixative buffer, 10 μl per sample (around 10^6 cells, 15min, R.T.). After fixation, cells were permeabilised with 100 μl saponin-based permeabilisation and wash reagent from the kit. After these treatments, Click-it EdU reaction cocktail was added (60 μl per sample, Table III). Cells were incubated at R.T. for 30 min. After EdU staining, continued surface staining with antibodies with RPE, PE-tandem, or Qdot conjugates if needed.

2.4 Calcium influx

Single cell suspensions from spleens were spun down and supernatants were discarded. 2 ml ACK buffer (Sigma-Aldrich) was used to lyse red blood cells (RBCs). 1 min after lysis, the same volume of complete culture medium was added to stop the

reaction and spun down again (repeated this step until RBCs have been lysed completely).

In some experiments, harvested cells were "calmed" by culturing in complete culture medium at 37 ˚C, 5% CO_2 for 1 h (Khalil, Cambier et al. 2012). After this, cells were spun down and re-suspended with HBSS buffer at the concentration of 2 x 10^6 cells / ml. DMSO dissolved Indo-1 (BD Biosciences, 1mM stock) or Fluo-4 (Thermo Fisher Scientific, 1mM stock) was added to the cell suspension to a final concentration of 1 μM / ml. Cell suspensions were left in the dark at RT for 1 h to load Indo-1 or Fluo-4. The reaction was stopped by adding twice the volume of HBSS-10% FBS. Cell suspensions were spun down and re-suspended with 200 μl HBSS-10% FBS again to allow complete de-esterification of extra AM moieties, Indo-1or Fluo-4 (37 ˚C, 5% CO_2 for 30 min). Cells were then labelled with anti-CD43 antibody as a dump marker in FACS buffer at 4 ˚C for 30 min, washed once, and processed by flow cytometry.

Samples were analysed by BD LSRFortessa Analyzer (BD Biosciences) with BD FACSDiva. Laser line used was 405 (Violet), filters were set for BUV395 (379/28, calcium bound) and BUV496 (525/50, calcium free) for Indo-1. Raw data was exported and the ratio of bound to free was calculated in FlowJo (FlowJo, LLC) as a Derived Parameter. The signalling of Fluo-4 was detected by using laser 488 (Blue), filter (530/30) in the same machine.

2.5 Detection of protein phosphorylation

BD Phosflow™ (BD Biosciences) was used to analyse intracellular phosphoproteins. Single cell suspensions from non-immunised mice were obtained as described in 2.3.1. Single cells were calmed in complete culture medium at 37 ˚C, 5% CO_2 for 2 h after red blood cells lysis by ACK buffer (Khalil, Cambier et al. 2012). Anti-IgM F(ab)$_2$ antiserum (Jackson Lab) was added to cell suspensions (2 x 10^6 cells in 200 μl) at a final concentration of 10 μg/ml, incubated at RT for 5 min. After stimulation, the same amount of pre-warmed Fix Buffer I (BD Biosciences) was added immediately, mixed well and incubated at 37 ˚C for 10 min. Cells were spun down and resuspended in 400 μl pre-cold Perm Buffer III (BD Biosciences), incubated on ice for 30 min. Cells were then washed with 1 ml ddH$_2$O once, and 1 ml PBS once. As a negative control, cells were treated with Lamda Protein Phosphatase (Lambda PP, New England BioLabs). 2.5 μl Lamda Protein Phosphatase was added to a final volume of 100 μl, incubated at 30 ˚C for 30 min. After this, both negative control and experimental samples were incubated with antibody cocktails for surface and intracellular markers of interest at 4 ˚C for 30 min. Samples were ready to analyse by BD LSRFortessa Analyzer (BD Biosciences) with BD FACSDiva.

2.6 Fluorescence-activated cell sorting (FACs)

Single cell lymphocyte suspension was obtained and stained as described before. Cells were suspended and stained in RPMI1640 complete culture medium. Fc gamma receptors II and III on cell surface were blocked with anti-CD16/32 antibody at 4 ˚C

for 30 min in 200 µl. Cells then were stained with antibody cocktail at 4 ˚C for 30 min in 200 µl and washed twice at 150 g, 4 ˚C for 4 mins with FACS buffer before analysis. Dead cells were excluded by Hoechst 33342. Single cells were sorted in BD FACSAria^TM Fusion high-speed cell sorter (BD Biosciences) directly into 96-well flat bottomed microtitre cell culture plate (Falcon) for single cell culture. For bulk sorting, gated targeting cells were directly harvested in tubes for mRNA extraction. Samples for mRNA extraction were spun down immediately at 200 g, 4 ˚C for 5min after sorting. Supernatant was carefully discarded from each sample. Cell pellets were frozen in liquid nitrogen and stored at -80 ˚C for mRNA extraction.

Table I: RPMI1640 complete culture medium

Constituent	Manufacturer	Final concentration
RPMI-1640 Medium (with phenored, L-Glutamine and 2-Mercaptoethanol)	Sigma-Aldrich	89% (V/V)
FBS (heat-inactivated)	Thermo Fisher Scientific	10% (V/V)
Penicillin. Streptomycin (10000 units)	Thermo Fishe Scientific	1% (V/V)

Table II: FACS buffer

Constituent	Manufacturer	Final concentration
PBS (without Ca and Mg)	Sigma-Aldrich	98% (V/V)
FBS (heat-inactivated)	Thermo Fisher Scientific	1% (V/V)
EDTA 500 mM	Sigma-Aldrich	2 mM
Penicillin. Streptomycin (10000 units)	Thermo Fishe Scientific	1% (V/V)

Table III: Click-it EdU reaction cocktail (Life Technologies)

Constituent	Amount for 10^6 cells (1 sample, µl)
PBS	43.8
CuSO$_4$	1
Alexa Flour 647 azide	0.25
1X Click-it EdU buffer	5
Click-it Wash Buffer	10

Table IV: Antibodies used in flow cytometry

Target	Clone	Conjugation	Dilution	Manufacturer
CD16/32	93	Purified	1:200	eBiosciences
B220	RA3-6B2	FITC/BV510/BV421	1:200	Biolegend
B220	RA3-6B2	APC	1:1000	eBiosciences
B220	RA3-6B2	PE	1:300	BD Biosciences
CD45.1	A20	PerCP-Cy5.5	1:150	Biolegend
CD45.1	A20	PE/FITC/PE-Cy7	1:100	eBiosciences
CD45.2	104	PerCP-Cy5.5	1:150	Biolegend
CD45.2	104	APC/FITC/PE	1:100	eBiosciences
CD43	S7	Biotin	1:100	BD Biosciences
IgD	11-26c.2a	BV421/BV510	1:200	Biolegend
IgM	Poly-clonal	FITC	1:300	Southern Biotech
IgM	11/41	APC-AF780/PE-Cy7	1:300	eBiosciences
IgMa	DS-1	PE	1:300	BD Biosciences
IgMa	DS-1	FITC/BV421	1:300	BD Biosciences
IgMb	AF6-78	PE	1:300	BD Biosciences
IgMb	AF6-78	FITC	1:300	BD Biosciences
IgG1	X56	APC	1:100	BD Biosciences
Fas (CD95)	Jo2	BV605	1:300	BD Biosciences
CD38	90	FITC/PerCP-Cy5.5/APC	1:500	Biolegend
CD138	281-2	BV711	1:300	Biolegend
PD-1	J43	PE	1:200	Biolegend
CD44	IM7	PerCP-Cy5.5	1:200	eBiosciences
CD11c	HL3	PE-Cy7	1:300	BD Biosciences
CD4	RM4.5	eFlour450	1:200	eBiosciences
CD4	GK1.5	BV510	1:200	Biolegend

CD3	145-2C11	PE	1:200	eBiosciences
CD3	17A2	BV510/BV421	1:200	Biolegend
CD62L	MEL-14	BV510	1:200	Biolegend
CXCR5	2G8	Purified	1:125	BD Biosciences
Rat IgG	Poly-clonal	AF647	1:200	Jackson Lab
CD5	53-7.3	Biotin	1:200	Biolegend
CD5	53-7.3	PE-Cy5	1:200	BD Biosciences
Streptavidin		FITC	1:300	BD Biosciences
Streptavidin		PE-Cy7	1:400	eBiosciences
Streptavidin		BV711/BV421	1:300	Biolegend
NP		PE	1:500	In house
Lambda	JC5-1	PE	1:500	Southern Biotech
Kappa	H139-52.1	FITC	1:500	Southern Biotech
CD19	eBio1D3	APC	1:100	eBiosciences
CD19	6D5	AF700	1:100	Biolegend
CD21	7G6	APC/FITC	1:400	BD Biosciences
CD23	B3B4	FITC	1:300	BD Biosciences
CD23	B3B4	PE-Cy7	1:500	eBiosciences
CD11b	M1/70	APC	1:500	eBiosciences
Ly6c	HK1.4	BV421	1:200	Biolegend
Ter-119	TER-119	Pacific Blue	1:200	Biolegend
AA4.1(CD93)	AA4.1	PerCP-Cy5.5	1:100	Biolegend
CD24	M1/69	BV510	1:200	Biolegend
C-kit	ACK2	BV605	1:200	Biolegend
IL7Ra	A7R34	PE-Cy	1:200	eBiosciences
CD25	7D4	Biotin	1:400	BD Biosciences
CD69	H1.2F3	APC	1:200	eBiosciences
MHCII	M5/114.15.2	PerCP-Cy5.5	1:200	Biolegend
CD86	GL1	PE-Cy5	1:300	eBiosciences
CD86	GL1	BV650	1:200	Biolegend
Annexin V		APC	1:20	BD Biosciences
7-AAD			1:20	eBiosciences
aCaspase 3	C92-605	Purified	1:100	BD Biosciences
Swine anti-Rabbit	Poly-clonal	Biotin	1:200	DAKO
Foxp3	FJK-16s	eFluor450	1:100	ThermoFisher
IgM	F(ab')$_2$ Fragment	Purified	1:100	Jackson Lab
Syk (Y352)	17A/P-ZAP70	PE	1:50	BD Biosciences
BLNK (pY84)	J117-1278	AF647	1:50	BD Biosciences

2.7 Single cell culture

To obtain plasma cell colony from single Fo B cell, NB-21.2D9 feeder cells (kind gift from Professor Garnett Kelsoe, Duke University) were employed in the single cell culture system. NB-21 feeder cells are retrovirally transfected to express mouse CD40L, BAFF and IL-21 in order to support and induce B cells to become plasma cells and support immunoglobulin production (Kuraoka, Schmidt et al. 2016).

6 days before single cell sorting, NB-21.2D9 fibroblast cells were thawed. One frozen vial of cells was suspended with 15 ml pre-warmed feeder cell maintenance medium and seeded in a 10 cm petri dish. 4 days before single cell sorting, NB-21.2D9 cell cultures were divided into three dishes to produce a new generation. 0.05% Trypsin-EDTA was used to dissociate and detach the cells from the culture dish. Once cells were tap-slided from the dish, 10 ml pre-warmed feeder cell culture medium was added to dilute Trypsin-EDTA. Cell suspension was spun down at 400 g for 5 min at 4 °C, and cell were suspended in pre-warmed feeder cell maintenance medium and counted. NB-21.2D9 cells were seeded at the total number of 5×10^5 cells in 15 ml feeder cell culture medium per 10 cm dish. 1 day before single cell sorting, NB-21.2D9 cells were harvested. After counting, cells were suspended in B cell complete culture medium, and were adjusted to the concentration of 1×10^4 cells/ml. 100 µl of the NB-21.2D9 cell suspension was added to each well in a 96-well cell culture plate. Feeder cells seeded 96-well plates were cultured at 37 °C, 5% CO_2, overnight.

On the day of cell sorting, recombinant mouse IL-4 (Peprotech) was diluted with pre-warmed B cell complete culture medium at the concentration of 4 ng/ml. 100 µl of B cell complete culture medium with IL-4 was added to each well in the 96 well-plate to make a final IL-4 concentration of 2 ng/ml. Single Fo B cell was FACS sorted (as described in 2.6) directly into each well and incubated at 37 °C, 5% CO_2 immediately after sorting to start single B cell culture.

2 days after sorting, 100 µl culture supernatant was removed from each well. 200 µl pre-warmed B cell complete culture medium was gently added into each well. From day 3 to day 8, 200 µl of culture medium was replaced with 200 µl fresh pre-warmed B cell complete culture medium daily. Around 200 µl single cell culture supernatants were directly harvested 10 days after single cell culture, and 2.5 µl of 10% NaN_3 was added into each supernatant. Supernatant from each well were aliquoted and stored at -20 °C for future use.

Table V: Feeder cell maintenance medium

Constituent	Manufacturer	Final concentration
DMEM, [+] 4.5 g/L D-glucose, [+] L-Glutamine	Invitrogen	88% (V/V)
Fetal Bovine Serum	Thermo Fisher Scientific	10% (V/V)
Penicillin. Streptomycin (10000 units)	Thermo Fishe Scientific	1% (V/V)
MEM NEAA	Invitrogen	1% (V/V)

Table VI: B cell complete culture medium

Constituent	Manufacturer	Final concentration
RPMI-1640, [+] L-Glutamine	Invitrogen	86% (V/V)
Fetal Bovine Serum (Hyclone)	Thermo Fisher Scientific	10% (V/V)
2-ME	Invitrogen	55 uM
Penicillin. Streptomycin (10000 units)	Thermo Fishe Scientific	1% (V/V)
HEPES	Invitrogen	10 mM
Sodium Pyruvate	Invitrogen	1 mM
MEM NEAA	Invitrogen	1% (V/V)

2.8 Immunofluorescence

2.8.1 Cryosection

Spleens were frozen on dry ice in a pre-labelled aluminium foil paper and stored at -80 ˚C. Lymph nodes were well-positioned in OCT tissue-freezing solution (Leica Microsystems), frozen on dry ice and stored in -80 ˚C. 6 μm sections from spleens and popliteal LNs were obtained by cryosection (Bright Instruments). Sections were placed onto pre-labelled multi-spot slides (Hendley-Essex) and air dried at room temperature (R.T.) for at least 30 min. Slides were fixed in acetone (Fisher scientific) at 4 ˚C for 20 min and air dried for another 10 min. After fixation, slides were stored at -20 ˚C for later use.

2.8.2 Immunofluorescence for tissue sections

Slides were allowed to recover to RT before staining. After this, slides were rehydrated by putting them into a glass tank filled with PBS for 5 min. 80 μl of 10% normal horse serum (Sigma-Aldrich) in PBS-10%BSA (Sigma-Aldrich) was added as

blocking buffer and incubated at RT for 20 min. If intracellular or nuclear staining was needed, 0.2% Triton X-100 (Sigma-Aldrich) in PBS was added to each spot for permeabilization (10 min, RT). Slides were then incubated with primary antibody cocktails (Table V) for 1 hour in a dark humid chamber with gently shaking at RT. Secondary and tertiary antibodies (Table VI) were added to each spot and incubated at the same condition as primary antibodies. Between each step of incubation, slides were washed in PBS for 5 min. All the antibodies were diluted in PBS-10% BSA (Sigma-Aldrich). After final wash, slides were dried and mounted with mounting medium (ProLong Gold antifade reagent, Invitrogen). Mounting medium was cured overnight at RT in the dark. After this, mounted slides were used for wide field fluorescence microscopy or stored at -20 ˚C for later observation.

2.8.3 Immunofluorescence for auto-immune slides

Auto-immune slides were from the Rat Liver, Kidney, Stomach Kit (NOVA Lite). Sera from coagulated blood samples of young or aged mice were produced by clotting at 37 ˚C for 2 hours and then spun down at 10000 g, RT for 5 min. Supernatants (sera) were carefully harvested and put into pre-labelled autoclaved clean microtubes.

Slides were allowed to warm to RT before staining. 50 μl net sera were added to spots. At least one positive and negative control was done on each slide. Positive controls of anti-mitochondrial antibodies, anti-nuclear antibodies and anti-smooth muscle antibodies were used from the kit. PBS and IFA system negative control from the kit were used as negative control. Loaded slides were incubated overnight at 4 ˚C. The

second day, slides were washed in PBS for 10 min and FITC conjugated rat anti-mouse IgG1 (H+L) (Southern Biotech) antibody was added to spots required. Slides were incubated in a humid dark chamber for 1 hour at RT. 50 μl Hoechst 33342 was applied to each spot and incubated for 2 min. After this, slides were well washed and mounted with mounting medium from the kit. Slides were cured in the dark overnight. Slides were sealed with transparent nail polish. Slides observed in a widefield fluorescence microscopy (20 x) or stored in -20 ˚C for later observation.

2.8.4 Microscopy

Both tissue sections slides and auto-immune slides were tile scanned and observed under Zeiss AxioScan Z1 scanning fluorescence widefield microscope (Carl Zeiss). Beam Splitter for Alexa Fluor 647 was 660, for Alexa Fluor 488 was 498, for Alexa Flour 405 was 395, for Alexa Flour 555 was 568. Exported tile scanned images were off-line processed with software Zen, Blue edition (Carl Zeiss) and ImageJ-Fiji.

Table VII: Primary antibodies used in immunofluorescence

Target	Isotype	Clone	Dilution	Manufacturer
B220	Rat anti-mouse	RA3-6B2	1:100	BD Biosciences
CD4				
IgM	Goat anti-mouse	Poly-clonal	1:200	Southern Biotech
IgD	Rat anti-mouse	11-26c.2a	1:200	Biolegend
CD169	Rat anti-mouse	3D6.112	1:100	Biolegend
CD1d	Rat anti-mouse	1B1	1:100	Bioegend
IRF4	Goat anti-mouse	Poly-cloncal	1:50	SantaCruz
NP	Rabbit Ig conjugated		1:500	In house

Table VIII: Secondary antibodies used in immunofluorescence

Target	Conjugation	Dilution	Manufacturer
Donkey anti-sheep (goat)	AF488	1:200	Jackson ImmunoResearch
Donkey anti-Rabbit	Cy3	1:200	Jackson ImmunoResearch
Streptavidin	BV421	1:200	Biolegend

2.9 Immunisation

2.9.1 T-cell dependent antigen immunisation

T cell dependent immune responses were triggered by subcutaneous immunisation with 20 μg alum-precipitated NP-CGG (4-hydroxy-3-nitrophenyl acetyl Chicken γ-globulin) on the plantar surface of rear feet and (or) intraperitoneal (i.p.) immunisation with 50 μg alum-precipitated NP-CGG. NP$_{18}$-CGG was a gift from Ms Chandra Raykundalia.

To prepare the antigen, 5 mg/ml of NP-CGG was mixed with equivalent volume of alum (9% $AlK(SO_4)_2$ in ddH_2O) (Zhang, Garcia-Ibanez et al. 2017), 10 M NaOH was added to the mixture to adjust its pH value to 6.5~7. Then, the mixture was rotated in the dark for at least 45 min to allow for maximum precipitation. After spinning at 250 g, R.T. for 5 mins, the pellet was washed in PBS twice. Then the pellet was suspended in PBS at 1 mg/ml for foot immunisation and 250 μg/ml for i.p. immunisation, 1×10^5 chemically inactivated Bordetella pertussis (b.p.) bacteria (LEE laboratories, BC, USA) were added as an adjuvant in all primary immunisations.

For most experiments, popliteal LNs and spleens were harvested at 8 days after immunisation. In pilot experiments, LNs and spleens were harvested at days 4, 5, 6, 8 and 14.

2.9.2 T-independent antigen immunisation

T cell independent immune response was induced by i.p. immunisation of 30 µg NP-Ficoll (Biosearch Technologies) in 200 µl PBS. Spleens were harvested and the immune response was evaluated after 5 days of immunisation.

2.9.3 T-dependent and T-independent mix immunisation

Sheep red blood cells (SRBCs) can induce mixed activation of both T-D and T-I responses. SRBCs (TCS Biosciences) were washed in PBS for twice. Mice were then i.v. immunised with 2 $\times 10^8$ cells in 200 µl PBS. Normally, spleens were harvested 5 days after immunisation. In pilot experiments, spleens were harvested at days 1, 2, 3, 4, 5 and 8 after immunisation.

2.10 Enzyme-linked immunosorbent assay (ELISA)

2.10.1 ELISA for NP-specific antibody titre and affinity

Samples used for ELISA were sera from coagulated blood samples of immunised or non-treated mice. Serum samples were collected and preserved as described in 2.8.3. Flat-bottom plates (Thermo Fisher Scientific) were coated with either NP_{15}-BSA (in house) or NP_2-BSA (in house) at 5 µg/ml in coating buffer (Table VIII), 4 ˚C, overnight. NP_{15}-BSA was used to detect the titres of all NP-specific Ig class switched

antibodies (eg. IgG or IgG1). NP_2-BSA was used to detect titres of the high affinity fraction of NP-specific Ig class switched antibodies (eg, IgG or IgG1) and the titres of all NP-specific IgM. The second day, plates were washed twice in wash buffer (Table VIII). 200 µl blocking buffer (PBS-1%BSA) was added and incubated at 37 ˚C for 1~1.5 h. Serum samples were serially diluted in seven 3x dilutions, normally with a starting dilution of 1 : 30. Plates with loaded samples were incubated at 37 ˚C for 1 h. After incubation, plates were washed in wash buffer (PBS-0.05%Tween 20) and incubated with AP-conjugated secondary antibodies (eg. anti-IgM, anti-IgG, anti-IgG1, anti-IgG3 et. al. Southern Biotech, Table VII), diluted in blocking buffer, at 37 ˚C for 45 min. Plates were well-washed before adding substrate buffer.

The substrate of AP was p-nitrophenyl phosphate dissolved in Tris buffer (SIGMAFAST, Sigma-Aldrich). One tablet from each was dissolved in 20 ml ddH_2O. After both tablets fully dissolved, 100 µl of this substrate buffer was added to develop the colour. The absorbance was read at 405 nm by using a Synergy HT Microplate Reader (BioTek). OD values were exported into Excel. OD values were plotted against dilution and smoothed lines were drawn through each dilution series. Relative antibody titres were read as maximal dilution where OD was above an arbitrary threshold. Antigen affinity was measured as the ratio of NP_2 antibody titre to NP_{15} antibody titre. To make OD values from different plates comparable, a standard sample was added into each plate and used to normalised OD values in different plates.

2.10.2 ELISA for Pigeon cytochrome C (PCC) specific antibody

In order to measure PCC-specific antibody titres, plates were coated with PCC (Sigma-Aldrich). PCC detection plates were coated with PCC diluted in coating buffer at the concentration of 10 µg/ml.

In both NP and PCC ELISA assays, negative controls and positive controls were included into each plate.

2.10.3 ELISA for serum total IgM and IgG1

Plates were coated with 2.5 µg/ml of anti-Kappa (Southern Biotech) and 2.5 µg/ml anti-Lambda (Southern Biotech) antibodies, to make a final total concentration of 5 µg/ml total antibodies.

Table IX: Antibodies used in ELISA

Target	Dilution	Manufacturer
Goat anti-mouse IgM-AP	1:2000	Southern Biotech
Goat anti-mouse IgG3-AP	1:1000	Southern Biotech
Goat anti-mouse IgG1-AP	1:1000	Southern Biotech
Goat anti-mouse IgG-AP	1:1000	Southern Biotech

Table X: Reagents used in ELISA

Reagents	Ingredients
Coating buffer	Na_2CO_3 1.95g, $NaHCO_3$ 2.93g in 1 L ddH_2O, ph=9.6
Blocking/Dilution buffer	PBA-1%BSA (Sigma)
Wash buffer	PBS-0.05% Tween 20 (Sigma)
Substrate	2 tablets in 20 ml ddH_2O

2.11 Real-time (RT) PCR

2.11.1 Extraction of total mRNA

mRNA was extracted from spleen sections or sorted cells. Before extraction, all samples were stored and kept at -80 ˚C. RNeasy Mini kit or Micro kit (Qiagen) was used depending on the amount of cells. Spleen sections which contain more than 1 million cells were treated with Mini Kit, smaller quantities were treated with the Micro kit. The procedures of mRNA extraction were strictly following manufacturer's instructions. mRNA was eluted in 15 µl (Micro kit) or 30 µl (Mini Kit) of RNase free water.

2.11.2 Reverse-transcription to generate cDNA

3 µl of random oligo-dN6 primers (Promega Biosciences) was added to each 30 µl mRNA sample. Primer-template mixtures were denatured at 70 ˚C for 10 min, and placed immediately on ice for oligo-dT binding. The reverse-transcription reaction system (Table X) was set up by adding 27 µl reaction buffer to 33 µl of template-primer mixture and left to incubate at 41 ˚C for 1 h, followed by 10 min inactivation at 90 ˚C. cDNA was stored at -20 ˚C for further use.

2.11.3 Semi-quantitative RT-PCR

RT-PCR was normally carried out in 384-well plates (Applied Biosystem). Taqman was performed in a reaction volume of 5.5 µl, including 0.5 µl cDNA template, varied optimalised amounts of primers and probes (Table IX), Taqman Universal PCR Master Mix (Applied Biosystem) and ddH$_2$O. mIgh and mIgd relative expression

levels were detected using SYBR Green chemistry, using the reaction buffer SensiMix SYBR Hi-ROX (Bioline). PCR was performed in an ABI 7900 real-time PCR machine (Applied Biosystems). The PCR program was run by using the software SDS 2.2.2 (Applied Biosystems), 95 ˚C for 10 min for denaturation, then elongation at 95 ˚C for 15 s followed at 60 ˚C for 1 min for 40 cycles.

Data were exported and analysed by using the software RQ Manager 1.2.1 (Applied Biosystems). mRNA relative expression level was calculated by using ΔCt value, which normalised to the housekeeping gene (β2-microglobulin).

Table XI: Primers information

Target		Sequence information
β2-micro globμlin	Forward	CTGCAGAGTTAAGCATGCCAGTAT
	Reverse	ATCACATGTCTCGATCCCAGTAGA
	Probe	CGAGCCCAAGACC
mIghm	Forward	TGACCGAGAGGACCGTGGA
	Reverse	CTTGAACAGGGTGACGGTGGT
	Probe	
mIghd	Forward	AACACCATCCAACACTCGTGTA
	Reverse	CTTGATGAAGGTGACGAAGCCA
	Probe	

Table XII: Reverse-transcriptional system (per sample)

Reagent	Volumn (μl)
5X first strand buffer (Invitrogen)	12
0.1 M DTT (Promega)	6
10 mM dNTPs (Invitrogen)	3
M-MLV reverse transcriptase (Invitrogen)	3
RNasin RNase inhibitor (Promega)	1.5
RNase free water (Qiagen)	1.5
Random primers (Promega)	3
Total mRNA Templates	30

2.12 Western Blot

2.12.1 Sample preparation

Single splenocytes suspension was obtained as described (chapter 2.3.1). 1×10^7 splenocytes were suspended in 90 µl MACS buffer (PBS (Thermo Fisher Scientific), 0.5% BSA (Sigma-Aldrich), 2 mM EDTA (Sigma Aldrich). 10 µl of anti-CD43 antibody labelled microbeads (Miltenyi Biotec) was added to each 1×10^7 of cells, mixed well and incubated at 4 ˚C for 15 min. After incubation, splenocytes were washed with MACS buffer 1-2 ml each 1×10^7, spun down and re-suspended each 1×10^8 cells with 500 µl MACS buffer (if cell number was below 10^8, with 500 µl MACS buffer). Cell suspensions were then applied to a pre-washed LS column (Miltenyi Biotec) inside a magnetic field. The column was eluted with 9 ml MACS buffer inside a magnetic field. All pass-through fluid was collected, and re-suspended with complete RPMI1640 culture medium. Harvested cells were left to calm for 1 h in complete RPMI1640 culture medium at 37 ˚C (Khalil, Cambier et al. 2012).

2×10^6 isolated B cells in 200 µl complete culture medium were stimulated with 10 µg/ml Anti-IgM F(ab)$_2$ (Jackson Lab) for 0 min, 5 min, 10 min, 30 min or 60 min. After stimulation, 1 ml 0.5% NaN$_3$ was added immediately to stop the reaction. After spinning down, supernatants from samples were completely removed and discarded. 200 µl RIPA Lysis and Extraction Buffer (Thermo Fisher Scientific) with 1X Halt Protease & Phosphatase Single-Use Inhibitor Cocktail (Thermo Fisher Scientific) was

added, and incubated on ice for at least 30 min. Cell lysates were then stored at -20 ˚C for future use.

2.12.2 Gel electrophoresis of Protein

10 µl DNase (Qiagen) was added into aliquotes of cell lysates. The mixture was incubated at RT for 30 min to eliminate chromatin pellets. Then 5X Sample Buffer (10% SDS, 300mM Tris-HCL, 0.05% Bromophenol blue, 50% Glycerol, 10% 2-mercaptoethanol), 100 mM DTT (Sigma-Aldrich) was added to each cell lysates, mixed well and heated to 95 ˚C for 10 min.

After the incubation, 15 µl of each sample was loaded to NuPAGE 4-12% BT Gel (Thermo Fisher Scientific) with 5 µl Prime-Step Prestained Broad Range Protein Ladder (BioLegend). The gel was run at constant voltage at 10 V/cm for 2 h in an electrophoresis tank filled with 1X Running Buffer (Thermo Fisher Scientific).

Before wet transfer, a polyvinylidene difluoride (PVDF) membrane (Immobilon) was activated by methanol (Fisher Scientific) for 10 min and washed with 1X transfer buffer (20X transfer buffer (Thermo Fisher Scientific), 20% methanol (Fisher Scientific)) to eliminate any residual methanol drops on the membrane. 2-Gel transfer system was set as (-) pre-wet pads, Blotting Filter Paper (Immobilon), gel, membrane, Filter Paper, pre-wet pads, Filter Paper, gel, membrane, filter paper, pre-wet pads (+), from (-) negative pole to (+) positive pole. The Electrophoresis system was filled with

transfer buffer, and the rest of tank was filled with ddH$_2$O, intended to cool the whole system. The transfer was run at a constant voltage at 4 V/cm for 2 h.

2.12.3 Immunoblot

Protein loaded membrane was blocked in TBST-5% BSA (Sigma-Aldrich) for 30 min at RT with gentle shaking. The membrane was then blotted either with Tris-buffered saline with Tween 20 (TBST)-5% BSA diluted mouse anti-Phosphotyrosine antibody (Bio X Cell) or anti-Beta Actin Rabbit Polyclonal (Proteintech), incubated at 4 ˚C overnight. The second day, membranes was washed three time in TBST at RT for 5-10 min under gentle shaking. The membrane was then blotted with TBST-5% BSA diluted secondary antibodies, anti-mouse or rabbit IgG HRP-linked antibody (Cell Signaling Technology) at RT for 1 h under gentle shaking. After the membrane was washed three times it was ready for imaging. Freshly prepared Clarity Western ECL Substrate (BIO-RAD) was spread on the membrane, incubated for 1 min and then discarded. The image was taken in a ChemiDoc^{TM} MP imaging system (BioRad) immediately afterwards. High resolution pictures were selected, analysed and exported by using software Image Lab 5.1 (BioRad).

2.13 Data analysis

GraphPad Prism 6 was used to perform statistical analysis and generate graphs. Comparison which involved two groups and only one variable parameter were tested for significance using unpaired two-tailed T test. Comparisons which involved two

groups, but two variable parameters were analysed using multiple t tests. P values were corrected for multiple comparisons using the Sidak-Bonferroni method.

P values < 0.05 were considered significant (*). P values were indicated with stars in most figures: * $p < 0.05$; ** $p < 0.01$; *** $p < 0.001$; **** $p < 0.0001$.

Comparisons in heterozygous mice which involved two groups and two variables were analysed using two-way ANOVA, corrected for multiple comparisons using Tukey's multiple comparisons test to compute CIs and significance. Significance and confidence level: 0.05 (95% confidence interval).

Chapter 3 . Characterization of B cell development in mice with polyclonal chimeric IgMg1 B cell receptors

3.1 Introduction

3.1.1 B cell receptor signalling strength and B cell development

B cells of mice and men can express five major classes of BCRs: IgM, IgD, IgG, IgE and IgA (Bengten, Wilson et al. 2000). Naïve follicular B cells express IgM and IgD simultaneously, while MZ B cells and B1 cells express high levels of IgM, with very little IgD expressed on their surface. After activation B cells start class switch recombination leading to the expression of downstream Ig classes (Chaudhuri and Alt 2004). Different subclasses of BCRs not only have different extracellular domains, but also contain additional cytoplasmic signalling regions that can lead to different downstream signalling strength. IgG1 contains a small cytoplasmic region that has been shown to mount higher downstream signalling after BCR stimulation (Waisman, Kraus et al. 2007, Weston-Bell, Forconi et al. 2014).

Previous studies have revealed that BCR signalling and its strength play important roles in B cell development and affect B cell fate decisions during B cell maturation (Niiro and Clark 2002, Monroe 2006, Pillai and Cariappa 2009). In bone marrow, B cells develop following the sequence from pre-pro B cells, pro-B cells, pre-B cells to immature B cells (Cambier, Gauld et al. 2007, Hobeika, Maity et al. 2016). Pre-BCRs with fully rearranged heavy chains and surrogate light chains are transiently expressed

on the surface of pre-B cells and tested for signalling capability as positive selections for pre-B cells (Saijo, Schmedt et al. 2003, Monroe 2006). During the immature B cell stage, B cells can be negatively selected if their BCR binds autoantigens, which is a first test for auto-reactivity. Here, B cells with strong self-binding strength are induced into apoptosis, B cells with weak to medium auto-reactivity are induced into an anergic state. Anergic B cells and non-self-binding B cells are allowed further maturation (Brink and Phan 2018). Light chain rearrangement during immature B cell stage can rescue some of the strong self-binding cells (Gay, Saunders et al. 1993, Tiegs, Russell et al. 1993). This mechanism is termed receptor editing and confers B cells a second chance for the production of a new BCR containing the same heavy chain with a new V-J combination light chain, which may generate a BCR that has no or only weak auto-reactivity.

After exiting bone marrow, immature B cells differentiate into transitional B cells (T1 B cells) that enter the periphery. T1 B cells are further selected and differentiate depending on their affinities toward self-antigens, particularly tissue-specific autoantigens (Russell, Dembic et al. 1991, Jacobi and Diamond 2005). During the final maturation of these surviving B cells, tonic BCR signalling strength can also affect B cell fate commitment (Cariappa, Tang et al. 2001, Cariappa, Takematsu et al. 2009, Pillai and Cariappa 2009). B cells with higher BCR signalling prefer to differentiate into follicular B cells (Loder, Mutschler et al. 1999, Niiro and Clark 2002), while lower BCR signalling may lead to MZ B cell differentiation (Cariappa, Tang et al. 2001, Pillai, Cariappa et al. 2005). Very recently, provoking work from the

Rajewsky group showed the instructive role of the BCR in driving mature B cell re-differentiation from B2 to B1 cells (Graf R, Science 2019).

3.1.2 B cell receptor signalling strength and B cell anergy

There is a link between hyper-active BCR signalling and B cell auto-reactivity or B cell anergy. During B cell development, B cells with increased tonic BCR signalling due to expression of a weak to medium self-binding BCR can be induced into anergy. Studies in mutant mice, where BCR signalling has been artificially increased by mutating individual BCR signalling repressors, e.g. SHP-1, show that this can lead to spontaneous generation of polyclonal auto-reactive antibodies beyond a certain age (Hibbs, Tarlinton et al. 1995, Getahun, Beavers et al. 2016). Autoreactive B cells observed in these models always maintain hyperactive BCR signalling, while autoreactive anergic B cells generally have absent or reduced activated BCR signalling after BCR ligation (Goodnow, Crosbie et al. 1988, Glynne, Ghandour et al. 2000). This is surprising, as BCR signalling by BCR self-antigen ligation as well as the mutation of repressors of the BCR signalling pathway should generate a similar effect -- generating B cells that display hyperactive BCR signalling. Why do B cells with mutant repressors fail to turn into an anergic state?

During normal B cell development, repressors of BCR signalling, such as SHP-1, are used by the immune system to maintain the anergic state of B cells (O'Neill, Getahun et al. 2011, Getahun, Beavers et al. 2016). The mutations of them make the immune

system incapable to counter-regulate BCR signalling by inducing B cells into anergic state. On the other hand, the immune system always creates a wide spectrum of BCR specificities that may include autoreactive B cells. Therefore, B cell development is highly evolved to deal with diverse signalling strength from BCR/ligand binding during development (Melamed, Benschop et al. 1998, Loder, Mutschler et al. 1999). B cells emerging during B cell development with autoreactive BCR can be dealt with, as long as repressors are available to inhibit BCR signalling and differentiate these cells into anergic cells, whereas, mutations in BCR signalling repressor molecules will generate mice with overt autoimmunity. Therefore, it is possible to create mouse model with poly-clonal anergic B cells if the modification only affects signalling strength from BCR/ligand binding.

Besides absent or reduced BCR signalling as the defining feature of anergy, there are some other recognized features shared by the majority of B cell anergy mouse models. Anergic B cells express lower levels of surface membrane IgM (Goodnow, Crosbie et al. 1988, Borrero and Clarke 2002, Merrell, Benschop et al. 2006). In some models, anergic B cells have shortened life spans, as they are less competitive to occupy survival niches (Cyster, Hartley et al. 1994, Cyster and Goodnow 1995, Mackay, Schneider et al. 2003). Furthermore, some studies report that anergic B cells are blocked at an immature or transitional stage and don't proceed into further development. This is called developmental blockage (Goodnow, Crosbie et al. 1989, Merrell, Benschop et al. 2006). In other models, anergic B cells are unable to enter follicles in the presence of competition from non-self-reactive naïve B cells and

display altered location to the T-B border (Fulcher and Basten 1994, Cyster and Goodnow 1995, Cambier, Gauld et al. 2007). Surprisingly, anergic B cells have been estimated to account for as much as 20-30 % of peripheral mature B cells pool (Grandien, Fucs et al. 1994, Wardemann, Yurasov et al. 2003). Two recent studies confirmed that all healthy individuals have a major compartment of silenced anergic auto-reactive B cells (Wardemann, Yurasov et al. 2003, Smith, Packard et al. 2015).

3.1.3 IgMg1 mouse model

Two different mouse models have shown that naïve B cells expressing the IgG1 cytoplasmic signalling chain show higher and longer-lasting calcium influx after stimulation. These are where B cells either express chimeric IgM with a IgG1 cytoplasmic signalling chain (IgM-G1) with all B cells monospecific for HEL, or where B cells are polyspecific with a normal VDJ repertoire but express only surface IgG1 (Horikawa, Martin et al. 2007, Waisman, Kraus et al. 2007). In attempt to enhance BCR signalling in a polyclonal B cell repertoire where B cells express normal polyclonal extracellular IgM and IgD, our collaborator Mike Snaith (Medimmune) generated a IgMg1 mouse model by adding the gene sequence encoding for the IgG1 cytoplasmic region downstream of the germ-line IgM extracellular region, while keeping germ-line VDJ regions to allow for regular random re-arrangements (described in Chapter 3, Fig. 3.1). As mentioned above, the strength of tonic BCR signalling impacts B cell fate decisions during development and hyper-activated BCR can induce either anergy or auto-reactivity. Therefore, it

may be interesting to characterize B cell development and evaluate the state of mature B cells in this mouse model.

3.1.4 Objective

The work presented in this chapter is based on our new IgMg1 BCR knock-in mouse model. Compared to IgM and IgD that does not have a cytoplasmic signalling domain, the IgG1 cytoplasmic region is supposed to transduce additional down-stream signalling after BCR stimulation. The aim of this part of my thesis is to how a change in BCR signalling in the IgMg1 mouse model impacts on B cell development, how does this modification change BCR signalling, and to characterize the emergence of mature B cell populations.

Aims are detailed as follows:

1. What is the impact of IgMg1 BCR signalling on B cell development in IgMg1 mice? on

    A. B cell development in BM stage

    B. B cell development in periphery stage

2. How does BCR signalling change in IgMg1 developing and mature B cells:

    A. Tonic BCR signalling strength

    B. Activated BCR signalling

3.2 Results

3.2.1 Expression of IgMg1 chimeric B cell receptor does not lead to major changes in bone marrow B cell development

To construct IgMg1 mice, a gene segment encoding for the cytoplasmic region of IgG1 was inserted down-stream of the IgM transmembrane encoding region. A targeting vector containing: genome sequence encoding IgM heavy chain constant regions M1 and M2 immediately 5' to cDNA encoding for the cytoplasmic tail extension of IgG1, and a neomycin selection cassette (inverted terminal repeats (ITRs) flanked neomycin cDNA), was microinjected into embryonic stem (ES) cells. The 75 bp sequence coding for the 25 C-terminal amino acids of the IgG1 cytoplasmic region was specifically targeted into the genome of C57BL6/N ES cells through homologous recombination. Positively recombined ES cells were selected by G418 (Geneticin) and screened by PCR. The positive selection cassette containing an ITR flanked neomycin gene was deleted by PiggyBac transposase mediated excision. Selected ES cells were then injected into blastocysts to generate high percentage chimeras. Chimeric founder mice were bred to generate homozygous IgMg1 mice. The Germ-line V-D-J regions remained intact in IgMg1 mice, which allows for random rearrangement during BCR development (Fig. 3.1A). Therefore, B cells in mice express IgMg1 chimeric B cell receptors: with IgM extracellular and transmembrane regions, but an IgG1 cytoplasmic tail (Fig. 3.1B).

Previous studies show that tonic signalling strength transduced from membrane-bound BCRs can affect B cell fate decisions during development (Niiro and Clark

2002, Monroe 2006, Pillai and Cariappa 2009). We reasoned that addition of the IgG1 cytoplasmic signalling tail to IgM might alter BCR signalling strength and therefore affect B cell development. To explore this, B cell development in IgMg1 mice was compared to that in IgMwt mice. B cell development has been generally divided into two stages. Bone marrow is the location for the differentiation and maturation of common lymphoid progenitors (CLPs), pro-B cells, pre-B cells and immature B cells. and periphery (mainly spleen) hosts further B cell development from transitional B cells to mature B cells (Mebius and Kraal 2005).

Bone marrow was collected from both IgMwt and IgMg1 mice. Percentages of developmental B subsets were assessed. Common lymphoid progenitor cells (CLPs) and pro-B cells (Fr.A) are gated from $CD19^-IgM^-CD3^-Ly6c^-Ter119^-CD93^+CD24^{low}C\text{-}kit^{int}IL7\text{-}Ra^+$ precursors. Within this population, CLPs are the $B220^-$ subset, while pro-B cells are the $B220^+$ (Fig. 3.2A) (Kondo, Weissman et al. 1997). CLPs and pro-B cells do not yet express BCR heavy chain and, as expected, no difference was detected for CLPs and pro-B cell development in IgMg1 mice (Fig. 3.2B). Pre-B cells are gated as $B220^+CD43^-IgM^-IgD^-$ bone marrow lymphocytes, BM transitional B cells are $B220^+CD43^-IgM^+IgD^{low}$, and immature B cells are $B220^+CD43^-IgM^+IgD^-$ subset (Fig. 3.3A). In IgMg1 and IgMwt mice, percentages of pre-B, transitional and immature B cells were comparable (Fig. 3.3 B). However, consistently higher percentages of mature B cells were observed in IgMg1 mice (Fig. 3.3B right). Overall, these observations indicate that the expression of IgMg1 does not lead to major changes in B cell development during the bone marrow stage.
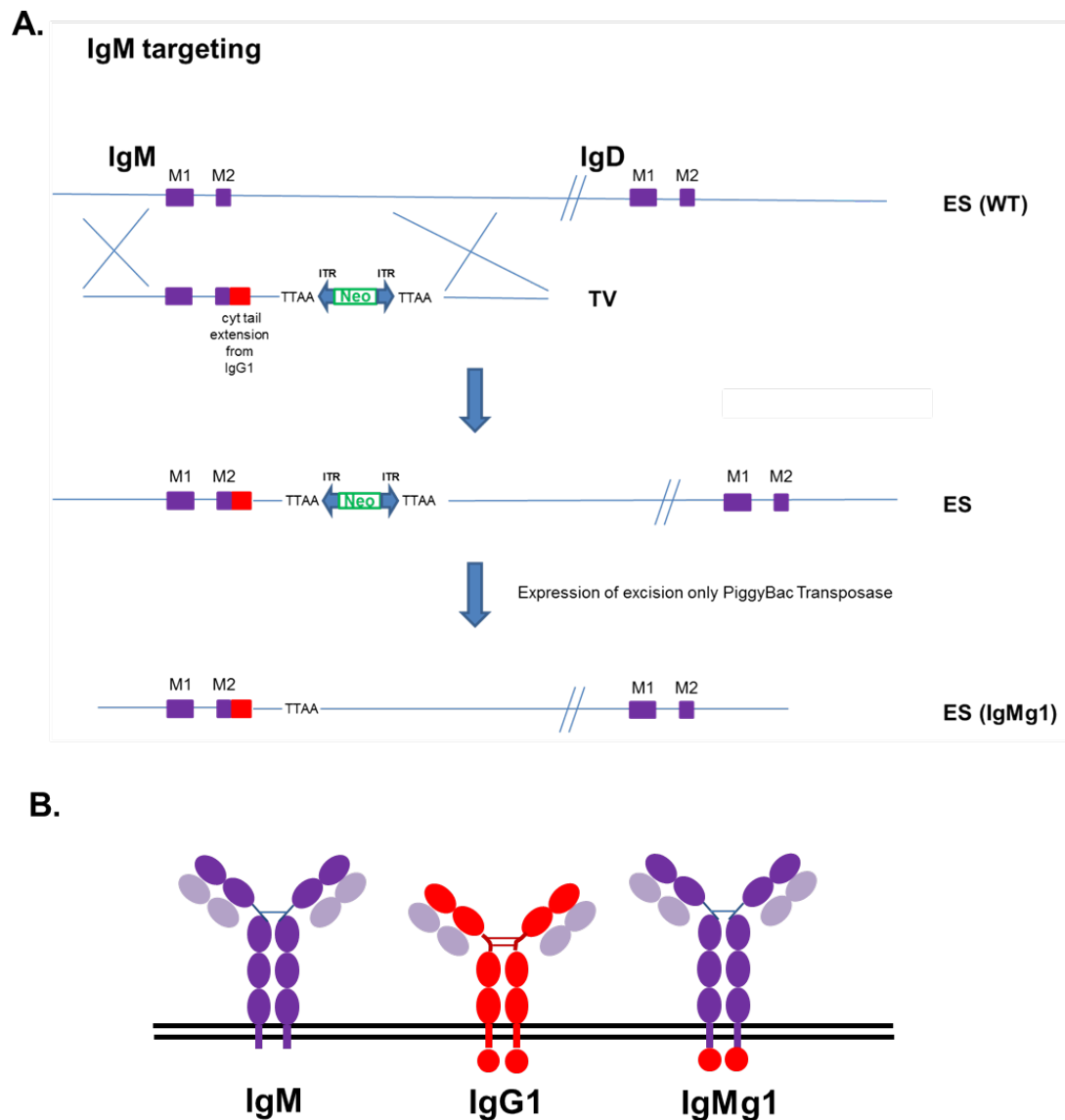
Figure 3.1: Schematic representation of Hc locus of both wild type and IgMg1 mice.

A. Detailed schematic process of IgM targeting. Genome sequence containing Hμ introns, two exons M1 and M2 (purple) with 75 bp cytoplasmic tail extension of IgG1 cDNA (red) was inserted into the genome of C57BL/6N ES cells through homologous recombination. Neomycin (Neo) was used for selection of the positively recombined clones. The selection cassette, inverted terminal repeats (ITR) flanked neomycin gene, was then deleted by Piggybac transposase-mediated deletion.

B. Schematic representation of the structure of wildtype IgM, IgG1 and chimeric BCR IgMg1
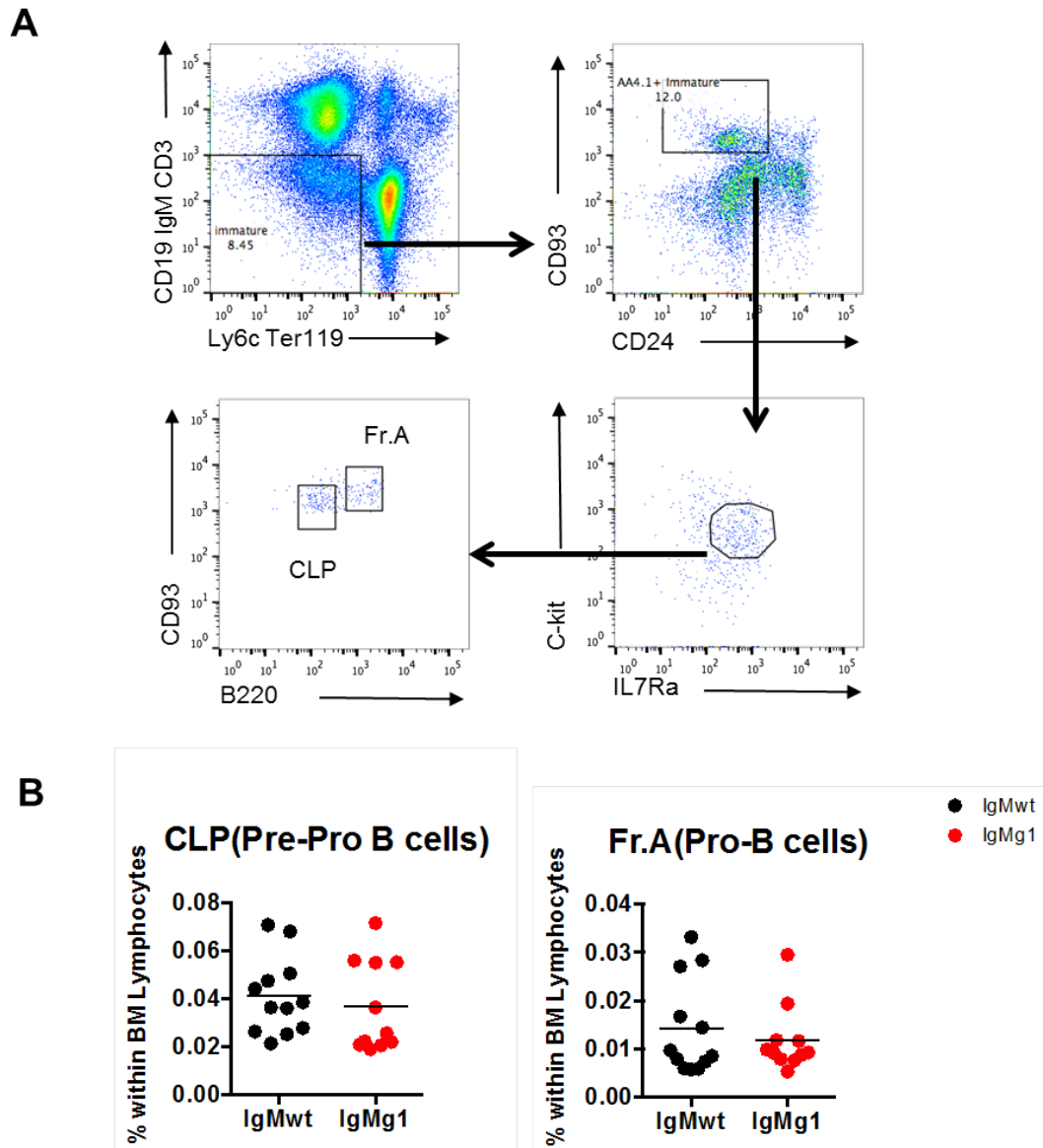
Figure 3.2: Bone marrow precursor cells development is normal in IgMg1 mice.

  A. Gate settings for both CLPs and Fr.A cells in bone marrow. CLPs and Fr.A all
      derive from the precursor CD19$^-$IgM$^-$CD3$^-$Ly6c$^-$Ter119$^-$ (top left)
      CD93$^+$CD24$^-$ (top right) C-kit$^+$IL7-Ra$^+$ (bottom right) population. CLPs are
      the B220$^-$, while Fr.A are the B220$^+$ cells (bottom left).
  B. The percentages of CLPs and pro-B cells within bone marrow lymphocytes
      and compared between IgMwt and IgMg1 mice.
ns, not significant; unpaired Student's t test. Bars indicate mean. Each symbol
represent sample from one mouse. Data are from three independent experiments.
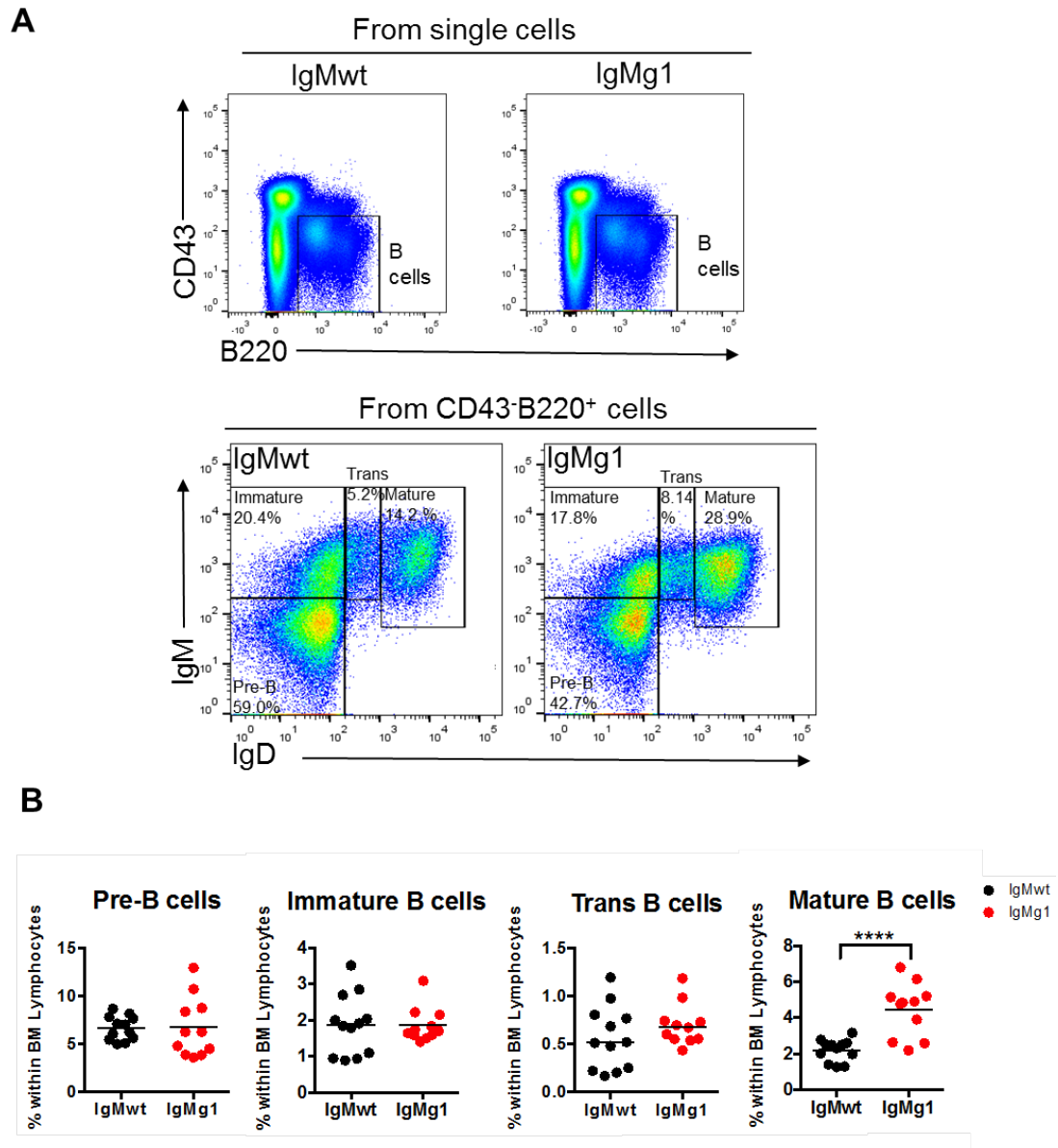
Figure 3.3: Pre-B and immature B cell development is normal in IgMg1 mice.

A. Gates to identify pre-B cells, immature B cells, transitional B cells and mature B cells in bone marrow. The four populations are all gated from CD43⁻B220⁺ cells (top), pre-B cells are IgM^-IgD^- cells, immature B cells are IgM^+IgD^- cells, transitional B cells are IgM^+IgD^{low} and mature B cells are IgM^+IgD^+ cells (bottom).

B. Percentages of pre-B, immature, transitional and mature B cells within bone marrow lymphocytes and compared between IgMwt and IgMg1 mice.

**** $p < 0.0001$; unpaired Student's t test. Bars indicate mean. Each symbol represent sample from one mouse. Data are from three independent experiments.

3.2.2 Peripheral B cell development is severely affected in IgMg1 mice

Immature B cells emigrate from the BM and become transitional B cells immediately when they enter the periphery. Transitional B cells mature in B cell follicles of the spleen to become MZ B cells or Fo B cells (Pillai, Cariappa et al. 2005, Pillai and Cariappa 2009). In order to test B cell development in peripheral lymphoid organs, B lymphocyte developmental stages were further assessed in the spleens of IgMg1 and IgMwt mice.

The spleens of IgMg1 mice were bigger than those of IgMwt mice, containing more splenocytes (Fig. 3.4B). Within splenocytes, the overall percentage of B cells in IgMg1 mice were slightly increased, whilst the absolute numbers almost doubled (Fig. 3.4C).

Transitional and mature B cell populations were further gated and analysed. Transitional B cells were gated as $CD19^+B220^+IgM^+CD93^+$ cells (Fig 3.5A). Within this population, T1 cells were gated as the $CD21^-CD23^-$ subset, and T2+T3 cells as $CD21^+CD23^+$ (Fig. 3.5A). Mature Fo and MZ B cells were gated from $CD19^+B220^+IgM^+CD93^-$ mature B cells (Fig. 3.5A). Fo B cells were $CD21^{int}CD23^{int}$ subset, while MZ B cells were $CD21^{high}CD23^{low/-}$ subset (Fig. 3.6A). Despite having more B cells, the percentages of transitional B cells, particularly T1 B cells were significantly lower in IgMg1 mice (Fig. 3.5B). The absolute numbers of transitional B cell populations, however, were comparable with their IgMwt counterparts (Fig.

3.5C). The increase in total B cell numbers in IgMg1 mice was due to the increased numbers of Fo B cells (Fig. 3.6B), which is the dominant mature B cell population in the periphery. On the contrary, the percentages of MZ B cells were significantly reduced in IgMg1 mice, despite their absolute numbers remained similar to those in IgMwt mice (Fig. 3.6C).

We further analysed B1 cell populations in both IgMwt and IgMg1splenocytes. B1 cells have been defined as $CD19^+IgM^+B220^+CD93^-CD21^-CD23^-IgD^{low}CD43^+$ (Fig. 3.7A). There was no significant change in splenic B1 cell numbers (Fig. 3.7B).

Overall, the expression of IgMg1 does not significantly affect B cell development in BM, however, it has a significant impact on peripheral B cell development with a strong increase in follicular B cell numbers, and reduced percentages, but no change in absolute numbers of transitional and other mature B cell populations. This phenomenon is possibly due to higher turn-over rate or longer life span of follicular B cells in IgMg1 mice.
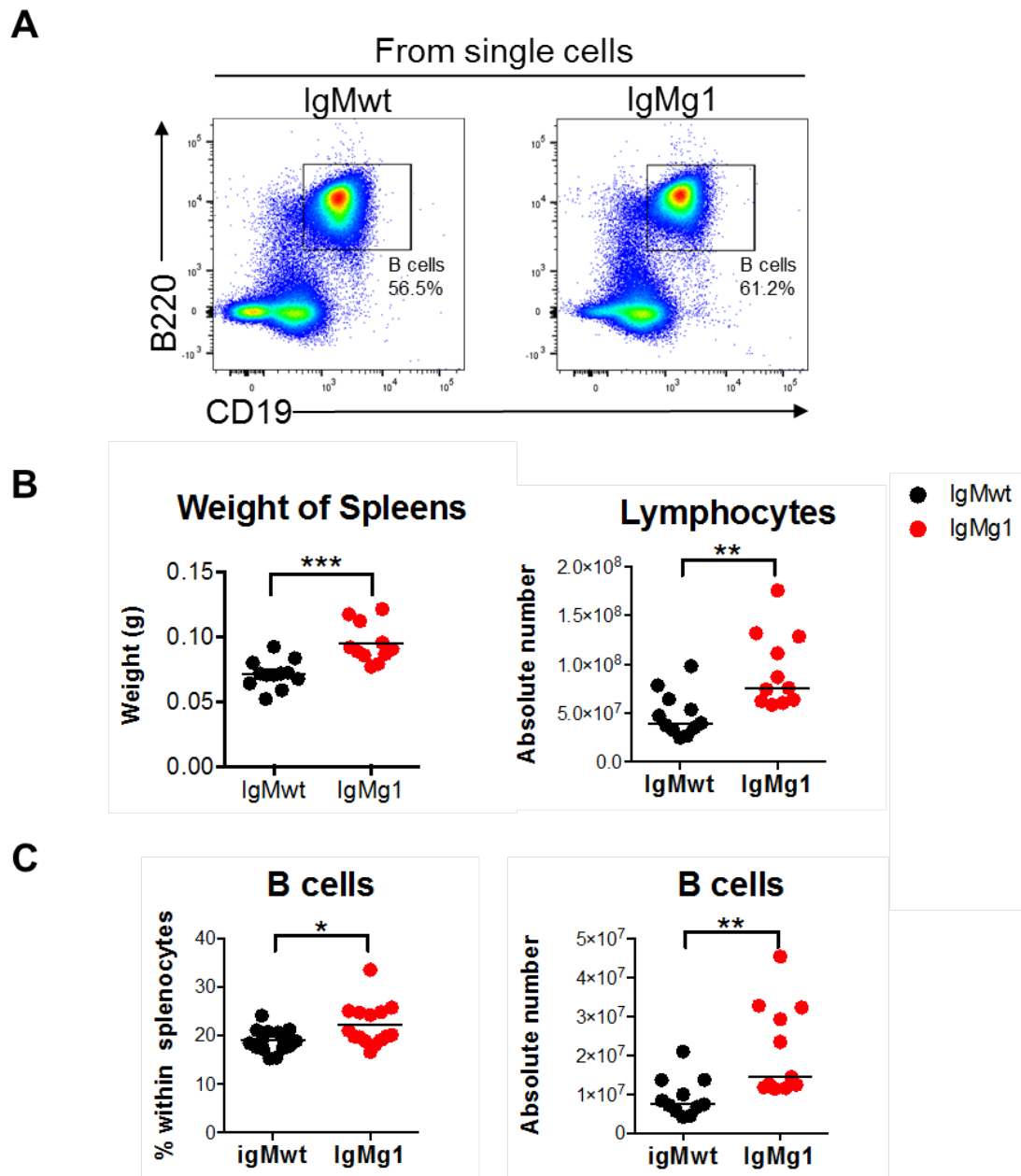
Figure 3.4: IgMg1 mice have bigger spleens with higher number of splenocytes and B cells.

A. Gate settings for CD19$^+$B220$^+$ B cells in IgMwt and IgMg1 spleens.
B. Weights of spleens and absolute numbers of splenocytes.
C. Percentages of B cells within spleen lymphocytes and their absolute numbers.
* $p < 0.05$; ** $p < 0.01$; *** $p < 0.001$; unpaired Student's t test. Bars indicate mean. Each symbol represent sample from one mouse. Data are from three independent experiments.
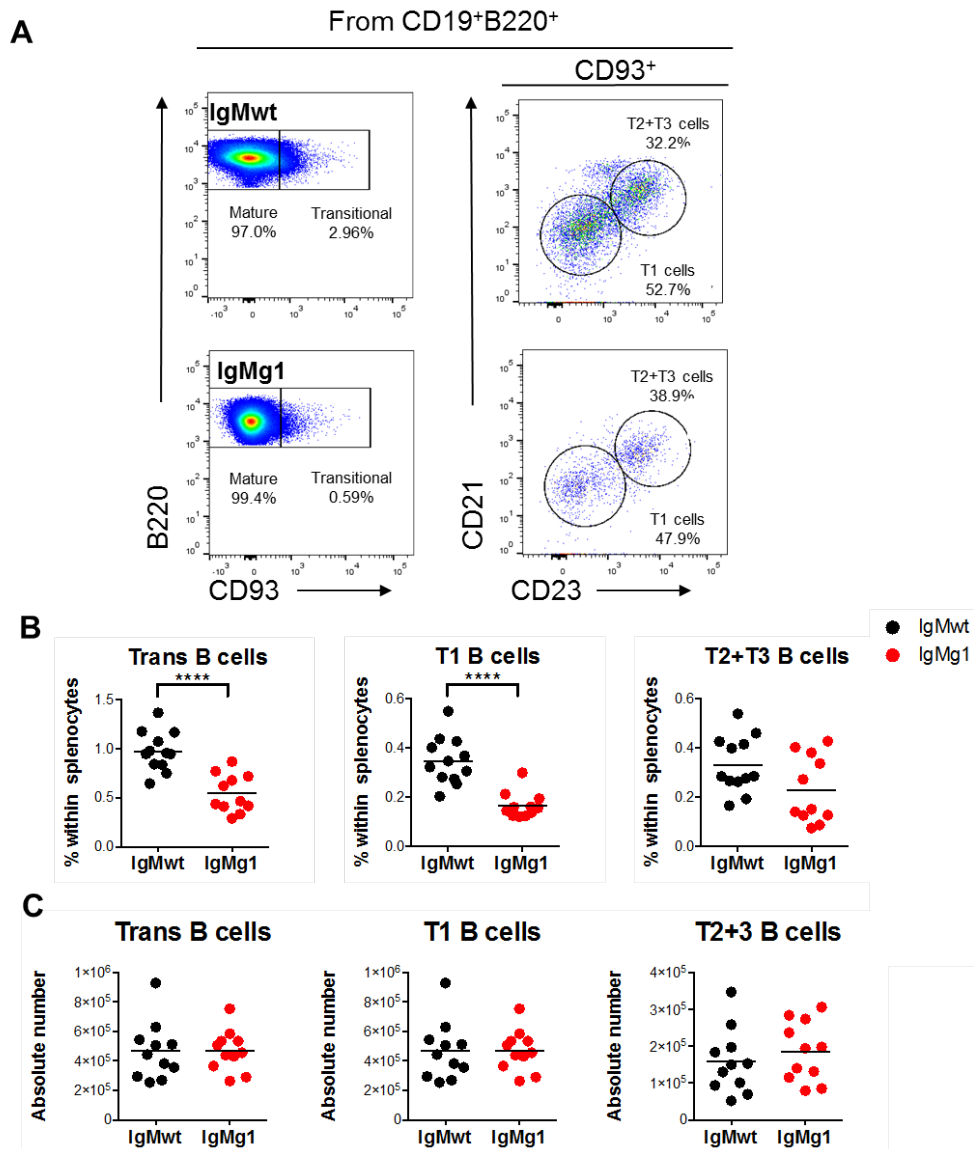
Figure 3.5: The percentages of transitional and T1 B cells are significantly reduced in IgMg1 mice.

A. Gate settings for transitional, T1, T2+3 cells in spleen. Transitional B cells are gated as $CD19^+B220^+CD93^+$ cells. T1 subset is $CD21^-CD23^-$ within the transitional population, while T2+T3 are $CD21^+CD23^+$ ones.
B. Percentages of transitional, T1 and T2+T3 B cells within spleen B cells.
C. Absolute numbers of transitional, T1 and T2+T3 B cells compared between IgMwt and IgMg1 mice.

$*$ $p < 0.05$; $****$ $p < 0.0001$; unpaired Student's t test. Bars indicate mean. Each symbol represents sample from one mouse. Data are from three independent experiments.
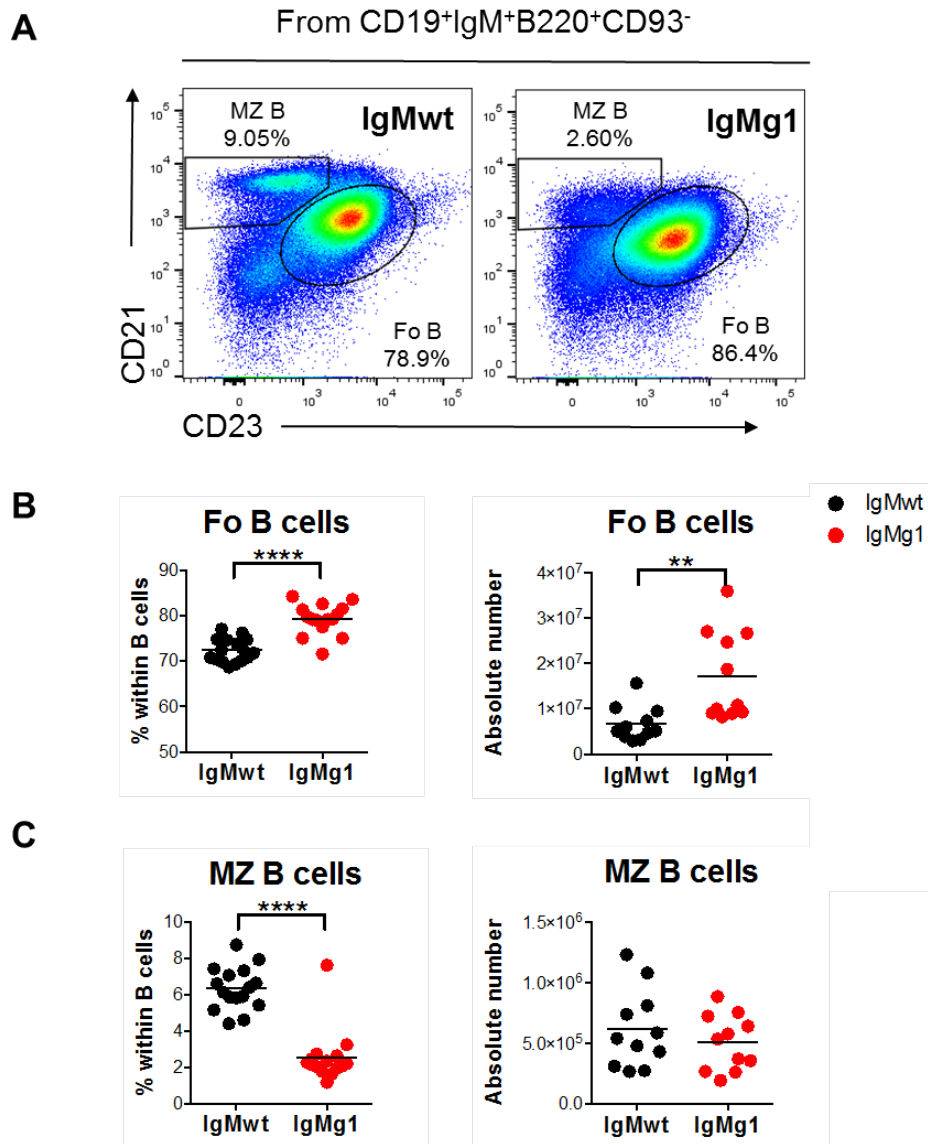
Figure 3.6: Peripheral follicular B cells and MZ B cell development is affected in IgMg1 mice.

A. Gate settings for Fo B cells and MZ B cells in spleen. These two populations are gated from CD19$^+$IgM$^+$B220$^+$CD93$^-$ mature B cells. Fo B cells are gated as CD21^{int}CD23^{int} cells. MZ B cells are gated as CD21^{high}CD23$^{low/-}$ cells.
B. Percentages and absolute numbers of Fo B cells.
C. Percentages and absolute numbers of MZ B cells.

** $p < 0.01$; **** $p < 0.0001$; unpaired Student's t test. Bars indicate mean. Each symbol represents sample from one mouse. Data are from three independent experiments.
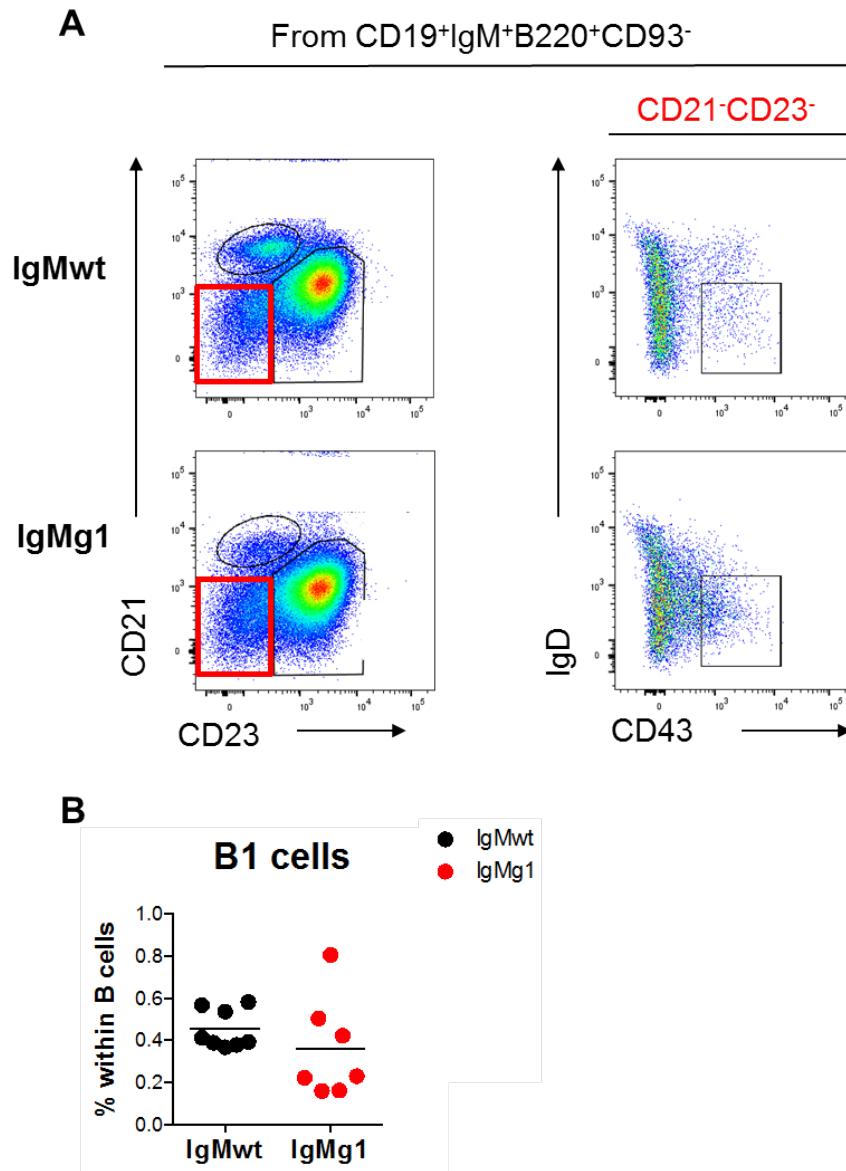
Figure 3.7: Spleen B1 cells are comparable between IgMwt and IgMg1 mice.

A. Gate scheme for B1 cells in spleen. These cells are gated from mature spleen B cells and they are CD21$^-$CD23$^-$IgD^{low}CD43$^+$ cells.

B. Percentages of B1 cells within spleen B cells and compared between IgMwt and IgMg1 mice.

ns, not significant; unpaired Student's t test. Bars indicate mean. Each symbol represents sample from one mouse. Data are from two independent experiments**.**

3.2.3 Slightly affected BM and significantly affected splenic B cell development in IgMg1 B cells

To better understand the inconsistent results of percentages and absolute numbers of B cell populations observed in homozygous mice, IgMg1/IgMwt heterozygous mice were constructed. This would enable to directly compare the development of IgMwt expressing B cells and IgMg1 expressing B cells competing in the same physiological environment. IgMg1 or C57BL/6 WT mice, which are Ig heavy chain allotype b (IgH^b), were crossed with BALB/c mice, which are Ig heavy chain allotype a (IgH^a), to generate IgH^a/IgH^b F1 mice. These IgH^a/IgH^b F1 mice are heterozygous for IgH; one allele being IgH^a and the other allele IgH^b (Fig. 3.8). Due to allelic exclusion, B cells in these mice can express only one IgH allele. In the absence of selection pressure this should lead to 50% IgH^a and 50% IgH^b B cells. B cell development and competition between IgH^a (IgMwt) and IgH^b (IgMwt or IgMg1) expressing B cells was assessed by testing the percentages of each population in these F1 mice. The percentages of B cell precursor B cell subsets CLPs and pro-B cells were similar in both groups (Fig. 3.9 A and B). Overall percentages of immature B cells were the same in IgMwt/IgMwt and IgMwt/IgMg1 IgH^a/IgH^b heterozygous mice (Fig. 3.9 C). However, immature IgH^b IgMg1 B cells developed at slightly smaller percentages than IgH^a IgMwt B cells (Fig. 3.10A). This was due to the IgH$^{a/b}$ allotypic differences or the different VDJ repertoires, but not the expression of the IgMg1 cytoplasmic chain, as we observed the same trend in numbers of immature B cells in IgM^{a}wt/IgM^{b}wt heterozygous mice (Fig. 3.10A). The number of IgH^b IgMg1 immature B cells in IgMg1/IgMwt heterozygous was slightly higher than IgH^b IgMwt

immature B cells when related to IgH^a IgMwt immature B cells (Fig. 3.10B). Overall mature B cell percentages were slightly increased in bone marrow of IgM^{a}wt/IgM^{b}g1 heterozygous mice (Fig. 3.9D). This may be explained by slight advantages of IgH^b IgMg1 B cells compared to both IgH^a and IgH^b IgMwt B cells, although this was not significant (Fig. 3.10C and D).

Taken together this confirms that IgMg1 does not endow B cells with a major advantage during B cell development in the bone marrow.

Further B cell development in the spleen was assessed in IgH^a IgMwt/IgH^b IgMwt and IgH^a IgMwt/IgH^b IgMg1 heterozygous mice. The overall percentages of transitional and T1 B cells tended to be lower in IgH^a IgMwt/IgH^b IgMg1 heterozygous mice (Fig. 3.11A and 3.11B left). IgH^b IgMg1 B cells displayed a significant survival disadvantage compared to both IgH^b and IgH^a IgMwt B cells during T1 stage (Fig. 3.12B). On the contrary, there were higher ratios of T2+3 B cells derived from IgH^b IgMg1 B cells (Fig. 3.12C). Overall percentages of mature Fo B cell were slightly higher while MZ B cells were slightly lower in IgH^a IgMwt/IgH^b IgMg1 heterozygous (Fig. 3.13A). Within those, IgH^b IgMg1 B cells displayed a major advantage in differentiating into Fo B cells (Fig. 3.13B) and an impaired MZ B cell fate commitment (Fig. 3.13C).

In summary this showed that IgH^b IgMg1 B cells display a significant survival disadvantage when competing with IgMwt B cells during T1 stage. This is in line

with the significantly reduced percentages of T1 cells in homozygous IgMg1 mice (Fig. 3.5). The higher ratio of IgH^b IgMg1 Fo B cells and lower ratio of IgH^b IgMg1 MZ B cells (Fig. 3.13B and C right) were also consistent with previous observations on their percentages in homozygous IgMg1 mice (Fig. 3.6). This suggests the percentages of B cell populations observed in homozygous IgMg1 mice reflect the impact of IgMg1 BCR signalling on peripheral B cell fate commitment rather than their absolute numbers.
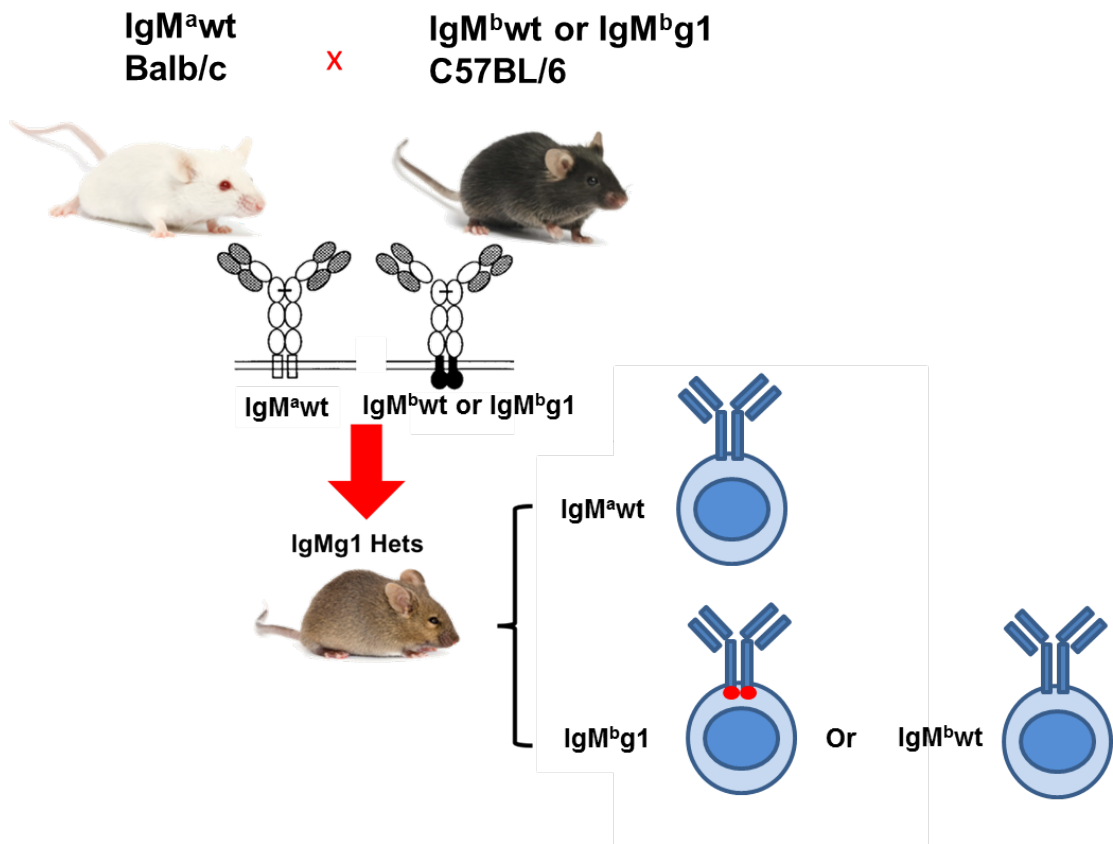
Figure 3.8: The construction of Ha/Hb heterozygous

Schematic representation of the generation of IgH^{a+} Balb/c and IgH^{b+} IgMg1 or IgMwt C57B/L6 heterozygous F1 mice. Due to allelic exclusion, B cells of F1 heterozygous mice will express either allele, and B cells are either IgM^{a+} or IgM^{b+}. This enables us to directly distinguish and compare two subsets of B cells developing alongside each other in F1 heterozygous mice.
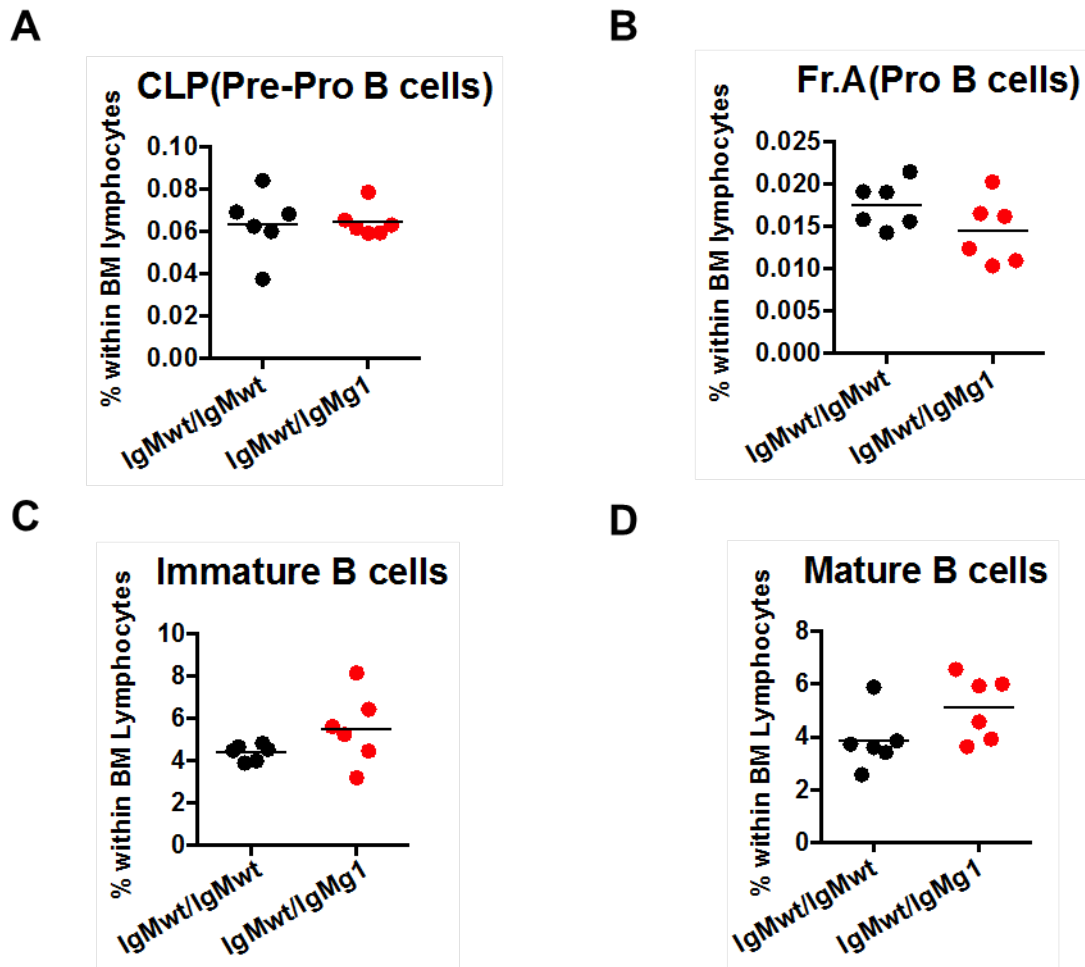
Figure 3.9: The percentages of B cell subsets within BM are comparable between IgMwt and IgMg1 heterozygous.

Gate setting of CLPs, Fr.A, immature B cells and mature B cells are the same as the ones displayed in Fig. 3.2 and Fig. 3.3
- A. Percentages of overall CLPs within bone marrow lymphocytes compared between IgM^awt/IgM^bwt and IgM^awt/IgM^bg1 heterozygous mice.
- B. Percentages of overall Fr.A (pro-B cells) within bone marrow lymphocytes
- C. Percentages of overall immature B cells within bone marrow lymphocytes.
- D. Percentages of overall mature B cells within bone marrow lymphocytes.

ns, not significant; unpaired Student's t test, Bars indicate mean. Each symbol represents sample from one mouse. Data is representative from two independent experiments.
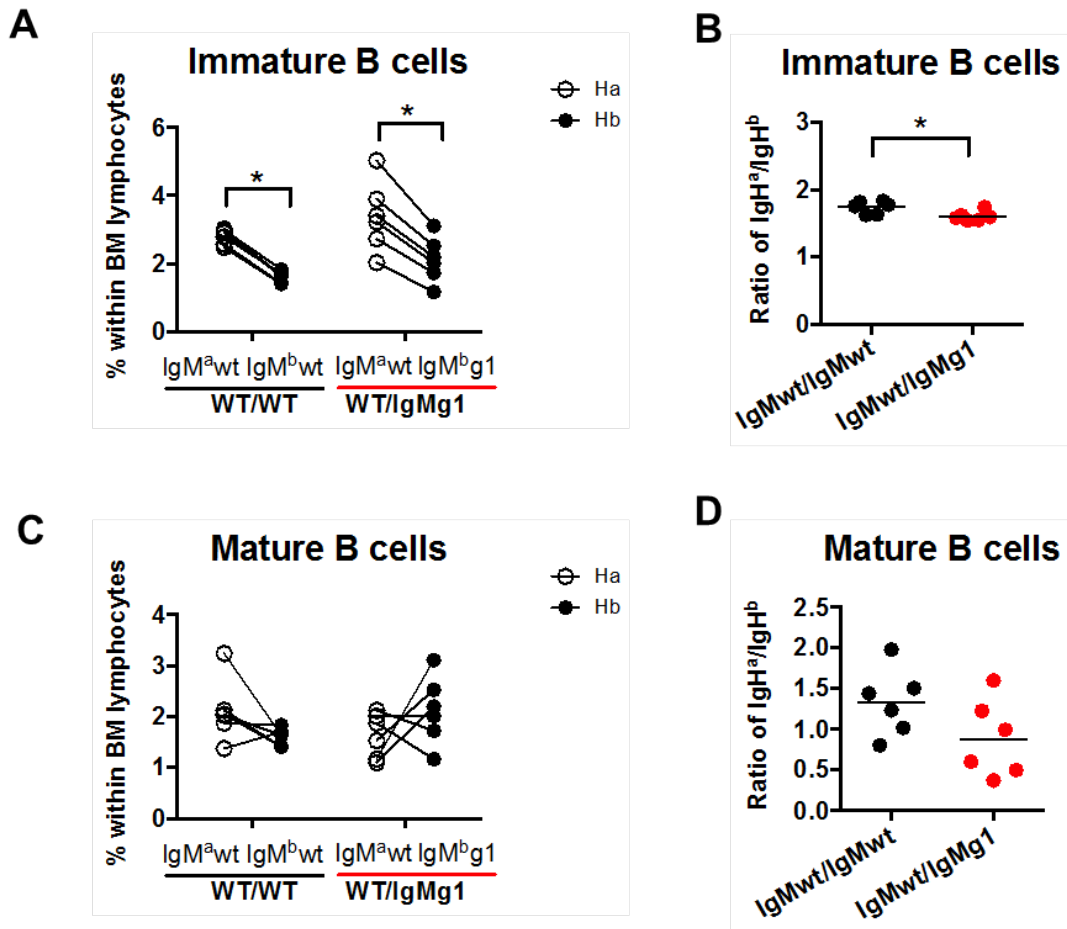
Figure 3.10: Bone marrow IgMg1 B cell development is normal in the presence of competition.

Gates for immature and mature B cells are the same as showed in Fig. 3.3.

A. Percentages of H^{a+} and H^{b+} immature BM B cells. Lines connect percentages of IgH^{a+} and IgH^{b+} cells from within the same heterozygous mouse.

B. Ratios of IgH^{a+} to IgH^{b+} immature B cell subsets within $IgM^{a}wt/IgM^{b}wt$ and $IgM^{a}wt/IgM^{b}g1$ heterozygous mice.

C. Percentages of H^{a+} and H^{b+} mature BM B cells. Lines connect percentages of IgH^{a+} and IgH^{b+} cells from within the same heterozygous mouse.

D. Ratios of IgH^{a+} to IgH^{b+} mature B cell subsets within $IgM^{a}wt/IgM^{b}wt$ and $IgM^{a}wt/IgM^{b}g1$ heterozygous mice.

$*$ $p < 0.05$; unpaired Student's t test in B, D. 2-Way ANOVA in A, C. Bras indicate mean. Each symbol represents sample from one mouse. Data are representative from two independent experiments.
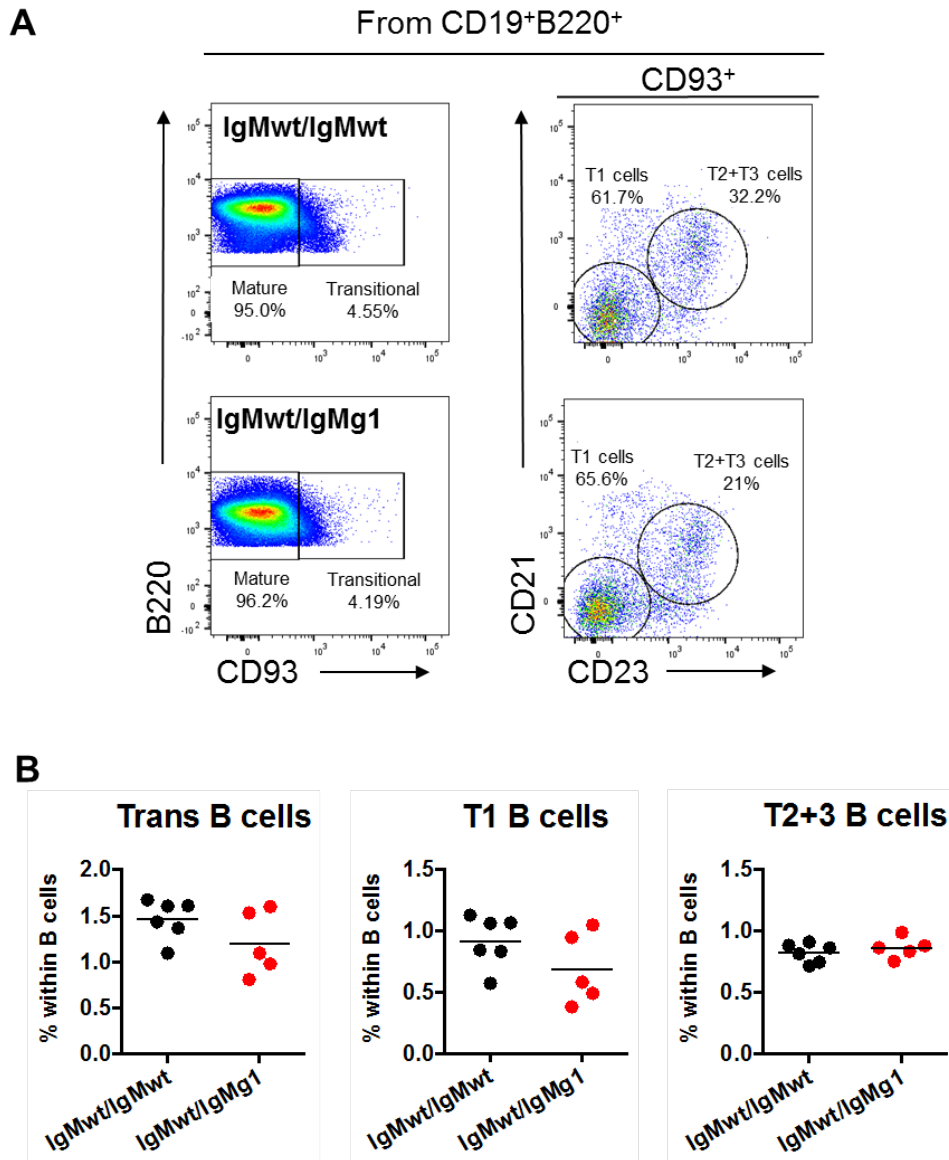
Figure 3.11: The percentages of transitional and T1 B cells are slightly reduced in IgMawt/IgMbg1 heterozygous mice.

A. Gate settings for transitional, T1, T2+3 cells in spleen. Transitional B cells are gated as CD19$^+$B220$^+$CD93$^+$ cells. T1 are CD21$^-$CD23$^-$ subsets within the transitional population, while T2+3 are CD21$^+$CD23$^+$ ones.
B. The percentages of overall transitional, T1 and T2+3 B cells within spleen B cells.

ns, not significant; unpaired Student's t test. Bars indicate mean. Each symbol represents sample from one mouse. Data are representative from two independent experiments.

A From CD19+B220+CD93+ Trans B cells

T1

T2+3

IgMwt/IgMwt

IgMb 41.2%
IgMa 50.3%

IgMb 38.2%
IgMa 38.9%

IgMwt/IgMg1

IgMb 25.7%
IgMa 68.3%

IgMa 44.9%
IgMa 39.5%

B T1 B cells
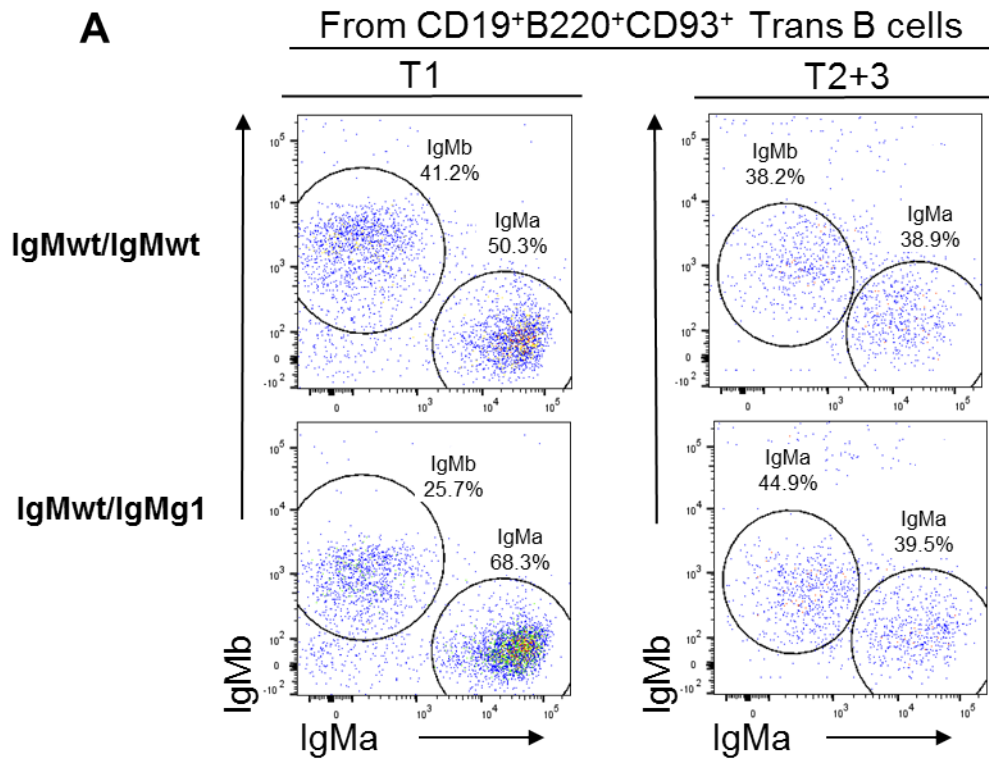
C T2+3 B cells

Figure 3.12: IgMg1 B cells are less efficient in generating T1 B cells.

A. Gates for IgM^b WT or IgMg1 B cells, and IgM^a WT B cells within both T1 and T2+3 B cells.
B. Percentages of H^{a+} and H^{b+} T1 B cells. Lines connect percentages of IgH^{a+} and IgH^{b+} cells from the same heterozygous. Ratios of IgH^{a+} to IgH^{b+} T1 B cell subsets within each heterozygous.
C. Percentages of H^{a+} and H^{b+} T2+3 B cells. Lines connect percentages of IgH^{a+} and IgH^{b+} cells from the same heterozygous. Ratios of IgH^{a+} to IgH^{b+} T2+3 B cell subsets within each heterozygous.

* $p < 0.05$; ** $p < 0.01$; **** $p < 0.0001$; unpaired Student's t test in B, C right; 2-Way ANOVA in B, C left. Horizontal bars indicate mean. Each symbol represents sample from one mouse. Data are representative from two independent experiments.
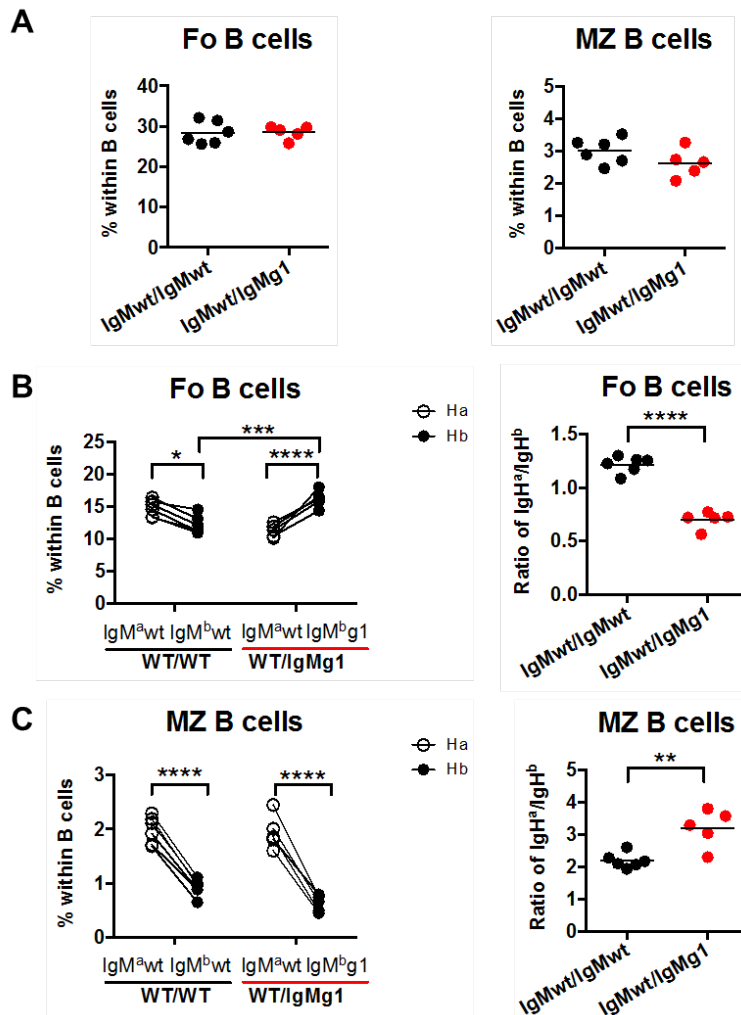
Figure 3.13: IgMg1 B cells are more efficient than IgMwt B cells in generating Fo B cells, while less competitive in generating MZ B cells.

Gates for Fo and MZ B cells are the same as in Fig. 3.6, sub-populations are the same as Fig.3.12

  A. The percentages of total Fo and MZ B cells within spleen B cells.
  B. Percentages of H^{a+} and H^{b+} Fo B cells. Lines connect percentages of IgH^{a+} and IgH^{b+} cells from the same heterozygous mouse. Ratios of IgH^{a+} to IgH^{b+} Fo B cell subsets within each heterozygous mouse.
  C. Percentages of H^{a+} and H^{b+} MZ B cells. Lines connect percentages of IgH^{a+} and IgH^{b+} cells from the same heterozygous mouse. Ratios of IgH^{a+} to IgH^{b+} MZ B cell subsets within each heterozygous mouse.

$*$ $p < 0.05$; $**$ $p < 0.01$; $***$ $p < 0.001$; $****$ $p < 0.0001$; unpaired Student's t test in A, B, C right; 2-Way ANOVA in B, C left. Horizontal bars indicate mean. Each symbol represents sample from one mouse. Data are representative from two independent experiments.

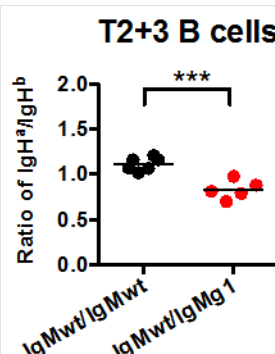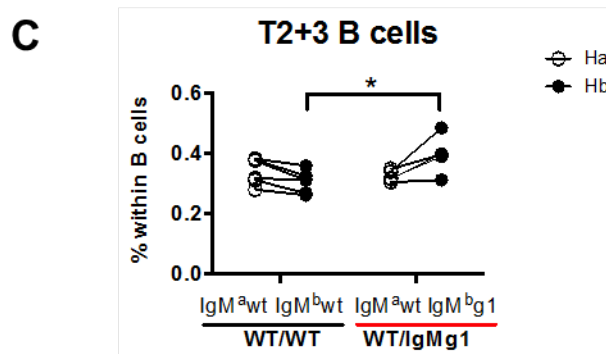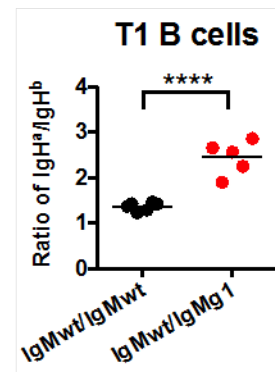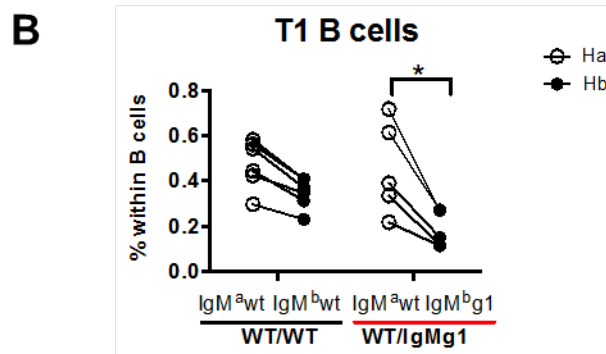BM chimeras were also constructed and B cell development in these bone marrow chimeric mice was also assessed to detect CD45.2$^+$ IgMg1 B cell development with the presence of CD45.1$^+$ IgMwt counterparts. To construct BM chimeras, lethally irradiated C57BL/6 mice were reconstituted with equal numbers of CD45.2$^+$ (IgMg1 or C57BL/6 IgMwt) and CD45.1$^+$ (C57BL/6-Ly5.1) bone marrow cells and were allowed to settle for 7-8 weeks (Fig. 3.14).

This showed CD45.2$^+$ BM cells had a developmental advantage over CD45.1$^+$ BM cells after reconstitution. In BM mature B cells, CD45.2$^+$ B cells accounted for around 75% of this population in IgMwt/IgMwt chimeras, with a ratio of CD45.2$^+$ B cells to CD45.1$^+$ B cells of around 3, while in IgMg1/IgMwt chimeras the ratio reached around 6 (Fig. 3.15B). This developmental advantage of CD45.2 BM cells was more obvious in early stages, such as in pre-B cells and immature B cells, where the ratios were larger than 10 in IgMwt/ IgMwt mice. However, CD45.2$^+$ IgMg1 precursor cells appear to be less competitive than IgMwt, as the ratio tended to be lower in IgMg1 chimeras (Fig. 3.15B).

In spleens, the ratio of CD45.2$^+$ to CD45.1$^+$ total B cells in IgMg1 BM chimeras remained higher at around 5 than in IgMwt BM chimeric mice, which was around 3.5 (Fig. 3.16A left). However, IgMg1 B cells do not show any advantage at T1 B cell stage, where the ratio of IgMg1 to IgMwt B cells tends to be lower than in WT chimeras (Fig. 3.16A middle), which is consistent with B cell blockage during T1

stage observed in homozygous IgMg1 mice (Fig. 3.8). The ratios of CD45.2$^+$ B cells to CD45.1$^+$ B cells reversed in T2+3 cells, to be as low as 0.3 in both WT and IgMg1 chimeras (Fig. 3.16A right). The ratio increased to be even higher in IgMg1 Fo B cells, which was around 8 and almost double that of WT chimeras (Fig. 3.16C top left), confirming IgMg1 B cells prefer follicular B cell fate (Fig. 3.9). On the contrary, there were at least 4-fold fewer marginal zone B cells in IgMg1 mice compared with their wildtype counterparts (Fig. 3.16B and C).

In summary, B cell development in bone marrow chimeras were quite consistent with the observations in homozygous mice (Fig. 3.7, 3.8 and 3.9) and IgH^a/IgH^b heterozygous mice. The ratio (CD45.2$^+$ to CD45.1$^+$) of peripheral mature B cells was around 5 in IgMg1 chimeras, and 3.5 in WT chimeras (Fig. 3.16A left).
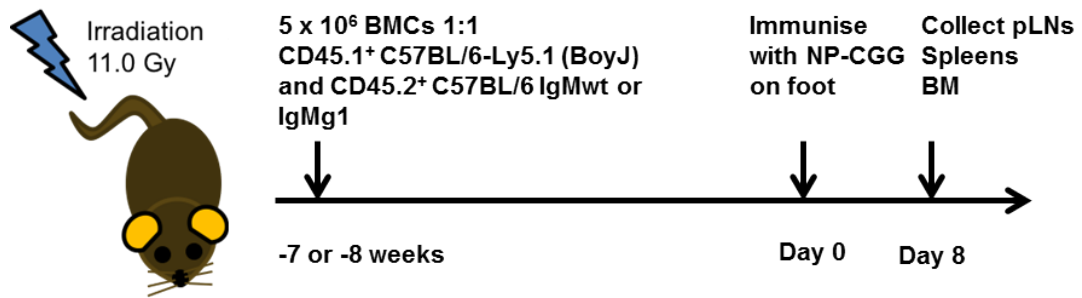
Figure 3.14: The construction of bone marrow chimeras.

Wildtype C57BL/6N of at least 20 g were fed on Baytril in water for one week before irradiation. Mice received 5.5 Gy irradiation in the morning and another 5.5 Gy irradiation in the afternoon. Right after the second irradiation, mice were adoptively transferred with a total amount of 5×10^6 bone marrow cells through i.v. injection. CD45.1$^+$ C57BL/6-Ly5.1 (BoyJ) and CD45.2$^+$ C57BL/6N (or IgMg1) were mixed at a ratio of 1:1. Mice were left to reconstitute for 7-8 weeks before immunisation.
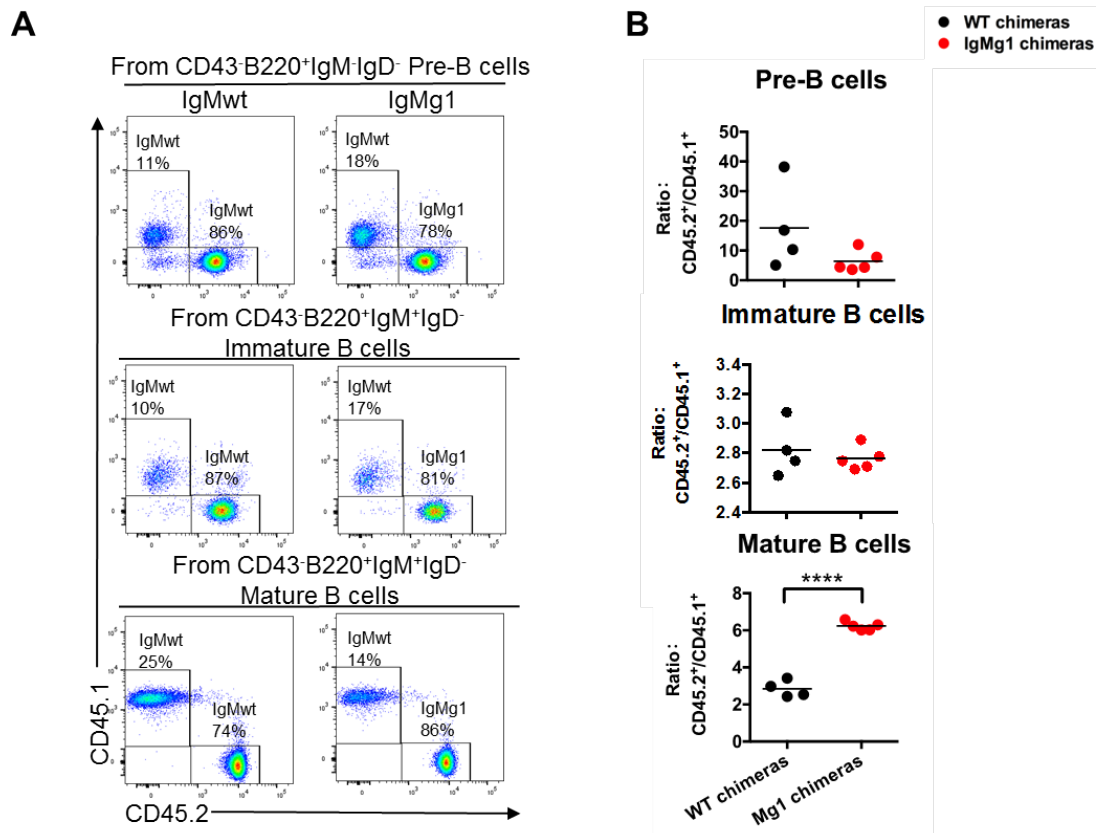
Figure 3.15: Increased IgMg1 mature B cell populations during BM stage.

The construction of bone marrow chimeras was described in Fig. 3.14. Gate settings for pre-B, immature and mature B cell populations in BM are the same in Fig. 3.3.
   A. Gate settings for CD45.1$^+$ and CD45.2$^+$ B cell subsets in BM pre-B cells, immature B cells and mature B cells from both IgMwt and IgMg1 mice.
   B. Ratios of CD45.2$^+$/CD45.1$^+$ are calculated and compared between groups. Ratios of CD45.2$^+$/CD45.1$^+$ is defined as percentages of CD45.2$^+$ subsets divide the percentages of CD45.1$^+$ subsets

**** $p < 0.0001$; unpaired Student's t test. Bars indicate mean. Each symbol represents sample from one mouse. Data are representative from two independent experiments.
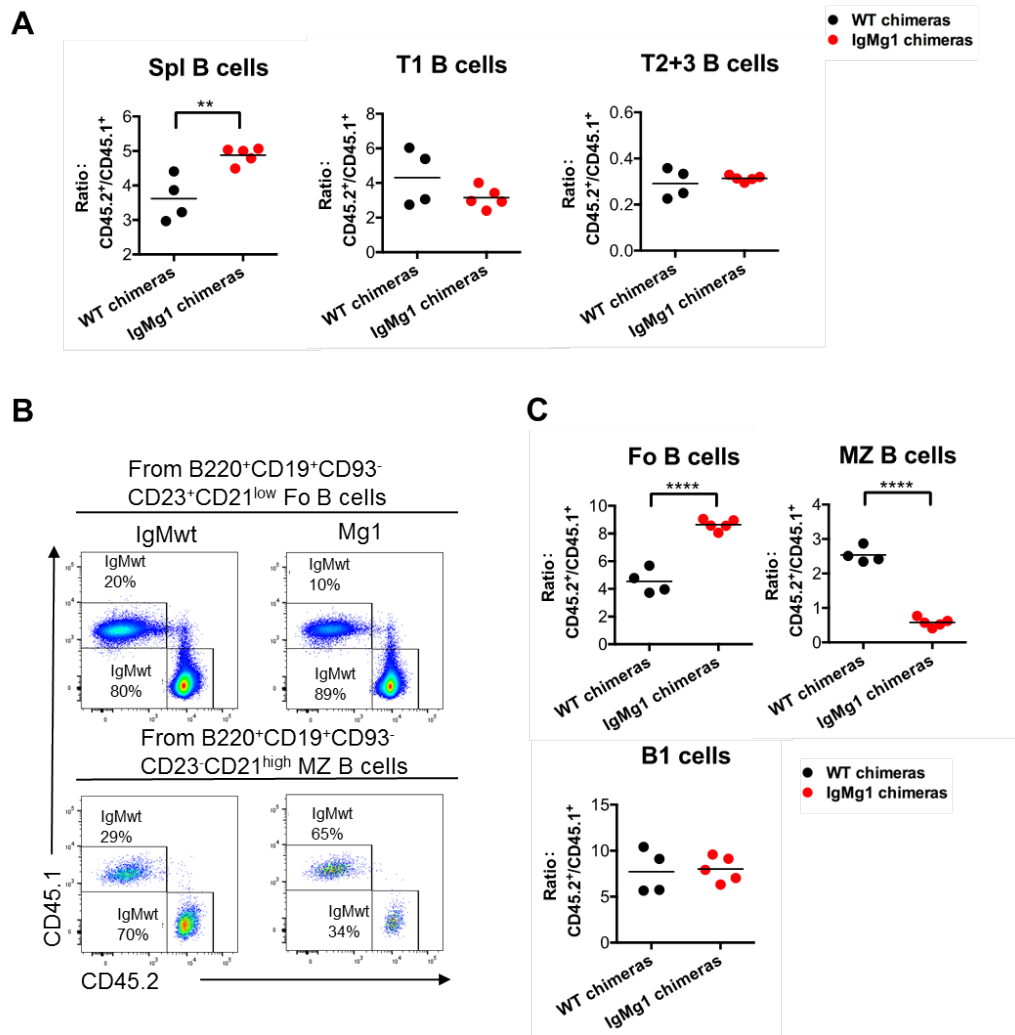
Figure 3.16: Increased differentiation of Fo B cells and decreased MZ B cells differentiation during peripheral development for IgMg1 B cells.

The construction of bone marrow chimeras was described in Fig. 3.14. Gate settings for spleen B, T1, T2+3, Fo, MZ, and B1 cells are the same in Fig. 3.4-3.7.

A. Ratios of $CD45.2^+/CD45.1^+$ are calculated and compared between groups. Spleen mature B cells and transitional B cell populations have been analysed and displayed.

B. Gate settings for $CD45.1^+$ and $CD45.2^+$ B cell subsets in spleen follicular and MZ B cells from both IgMwt and IgMg1 mice.

C. Ratios of $CD45.2^+/CD45.1^+$ are calculated and compared between groups. Ratio of $CD45.2^+/CD45.1^+$ is defined as percentages of $CD45.2^+$ subsets divide the percentages of $CD45.1^+$ subsets

**p < 0.01; ****p < 0.0001; unpaired Student's t test. Bars indicate mean. Each symbol represents sample from one mouse. Data are representative from two independent experiments.

**3.2.4 Increased Igλ light chain usage during B cell development**

The significant reduction in the percentage of T1 B cells in spleens of IgMg1 mice (Fig. 3.5 and 3.11) suggests that IgMg1 B cells experienced enhanced negative selection during B cell development. Immature stage in bone marrow and T1 stage in spleen are the two major self-reactive selection checkpoints during B cell development (Pelanda and Torres 2012). Negative selection at the immature stage may induce B cell apoptosis, or alternatively, B cells can undergo secondary light-chain rearrangements (Gay, Saunders et al. 1993, Tiegs, Russell et al. 1993, Prak and Weigert 1995). The first light chain rearrangement during B cell development happens in the Igκ light chain locus. This, in mice, leads to preferential expression of Igκ light chains, with 90% of mature B cells expressing Igκ containing BCR. The Igλ light chain locus is normally silenced and lambda light chain rearrangement is only activated if kappa light chain rearrangement completely fails (Prak, Trounstine et al. 1994, Prak and Weigert 1995). Thus, expression of Igλ light chain can serve as an indicator of negative selection B cells experienced during immature stage. We therefore measured the frequency and ratio of Igλ to Igκ light chain expressing B cells in BM immature, transitional B cells and all mature B cell populations. During immature stage the Igλ/Igκ ratio was varied between experiments (Fig. 3.17B left, solid and circle), however tended to be higher in the IgMg1 mice in each experiment (Fig. 3.17B left). This ratio increased to be significantly higher in IgMg1 BM transitional B cells (Fig. 3.17B right) and in all mature B cell populations of IgMg1 mice (Fig. 3.17C). These results indicate that during immature stage of B cell

development the expression of IgMg1 makes B cells more prone to be negatively selected.

The ratio of Igλ to Igκ was then assessed in BM chimeras, which was described in Fig. 3.14. In IgMwt/IgMwt chimeras, both CD45.1$^+$ and CD45.2$^+$ B cells displayed similar lambda chain usage (Fig. 3.18C). In IgMwt/IgMg1 chimeras, however, there were significantly higher percentages of Igλ$^+$ B cells in CD45.2$^+$ IgMg1 B cells and this started from immature stage (Fig. 3.18C). Consistent with the observation in homozygous IgMg1 mice, the ratios of Igλ$^+$ mature B cells in both BM and spleens in IgMg1 chimeric mice were significantly higher (Fig. 3.19B and D). This confirms enhanced λ chain usage in IgMg1 B cells, indicating that IgMg1 B cells are regarded to be more auto-reactive during negative selection of B cell development.

A

IgD⁺IgM⁺ mature BM B cells

IgM⁺B220⁺ mature spleen B cells
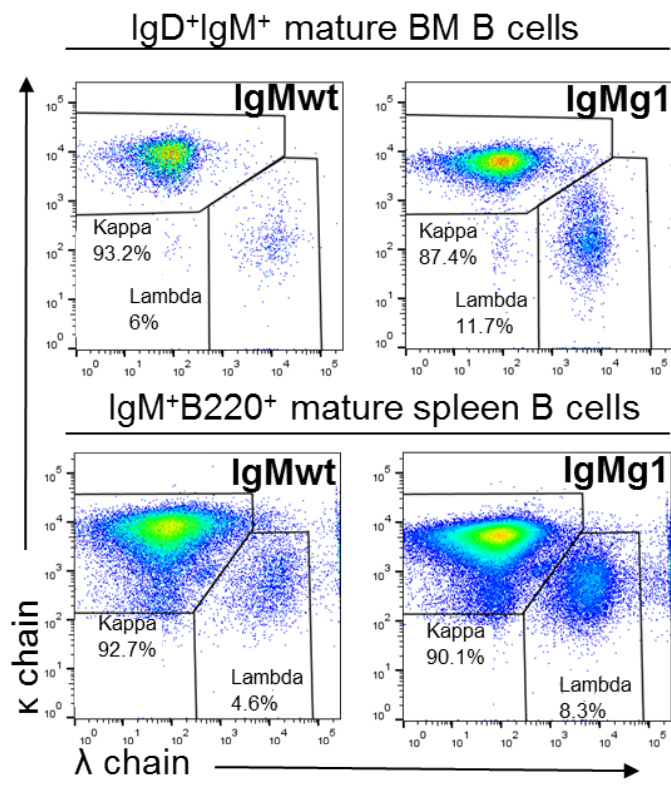
B
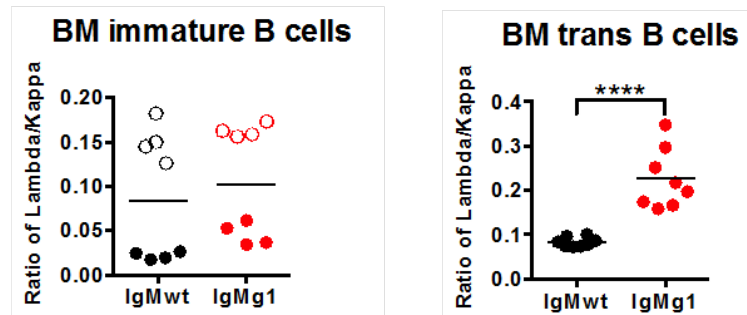
C
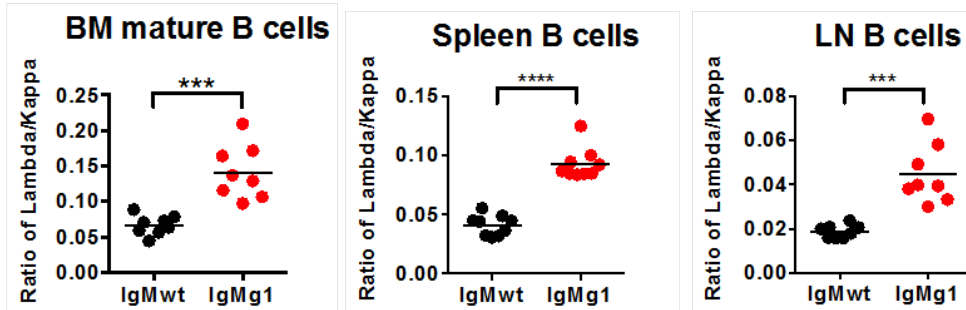
Figure 3.17: Enhanced IgL Lambda chain usage in IgMg1 mice.

Gates for BM immature and mature B cells are the same as the ones displayed in Fig. 3.3. Spleen and LN B cells are gated as the one displayed in Fig. 3.7

A. Gate settings for IgL Lambda$^+$ and Kappa$^+$ B cells in BM and spleen mature B cells.
B. Ratio of percentage of IgL Lambda$^+$ B cells to Kappa$^+$ B cells in BM immature and transitional B cells.
C. Ratio of percentage of Lambda$^+$ B cells to Kappa$^+$ B cells in BM mature B cells, spleen B cells and LN B cells. This ratio has been regarded as an indicator of lambda chain usage.

***p < 0.001; ****p < 0.0001; unpaired Student's t test. Bars indicate mean. Each symbol represents sample from one mouse. Data are from two independent experiments.
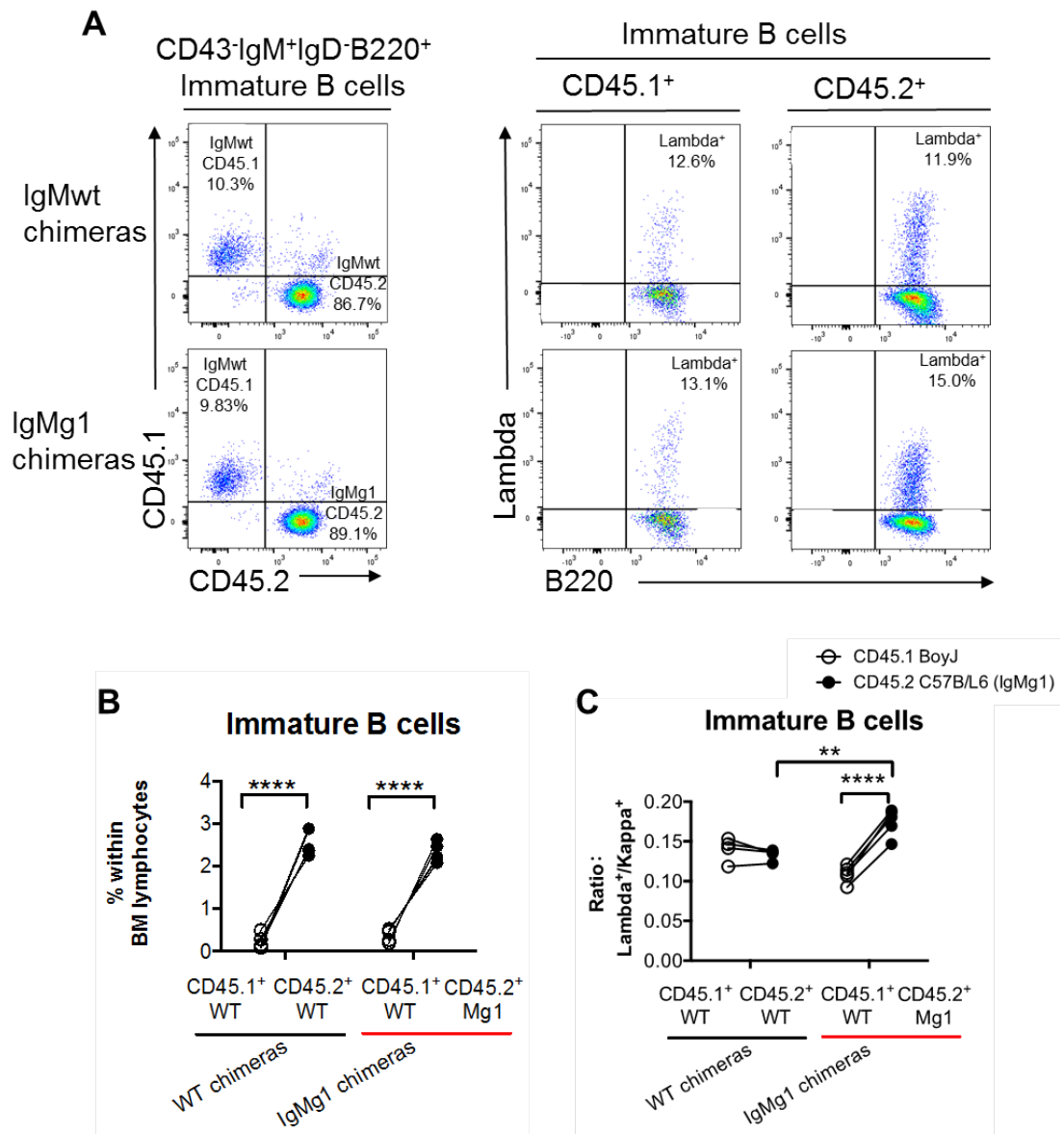
Figure 3.18: Higher IgL Lambda chain usage in IgMg1 immature B cells in bone marrow chimeric mice.

A. Gate settings of IgL Lambda$^+$ B cells in CD45.1$^+$ and CD45.2$^+$ BM immature B cells.
B. The percentages of total immature B cells within BM lymphocytes from both IgMwt and IgMg1 chimeras.
C. Ratio of percentage of IgL Lambda$^+$ B cells to IgL Kappa$^+$ B cells in both CD45.1$^+$ and CD45.2$^+$ immature B cells from IgMwt and IgMg1 chimeras. This ratio has been regarded as an indicator of lambda chain usage.

**p < 0.01; ****p < 0.0001; 2-way ANOVA. Each symbol represents sample from one mouse. Data are representative from two independent experiments.
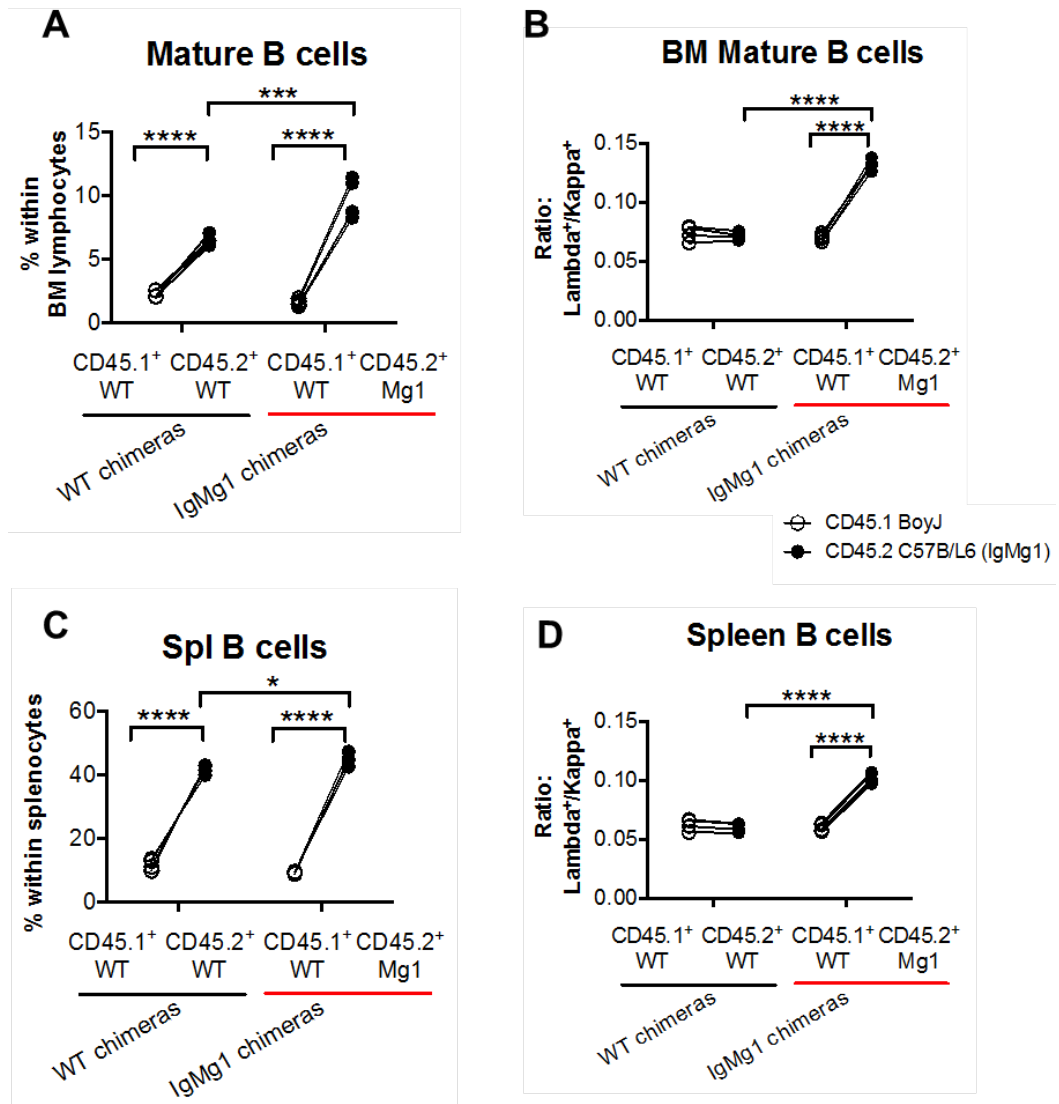
Figure 3.19: Higher IgL Lambda chain usage in IgMg1 mature B cells.

Gates for BM mature B cells and spleen B cells are the same as the ones displayed in Fig. 3.3 and Fig. 3.4.

    A. Percentages of total mature B cells within BM lymphocytes from both IgMwt and IgMg1 chimeras.

    B. Ratio of percentage of IgL Lambda$^+$ B cells to IgL Kappa$^+$ B cells in both CD45.1$^+$ and CD45.2$^+$ BM mature B cells from IgMwt and IgMg1 chimeras.

    C. Percentages of total spleen B cells within splenocytes from both IgMwt and IgMg1 chimeras.

    D. Ratio of percentage of IgL Lambda$^+$ B cells to IgL Kappa$^+$ B cells in both CD45.1$^+$ and CD45.2$^+$ spleen B cells from IgMwt and IgMg1 chimeras.

$*p < 0.05$; $****p < 0.0001$; 2-way ANOVA. Each symbol represents sample from one mouse. Data are representative from two independent experiments.

3.2.5 Reduced expression of surface IgM on IgMg1 B cells from the immature stage of development

The significantly reduced numbers of T1 cells and enhanced lambda chain usage in IgMg1 mice indicate IgMg1 B cells are more prone to undergo negative selection similar to self-reactive B cells during development. Previous studies showed that the majority of B cells displaying auto-reactivity are either deleted or induced into anergic state during B cell development (Brink and Phan 2018). Down-regulation of surface IgM has been observed in anergic B cells in the majority of anergic mouse models (Erikson, Radic et al. 1991, Goodnow, Brink et al. 1991, Benschop, Aviszus et al. 2001, Borrero and Clarke 2002). Thus, surface IgM and IgD expressions in IgMg1 B cells were assessed.

Flow cytometry showed that membrane IgM (mIgM) expression was reduced in all IgMg1 B cell subsets compared to IgMwt counterparts. mIgM expression level was reduced in IgMg1 mice since mIgM is initially expressed on immature B cells, and in IgMg1 mice mIgM expression level of immature B cells was 74% of IgMwt B cells (Fig. 3.20A and B). Lower expression of mIgM was also found in transitional and mature BM B cells, which were 65% and 53% of their WT counterparts, respectively (Fig. 3.20C and D left). In the spleen transitional B cell populations, mIgM expression in IgMg1 B cells were 49% in T1 B cells and 40% in T2+3 B cells of the expression levels on IgMwt B cells (Fig. 3.21A, B and C, D). While IgMwt B cells express mIgM at 2-fold higher levels when they differentiate into MZ B cells, mIgM levels remained low and were more than 3-fold lower in IgMg1 MZ B cells compared to

IgMwt MZ B cells (Fig. 3.22C and D). Fo B cells in IgMg1 mice express 2-fold lower surface IgM than their WT counterparts (Fig. 3.22B and D left). Different from this, initial expression of mIgD during T1 stage in the spleen was comparable between IgMg1 and IgMwt mice (Fig. 3.21B). However, mIgD expression levels were slightly decreased in BM mature B cells (Fig. 3.20D), T2+3 cells (Fig. 3.21D) and Fo B cells (Fig. 3.22D). MZ B cells in IgMg1 and IgMwt mice also displayed low but similar levels of mIgD expression (Fig. 3.22B). Overall, mIgM expression was significantly downregulated in all IgM expressing B cell populations, but the expression of mIgD was only slightly reduced mainly in re-circulating B cells, such as Fo B cells. The expression of mIgM and mIgD on B cells is dynamically regulated and is tightly connected with BCR signalling and the responsiveness of B cells (Goodnow, Crosbie et al. 1989, Zikherman, Parameswaran et al. 2012). The changes in mIgM and mIgD expression levels suggest BCR signalling or the state of B cell activation may be altered in IgMg1 mice.
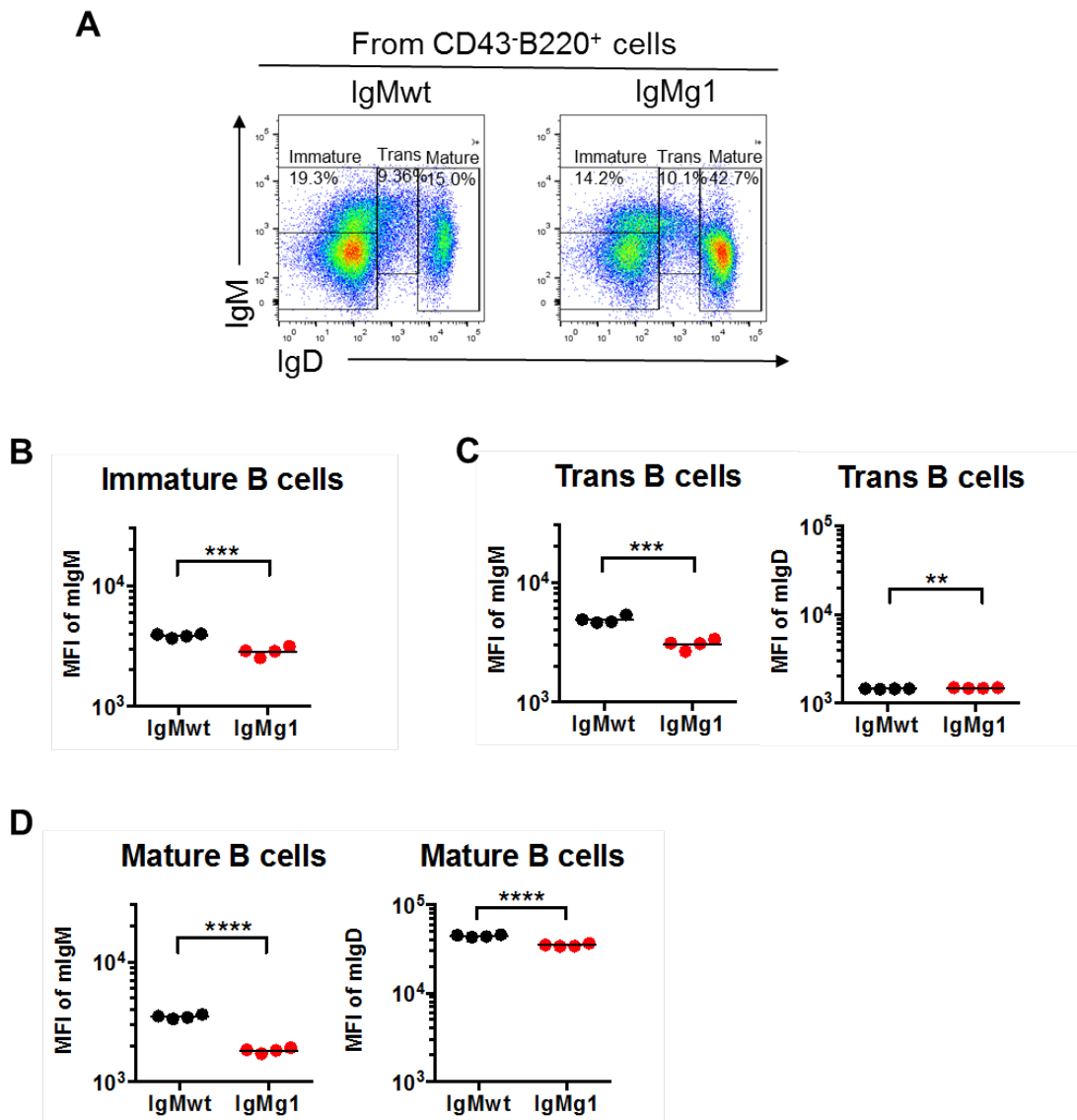
Figure 3.20: Reduced surface IgM (mIgM) and IgD (mIgD) expression in immature and mature BM B cells.

A. Representative 2-D plot displaying IgD and IgM expression in both immature and mature BM B cells.
B. The MFI of mIgM in immature B cells from both IgMwt and IgMg1 mice.
C. The MFI of mIgM in BM transitional B cells from both IgMwt and IgMg1 mice
D. The MFI of mIgM and mIgD in BM mature B cells from both IgMwt and IgMg1 mice

$**p < 0.01$; $***p < 0.001$; $****p < 0.0001$; unpaired Student's t test. Bars indicate mean. Each symbol represents sample from one mouse. Data are representative from four independent experiments.
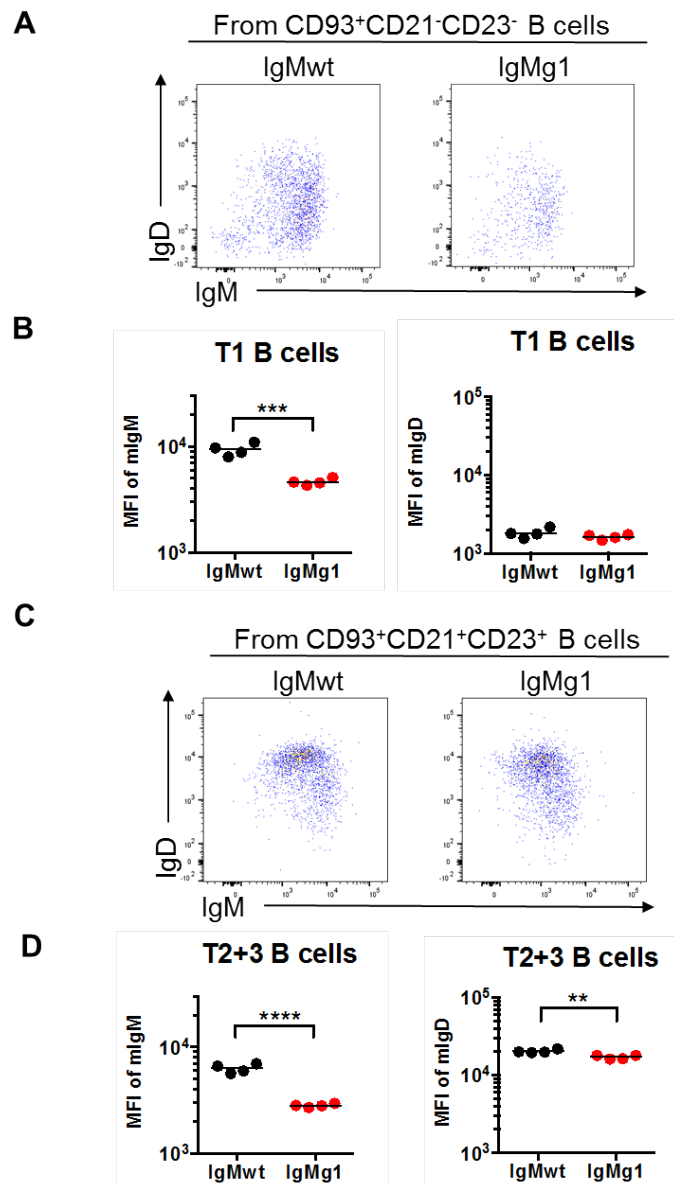
Figure 3.21: Reduced surface IgM (mIgM) and IgD (mIgD) expression in transitional B cells.

A. Representative 2-D plot displaying IgD and IgM expression in T1 B cells.
B. The MFI of mIgM in T1 B cells from both IgMwt and IgMg1 mice.
C. Representative 2-D plot displaying IgD and IgM expression in T2+3 B cells.
D. The MFI of mIgM and mIgD in T2+3 B cells from both IgMwt and IgMg1 mice

***$p < 0.001$; ****$p < 0.0001$; unpaired Student's t test. Bars indicate mean. Each symbol represents sample from one mouse. Data are representative from four independent experiments.
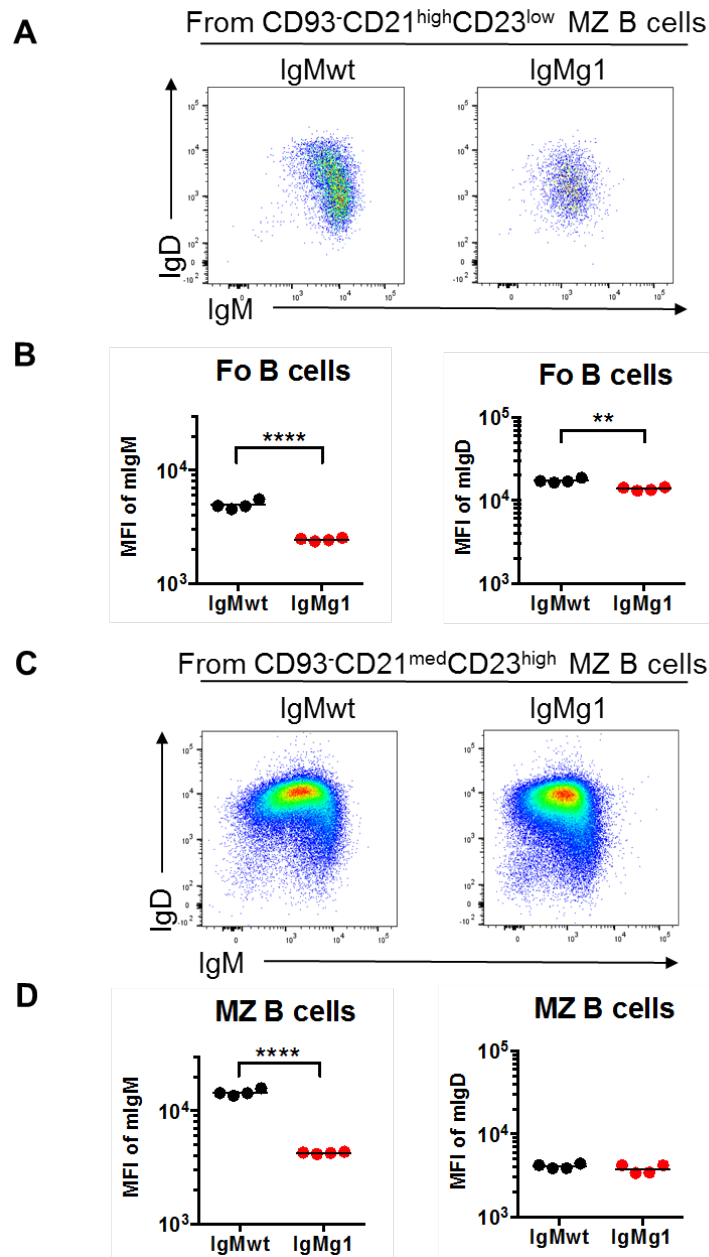
Figure 3.22: Reduced surface IgM (mIgM) and IgD (mIgD) expression in spleen MZ and Fo B cells.

A. Representative 2-D plot displaying IgD and IgM expression in MZ B cells.
B. The MFI of mIgM in Fo B cells from both IgMwt and IgMg1 mice.
C. Representative 2-D plot displaying IgD and IgM expression in Fo B cells.
D. The MFI of mIgM and mIgD in MZ B cells from both IgMwt and IgMg1 mice
$***p < 0.001$; $****p < 0.0001$; unpaired Student's t test. Bars indicate mean. Each symbol represents sample from one mouse. Data are representative from four independent experiments.

To test whether the lower IgMg1 BCR expression was due to transcriptional regulation, primers were designed to specifically amplify mRNA encoding for membrane bound IgM or IgD (Fig. 3.23A). Surprisingly, there was no significant difference in relative mRNA levels encoding for mIgM between IgMwt and IgMg1 mice (Fig. 3.23B), suggesting that the reduced mIgM expression was not due to transcriptional regulation.
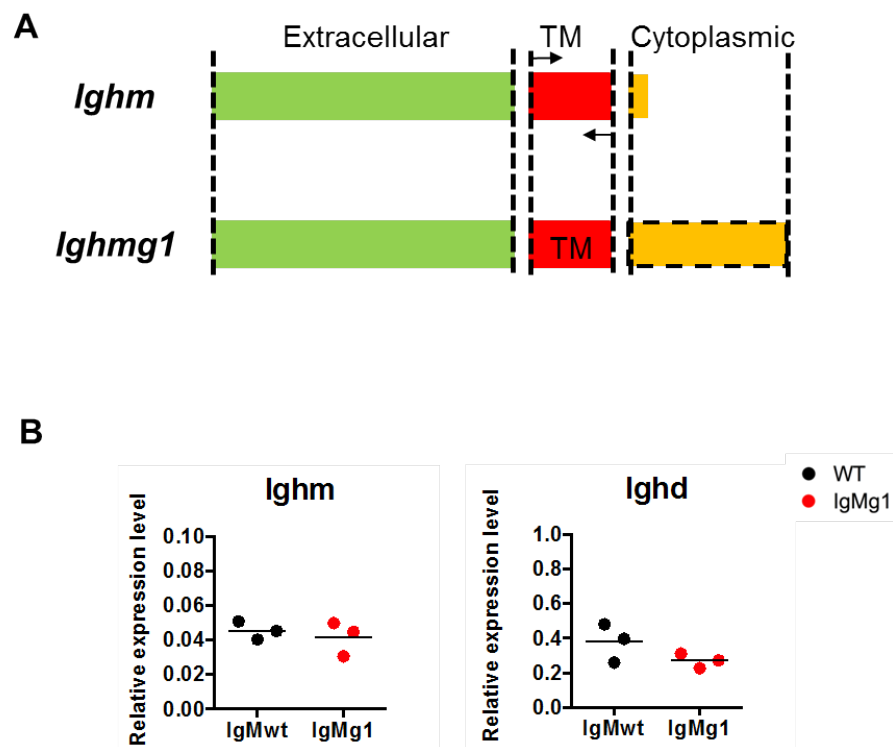
Figure 3.23: Ighm mRNA expression level is comparable between IgMwt and IgMg1 mice.

A. Schematic mRNA sequences encoding for membrane-bound IgM (Ighm) and IgMg1 (Ighmg1), extracellular part (green), transmembrane (TM) part (red), cytoplasmic part (yellow). Forward and reverse primers are designed as indicated (arrow shows).
B. Relative mRNA expression levels of Ighm and Ighd. Relative mRNA levels are normalised to house-keeping gene β-2 microglobulin, compared between IgMwt and IgMg1 mice.

Bars indicate median. Each symbol represent sample from one mouse.

3.2.6 Evidence for hyper-active tonic signalling transducing from IgMg1 during B cell development

As B cell fate is tightly regulated by their tonic BCR signalling strength (Niiro and Clark 2002, Monroe 2006, Pillai and Cariappa 2009), the effects on peripheral B cell development seen in IgMg1 mice suggested that tonic BCR signalling strength had changed in IgMg1 B cells. In order to directly measure tonic BCR signalling strength in all B cell subsets in IgMg1 and IgMwt mice, Nur77-GFP reporter mice were utilised (Moran, Holzapfel et al. 2011). Nur77 is an inducible orphan nuclear receptor, its expression is rapidly up-regulated after cognate receptor-antigen ligation in both T and B cells (Winoto and Littman 2002). As the expression of GFP is under the control of Nur77 regulatory region *Nr4a1*, the expression of GFP is immediately induced after TCR or BCR activation and the intensity of GFP can reflect TCR and BCR signalling strength (Zikherman, Parameswaran et al. 2012).

During BM development, mIgM starts signalling after initial expression on immature B cells (Tze, Schram et al. 2005). During this stage, IgMg1 transduced stronger signalling than wildtype IgM (Fig. 3.24B and C left). At transitional stage IgMg1 B cells showed significantly stronger tonic signalling than their wildtype counterparts (Fig. 3.24B and C middle). Only 25% of IgMwt transitional B cells expressed stronger than background signalling, while around 60% of IgMg1 B cells expressed Nur77-GFP levels higher than background (Fig. 3.24D middle). The average Nur77-GFP expression in transitional B cells was 1.7 times higher than background in IgMwt B cells, while transitional IgMg1 B cells expressed 3 times higher Nur77-GFP

than background (Fig. 3.24C middle). This hyper-active signalling in IgMg1 B cells disappeared once B cells had entered the mature BM B cell stage, with the average Nur77-GFP expression level not further increasing, and IgMwt B cells reaching slightly higher levels of Nur77-GFP expression than IgMg1 B cells (Fig. 3.24B and C right). This was also reflected in the frequency of Nur77^{+} B cells being slightly lower in mature IgMg1 B cells than in IgMwt B cells (3.24B and C right).

In the periphery, both T1 and T2+3 IgMg1 B cells tended to have slightly lower Nur77-GFP expression than their WT counterparts, although none of this was significant (Fig. 3.25A and B). Relative Nur77-GFP expression levels in transitional B cells reached levels of around 4 to 6 times above background (Fig. 3.25B) and around 50% considered positive by Overton subtraction (Fig. 3.25C). The average Nur77-GFP expression level increased in MZ B cells compared to transitional B cells, being around 7 in IgMwt mice and around 9 in IgMg1 mice (Fig. 3.26A). Around 90% MZ B cells from IgMg1 mice expressed Nur77-GFP higher than background (Fig. 3.26C left). Average Nur77-GFP expression levels in Fo B cells were similar to transitional B cells (Fig. 3.26B). Fo B cells in IgMg1 mice tended to show slightly lower expression levels but had a similar percentage of Nur77^{+} B cells of around 60% (Fig. 3.26B and C).

In summary, IgMg1 was able to transduce stronger tonic BCR signalling at the stage when it was firstly expressed on immature B cells. This stronger signal became attenuated during BM development, indicating negative regulation of IgMg1 B cells

happening during BM B cell development. IgMg1 MZ B cells showed considerably stronger tonic BCR signalling, while the remaining peripheral IgMg1 B cell populations showed slightly repressed tonic BCR signalling.

A From BM B220⁺CD43⁻ cells

B From BM B220⁺CD43⁻ cells

C

Immature B cells
Trans B cells
Mature B cells

D

Nur77⁺ immature B
Nur77⁺ trans B
Nur77⁺ mature B
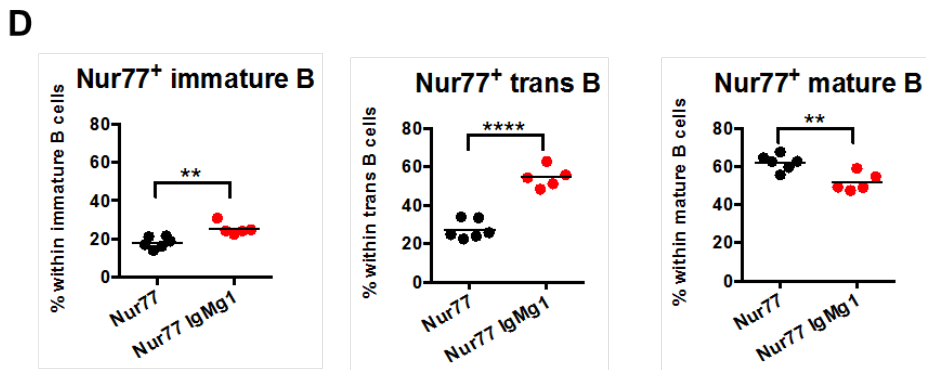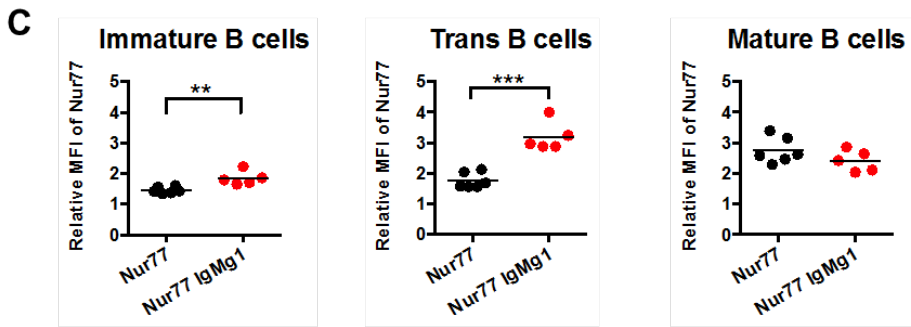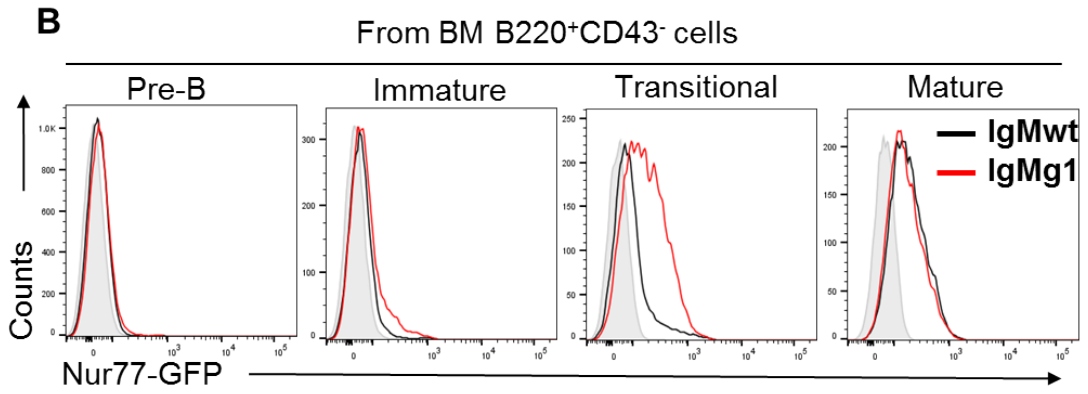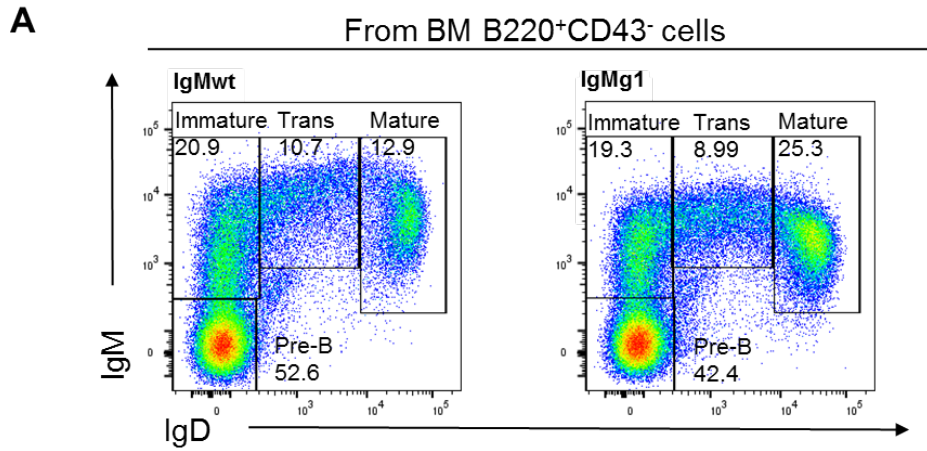
Figure 3.24: Dynamic Nur77-GFP expression levels during B cell development in BM.

A. Gate settings for the four different stages of BM B cell populations: pre-B cells, immature B cells, transitional B cells and mature B cells.
B. Overlays of both Nur77 IgMwt (black) and Nur77 IgMg1 (red) B cells Nur77-GFP expression levels in the above four B cell populations. Non-fluorescent counterpart of each cell population is gated as negative control (gray).
C. Relative MFI (median FI) of Nur77-GFP expression level and compared between groups. Data merged from two independent experiments. Nur77-GFP expression level are normalised between independent experiments by defining the MFI (median FI) of the Nur77-GFP negative control (grey curve) as 1.
D. Percentages of Nur77$^+$ B cells and compared between groups. The percentages of Nur77$^+$ B cells were calculated by Overton subtraction.

**p < 0.01; ****p < 0.0001; unpaired Student's t test. Bars indicate mean. Each symbol represents sample from one mouse. Data are combined from two independent experiments.
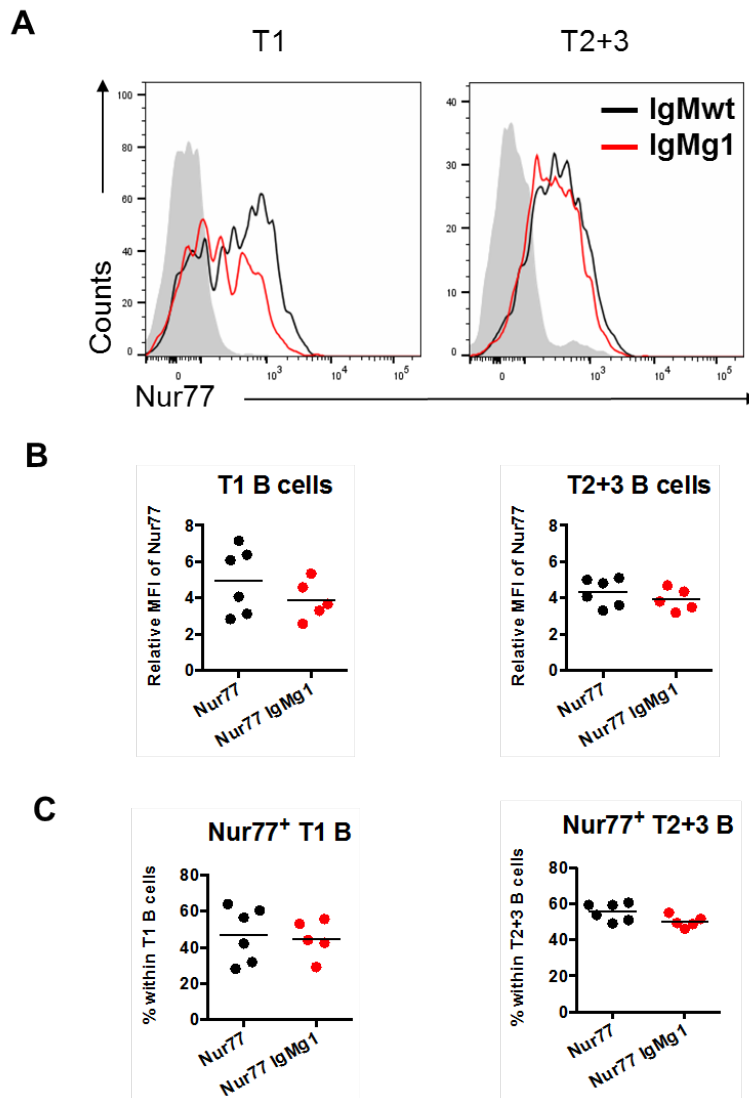
Figure 3.25: Nur77-GFP expression level is comparable in IgMg1 transitional B cells.

Gate settings for transitional B cells are the same as the ones displayed in Fig 3.5.
  A. Overlays of Nur77-GFP expressions in both T1 and T2+T3 B cells from Nur77 IgMwt (black) and Nur77 IgMg1 (red) mice. Non-fluorescent counterpart of each cell population is gated as negative control (gray).
  B. Normalised Nur77-GFP expression level in T1 and T2+T3 B cells. Nur77-GFP expression level is normalised between independent experiments by defining the MFI of the Nur77-GFP negative control (grey curve) as 1.
  C. The percentages of Nur77^{+} B cells and compared between groups. The percentages of Nur77^{+} B cells were calculated by Overton subtraction.
ns, not significant; unpaired Student's t test. Bars indicate mean. Each symbol represent sample from one mouse. Data are combined from two independent experiments.
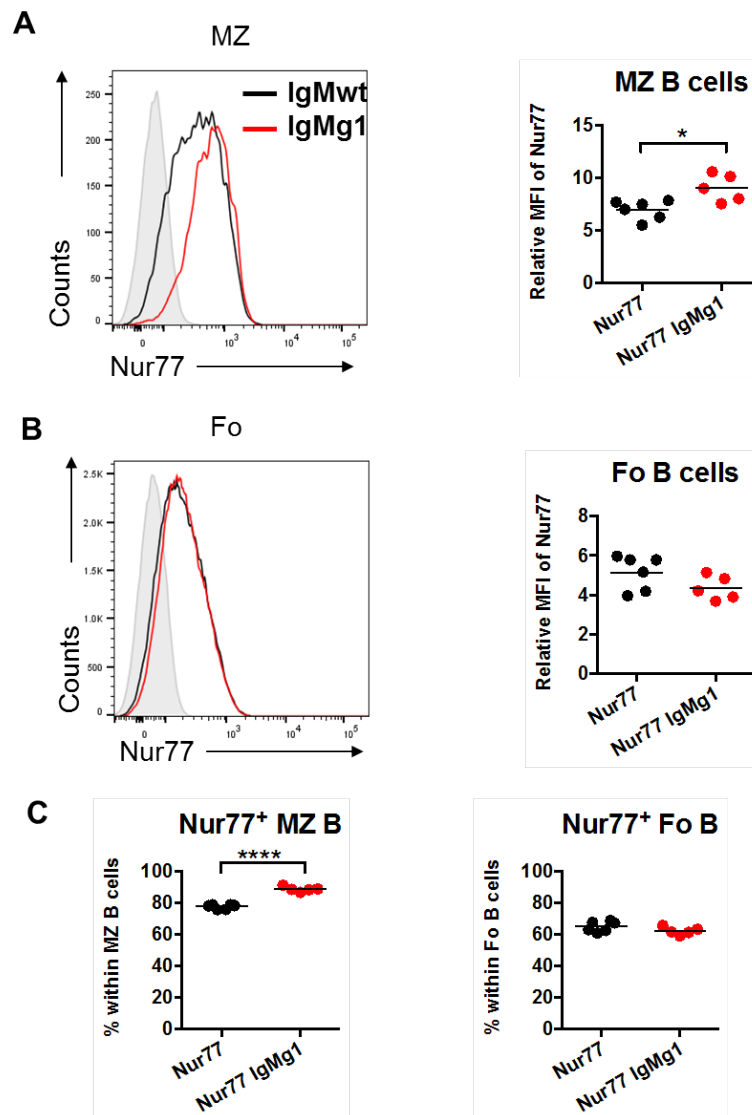
Figure 3.26: Nur77-GFP expression level is enhanced in MZ B cells.

Gate settings for MZ and Fo B cells are the same as the ones displayed in Fig 3.6.

A. Overlays of Nur77-GFP expressions in both MZ and Fo B cells from Nur77 IgMwt (black) and Nur77 IgMg1 (red) mice. Non-fluorescent counterpart of each cell population is gated as negative control (gray).

B. Nur77-GFP expression levels in MZ and Fo B cells and compared between groups.

C. The percentages of Nur77$^+$ B cells and compared between groups. The percentages of Nur77+ B cells were calculated by Overton subtraction.

***p < 0.001; ****p < 0.0001; unpaired Student's t test. Bars indicate mean. Each symbol represent sample from one mouse. Data are combined from two independent experiments.

3.2.7 Dampened calcium influx and phosphorylation signalling after activating IgMg1 B cells through BCR

The Nur77-GFP expression experiments demonstrated that tonic BCR signalling strength in IgMg1 mice were either higher, shown in MZ B cells, or were comparable to their wildtype counterparts, shown in mature follicular B cells. In order to test whether IgMg1 BCR leads to similar changes after BCR activation, the calcium influx of splenic B cells after activation with anti-IgM antibody was assessed. Splenic B cells were stained with Indo-1, and stimulated with anti-IgM to activate B cells directly through their BCRs. Basal soluble Ca^{2+} levels (R0) were comparable between IgMg1 and IgMwt B cells (Fig. 3.27B and C). After stimulating with anti-IgM, IgMwt B cells mounted an instant and strong calcium influx (Fig. 3.27A and B). IgMg1 B cells generated a slower and remarkably weaker calcium influx after activation (Fig. 3.27B), reflected by weaker peak flux (Rp/R0) and longer time taken to reach peak levels after stimulation (Fig. 3.27B and C).

The changes observed in signalling pattern of Ca^{2+} influx indicate that activated signalling transduced from IgMg1 BCR in mature B cells is lower than that of IgMwt BCR.

A

Anti-IgM

IgMwt

IgMg1

Bounding

Free

Time(s)

B

Anti-IgM

Ratio: Bounding / Free

IgMwt
IgMg1

3.9

3.7

3.5

3.3

3.1

Time (s)   100   200   300   400   500

C

R0

Rp / R0

Time to peak

Ratio: Bound / Free

Ratio

Time (s)

*

**

IgMwt   IgMg1   IgMwt   IgMg1   IgMwt   IgMg1
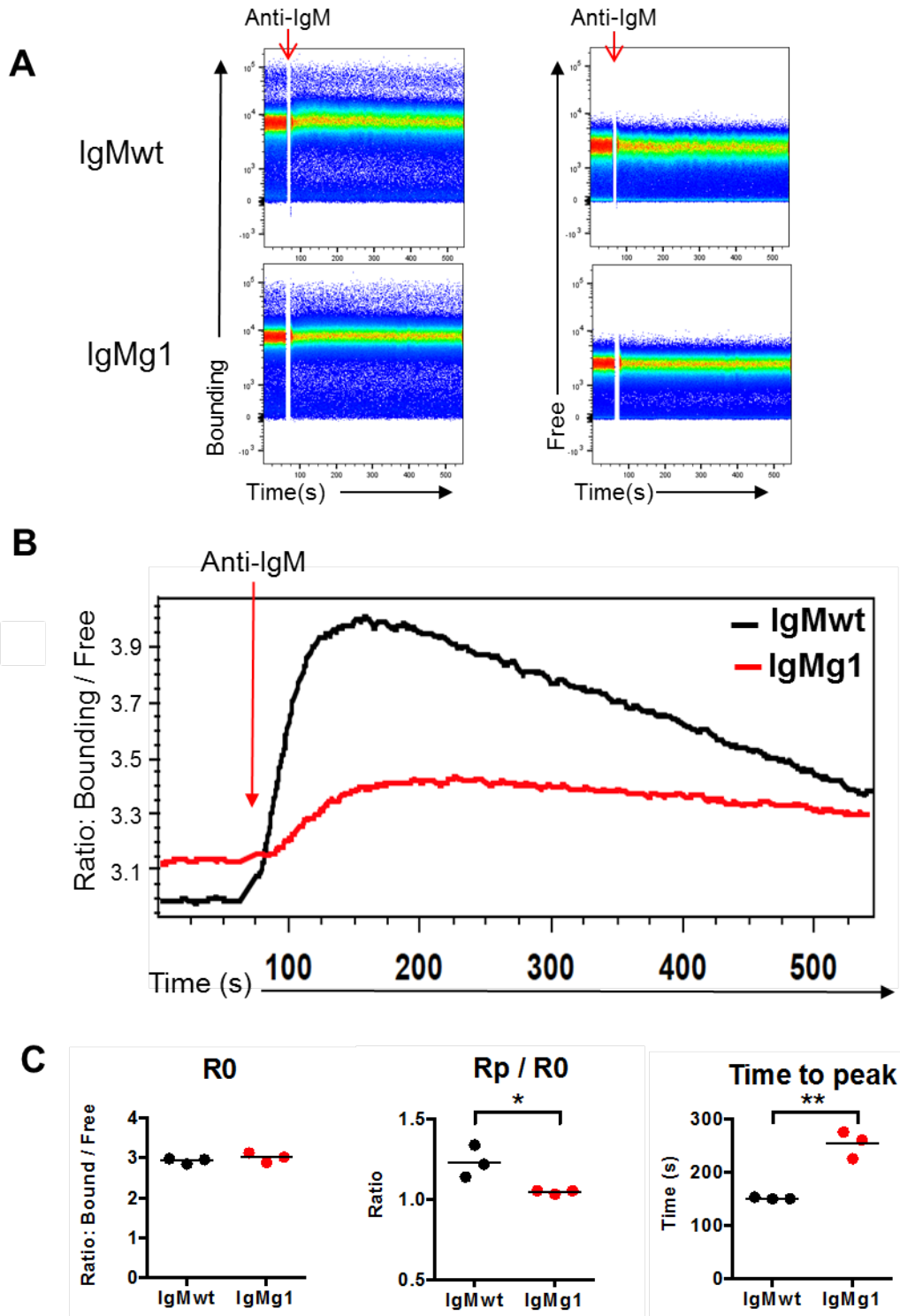
Figure 3.27: Lagging and weaker calcium influx of IgMg1 B cells after stimulation through IgM, after Indo-1 loading.

A. Calcium influx in both IgMwt and IgMg1 B cells. Left: emission of Indo-1 after binding to Ca^{2+}; Right: emission of free Indo-1. RBC-depleted splenocytes are calmed at 5% $CO2$ at 37 C° for three hours. Then labeled with 1 μM Indo-1 for 1 hour at RT. After labelling, cells are stained with anti-CD43. The stained cells were first acquired for 1min to record the basal soluble calcium level, then stimulated with 10 μg/ml anti-IgM F(ab')$_2$ antibody and acquired their calcium influx for 8min.

B. Overlays of kinetic calcium influx from both IgMwt and IgMg1 splenic B cells.

C. Strength and lasting time for calcium influx. The strength of calcium influx is calculated as the ratio between peak value (Rp) to basal value (R0). Time to peak is the duration of time used from start to reach the peak.

*$p < 0.05$; **$p < 0.01$; unpaired Student's t test. Bars indicate median. Each symbol represent sample from one mouse.

3.2.8 Weaker BCR-activation induced SYK and BLNK phosphorylation in IgMg1 B cells

To further confirm these observations and test phosphorylation levels of specific signal transducing proteins downstream of the BCR, PhosFlow was utilized to detect tonic and BCR activation induced signalling in various B cell subsets. In bone marrow immature and mature B cells, tonic p-SYK and p-BLNK levels were quite comparable (Fig. 3.28A, B and C). While BCR activation with anti-IgM induced a clear increase in p-SYK and p-BLNK in IgMg1 B cells, these levels were consistently and dramatically lower than the ones induced in IgMwt B cells (Fig. 3.28B and C), indicating that downstream BCR activation induced signalling in IgMg1 B cells is repressed from immature B cell stage.

In the spleen, tonic and activated p-SYK and p-BLNK levels were detected in the two major peripheral mature B cell populations − mature Fo B cells and MZ B cells. Of these, MZ B cells showed significantly increased tonic p-SYK signalling in IgMg1 B cells (Fig. 3.29A and B), consistent with the stronger Nur77-GFP reporter levels observed in these cells (Fig. 3.26A). However, tonic p-BLNK levels were similar in MZ B cells and Fo B cells (Fig. 3.29C). Within 5 minutes of BCR activation with anti-IgM, p-SYK was significantly elevated in IgMwt B cells, with the strongest increases happening in MZ B cells (Fig. 3.29B). This increase was less in all IgMg1 B cell populations. Again, this attenuation of signal was strongest in MZ B cells, while the attenuation of the weak signal seen in Fo B cells was not significant (Fig. 3.29A and B). BCR-stimulation induced BLNK phosphorylation in different splenic B cell

populations with a similar pattern to what was seen for p-SYK. In both populations of splenic IgMg1 B cells, BLNK phosphorylation was significantly attenuated compared to their WT counterparts (Fig. 3.29C).

The reduced elevation levels of p-SYK and p-BLNK after BCR ligation in both immature and mature IgMg1 B cells were consistent with pervious observations of weaker calcium influx. Together, these results suggest that IgMg1 B cells represent anergic B cells. Despite immature B cells displaying slightly stronger tonic Nur77-GFP expression level in IgMg1 mice (Fig. 3.24), the tonic p-SYK and p-BLNK levels were quite comparable to WT counterparts. Furthermore, BCR ligation induced BCR signalling was significantly reduced in immature B cells from IgMg1 mice, indicating IgMg1 B cells are induced into anergy during this stage.

123
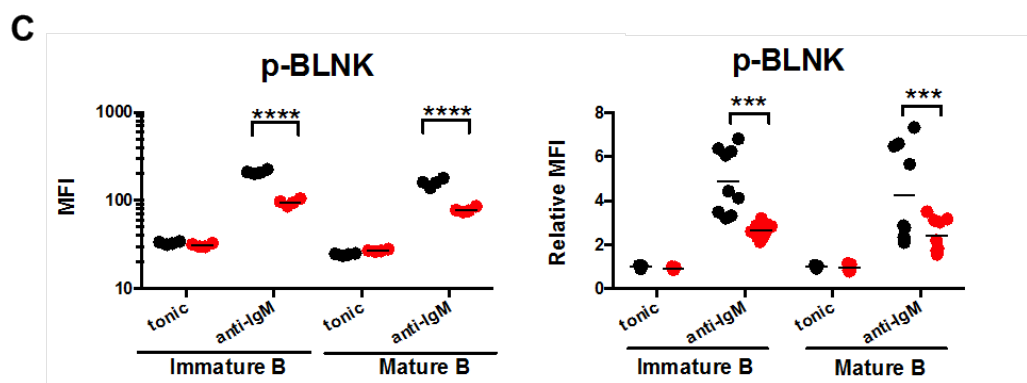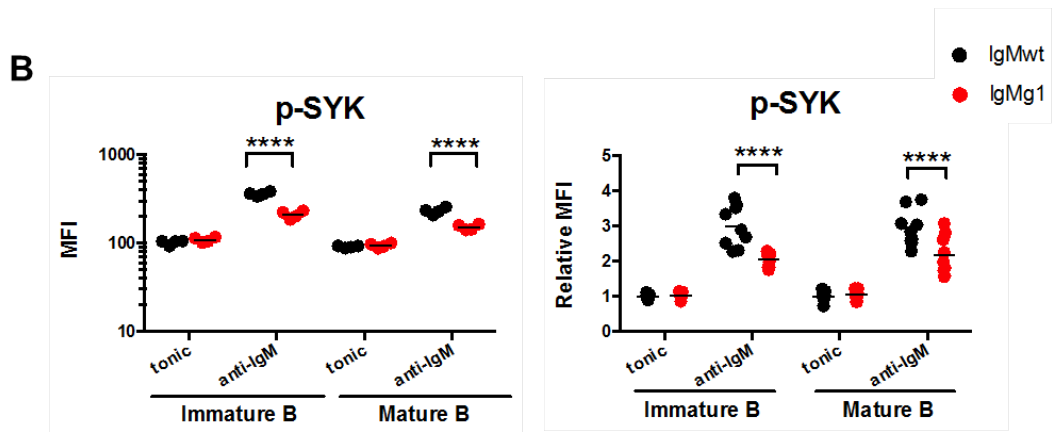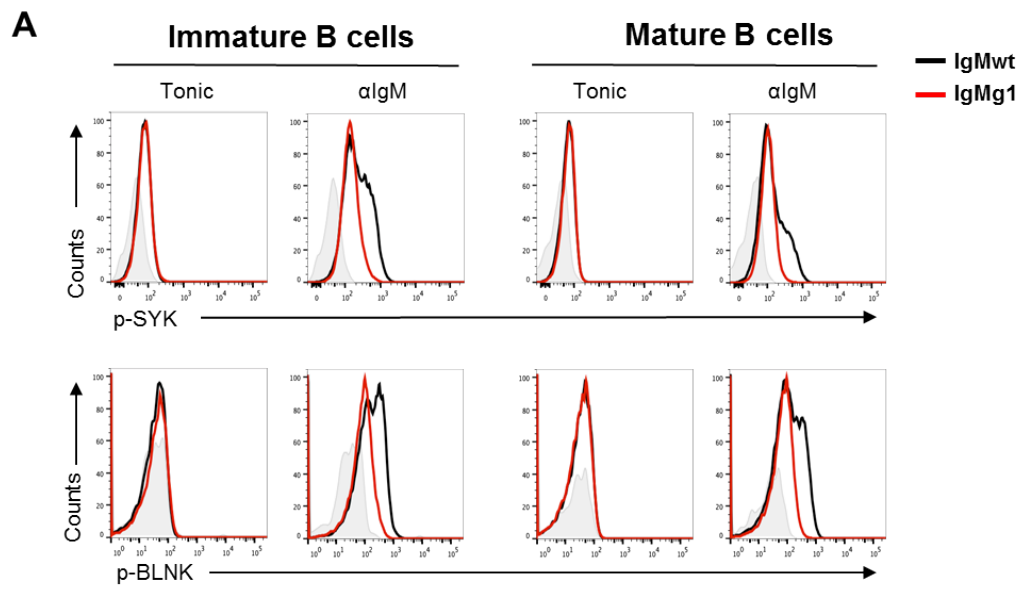
Figure 3.28: Comparable tonic signalling, but constant lower activated phosphorylation levels of SYK and BLNK in immature and mature B cells in BM.

Gates for BM immature and mature B cells are the same as displayed in Fig. 3.3.

A. Overlays of phosphorylated SYK and BLNK from both IgMg1 (red line) and IgMwt (Black line) mice. BM lymphocytes are collected, for activated signalling, lymphocytes are stimulated with 10 µg/ml anti-IgM antibody for 5min.Both non-treated (tonic) and treated (activated) cells are fixed and permeabilised. Anti-pSYK and anti-pBLNK are added along with other needed antibodies to stain the cells. Lambda-phosphatase treated counterparts are set as negative control (gray histogram).

B. Tonic and activated relative p-SYK MFI levels. The MFI of tonic and activated p-SYK in immature and mature B cells of one representative experiment is shown (left). In order to merge data from two independent experiments (right), the relative MFI of p-SYK is calculated by taking the average MFI for tonic IgMwt in each population as 1.

C. Tonic and activated relative p-BLNK MFI levels. The MFI of tonic and activated p-BLNK in immature and mature B cells of one representative experiment is shown (left). In order to merge data from two independent experiments (right), the relative MFI of p-BLNK is calculated by taking the average MFI for tonic IgMwt in each population as 1.

***$p < 0.001$; ****$p < 0.0001$; 2-way ANOVA. Bars indicate mean. Each symbol represents sample from one mouse. Data are representative from two independent experiments.

A

Follicular B cells   Marginal zone B cells

Tonic   αIgM   Tonic   αIgM

— IgMwt
— IgMg1

B

p-SYK   p-SYK

● IgMwt
● IgMg1

C

p-BLNK   p-BLNK

125
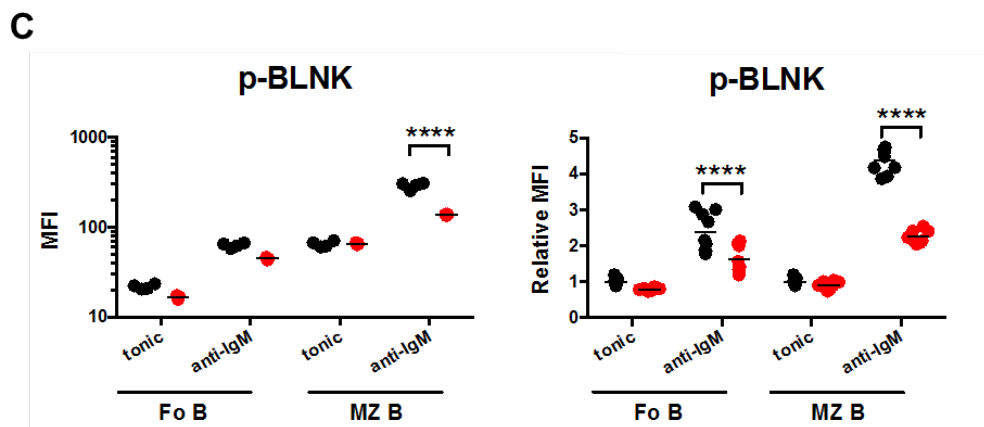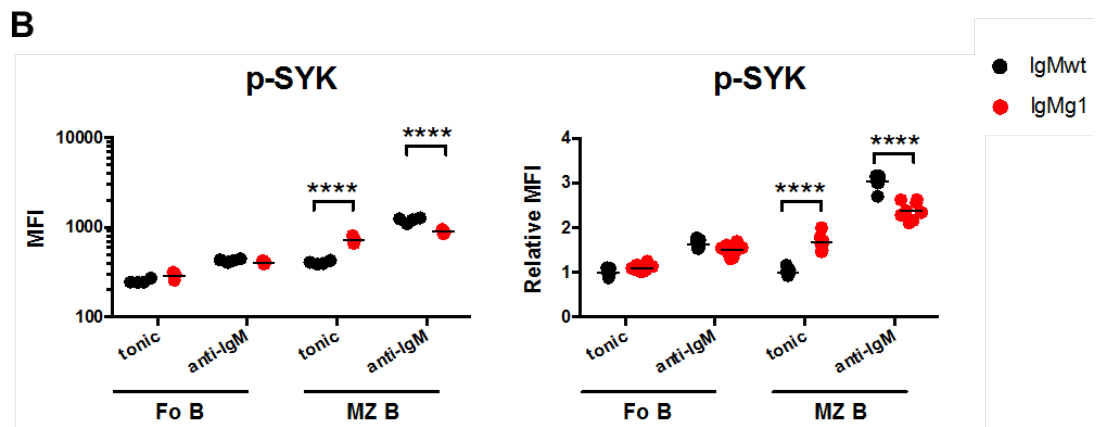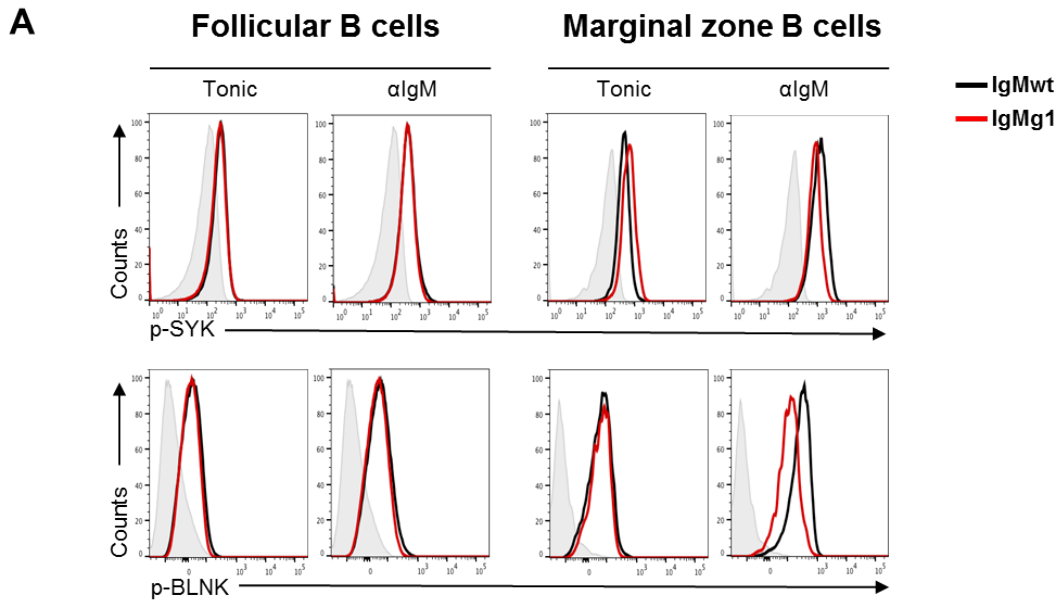
Figure 3.29: Higher tonic signalling while reduced activated signalling in IgMg1 MZ B cells.

Gates for Fo and MZ B cells are the same as displayed in Fig. 3.6.

A. Overlays of phosphorylated SYK and BLNK from both IgMg1 (red line) and IgMwt (Black line) mice. Lymphocytes are isolated from spleens, either non-treated or treated as described before (Fig. 3.29). Lambda-phosphatase treated counterparts are set as negative control (gray histogram).

B. Tonic and activated relative p-SYK MFI levels. The MFI of tonic and activated p-SYK in Fo and MZ B cells of one representative experiment is shown (left). In order to merge data from two independent experiments (right), the relative MFI of p-SYK is calculated by taking the average MFI for tonic IgMwt in each population as 1.

C. Tonic and activated relative p-BLNK MFI levels. The MFI of tonic and activated p-BLNK in Fo and MZ B cells of one representative experiment is shown (left). In order to merge data from two independent experiments (right), the relative MFI of p-BLNK is calculated by taking the average MFI for tonic IgMwt in each population as 1.

****$p < 0.0001$; 2-way ANOVA. Bars indicate mean. Each symbol represents sample from one mouse. Data are from two independent experiments.

3.2.9 Activation markers are not elevated but are slightly lower in IgMg1 B cells

Nur77-GFP expression levels in peripheral Fo B cells were quite comparable between IgMwt and IgMg1 mice (Fig. 3.26B). In line with this, the basal intracellular Ca^{2+} of splenic B cells in IgMg1 mice were also similar to their WT counterparts (Fig. 3.27B), as were the tonic p-SYK and p-BLNK levels in Fo B cells (Fig. 3.29B). Together, these results suggest that the dominant splenic B cell population, naïve Fo recirculating B cells, is not hyper-activated in IgMg1 mice. To further test this, the expression levels of activation markers CD25, CD69 and CD86 on IgMg1 B cells were compared to their WT counterparts. These markers are induced on the surface of all lymphocytes and are up-regulated after B cell activation (Dugas, Paul-Eugene et al. 1991, Ziegler, Ramsdell et al. 1993, Nashar, Webb et al. 1996). They would be expected to be increased if B cells in IgMg1 mice received increased tonic BCR signalling.

Flow cytometry showed that the expression of CD25 and CD86 was quite comparable between IgMg1 and IgMwt total splenic B cells, whereas background CD69 expression was slightly but significantly lower in IgMg1 splenic B cells (Fig. 3.30A and B). IgMg1 B cells from total LNs showed similar expression level of both CD25 and CD69 on their surface (Fig. 3.30C and D). Together these results confirm that at least the peripheral Fo B cell subset is not hyper-activated, whereas MZ B cells in IgMg1 mice displayed hyper-activated steady state reflected by higher tonic Nur77-GFP, p-SYK and p-BLNK levels. Further detailed flow cytometric markers and gating strategies in splenic B cells are needed to separate this population and detect CD25 and CD69 expression levels on them.
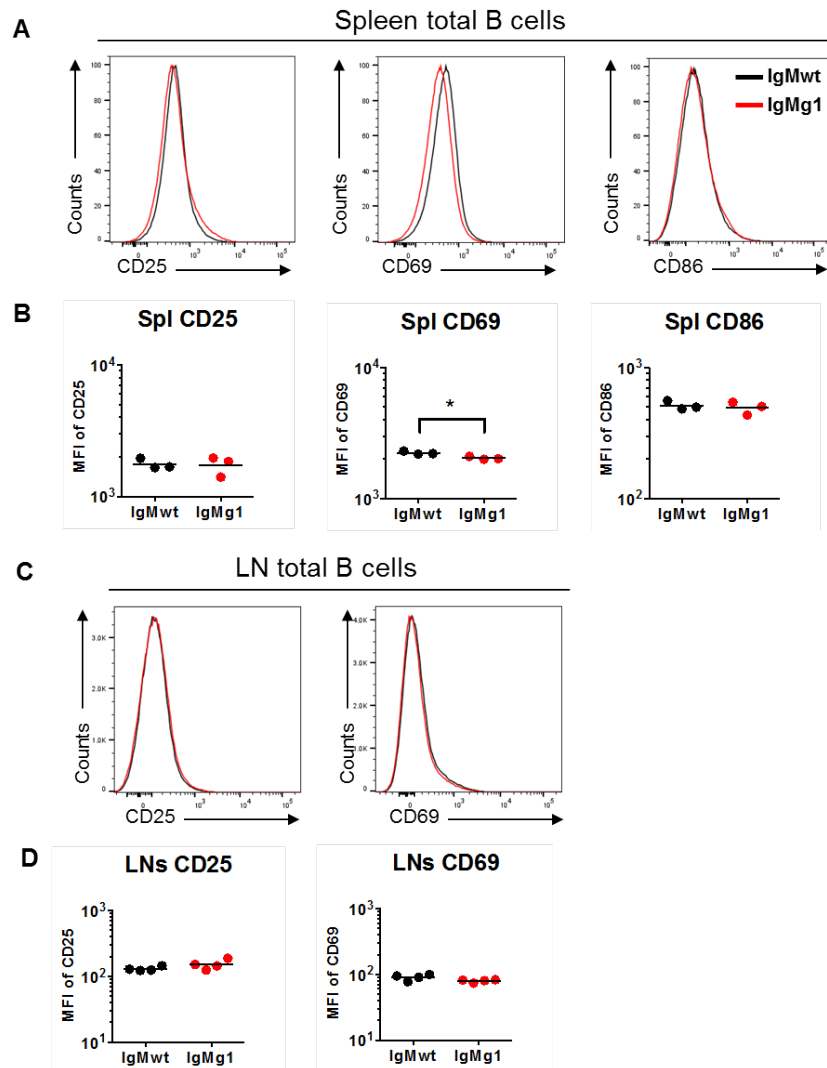
Figure 3.30: Activation markers expression levels were either comparable or lower on IgMg1 B cells.

Gates for B cells were the same as showed in Fig. 3.4
  A. Overlays of surface CD25, CD69 and CD86 expression levels on total splenic B cells from IgMwt (black) and IgMg1 (red).
  B. Surface CD25, CD69 and CD86 expression levels on total spleen B cells from IgMwt (black) and IgMg1 (red).
  C. Overlays of surface CD25 and CD69 expression levels on total LN B cells from IgMwt (black) and IgMg1 (red).
  D. Surface CD25 and CD69 expression levels on total LN B cells from IgMwt (black) and IgMg1 (red).
*p < 0.05; unpaired Student's t test. Bars indicate mean.

3.2.10 Down-regulation of IgM expression and altered MZ B cell localisation in IgMg1 mice

Anergic B cells are not just characterised by their reduced BCR signalling after activation, other features include: the down-regulation of surface IgM, altered localisation to unusual anatomical sites, and blockade of B cell development (Cambier, Gauld et al. 2007). Results shown above show that IgMg1 B cells display reduced activated signalling and down-regulate mIgM. Although there were no obvious signs that B cell development was blocked, IgMg1 B cells experienced increased negative selection during immature and transitional stages, as evidenced by the increased IgL λ/κ ratio. It was therefore interesting to test if there was any change in micro-anatomical location of mature IgMg1 B cells.

To explore this, the anatomical structures of spleen white pulp were detected by fluorescence immunohistology, looking for the presence and location of Fo and MZ B cells. Spleens from both non-immunised IgMg1 and IgMwt mice were cryo-sectioned. Fluorophore-labelled anti-IgM and anti-IgD antisera and CD4 and CD169 antibodies were used to mark different micro-anatomical regions of the splenic white pulp (Fig. 3.31). Using this marker combination, the B cell follicles are $IgD^{hi}IgM^{med}CD4^{-}$ $CD169^{-}$, the MZ region is $IgD^{lo}IgM^{hi}$ $CD4^{-}CD169^{-}$, and the T zone is $IgD^{-}IgM^{-}$ $CD4^{+}CD169^{-}$. CD169-specific staining of macrophages was used to identify the marginal sinus macrophages, separating follicles from MZ (Fig. 3.31A). IgM was expressed at much lower levels in the B cell follicles of IgMg1 mice than in IgMwt mice, confirming the lower expression of surface and also intracellular IgM on B cells

of IgMg1 mice (Fig. 3.21 and 3.22). There was no obvious difference in the location of follicular B cells or of B cell follicle size (Fig. 3.31). However, the MZ seemed to have disappeared in IgMg1 spleens, shown by a loss of IgM^{high}IgD^{low} MZ cells around the IgD^{high} follicular areas (Fig. 3.31B). This difference in MZ compartment was more pronounced seen in flow cytometry, which showed a 65% reduction of the percentages of MZ B cells (Fig. 3.6C).

As IgMg1 MZ B cells significantly down-regulate mIgM (Fig. 3.22), it is possible that the disappearance of MZ area in IgMg1 spleen was due to IgM levels being too low to be detected by immunofluorescence. CD1d is highly expressed on MZ B cells (Roark, Park et al. 1998, Makowska, Faizunnessa et al. 1999, Pillai, Cariappa et al. 2005). To confirm MZ B cell absence, we stained spleen sections with B220 and CD1d (Fig. 3.32). This showed B220^{+}CD1d^{+} MZ B cells present in both marginal zone area and follicular region of spleen from IgMwt mice (Fig. 3.32A right). There were still some MZ B cells in IgMg1 mice, but all of them were relocated to the follicular areas (Fig. 3.32B). The normal micro-anatomincal location of follicular B cells confirms that there is little change in the activation state of these cells. The small number of MZ B cells in IgMg1 mice however do show signs of increased tonic activation, which is reflected by their increased appearance in follicular areas and the T-B borders, indicating that these cells may be in an increased state of shuttling between follicles and the MZ (Arnon, Horton et al. 2013) (Figure. 3.32B).
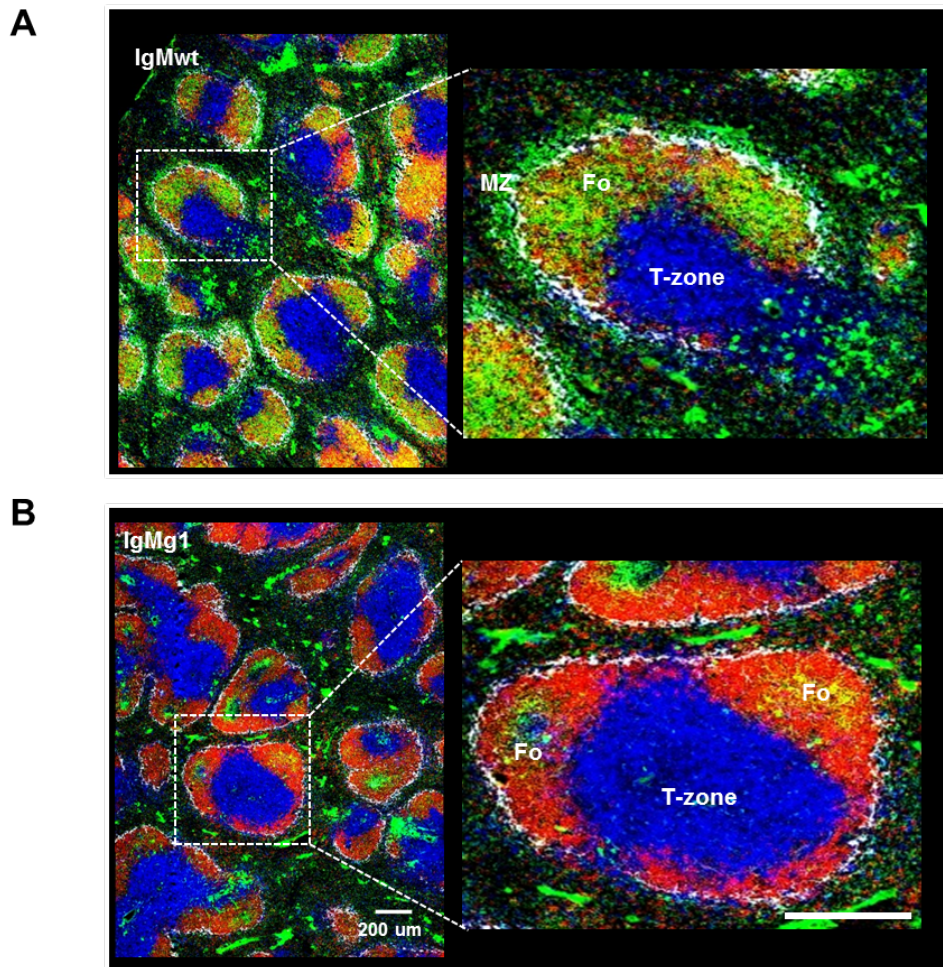
IgM/**IgD**/**CD4**/**CD169**

Figure 3.31: Immunofluorescence images of spleen sections from both IgMwt and IgMg1 non-immunised mice.

A. Immunofluorescent staining of spleen cryosection from IgMwt non-immunised mice. Sections are stained for anti-IgM (green), anti-IgD (red), anti-CD4 (blue) and anti-CD169 (gray). MZ B cells are $IgM^{high}IgD^{low}CD4^-$ (green); Fo B cells are $IgM^{medium}IgD^{high}CD4^-$ (yellow); T cell were are $IgM^-IgD^-CD4^+$ (blue).

B. Immunofluorescent staining of spleen cryosection from IgMg1 non-immunised mice. Sections are stained for anti-IgM (green), anti-IgD (red), anti-CD4 (blue) and anti-CD169 (gray). MZ B cells are $IgM^{high}IgD^{low}CD4^-$ (green); Fo B cells are $IgM^{medium}IgD^{high}CD4^-$ (yellow); T cell are $IgM^-IgD^-CD4^+$ (blue).

A

IgMwt
B220/CD1d/IgD

IgD

IgD/CD1d

B220/CD1d

B220/CD1d

T-zone

Fo

MZ

IgD/CD1d

B220/CD1d

B

IgMg1
B220/CD1d/IgD

IgD

IgD/CD1d

B220/CD1d

B220/CD1d

Fo

T-zone

300 um

50 um

10 um
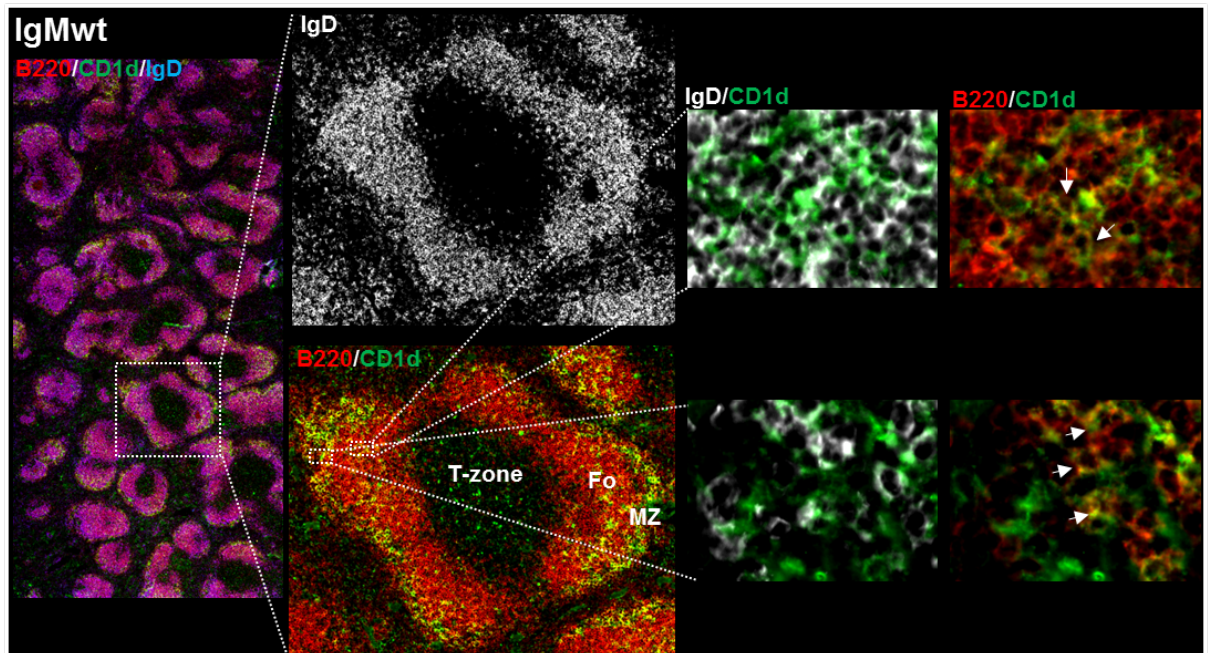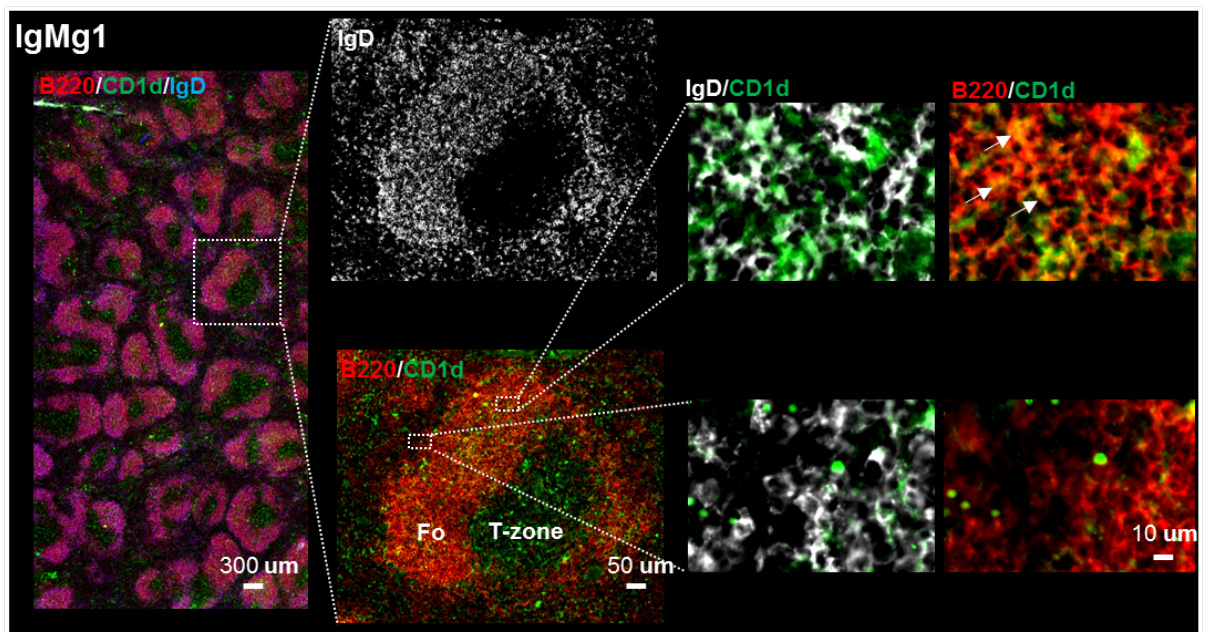
Figure 3.32: Impaired MZ B cell differentiation and the dislocation of them to follicular region.

A. Immunofluorescent staining of spleen cryosection from IgMwt non-immunised mice. Sections are stained for anti-B220 (red), IgD(Blue or white) and anti-CD1d (green). MZ B cells are CD1d$^+$B220$^+$ (yellow); Fo B cells are CD1d$^-$B220$^+$ (red). Arrow indicates CD1d$^+$B220$^+$ MZ B cells.

B. Immunofluorescent staining of spleen cryosection from IgMg1 non-immunised mice. Sections are stained for anti-B220 (red), IgD(Blue or white) and anti-CD1d (green). MZ B cells are CD1d$^+$B220$^+$ (yellow); Fo B cells are CD1d$^-$B220$^+$ (red). Arrow indicates CD1d$^+$B220$^+$ MZ B cells.

3.2.11 Changed surface chemokine receptor expression levels in IgMg1 MZ B cells

Chemokine receptors are dynamically expressed on the surface of lymphocyte. These receptors have a role in locating cells to different micro-anatomical compartments, for example, guiding cells to local responding site after stimulation. Thus, altered localisation of IgMg1 MZ B cells should be reflected by changes on their surface chemokine receptor expression levels. CCR7 guides cellular migration towards the T zone, is highly expressed on T cells, and is up-regulated during initial B cell activation in order to attract B cells towards T-B border (Forster, Schubel et al. 1999, Okada and Cyster 2007, Forster, Schubel et al. 2016), reacting to chemotactic cues from CCL19 and CCL21 produced by T zone stroma. CCR7 has also been reported to play roles in locating MZ B cells to follicles (Muppidi, Arnon et al. 2011), indicating its potential role in MZ B cell shuttling (Arnon, Horton et al. 2013). Another important chemokine receptor is CXCR5, which is highly expressed on B cells. Its ligand CXCL13 is enriched in B cell follicles and forms a gradient from follicle to outer regions. CXCL13 and CXCR5 paired to help B cells localise to B cell follicles. In order to follow these processes, the expression levels of CCR7 and CXCR5 on IgMg1 and IgMwt B cells were detected by flow cytometry.

Follicular and MZ B cells subpopulations were gated as described before (Fig.3.6). While there was no significant difference in CCR7 expression on follicular B cells, the expression of CCR7 on MZ B cells was slightly but significantly higher in IgMg1 mice (Fig. 3.33A). CXCR5 expression was unchanged between IgMg1 and IgMwt

MZ B cells (Fig. 3.33B). Higher expression level of CCR7 suggests that IgMg1 MZ B cells are more sensitive to the CCL19/21 chemokine gradient produced by the T zone, and confirms that these cells are in a pre-activated stage with increased movement into the follicular areas.
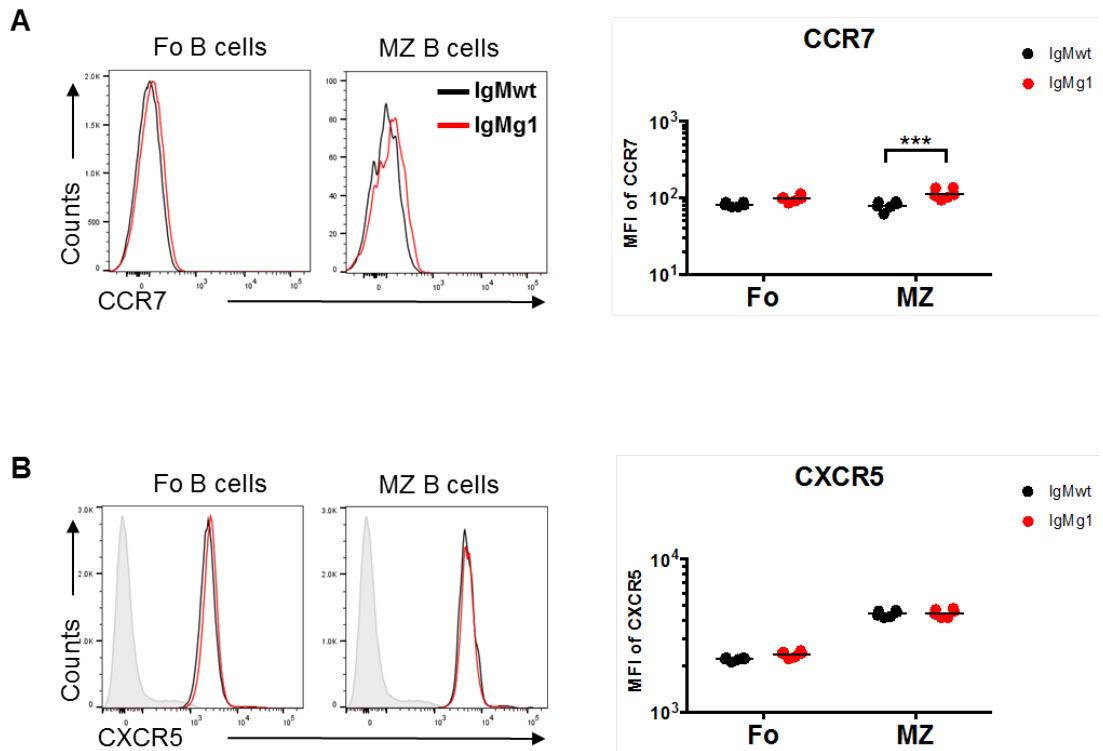
Figure 3.33: Increased CCR7 expression but similar CXCR5 expression on MZ B cells in IgMg1 mice.

Gates for MZ and Fo B cells are similar as showed before in Fig. 3.6.
- A. Overlays and summarizing statistics of surface CCR7 expression levels on follicular and MZ B cells from IgMwt (black) and IgMg1 (red).
- B. Overlays and summarizing statistics of surface CXCR5 expression levels on spleen B cells from IgMwt (black) and IgMg1 (red). Gray: CXCR5 expression level on T cells as a control.

***p < 0.001; 2-way ANONA. Bars indicate mean. Data are representative from two independent experiments.

3.3 Discussion

3.3.1 IgMg1 B cells have been induced into anergic state during B cell development

Previous studies on BCR signalling have shown that mutations in repressors

of BCR signalling result in hyper-activated B cells and auto-immune diseases (Hibbs,

Tarlinton et al. 1995, O'Keefe, Williams et al. 1996, Getahun, Beavers et al. 2016).

Mutation of CD22 for example, leads to enhanced calcium influx, higher expression

levels of CD86 and increased proliferation after BCR ligation (O'Keefe, Williams et

al. 1996). B cells of Lyn$^{-/-}$ mice show enhanced Jun N-terminal kinase (JNK) activity

and increased calcium influx after activation through BCR (Chan, Lowell et al. 1998,

Cornall, Cyster et al. 1998). Furthermore, loss of SHP-1 in anergic B cells leads to

restoration of activated BCR signalling (O'Neill, Getahun et al. 2011, Getahun,

Beavers et al. 2016). In this study, we were trying to enhance BCR signalling by

adding the IgG1 cytoplasmic region to IgM. However, contradictory to what we

expected, after BCR ligation by anti-IgM, immature B cells display reduced BCR

signalling, shown by significantly lower elevation of p-SYK and p-BLNK,

resembling anergy. This anergic-like signalling pattern was also observed in all

mature B cell populations. Following stimulation via BCR ligation, recirculating

IgMg1 Fo B cells generate lower signalling levels than IgMwt B cells, reflected by

lower calcium influx and weaker elevation of protein phosphorylation. Additionally,

BM immature B cells, another circulating naïve B cell population, also display

significantly lower elevation of p-SYK and p-BLNK after BCR ligation. More

significant inhibition of activated BCR signalling is observed in MZ B cells. The

defining feature of B cell anergy is the absence of or reduced signalling down-stream of the BCR (Goodnow, Crosbie et al. 1988, Shlomchik 2008), these results suggest that rather than being hyper-activated after BCR ligation, both immature and mature B cells in IgMg1 mice are in a state of anergy.

Anergic B cells in the classical anergic HEL mouse model (MD4 × ML5) and lupus mouse models display a hyper-activated tonic state (Cambier, Gauld et al. 2007), which leads to the assumption that anergic B cells are hyper-activated cells at steady state. In this IgMg1 mouse model, BM immature B cells display slightly higher tonic Nur77-GFP levels compared to WT, but display comparable tonic p-SYK and p-BLNK expression levels. The two recirculating naïve mature B cell subsets, spleen Fo B cells and BM mature B cells, show slightly lower or comparable tonic BCR signalling levels in IgMg1 mice compared to WT, reflected by: Nur77-GFP expression levels, basal soluble calcium level after *in vitro* rest and tonic p-SYK and p-BLNK levels (Fig. 3.26, 3.27, 3.29 and 3.30). However, MZ B cells in IgMg1 mice are hyper-activated at the steady state, showing significantly stronger tonic BCR signalling and up-regulated surface expression of CCR7. As recirculating B cells are the dominant mature B cell populations in IgMg1 mice, these results demonstrate that unlike anergic HEL-specific B cells, the majority of B cells in IgMg1 mice are not hyper-activated at the tonic state.

Apart from reduced BCR signalling after IgM ligation, surface IgM expression on all B cell populations in IgMg1 mice is found to be ≤50% that of their WT counterparts.

The down-regulation of surface IgM is observed in the majority of anergic B cell mouse models (Cambier, Gauld et al. 2007), and has been used to define anergic B cell populations in humans (Duty, Szodoray et al. 2009). There is a trend of increased suppression of surface IgM expression from immature B cells to mature B cells in IgMg1 mice during B cell development. However, the enhanced suppression of IgM does not seem to link with a more stringent anergic state. With less than 30% reduction of surface IgM expression compared to IgMwt B cells, IgMg1 immature B cells show more significant repression of activated BCR signalling than IgMg1 Fo B cells, which show more than 50% reduction of surface IgM expression.

In some models of B cell anergy, anergic B cells were reported present in ectopic locations, such as the T-B border (Mandik-Nayak, Bui et al. 1997, Noorchashm, Bui et al. 1999, Cambier, Gauld et al. 2007). In the IgMg1 model, MZ B cells are ectopically present in the follicular region, which can be interpreted as a movement towards the T zone.

In the IgMg1 model, significantly reduced BCR signalling following BCR ligation, combined with the reduced surface IgM expression in all B cell populations again strongly suggests that B cells in IgMg1 mice have entered an anergic state, and this phenotype begins to show at the immature B cell stage.

3.3.2 Extra signalling from the cytoplasmic region of IgG1 leads to anergy induction during immature B cell stage of B cell development

B cell anergy is induced by extra signalling from BCR ligation with self-antigen during negative check points of B cell development (Brink and Phan 2018). Results from Nur77-GFP reporter mice show that IgMg1, containing the IgG1 cytoplasmic region, is initially able to transduce stronger downstream signalling than IgM in immature and transitional B cells during BM stage. As IgMg1 is intrinsically able to transduce a stronger down-stream BCR signal, IgMg1 BCRs with low affinity toward self-antigen may transduce signalling that is relatively stronger than WT IgM BCR with the same specificity. This stronger signalling from IgMg1/self-ligand binding could be translated into increased negative selection during B cell development.

There are two negative selection checkpoints against auto-reactivity during B cell development: (i) immature B cell stage and (ii) transitional T1 stage. During these two stages, self-antigens are displayed in the BM micro-environment or are expressed on peripheral tissues (Mandik-Nayak, Bui et al. 1997, Noorchashm, Bui et al. 1999, Cambier, Gauld et al. 2007) . Depending on their affinity toward self-antigen, B cells are either deleted, modified, induced into anergy, or allowed to further differentiate (Jacobi and Diamond 2005, Meffre and Wardemann 2008, Pelanda and Torres 2012). The Nur77-GFP expression level is attenuated during BM development in IgMg1 mice, with significantly decreased Nur77-GFP expression in BM mature B cells compared to transitional B cells. There is no such attenuation of Nur77-GFP

expression during peripheral development of IgMg1 B cell subsets. Furthermore, IgMg1 immature B cells have already acquired the features of anergic B cells. Thus the key process of anergy induction should happen no later than immature B cell stage. This is consistent with a previous observation showing that the main strategy of negative regulation at the immature B cell and T1 stages are different. Immature B cells are more resistant to apoptosis induction, while 70-80% of T1 cells are deleted (Carsetti, Kohler et al. 1995). Thus, anergy induction or light chain editing could be the main strategies adopted at the immature B cell stage to deal with auto-reactive B cells (Gay, Saunders et al. 1993, Tiegs, Russell et al. 1993, Prak and Weigert 1995). However, auto-reactive B cells are mainly deleted at the T1 stage (Russell, Dembic et al. 1991, Jacobi and Diamond 2005) . In line with this, results in this study show either percentages or absolute numbers of IgMg1 T1 B cells are significantly reduced in IgMg1homozygous mice or in IgMwt/IgMg1 heterozygous.

Previous studies show that the maintenance of unresponsiveness of anergic B cells requires continuous presence of inhibitory signalling by both SHP-1 and SHIP-1 (O'Neill, Getahun et al. 2011, Getahun, Beavers et al. 2016). These pathways could be involved in the maintenance of a low-responsive state of IgMg1 B cells as well. After BCR stimulation, the elevation of p-SYK in IgMg1 Fo B cells is quite similar to IgMwt Fo B cells. However, there is a significantly reduced elevation of p-BLNK in IgMg1 Fo B cells, suggesting that the signalling transduction from p-SYK to p-BLNK is impaired in IgMg1 Fo B cells. SHP-1 is known to down-regulate p-SYK activity (Maeda, Scharenberg et al. 1999, Rolli, Gallwitz et al. 2002) and is reported to repress

phosphorylation of BLNK by p-SYK in B cells (Mizuno, Tagawa et al. 2000). Thus SHP-1 could inhibit signalling transduction from p-SYK to BLNK and maintain the low-responsive state of IgMg1 B cells. The impaired phosphorylation of BLNK might lead to weaker calcium influx and decreased elevation of total phosphotyrosines observed in IgMg1 splenic B cells. The function of SHP-1 and the mechanism behind the maintenance of the low-responsive state of IgMg1 B cells could be further studied.

3.3.3 The expression of IgMg1 chimeric BCR affected B cell development

In both IgMg1 homozygous and heterozygous mice, no major effect on IgMg1 B cell development during BM stage is detected, despite significantly higher numbers of mature IgMg1 B cells in BM. The majority of BM mature B cells come from recirculation of peripheral mature Fo B cells, but 15% derive from direct maturation in BM (Cariappa, Chase et al. 2007, Lindsley, Thomas et al. 2007). The increased number of mature IgMg1 B cells could either come from enhanced circulation from the periphery, or from increased direct maturation of IgMg1 Fo B cells in BM.

During peripheral stage, the percentages of T1 B cells are significantly reduced in IgMg1 homozygous mice. Consistent with this trend, H[b] IgMg1 B cells are less competitive at differentiating into T1 B cells compared to H[a] IgMwt B cells. However, IgMg1 B cells show a survival advantage when they differentiate into T2+3 cells, which leads to only a slightly reduced percentage of T2+3 B cells in homozygous IgMg1 mice and a higher percentage of T2+3 B cells in IgMwt/IgMg1 heterozygous mice. These results suggest that IgMg1 T1 B cells can possibly proliferate faster to

generate more daughter T2+3 B cells. T2 B cells are the direct precursors of MZ and Fo B cells (Pillai, Cariappa et al. 2005). Previous studies have shown that fate decisions of MZ and Fo B cells are highly sensitive to BCR signalling strength (Cariappa, Tang et al. 2001, Samardzic, Marinkovic et al. 2002). Results of peripheral B cell development demonstrate that the changed signalling from the IgMg1 BCR seem to preferentially promote Fo B cell generation. The larger Fo B cell populations in IgMg1 mice could be explained by three different situations. Firstly, altered signalling in IgMg1 T2 B cells could favour Fo B cell differentiation. Secondly, the proportion of T2 cells committing to Fo B cell fate could be the same in IgMg1 and IgMwt mice, but T2 IgMg1 B cells could proliferate faster to produce higher numbers of Fo B cells. Thirdly, the percentages of precursor cells and proliferation rate both be unchanged in T2 IgMg1 B cells, but newly generated Fo B cells in IgMg1 mice could have a longer life span. Additional experiments are needed to verify these possibilities and reveal the mechanisms of the impact of IgMg1 BCR signalling on peripheral B cell fate decisions.

Studies have shown that silenced or non-silenced self-reactive B cells are retained in the mature Fo B cell compartment (Wardemann, Yurasov et al. 2003, Zikherman, Parameswaran et al. 2012). This can be evolutionarily advantageous. MZ B cells have higher levels of tonic BCR signalling (Fig. 3.26 and 3.29) and CD21 (Oliver, Martin et al. 1999, Cariappa, Tang et al. 2001), can be immediately activated and can mount an immune response when they encounter cognate antigen, without the need for T cell help (Oliver, Martin et al. 1997, Oliver, Martin et al. 1999). On the contrary, Fo B

cells have relatively fine-tuned tonic BCR signalling (Noviski, Mueller et al. 2018)), which is lower than MZ B cells (Fig. 3.26 and 3.29). They localise in B cell follicles and are less likely to encounter antigen directly from blood. Fo B cells are normally involved in the T-D immune response and require co-stimulation signals from T cells for complete activation. Thus, Fo B cells can be better controlled and are more easily supervised during their activation. From this point of view, with the extra signalling from the IgG1 tail, IgMg1 B cells are treated as auto-reactive B cells and are more likely to be induced into Fo B cell fate.

3.3.4 Outlook on the next chapter

The results of the current studies on IgMg1 B cells suggest that these cells have been induced into an anergic state during B cell development. By preserving germ-line VDJ regions and allowing for random rearrangements, mature B cells in IgMg1 mice should be poly-clonal anergic B cells. This enables us to further study the behaviours of poly-clonal anergic B cells during immune responses, with a focus on the regulation of anergic B cells during GC reactions.

Chapter 4 . Antigen-induced differentiation of anergic B cells in the IgMg1 mouse model

4.1 Introduction

4.1.1 Animal models of B cell anergy and their limitations

The functional silence of self-antigen-specific B cells was first described by Goodnow *et.al* using hen egg lysozyme (HEL)-specific B cell receptor (BCR) transgene mouse model which also has general endogenous expression of HEL (Goodnow, Crosbie et al. 1988). The general knowledge of B cell anergy has developed based on this model (Glynne, Ghandour et al. 2000, Burnett, Langley et al. 2018). However, the application of this HEL mouse model to study breakage of immune tolerance in autoimmune diseases such as lupus failed. The limitation of BCR specificities, being only HEL-specific, contributed to the failure of these experiments (Shlomchik 2008). More recently generated animal models of B cell anergy which are specific for natural endogenous auto-antigens, such as chromatin and insulin to study lupus or diabetes, are also limited by the fact that specificity only toward one or limited number of auto-antigens can be investigated. The endogenous wild type VDJ repertoire for the BCR is lost in all of these BCR transgene anergic models and B cells are not able to respond to other self-antigens. Further, the anergic patterns in these animal models varied (Erikson, Radic et al. 1991, Santulli-Marotto, Retter et al. 1998, Benschop, Aviszus et al. 2001, Rojas, Hulbert et al. 2001). The diversity of these anergic phenotypes can be partly explained by their distinct BCRs binding to different self-

antigens in different ways, such as different affinities for self-antigens, different sites of encountering the antigen (Cambier, Gauld et al. 2007). As anergic B cells have been estimated to account for almost a quarter of peripheral mature B cells and have a wide spectrum of both BCR specificities and affinities (Grandien, Fucs et al. 1994, Cambier, Gauld et al. 2007), a mouse model with poly-clonal anergic B cells would be useful to study this diverse population.

Until recently, the main interest of anergic B cell studies remained to be the relationship between anergic B cells and auto-immune diseases. Less attention has been paid to why our immune system would risk to preserve such a big quantity of these potentially auto-reactive B cells.

It has been shown that anergic B cells can be involved in immune responses by recruiting them into germinal centres (GCs) (Cappione, Anolik et al. 2005, Sabouri, Schofield et al. 2014, Williams, Bonami et al. 2015). Very recently, the activation and salvage of HEL-specific anergic B cells through recruitment into the GC response and hypermutation away from self-specificity has been described by Burnett *et al.* (Burnett, Langley et al. 2018). This process has been labelled "clonal redemption". By generating BM chimeras, HEL-specific BCR transgenic B cells were exposed in a HEL expressing (self-antigen) environment, which induced an anergic state. These mice were then immunised with duck egg lysozyme (DEL) as a model for a non-self (foreign) antigen. DEL is highly crossreactive with HEL and has only 4 amino acid residues difference to HEL. It was observed that these HEL-specific anergic B cells

were recruited well into the GC response. During the GC reaction, HEL-specific B cells were allowed to evolve away from self-reactivity through mutations to remove self-binding. This was followed by an accumulation of higher affinity B cells specific for DEL (Schofield et al. 2014, Burnett, Langley et al. 2018). Molecular mimicry is adopted by many pathogens in order to mimic self-antigen and to escape immune surveillance (Pinschewer, Perez et al. 2004, Scherer, Zwick et al. 2007, Gristick, von Boehmer et al. 2016). Thus, keeping self-antigen cross-reactive B cells in the repertoire, but silencing them by inducing anergy, from which they can escape by clonal redemption, is a potential benefit in the defence against invasion of pathogens using molecular mimicry. This way these silenced self-reactive B cells can stay in the repertoire at low risk of causing auto-immune diseases.

The studies mentioned have shed light on the physiological function of anergic B cells, however, inevitably brought another question: how are anergic B cells regulated to accomplish clonal redemption during GC reactions?

4.1.2 B cell receptor signalling and B cell fate decisions during the GC response

The GC is the place where antigen-specific B cells undergo affinity maturation. This evolution towards higher affinity for specific epitope is not a random process but is based on complex selection within GCs. Currently, the favoured model is the "T cell centric" model (Mesin, Ersching et al. 2016), where B cells take a passive role and B cell fate decisions are directed by Tfh cells (Batista and Neuberger 2000, Allen,

Okada et al. 2007, Schwickert, Victora et al. 2011, Gitlin, Mayer et al. 2015). Another well-known model is antibody feedback, where B cells with higher BCR affinity could get greater access to antigens and thus present more antigen through p-MHCII in order to receive T cell help for selection (Meyer-Hermann, Mohr et al. 2012, Zhang, Meyer-Hermann et al. 2013). This suggests BCR affinity and signalling strength could be additional factors which drive the selection. In this model, stronger BCR signalling would cause B cells with higher affinity to become more competitive by presenting higher amounts of antigen as p-MHCII or forming stronger T - B cell interactions. The duration and strength of this T-B interaction will affect GC B cell fate decisions.

Potential differences in BCR signalling strength not only derives from the affinity of the BCR - antigen interaction, but can also come from intrinsic changes in the activation state of B cells. Compared to normal non-self-reactive naïve B cells, anergic B cells present a unique gene expression pattern and reduced BCR signalling after activation (Goodnow, Crosbie et al. 1988, Glynne, Ghandour et al. 2000). Being a large population within peripheral mature B cells (Grandien, Fucs et al. 1994, Wardemann, Yurasov et al. 2003), it is hard to ignore anergic B cells and their involvement into GC reactions. Clonal redemption has been proposed as a model where anergic B cells evolve away from auto-reactivity and towards specificity to cross-reactive foreign antigens in the GC (Sabouri, Schofield et al. 2014, Reed, Jackson et al. 2016, Burnett, Langley et al. 2018). However, the selection mechanisms behind clonal redemption are not clear. The study from Chan et al suggests that the

selection against auto-reactivity in GCs depends on the concentrations and locations of auto-antigens (Chan, Wood et al. 2012). Thus, the selection and modification of GC B cells generated from activated anergic B cells should also depend on the presence of self-antigen. It remains elusive how the positive selection signalling from foreign antigen and negative selection signalling from self-antigen work together to modify these B cells during GC reactions. Besides these hypothetical positive and negative signals, active BCR signalling in anergic B cells is intrinsically different from naïve non-self-reactive B cells, as shown by observations of *in vitro* stimulated anergic and normal mature B cells through their BCRs (Erikson, Radic et al. 1991, Goodnow, Brink et al. 1991, Benschop, Aviszus et al. 2001). It is not known how long this rewired BCR signalling in anergic B cells remains after they are activated and become GC B cells, and how far this rewired BCR signalling would affect BCR selection during the GC response.

Another potential effect which might affect BCR signalling in GC B cells are the isotypes of surface BCRs. During or preceding the GC response, the majority of GC B cells lose surface IgM expression and go through class-switch to express IgG1 or other isotypes (Toellner, Gulbranson-Judge et al. 1996, Toellner, Luther et al. 1998, Marshall, Zhang et al. 2011). Different BCR isotypes have different length cytoplasmic regions that can transduce different strength down-stream BCR signalling. Among these, the best understood is IgG1, which can signal independently of Igα/β and can transduce stronger downstream BCR signals (Waisman, Kraus et al. 2007, Engels, Konig et al. 2009, Weston-Bell, Forconi et al. 2014). IgE[+] GC B cells are

known to be disfavoured during GC selection. Despite having the same specificity, once GC B cells have switched to express IgE$^+$ on the surface, they are more prone to be induced into apoptosis (Yang, Sullivan et al. 2012, He, Meyer-Hermann et al. 2013). However, the mechanisms of the influence of different signalling patterns from different isotypes of BCRs on GC B cell selections remains to be revealed. In our IgMg1 mouse model, altered BCR signalling through IgMg1 would disappear after they cease IgM expression and switch to express other isotypes, such as IgG1.

4.1.3 Objective

The work presented in this chapter is based on the hypothesis that changed BCR signalling, in the poly-clonal IgMg1 knock-in mouse model described in Chapter 3, generated a mouse model with poly-clonal anergic B cells. *In vivo* responses of anergic B cells to TI-II antigens are not well studied. However, when stimulated *in vitro* with anti-IgM antibody to activate anergic B cells through BCR, anergic B cells are not able to respond or only mount reduced activated BCR signalling. In this chapter, the immune responses of these anergic IgMg1 B cells toward TI-II were analysed in order to test the capability of these cells to undergo plasma cell responses after activation through surface BCRs without T cell help. The ability of anergic B cells to join GC responses through clonal redemption is reported, however, factors involved into this directed selection within GC response are poorly understood. In this chapter, the immune response of these anergic IgMg1 B cells toward TD antigens and

the detailed process of GC reactions were investigated by immunisation and the study of antigen-induced B cell differentiation in time course experiments.

Aims are detailed as follows:

1. How do anergic IgMg1 B cells respond to TI-II and T-D antigens? Are they behaving differently to IgMwt non-self-reactive B cells?

    A. B cell differentiation in the TI-II immune response

    B. B cell differentiation in the T-D immune response

2. The dynamic process of GC reactions in IgMwt and IgMg1 mice.

    A. The emergence B cell populations generated during GC response

    B. Proliferation and apoptotic rates during the GC response

    C. Class switch of GC B cells

    D. BCR signalling strength during the GC response

3. Are IgMg1 B cells influencing Tfh differentiation

    A. Test the generation of Tfh cells during GC responses

4.2 Results

In Chapter 3 we have characterised the newly generated IgMg1 mouse, and noticed that IgMg1 B cells are displaying an anergic pattern, with clearly suppressed BCR signalling after activation. In this chapter we utilise this poly-clonal anergic B cell mouse model to study the impact of the changed signalling in anergic B cells on their *in vivo* activation and fate decisions.

4.2.1 Impaired TI-II immune response in IgMg1 mice

Previous studies aimed at revealing the role of anergic B cells in auto-immune diseases were limited by single or limited specificity of transgenic BCR(s) present in the B cell repertoire of anergic mouse models used in these studies. The *in vivo* response of anergic B cells toward TI-II antigens is poorly studied. Despite this, it has been shown that *in vitro* stimulation of anergic B cells through IgM ligation leads to absent or severely reduced activation BCR signalling (Erikson, Radic et al. 1991, Goodnow, Brink et al. 1991, Benschop, Aviszus et al. 2001). This indicates that the ability of anergic B cells responding to TI-II antigens might be impaired. Therefore, we studied the responses of our poly-clonal anergic IgMg1 B cells to the TI-II antigen NP-Ficoll *in vivo*.

In order to induce splenic TI-II B cell responses, both IgMg1 and IgMwt control mice were immunised with i.p. NP-Ficoll. Development of splenic plasma cells and NP-responding B cells was followed at the peak of the extrafollicular plasmablast

response (Garcia de Vinuesa, O'Leary et al. 1999). Fig. 4.1B shows percentages of plasma cells and antigen-specific plasma cells and B cells 5 days after NP-Ficoll immunisation. A summary of all experiments, normalized to remove variation between different immunisation experiments is shown in Fig. 4.1C. Flow cytometric analysis showed that significantly fewer NP-specific B cells were generated in IgMg1 mice at day 5 after immunisation with NP-Ficoll, with antigen-specific CD138$^-$ B blasts accounting for 0.7% of lymphocytes in IgMwt and 0.2% of B220$^+$ cells in IgMg1 mice (Fig. 4.1A, B and C left). Plasma cells are the main responding B cell population generated in TI-II immunisation (Garcia de Vinuesa, O'Leary et al. 1999). Both total plasma cells and NP-specific plasma cells were reduced by 50% in IgMg1 mice (Fig. 4.1B and C middle, right).

As NP-PE may bind B cells non-specifically, unimmunised control mice were used to identify non-specific background staining of B cells (Fig 4.2A). While five days after immunisation there was a clear increase of NP-specific CD138$^-$ B blasts in IgMwt mice, the percentages of NP-binding B cells in IgMg1 mice remained low and did not rise above the high background levels observed by flow cytometry (Fig. 4.2A and B). Staining of NP-specific plasma cells, however, was specific and no antigen-specific PCs were detected in unimmunised mice (Fig. 4.2 C). In summary, Fig. 4.1 and Fig 4.2 indicate that IgMg1 B cells can form plasma cells in response to NP-Ficoll, but at significantly lower efficiency than IgMwt B cells, while B blast numbers at day 5 post immunisation are severely reduced and not detectable using this method.

To confirm this observation, spleen sections from immunised IgMwt and IgMg1 mice were stained, to assess plasma cell clusters *in situ*. Transcription factor IRF4 is required for the generation of plasma cells, is strongly expressed by plasma cells (Klein, Casola et al. 2006) and therefore was selected as a marker for plasma cells. Anti-IgD, staining naïve B cells, was used to identify follicular areas. NP conjugated to sheep Ig was used to check the antigen-specificity of these plasma cells, CD4 was used to outline T-zone (Fig. 4.3A). Images confirmed that $IRF4^+NP^+IgD^-CD4^-$ plasma cell clusters (white arrow heads) accumulating in the splenic bridging channels in IgMg1 spleens were significantly smaller than their IgMwt counterparts (Fig. 4.3A, B and C). This further confirmed smaller numbers of antigen-specific B blasts (green arrow heads) formed in IgMg1 mice. There was no obvious difference in the migration of these cells, as they had similar locations in both IgMg1 and IgMwt mice in the outer T zone and bridging channels (Garcia de Vinuesa, O'Leary et al. 1999)(Fig, 4.3A).

Furthermore, NP-specific serum antibodies in IgMg1 mice were analysed. This showed that the median titres of antigen-specific IgM and IgG3 were also reduced by 30% and 32% respectively in IgMg1 mice, although these differences were not significant (Fig. 4.4). Surprisingly, although class switch recombination leads to a loss of expressed IgMg1 BCR, meaning IgG3 switched B blasts from IgMwt and IgMg1 mice should be genetically identical, IgM and IgG3 antibody titres in IgMg1 mice show a similar slight reduction.

Together, the results from both flow cytometry and immunofluorescence suggest IgMg1 B cells have a reduced ability to respond to TI-II antigens by forming lower numbers of B blasts and plasma cells. This is consistent with the *in vitro* BCR stimulation experiments described in chapter 3 (Fig. 3.27-3.30), which showed that anti-IgM stimulation induced BCR signalling of IgMg1 B cells results in a lower induction of protein phosphorylation and lagging calcium influx. This observation is consistent with IgMg1 B cells representing an anergic state that is not licensed to effectively differentiate into plasma cells without first undergoing GC differentiation (Burnett, Langley et al. 2018).
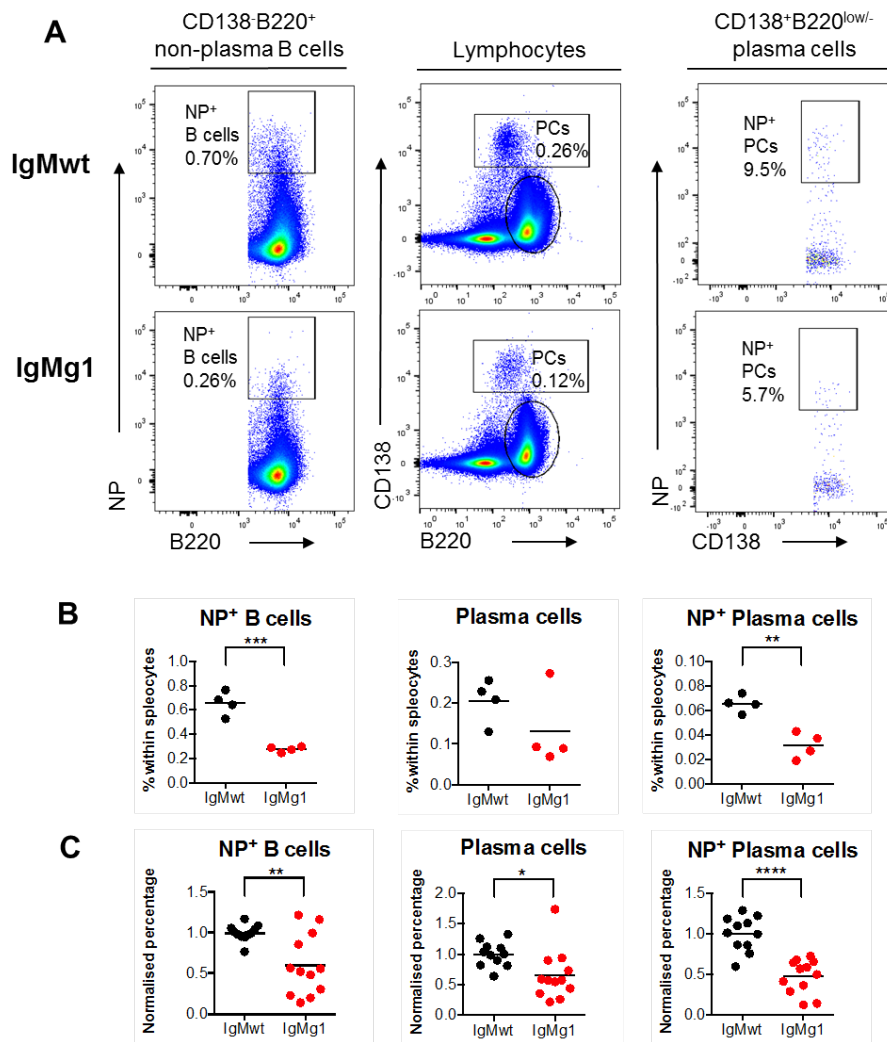
Figure 4.1: Impaired NP-Ficoll induced B cell response and plasma cell differentiation in IgMg1 mice.

Both IgMg1 and IgMwt mice are immunised i.p. with 30 μg NP-Ficoll. Spleens are collected 5 days after immunisation.

A. Gate settings of T-I immune response after NP-Ficoll immunisation. Gates for plasma cells (PCs), NP-specific B cells and NP-specific PCs are displayed.
B. The percentages of NP-specific B cells, total plasma cells and NP-specific plasma cells. Representative data from three independent experiments.
C. Normalized data merged from all three independent experiments. Data are normalized to the arithmetic average of the wild type data of each experiment, taking this as 1.

* p < 0.05; ** p < 0.01; **** p < 0.0001; unpaired Student's t test. Bars indicate mean. Each symbol represents sample from one mouse. Data are from three independent experiments.
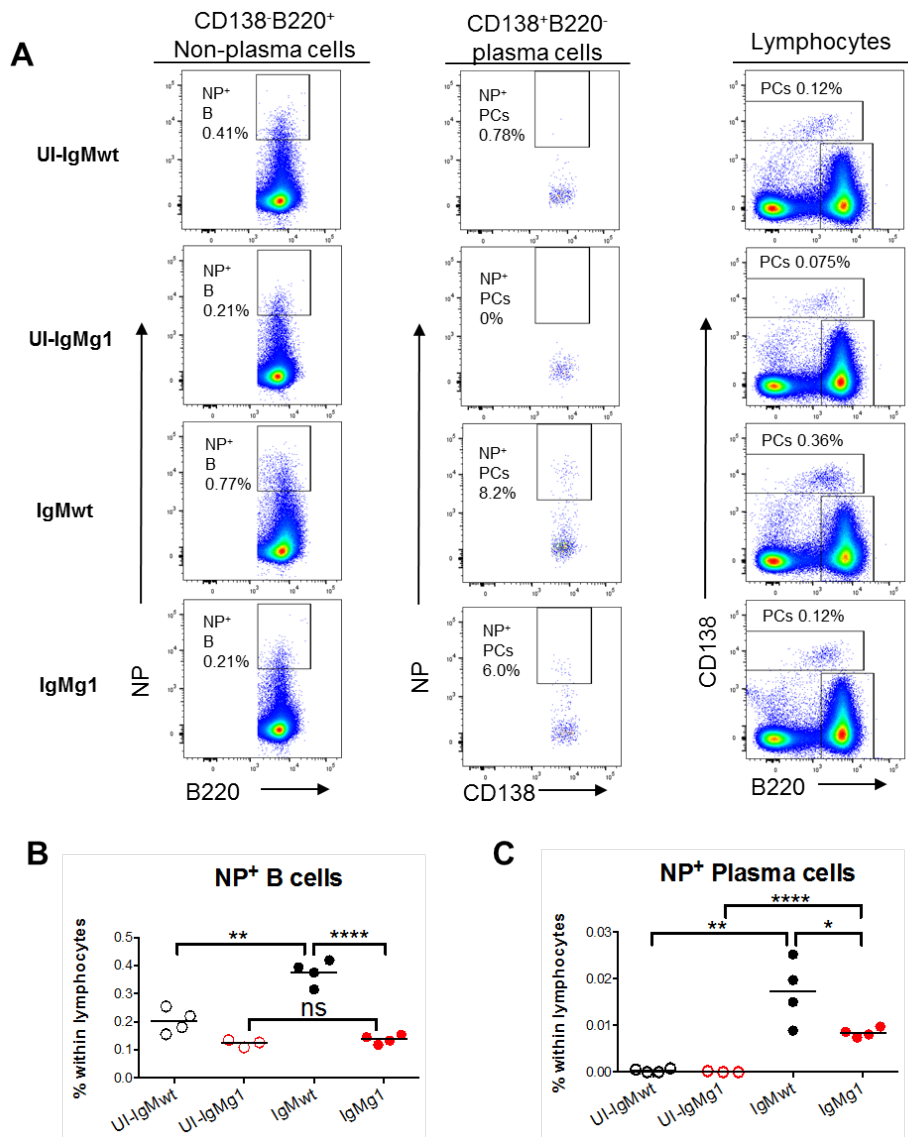
Figure 4.2: IgMg1 mice respond to NP-Ficoll less efficiently than IgMwt mice.

Both IgMg1 and IgMwt mice are immunised i.p. with 30 µg NP-Ficoll. Spleens are collected 5 days after immunisation. Spleens from unimmunised IgMwt and IgMg1 mice as control.

    A. Gate settings of T-I immune response after NP-Ficoll immunisation. Gate settings for plasma cells (PCs), NP-specific B cells and NP-specific PCs are displayed.

    B. The percentages of NP-specific B cells are calculated and compared with unimmunised mice.

    C. The percentages of NP-specific plasma cells are calculated and compared with unimmunised mice.

ns, non-significant; * $p < 0.05$; **** $p < 0.0001$; unpaired Student's t test. Bars indicate mean. Each symbol represent sample from one mouse.
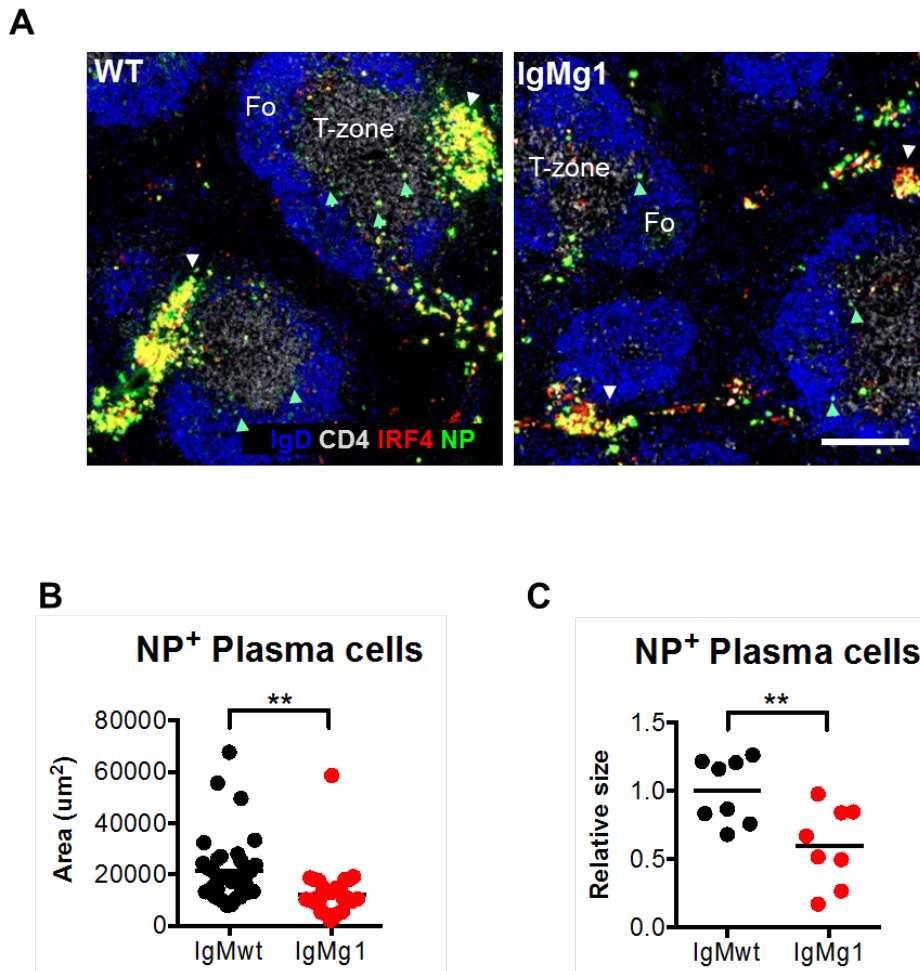
Figure 4.3: Smaller plasma cell clusters in IgMg1 spleen sections.

Spleen sections are from IgMg1 and IgMwt mice at day 5 after i.p. immunised with 30 µg NP-Ficoll.

A. Representative immunofluorescence images of spleen sections from both IgMwt and IgMg1 mice. Sections are stained with NP (green), IRF4 (red), IgD (blue) and CD4 (gray). Plasma cluster is indicated with white arrows. NP-specific B blasts are indicated with green arrows.

B. Area of NP-specific plasma clusters in IgMg1 and IgMwt mice. Each symbol represents one PC cluster, data are combined from 4 mice in one representative experiment.

C. Relative sizes of NP-specific plasma cell clusters are merged from two independent experiments. Data are normalized to the arithmetic average of the wild type data of each experiment, taking this as 1. Data analysis done by Dr. Juan Carlos Yam-Puc.

** $p < 0.01$; unpaired Student's t test. Bars indicate mean. Each symbol represents sample from one mouse. Data are from three independent experiments.
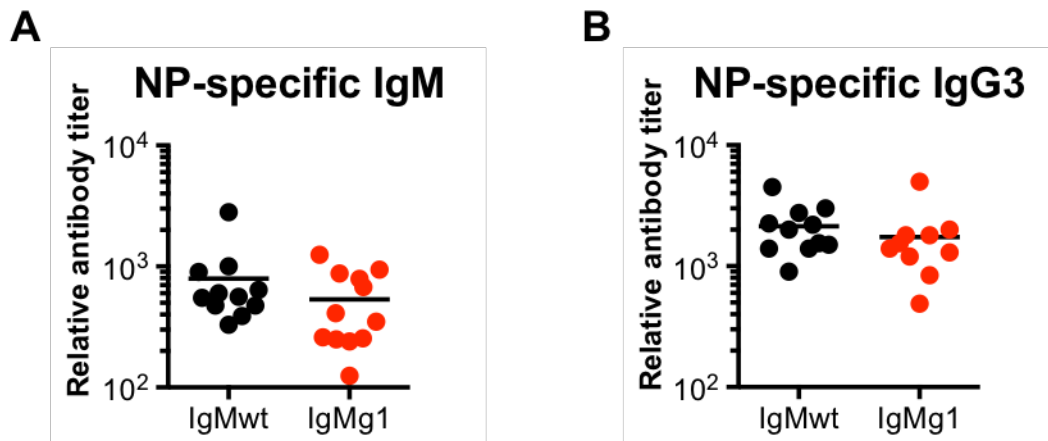
Figure 4.4: IgM and IgG3 tend to be slightly lower in IgMg1 mice.

Both IgMg1 and WT mice are immunised i.p. with 30 µg NP-Ficoll. Serum samples are collected 5 days after immunisation.

A. NP specific IgM antibody titers. NP2-BSA is used to coat plate and used to detect anti-NP IgM titers in both IgMg1 and WT serum samples.
B. NP specific IgG3 antibody titers. NP14-BSA is used to coat plate and used to detect anti-NP IgG3 titers in both IgMg1 and WT serum samples.

ns, not significant; unpaired Student's t test. Bars indicate mean. Each symbol represents sample from one mouse. Data are from three independent experiments.

4.2.2 Consistently larger NP-specific GC B cell compartment in IgMg1 mice 8 days after immunisation with T-D antigen

It was then of interest to know how anergic IgMg1 B cells would behave in a T-dependent antibody response. Mice were immunised in the foot with alum-precipitated NP-CGG with heat-inactivated *Bordetella pertussis* (BP) as an adjuvant. Eight days later, responding B cell populations in the popliteal LNs were analysed. Gate settings for different responding B cell populations are shown in Fig. 4.5. Plasma cells (PCs) were gated as $CD138^+B220^{low/-}$ cells. The NP-specific B cell response was analysed by gating on NP-PE binding B cells. Within this population, NP^+ GC B cells ($CD138^-B220^+NP^+CD38^{low/-}Fas^+$) and NP^+ memory B cells ($CD138^-B220^+NP^+CD38^+Fas^{low/-}$; MBCs) (Conter, Song et al. 2014) were gated (Fig. 4.5).

Fig. 4.6 shows representative percentages of all populations analysed from a representative experiment, while Fig. 4.7 shows a summary of all four experiments. Eight days post immunisation there were no significant changes in overall B cell (Fig. 4.6A, 4.7A) or plasma cell numbers (4.7B), however TD antigen led to an increase in the GC response (Fig. 4.7C). Memory B cell numbers did not significantly change (Fig 4.6D, 4.7D). Analysis of NP-specific B cells showed a more pronounced increase in overall NP-specific B cells (Fig. 4.6E, 4.7E) and NP-specific GC B cells in IgMg1 mice (Fig. 4.6 F, 4.7F). This indicates that IgMg1 B cells, in response to T-D antigens, differentiate more efficiently into GC B cells than IgMwt B cells. The larger population of NP^+ GC B cells (Fig. 4.6F, 4.7F) could either be due to a larger population of NP^+ precursor B cells in IgMg1 mice (Fig. 4.6E, 4.7E), or to a

preferential differentiation of activated NP-specific IgMg1 B cells into GC B cells. To test this, GC B cell percentages within the NP-specific B cells were calculated. While it is impossible to make firm conclusions about fate decisions at the time when GCs are formed, which is 3-5 d before the tissues were analysed (Toellner, Luther et al. 1998), this suggested that a significantly higher percentage of NP-specific B cells had committed to GC B cell fate in IgMg1 mice (Fig. 4.6G, 4.7G).

The analysis of the T-D B cell response 8 d after immunisation indicates that, in the presence of T cell help, IgMg1 B cells are prone to produce good GC response reflected by slightly more total GC B cells and significantly more NP^+ GC B cells. However, the size of both the plasma cell and memory B cell populations, which at this stage of the T-D immune response contains a mix of GC-derived and non-GC-derived cells, are the same (Sze, Toellner et al. 2000, Zhang, Tech et al. 2018), (Kurosaki, Kometani et al. 2015). This would support the idea that anergic B cells are licensed to form GC responses (Sabouri, Schofield et al. 2014, Reed, Jackson et al. 2016, Burnett, Langley et al. 2018), however, non-GC dependent differentiation and GC outputs of plasma cells and memory B cells is not increased, and might even be impaired.

Figure 4.5: Gate settings to analyse T-D immune response in both IgMg1 and WT mice.

Both IgMg1 and WT mice are immunised with 20 µg alum precipitated NP-CGG and heat-inactivated *Bordetella pertussis* (BP) as adjuvant on each plantar surface of foot. Popliteal LNs are collected 8 days after immunisation. Gates for plasma cells (PCs), NP-specific B cells, NP-specific GC B cells and NP-specific memory B cells (MBCs) are displayed.
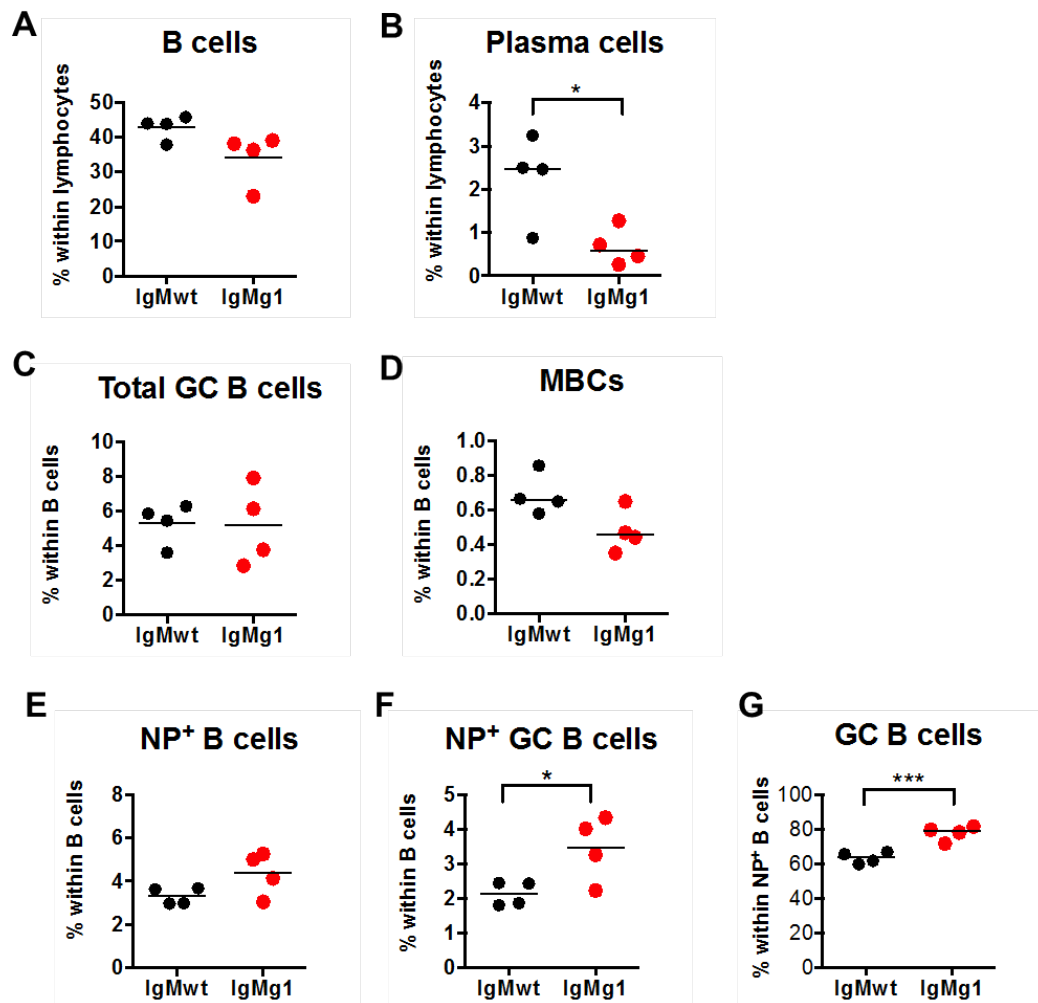
Figure 4.6: Increased GC response after T-D immunisation of IgMg1 mice.

Representative experiment of WT and IgMg1 mice are immunised with 20 µg alum precipitated NP-CGG and heat-inactivated Bordetella pertussis (BP) as adjuvant on the plantar surface of the hind feet. Popliteal LNs are collected 8 days after immunisation.

- A. Percentages of B cells within lymphocytes.
- B. Percentages of plasma cells within lymphocytes.
- C. Percentages of total GC B within B cells.
- D. Percentages of memory B cells within B cells.
- E. Percentages of NP-specific B cells within B cells.
- F. Percentages of NP-specific GC B cells within B cells.
- G. Percentages of NP-specific GC B cells within NP^+ B cells.

$* p < 0.05$; $*** p < 0.001$; unpaired Student's t test. Bars indicate mean. Each symbol represents sample from one mouse. Data were one representative experiment from four independent experiments.
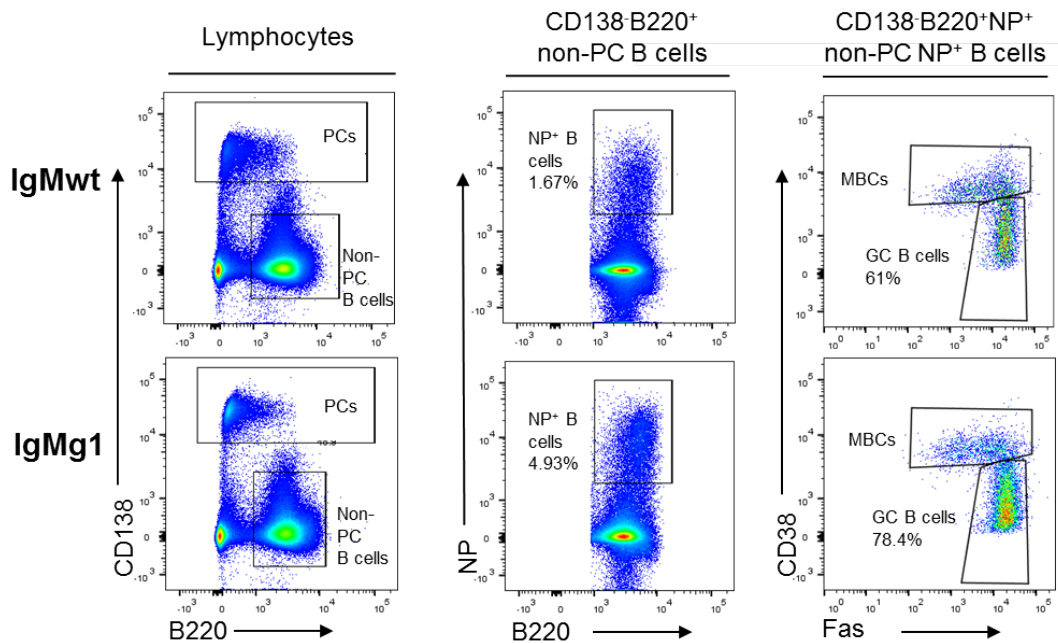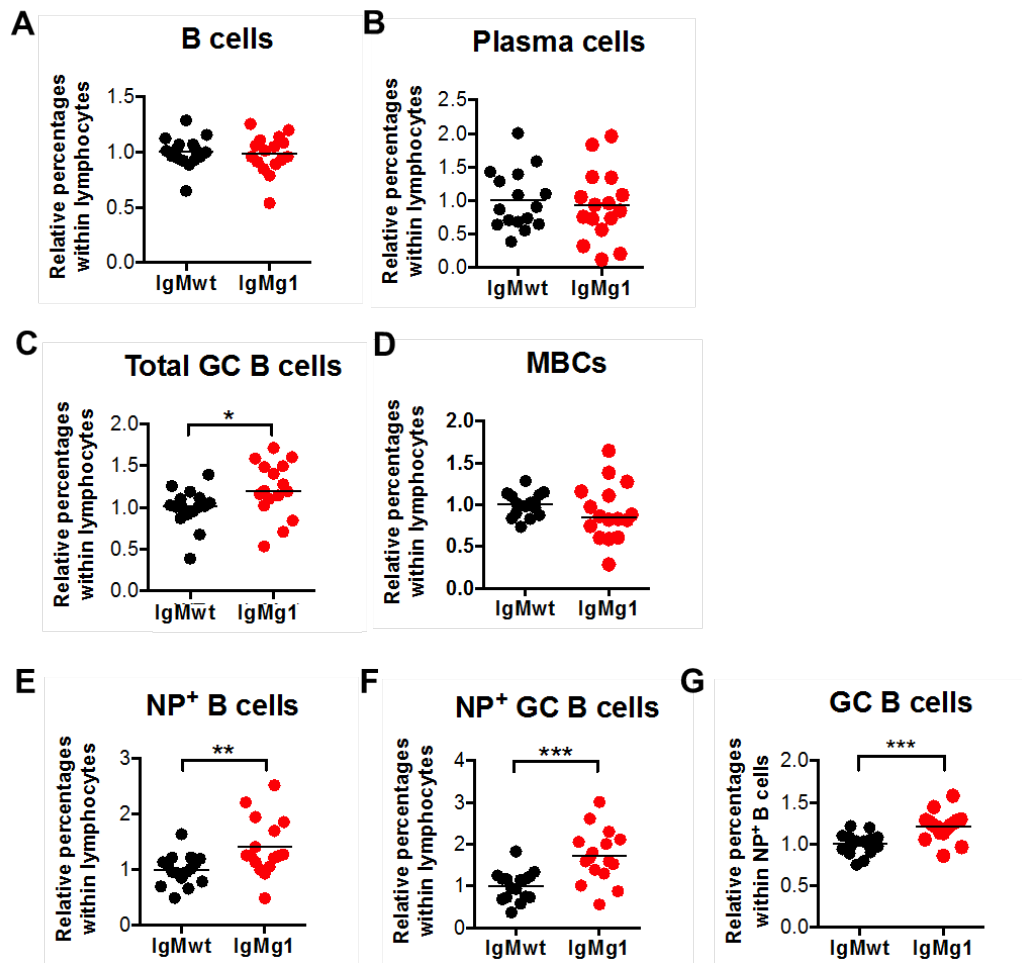
Figure 4.7: Increased GC response after T-D immunisation of IgMg1 mice.

Merged and normalised data of all four independent experiments. WT and IgMg1 mice are immunised with 20 µg alum precipitated NP-CGG and heat-inactivated Bordetella pertussis (BP) as adjuvant on plantar surface of foot. Popliteal LNs are collected 8 days after immunisation.

    A. Relative percentages of B cells merged from four independent experiments. Data are normalized to the arithmetic average of the wild type data of each experiment, taking this as 1.
    B. Relative percentages of plasma cells.
    C. Relative percentages of total GC B cells.
    D. Relative percentages of total memory B cells.
    E. Relative percentages of NP-specific B cells.
    F. Relative percentages of NP-specific GC B cells.
    G. Relative percentages of NP-specific GC B cells within NP$^+$ B cells.

$* \; p < 0.05$; $** \; p < 0.01$; $*** \; p < 0.001$; unpaired Student's t test. Bars indicate mean. Each symbol represents sample from one mouse. Data were merged from four independent experiments.

4.2.3 Delayed early B cell response after immunisation with SRBC in IgMg1 mice

The observations described above were based on results obtained at the peak time of either TI-II or T-D immune responses to the hapten NP. To better understand the early stages of the B cell response, time courses after i.v. immunisation with sheep red blood cells (SRBCs) were performed. SRBC immunisation induces polyclonal B cell activation. They represent complex and large antigens with repetitive carbohydrate epitopes that can induce fast primary responses in the spleen. Unlike hapten-carrier conjugates, such as NP-CGG, SRBCs can induce a relatively strong poly-clonal T-D immune response in the absence of adjuvants (McAllister, Apgar et al. 2017). IgMwt and IgMg1 mice were immunised with SRBC i.v. and numbers of plasma cells ($CD138^+B220^-$) and GC B cells ($CD138^-B220^+CD38^{low/-}Fas^+$) were followed over the first 8 days.

Immunisation with SRBCs leads to a significant increase in plasma cell and GC B cell differentiation from day 4 (Fig. 4.8B and C). Interestingly, while 3 days after immunisation there was no increase in plasma cells or GC B cells yet, there was a reproducible reduction of plasma cells and GC B cells in IgMg1 compared to IgMwt mice (two experiments with 4+4 and 4+3 animals; plasma cell reduction: p=0.0006 and p=0.001, GC B cell reduction: p=0.001 and p=0.06). Immunisation leads to a loss of GC B cells not specific for the immunogen in the first few days of the response (Szakal, Taylor et al. 1990). Therefore, it can be speculated that the smaller numbers of plasma and GC B cells 3 days after immunisation in IgMg1 may represent a

165

smaller population of newly emerging immunisation induced cells. A similar trend was seen on day 4 (Fig. 4.8). Five days after immunisation is the peak of the extra-follicular plasma cell response, and at the same time plasma cell output from GCs starts to be generated (Sze, Toellner et al. 2000, Zhang, Tech et al. 2018). From day 5 there is no longer a significant difference in plasma cell population between IgMg1 and IgMwt mice (Fig. 4.8A right and B), which could indicate a saturation of extrafollicular niches for plasma cells or the impact of increasing plasma cell output from the GC. GC B cells in IgMg1 mice appear in larger numbers from day 5, which may indicate that an equilibrium of proliferation and survival of GC B cells developing by day 5, which makes the effects of the slower onset of GC B cell differentiation and/or GC B cell recruitment disappear (Fig. 4.8A left and C).

The small changes in quantity of GC B cells are due to the combined effects of immigration, proliferation, emigration, and apoptosis. In order to test whether the changes in GC B cell numbers in IgMg1 mice were due to cell proliferation, *in vivo* EdU incorporation was measured.

To measure B cell proliferation rates, EdU was injected i.p. two hours before spleens were being taken. While there was no statistical difference in EdU uptake between IgMg1 and IgMwt mice, EdU incorporation into GC B cells tended to be slightly less on day 3 after immunisation in IgMg1 mice (Fig. 4.9A top and B). One day later, the proliferation rate of GC B cells increased to become slightly higher in IgMg1 mice (Fig. 4.9 A bottom and B). This is in line with changes in accumulation of GC B cells

3 and 4 d after immunisation (Fig. 4.8C). EdU incorporation into plasmablasts was the same on day 3, which would be in line with the hypothesis that the lower number of plasma cells was due to lower recruitment on day 3 (Fig. 4.10A and B). Four days post immunisation there was significantly less EdU incorporation into IgMg1 plasmablasts (Fig.4.10B), indicating that the lower percentages of plasma cells in IgMg1 mice on day 4 can be explained by changes in recruitment and proliferation.
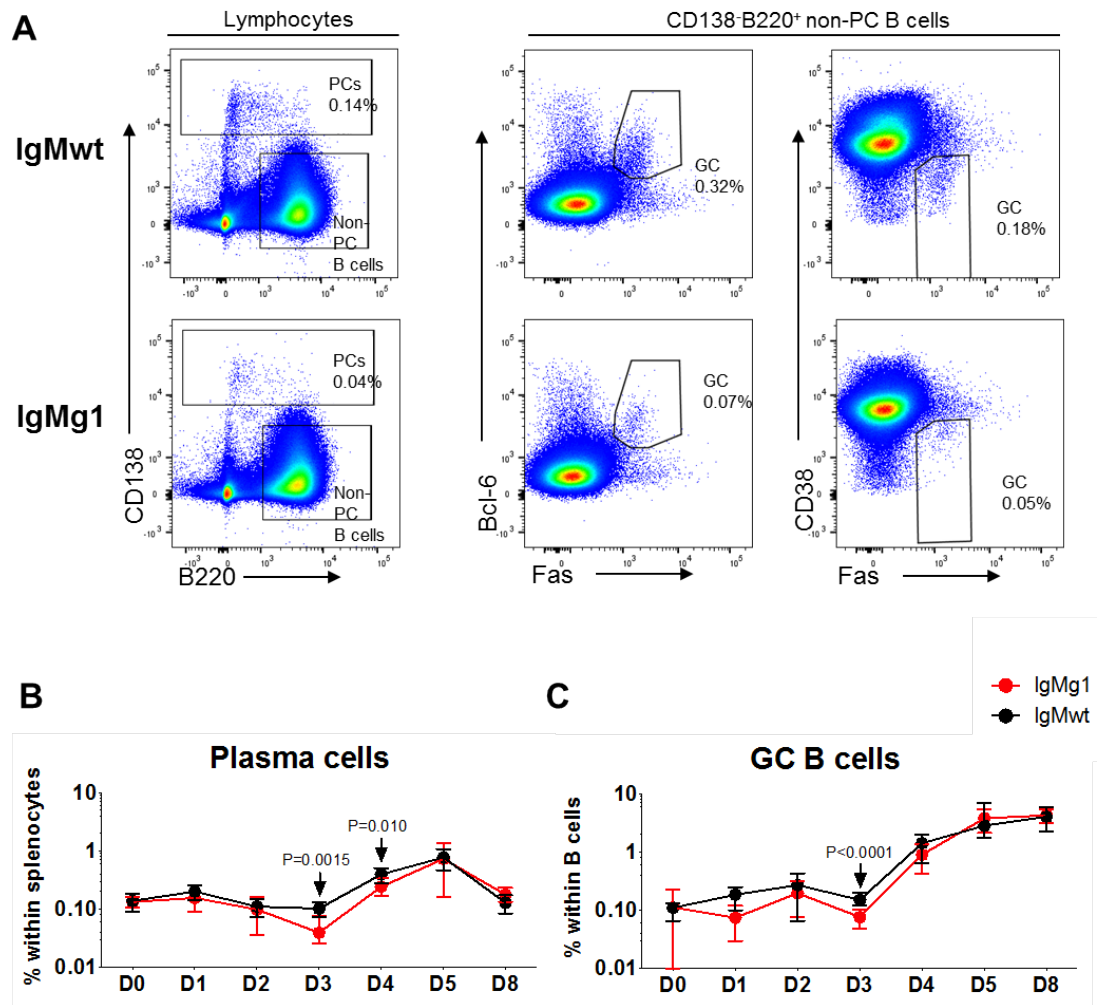
Figure 4.8: Early-delayed response of IgMg1 B cells towards SRBCs immunisation.

IgMwt and IgMg1 mice are i.v. immunised with 2 x10^{8} SRBCs. Spleens are collected at each indicated time point from day 0 to day 8 after immunisation.

   A. Gate settings for plasma cells (PCs) and GC B cells 3 days after immunisation.
   B. Percentages of IgMg1 (red) and IgMwt (black) GC B cells over time after immunisation.
   C. Percentages of IgMg1 (red) and IgMwt (black) plasma cells over time after immunisation.

Multiple t test. Bars and whiskers indicate mean ± SD. Data are combined from two independent experiments, with a total number of 6 to 8 mice per time point.
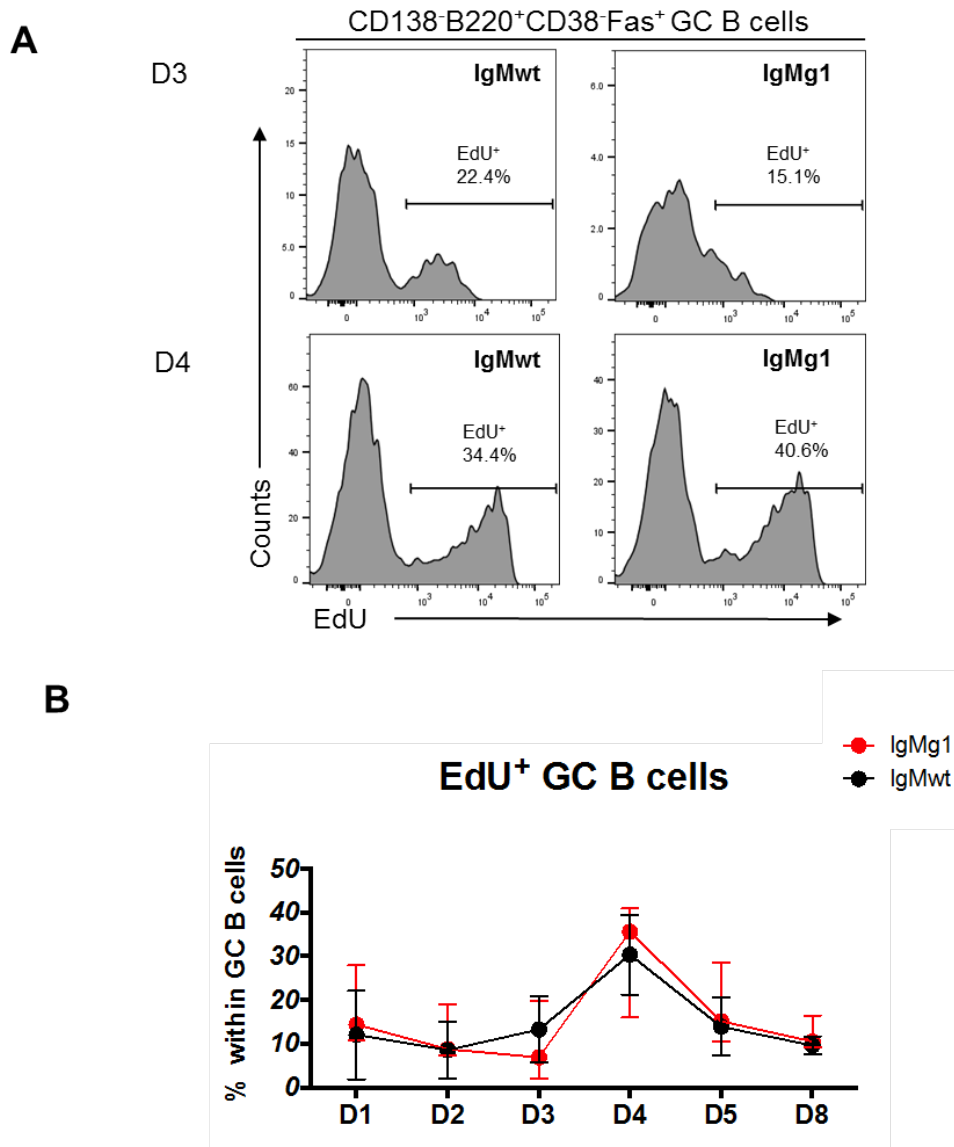
Figure 4.9: Similar EdU incorporation rate in GC B cells from both IgMwt and IgMg1 mice.

IgMwt and IgMg1 mice are i.v. immunised with 2×10^8 SRBCs, spleens are collected at each indicated time point from day 1 to day 8 after immunisation.

A. Representative histograms and thresholds for EdU^+ GC B cells 3 and 4 days after immunisation.

B. EdU incorporation rate within $CD38^-Fas^+$ GC B cells over time, showing IgMg1 (red) and IgMwt (black).

Multiple t test. Bars indicate mean ± SD. Data are combined from two independent experiments, with a total number of 6 to 8 mice per time point.
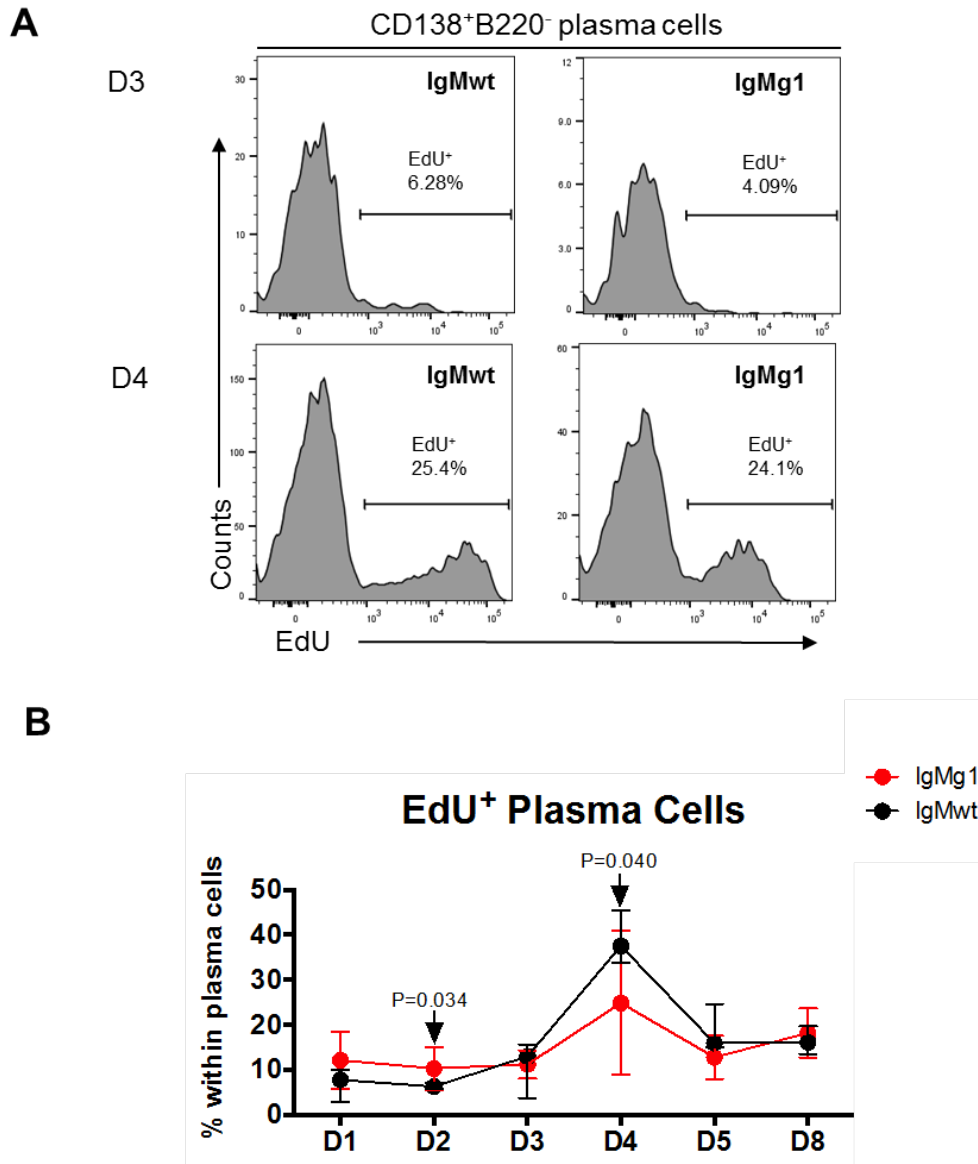
Figure 4.10: Slightly different EdU incorporation rate in plasma cells from IgMg1 mice.

IgMwt and IgMg1 mice are i.v. immunised with 2×10^8 SRBCs, spleens are collected at each indicated time point from day 1 to day 8 after immunisation.

A. Representative histograms and thresholds for EdU$^+$ GC B cells 3 and 4 days after immunisation.

B. EdU incorporation rate within CD38$^-$Fas$^+$ GC B cells over time, showing IgMg1 (red) and IgMwt (black).

Multiple t test. Bars indicate mean ± SD. Data are combined from two independent experiments, with a total number of 6 to 8 mice per time point.

4.2.4 Increased early apoptosis rate and higher proliferation rate during the TD antibody response to NP-CGG in IgMg1 mice

The kinetics of the GC response after SRBCs immunisation suggested a higher proliferation rate of GC B cells resulting in slightly larger GC in IgMg1 mice on day 5 after immunisation (Fig. 4.8-4.11). As there were also slightly larger GCs in IgMg1 mice 8 days after NP-CGG immunisation (Fig. 4.6 and 4.7), we next explored if this is also due to higher early rates of proliferation. We conducted time-course experiments in response to NP-CGG to assess GC B cell proliferation and apoptosis. Mice were immunised by plantar surface of foot injections with alum-precipitated NP-CGG with heat-inactivated *Bordetella pertussis* (b.p.), and responding B cell populations were analysed in popliteal LNs on days 4, 5, 6, 8 and14 after immunisation. EdU was i.p injected 2 hours before pLNs being taken. EdU incorporation rate was used to indicate cell proliferation rate. Intracellular staining of activated Caspase3 (aCaspase 3) was used to label apoptotic cells.

While there was no obvious difference in the total size of GCs (Fig. 4.11), IgMg1 mice showed a slightly higher frequency of proliferating GC B cells at day 8 after NP-CGG immunisation (Fig. 4.12A and B). Interestingly, this was preceded by a phase of increased apoptosis in IgMg1 GC B cells 6 days after immunisation (Fig. 4.12A and C).

This confirms observations from the SRBC time course experiments, showing an improved expansion of GC B cells in IgMg1 mice towards the peak of the response

171

despite increased apoptosis earlier on. This equilibrium of proliferation and apoptosis may lead to comparable percentages of total GC B cells in both IgMg1 and IgMwt mice 8 days after immunisation (Fig. 4.11B). Despite there being no obvious differences in the total number of GC B cells, there were subtle effects on the numbers of NP-responding GC B cells (Fig. 4.13). Reproducing the result of the single time point experiment described earlier (Fig. 4.7B), IgMg1 mice contained significantly higher numbers of NP-specific GC B cells 8 days after immunisation. This was also the case for the percentage of NP-specific GC B cells within B cells, which corresponds to the absolute numbers of hapten specific B cells generated (4.13B), as well as for the percentage of NP-specific GC B cells within the total GC B cell population (Fig. 4.13C).

GCs formed in response to NP-CGG are initially preferentially colonized by NP-binding cells (Toellner, Sze et al. 2018). At later stages these may be overtaken by GC B cells specific for the carrier-protein. This has been explained by the higher initial affinity of NP-specific B cells in the naïve repertoire, which may make it more difficult for B cells specific for more complex single copy epitopes on the carrier protein to be recruited and expand as GC B cells (Toellner, Sze et al. 2018). Fig. 4.13C shows a similar decline in the percentage of NP-binding B cells within GCs in IgMwt and IgMg1 mice, however this decline is delayed in IgMg1 mice, which may reflect small differences in recruitment and survival of the initial wave of NP-specific B cells and later recruited carrier specific B cells.
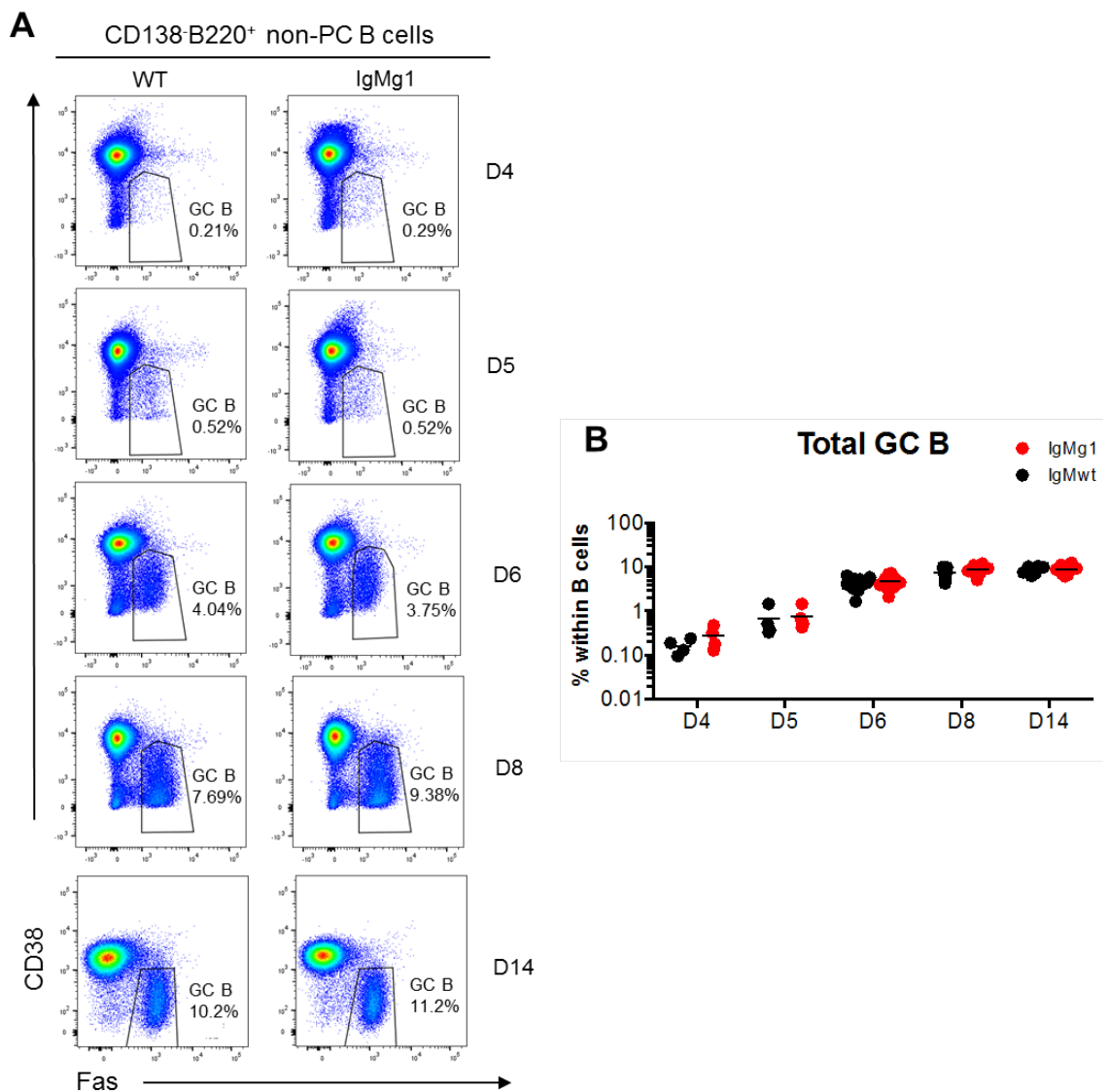
Figure 4.11: Comparable numbers of GC B cells after NP-CGG immunisation of IgMg1 and IgMwt mice.

Mice are immunised with 20 µg alum precipitated NP-CGG on plantar surface of foot, heat-inactivated *Bordetella pertussis* (BP) as adjuvant. After immunisation, popliteal LNs are collected sequentially from day 4 to day 14.
- A. Representative dot plots with gates for total GC B cells in IgMwt and IgMg1 mice 4 ad 14 days after immunisation.
- B. Percentages of GC B cells within B cells in WT and IgMg1 mice.

ns, not significant; multiple t test. Bars indicate mean. Each symbol represents sample from one mouse. Data are combined from three independent experiments.
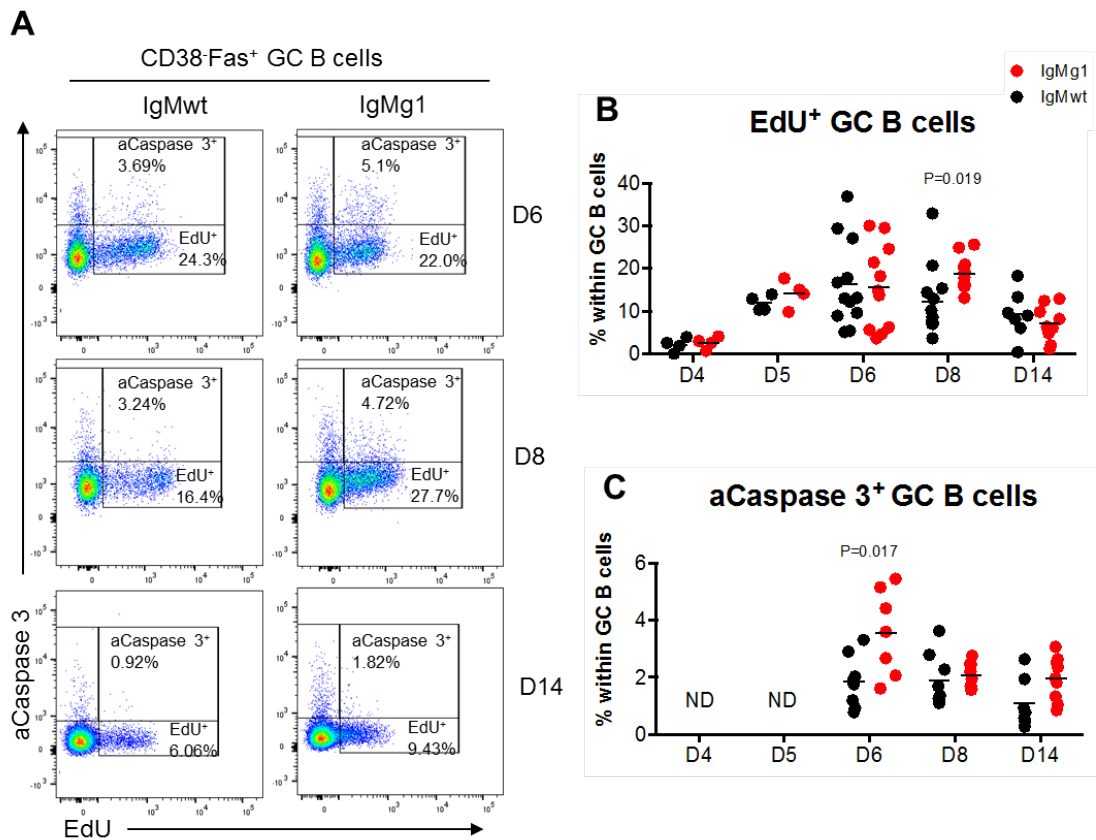
Figure 4.12: Increased apoptosis and proliferation of IgMg1 B cells in early stage GCs.

Mice are immunised with 20 μg alum precipitated NP-CGG and heat-inactivated *Bordetella pertussis* (BP) as adjuvant on plantar surface of foot. After immunisation, popliteal LNs are collected sequentially from day 4 to day 14. 2 hours before dissection, 200 μg EdU is injected by i.p. Gates for total GC B cells were displayed in Fig. 4.13.

  A. Representative samples and gate settings used to analyse proliferation and apoptosis in GC B cells. Apoptosis was detected by anti-aCaspase3 antibody, while proliferation was assessed by EdU incorporation rate.
  B. The percentages of EdU$^+$ GC B cells, and compared between WT and IgMg1 mice.
  C. The percentages of aCaspase3$^+$ GC B cells, and compared between WT and IgMg1 mice.

Multiple t test. Bars indicate mean. Each symbol represent sample from one mouse. Data are combined from three independent experiments.
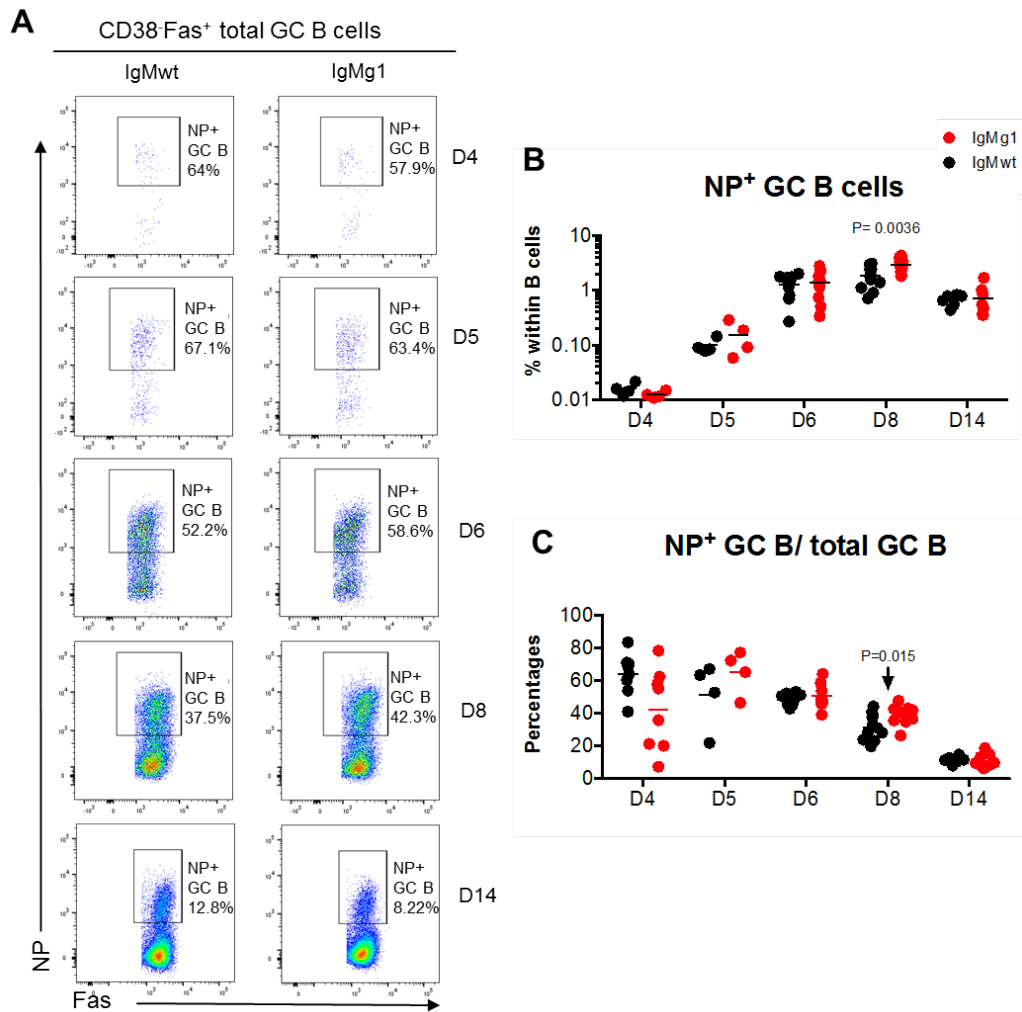
Figure 4.13: Delayed specificity shift within total GC response in IgMg1 mice.

Mice are immunised with 20 µg alum precipitated NP-CGG on plantar surface of foot, heat-inactivated *Bordetella pertussis* (BP) as adjuvant. After immunisation, popliteal LNs are collected sequentially from day 4 to day 14.

A. Gate settings for NP-specific GC B cells in IgMwt and IgMg1 mice after immunisation from day 4 to day 14.

B. The percentages of NP-specific GC B cells within B cells from IgMwt and IgMg1 mice.

C. Dynamic ratio changes of NP-specific GC B cells to total GC B cells. The ratio of NP-specific GC B cells to total GC B cells is calculated by using the percentages of NP-specific GC B cells divide the percentages of total GC B cells.

Multiple t test. Bars indicate mean. Each symbol represents sample from one mouse. Data are combined from three independent experiments.

In order to test whether there is a difference in B cell activation in the IgMg1 mouse, we tested expression levels of two early B cell activation markers (CD25 and CD69) on B cells responding to NP-CGG (Fig. 4.14A and B). This showed that the expression of CD25 and CD69 was similar between IgMwt and IgMg1 mice (Fig. 4.14B and D), suggesting a similar activation status of IgMg1 B cells in the presence of T cell help, at least as indicated by these two activation markers. This, of course, does not exclude that there are other changes in signals downstream of BCR signalling in early activated IgMg1 B cells.
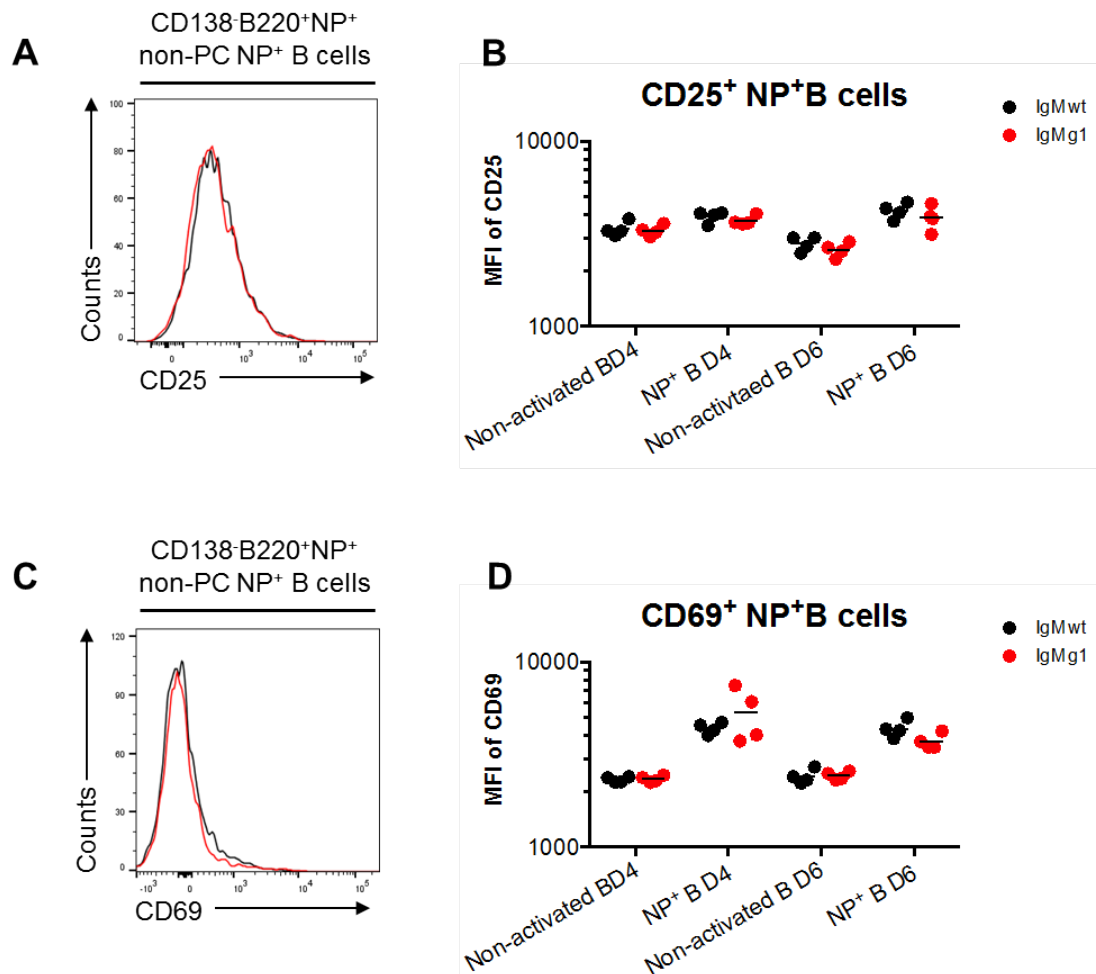
Figure 4.14: Similar expression levels of CD25 and CD69 in NP-specific B cells of IgMg1 and IgMwt mice.

Mice are immunised with 20 µg alum precipitated NP-CGG and heat-inactivated *Bordetella pertussis* (BP) as adjuvant on plantar surface of foot. After immunisation, popliteal LNs are collected day 4, 6 after immunisation.
   A. Overlays of CD25 expression levels on NP-specific B cells (activated) and NP⁻ B cells (non-activated) from day 4 after immunisation. Gates from NP-specific B cells was the same as Fig. 4.5. Red: IgMg1 NP-specific B cell; Black: IgMwt NP-specific B cells.
   B. MFI of CD25 expression levels.
   C. Overlays of CD69 expression levels on NP-specific B cells (activated) and NP⁻ B cells (non-activated), from day 4 after immunisation. Gates from NP-specific B cells was the same as Fig. 4.5. Red: IgMg1 NP-specific B cell; Black: IgMwt NP-specific B cells.
   D. MFI of CD69 expression levels.
Bars indicate mean. Each symbol represents sample from one mouse.

4.2.5 IgMg1 B cells have equal potential to become activated and populate GCs

IgMg1 B cells were shown to have reduced ability to respond to TI-II antigen (Fig. 4.1). The observation on NP-CGG induced immune responses described above (Fig. 4.7F, 4.13) showed there was a larger hapten-specific GC B cell population generated at the peak of the response in IgMg1 mice. Further, activated IgMg1 B cells were more prone to differentiate into GC B cells (Fig. 4.7G). These observations raise the possibility that IgMg1 B cells, being anergic B cells, are intrinsically programmed to preferentially differentiate into GC B cells. Gene expression patterns of anergic B cells are different from naïve B cells (Glynne, Ghandour et al. 2000), which can be the reason for the biased GC B cell fate decision. Negative selection happening in GCs may serve as a checkpoint for antigen-activated anergic B cells (Chan, Wood et al. 2012). In this environment, anergic B cells may undergo clonal redemption and, through hypermutation, turn into low-risk, useful cells that have lost self-reactivity and become highly specific for foreign antigens (Burnett, Langley et al. 2018).

In order to better resolve subtle changes in IgMg1 B cell recruitment, expansion, and loss from the GC, bone marrow chimeric mice were created to produce a system where IgMg1 and IgMwt B cells could differentiate in direct competition (chapter 3.14). Equal numbers of CD45.2 (IgMg1 or C57BL/6 IgMwt) and CD45.1 (BoyJ IgMwt) bone marrow (BM) cells were transferred into irradiated C57BL/6 mice (Fig. 3.14). Seven weeks later IgMwt/IgMwt chimeras were immunised with NP-CGG. Spleens in IgMwt/IgMwt chimeras contain on average 3.5 times higher numbers of

CD45.2 than CD45.1 mature B cells. This ratio is 5 times more CD45.2 than CD45.1 in IgMg1/IgMwt chimeras (Fig 3.16).

Eight days after NP-CGG immunisation, popliteal LNs were harvested from both IgMwt/IgMwt and IgMg1/IgMwt chimeras. Naïve and responding CD45.2$^+$ (IgMwt or IgMg1) and CD45.1$^+$ (IgMwt) B cell populations were analysed. The B220$^+$ NP-nonbinding CD138$^-$ population from the popliteal LN were gated as naïve control B cells (Fig. 4.15A and B). Similar to what is seen in the spleen (Fig. 3.19), non-activated naïve B cells in LN consist of on average 2 times more CD45.2 than CD45.1 B cells. In IgMg1/IgMwt chimeras this ratio becomes 4.5 times more CD45.2 than CD45.1 (Fig. 4.15C). Analysing the total NP-responding cells, neither IgMwt/IgMwt nor IgMg1/IgMwt chimeras displayed a significant change in the ratio of CD45.2/CD45.1 B cells (Fig. 4.15B and C). Similarly, there was no change in the ratio of CD45.2/CD45.1 in the NP-specific GC B cell population. Surprisingly, this seems to indicate that when in direct competition, IgMg1 B cells are just as capable as IgMwt B cells to populate GCs 8 days after immunisation.

As earlier experiments had indicated that NP-specific IgMg1 B cells have an increased capacity to populate GCs 8 days after immunisation (Fig. 4.6G, 4.7G, 4.13B), the sizes of the NP-specific GC B cell populations in both types of chimeras were calculated as well. Surprisingly, this confirmed a consistent trend toward larger GCs if IgMg1 B cells were present, with larger relative and absolute GC B cell compartments (Fig. 4.16A and B), and highly significant increased percentage of GC

B cells within NP-specific B cells (Fig. 4.16C). An increase in the size of the GC compartment in IgMg1/IgMwt chimeras (Fig. 4.7G and 4.16C) in the absence of a change in the ratio of IgMg1 to IgMwt B cells (Fig. 4.15C) could indicate that the presence of IgMg1 B cells in GCs produces an environment that allows enhanced B cell expansion or survival, or enable reduced loss from the GC. This change of environment does not seem dependent on B cell intrinsic signalling changes induced by the type of BCRs (IgMg1 or IgMwt) on individual GC B cells, but a general change in environment that is induced by the presence of IgMg1 B cells. In order to better resolve this, similar experiments performed at earlier time points following immunisation would be necessary, which could not be done due to time constraints.
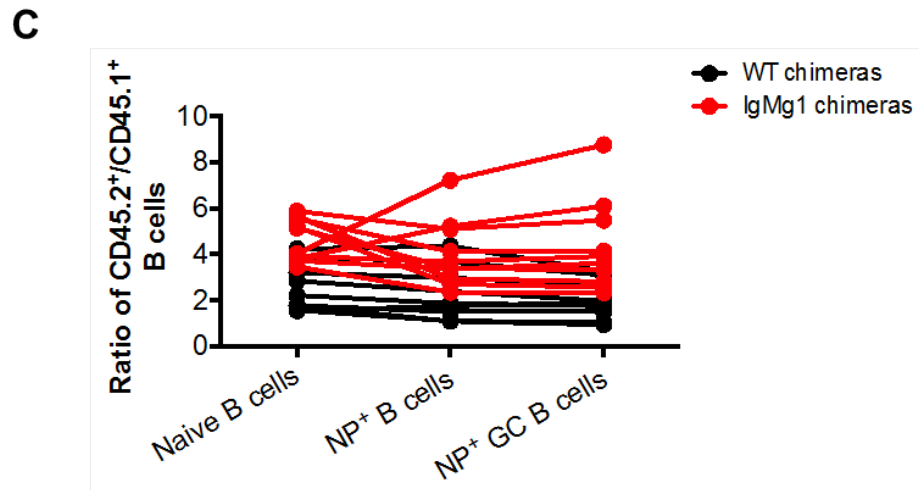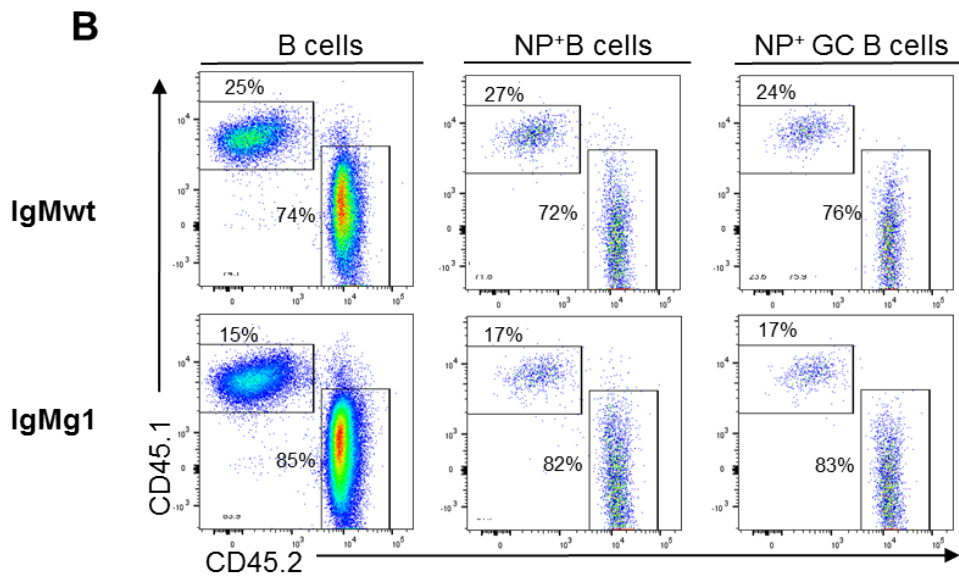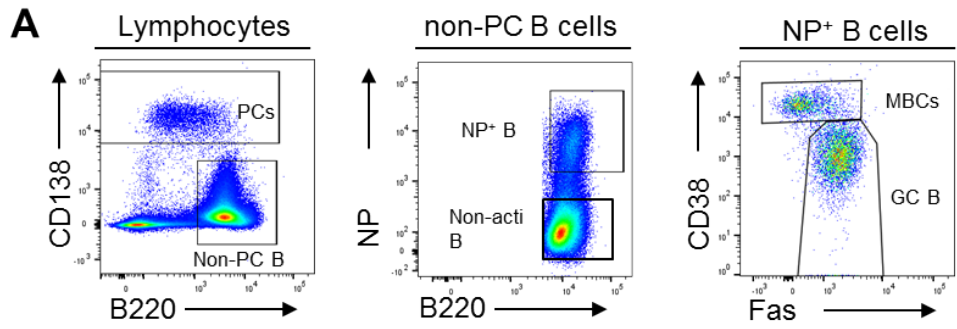
Figure 4.15: IgMg1 B cells compete equally well to be activated and commit to GC B cell fate.

Mice are immunised with 20 µg alum precipitated NP-CGG on plantar surface of foot, heat-inactivated *Bordetella pertussis* (BP) as adjuvant. After immunisation after 8 days, popliteal LNs are collected.

A. Gates for B cells, NP-specific B cells and NP-specific GC B cells.
B. Gates for $CD45.2^+$ and $CD45.1^+$ B cell sub-populations within each subset.
C. Ratio of $CD45.2^+/CD45.1^+$ have been calculated and compared between groups. Ratio of $CD45.2^+/CD45.1^+$ has been defined as percentages of $CD45.2^+$ subsets divide the percentages of $CD45.1^+$ subsets

2-way ANOVA. Each symbol represents sample from one mouse. Data are combined from two independent experiments.
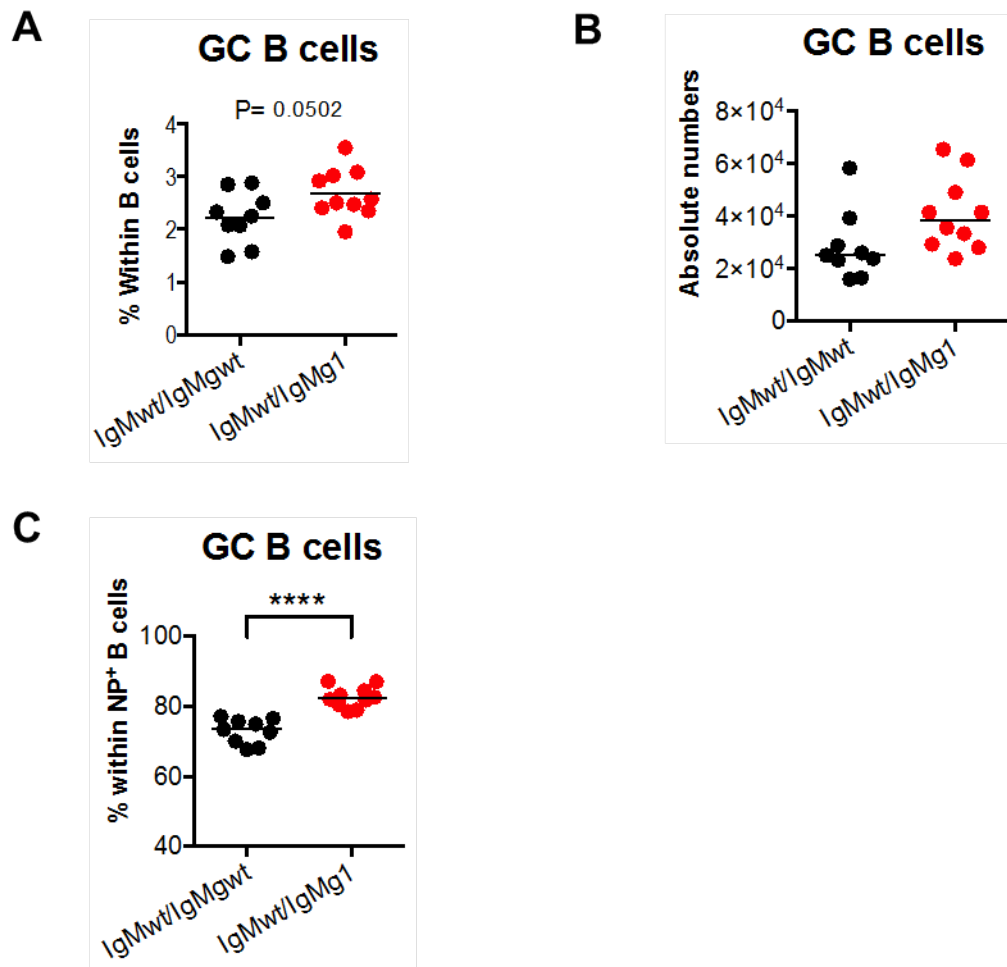
Figure 4.16: Overall more NP⁺ GC B cells in IgMg1 chimeras.

IgMwt and IgMg1 bone marrow chimeras are immunised with 20 µg alum precipitated on plantar surface of foot, heat-inactivated *Bordetella pertussis* (BP) as adjuvant. Popliteal LNs are collected 8 days after immunisation.
   A. The percentages of NP⁺ GC B cell within total B cells, and compared between IgMwt/IgMwt and IgMwt/IgMg1 mice.
   B. The absolute numbers of GC B cells, and compared between IgMwt/IgMwt and IgMwt/IgMg1 mice.
   C. The percentages of GC B cells within NP-specific B cells, and compared between IgMwt/IgMwt and IgMwt/IgMg1 mice.

****$p < 0.0001$; unpaired Student's t test. Bars indicate mean. Each symbol represents sample from one mouse. Data are combined from two independent experiments.

4.2.6 Changes in IgM and IgG1 usage in GC B cells of IgMg1 mice

GCs are known to be the place where Ig gene hypermutation happens and are populated by Ig class-switched B cells. IgMg1 BCR signalling changes may affect the efficiency of Ig class switching. While Ig class switched IgMg1 B cells become genetically identical to IgMwt Ig class switched B cells, it is still possible that rewiring of BCR signalling in IgMg1 B cells or epigenetic differences can lead to continued decreased signalling, leading to changes in the expansion and survival of Ig class switched B cells.

In order to test for Ig class usage, IgMwt and IgMg1 mice were immunised in the foot with NP-CGG in alum and *B.p.* adjuvant, and numbers of NP-specific IgM and IgG1 positive GC B cells followed on days 6, 8, and 14 after immunisation. GC B cells were gated as described before as CD138⁻B220⁺CD38$^{low/-}$Fas⁺ cells, and the changes of GC B cells followed over time after immunisation (Fig. 4.17A). Similar to what has been shown previously (Fig. 4.13C), this confirmed that while the size of the total GC response increased until 14 days post immunisation (Fig. 4.17A and B), the percentage of NP-binding GC B cells declined from day 6 to day 14 post immunisation, and this change in antigen-specificity was delayed in IgMg1 mice (Fig. 4.17C).

NP-specific IgG1 switched GC B cells were stained during the time course to NP-CGG immunisation (Fig. 4.18A). This showed that the main reason why IgMg1 GC B

cell numbers were increased on day 8 was the NP-specific IgG1 switched population (Fig. 4.18C). This difference disappears by day 14 post immunisation.

Together these results confirm the delayed specificity shift from early NP-binding to late non-NP-binding GCs in IgMg1 mice. This is in-line with a larger expansion of the IgG1$^+$NP$^+$ GC B cell population on day 8 after NP-CGG immunisation in IgMg1 mice. Whether this is due to changes in Ig class switch recombination or differences in BCR signalling in IgG1 switched IgMg1 B cells will be investigated in the following experiments.
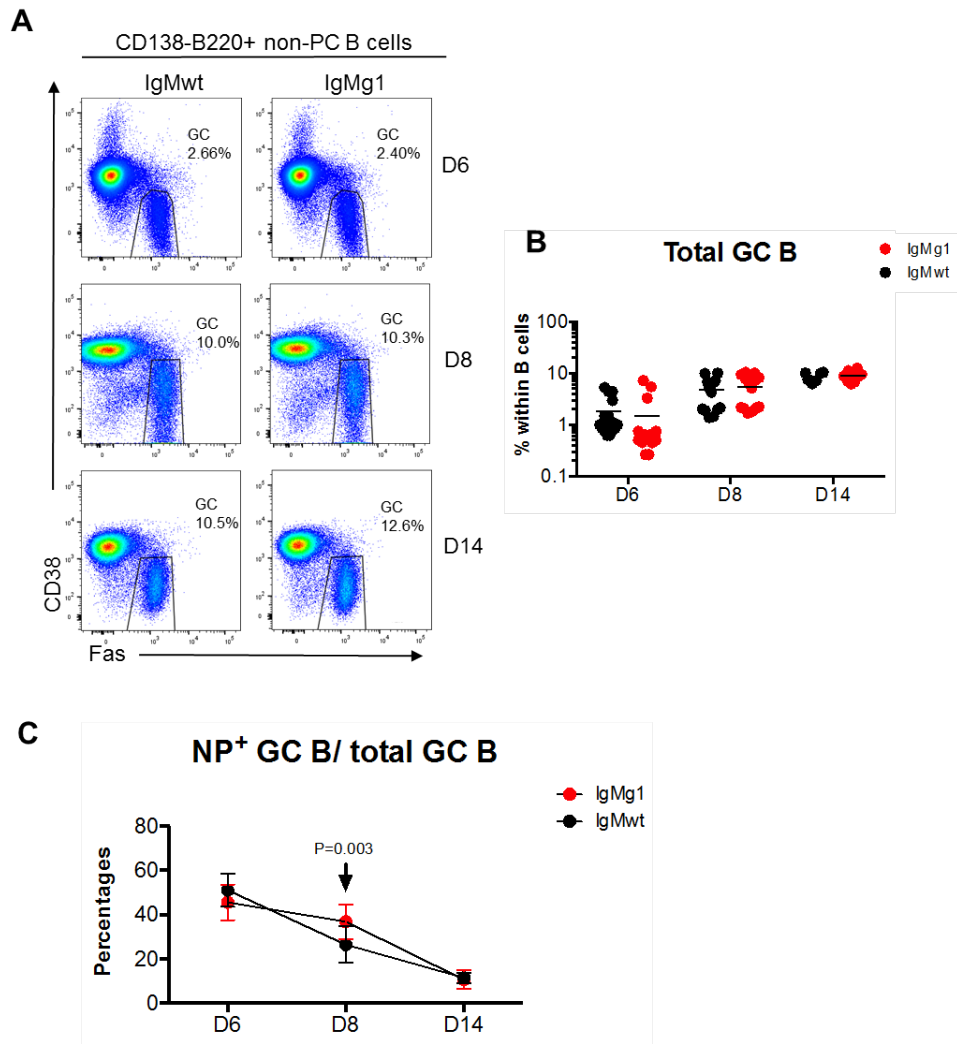
Figure 4.17: Delayed specificity shift of total GC B cells in IgMg1 mice.

Mice are immunised with 20 µg alum precipitated NP-CGG on plantar surface of foot, heat-inactivated *Bordetella pertussis* (BP) as adjuvant. After immunisation, popliteal LNs are collected sequentially from day 6 to day 14.
  A. Gate settings for total GC B cells in IgMwt and IgMg1 mice after immunisation.
  B. The percentages of total GC B cells within B cells from IgMwt and IgMg1 mice.
  C. Ratio of NP-specific GC B cells to total GC B cells over time. The ratio of NP-specific GC B cells to total GC B cells is calculated by using the percentages of NP-specific GC B cells within all B cells divided by the percentages of total GC B cells within all B cells.
Multiple t test. Bars indicate mean. Each symbol represents sample from one mouse. Data are combined from three independent experiments.

A CD38⁻Fas⁺ total GC B cells

B Q1:NP⁺IgG1⁻

C Q2:NP⁺IgG1⁺

D Q3:NP⁻IgG1⁻

E Q4:NP⁻IgG1⁺
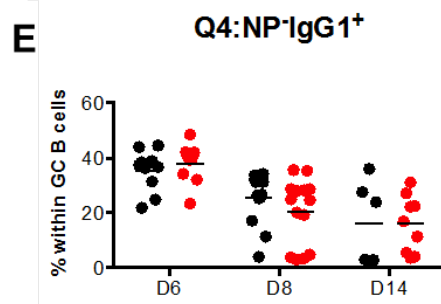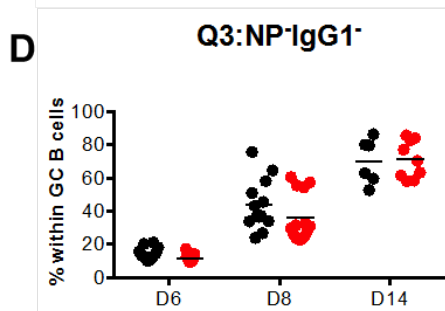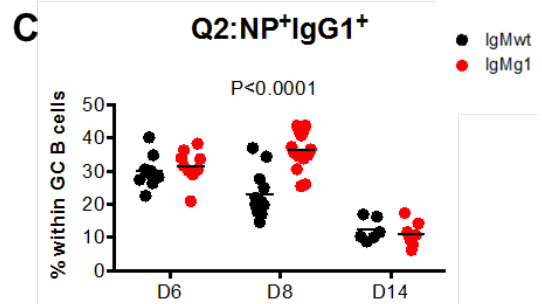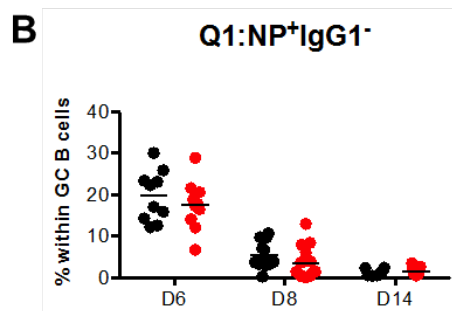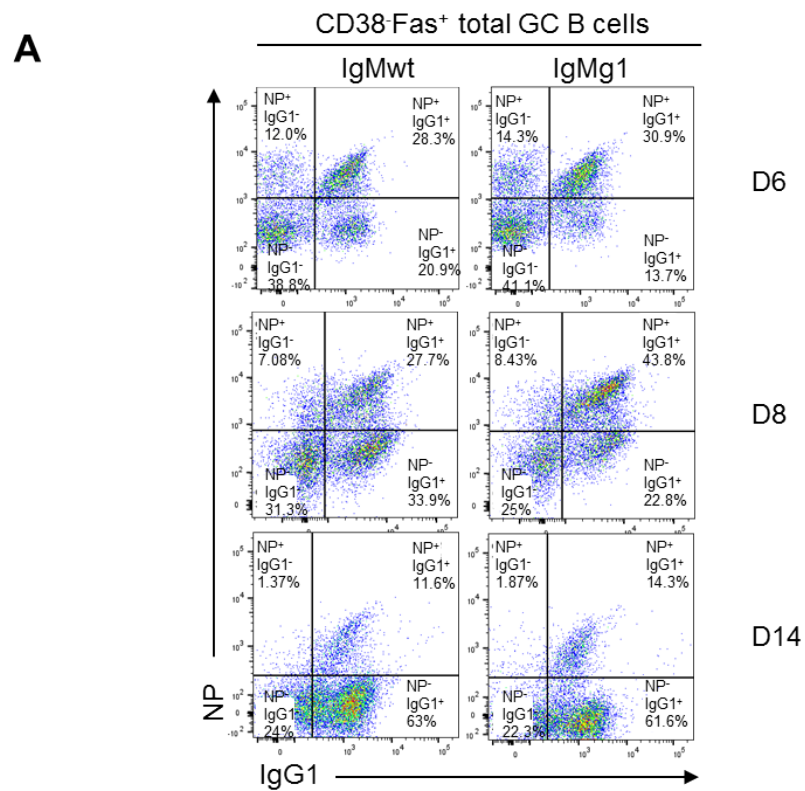
Figure 4.18: Accumulated NP⁺IgG1⁺ GC B cells on day 8 in IgMg1 mice.

Mice are immunised with 20 μg alum precipitated NP-CGG on the plantar surface of foot, heat-inactivated *Bordetella pertussis* (BP) as adjuvant. After immunisation, popliteal LNs are collected sequentially from day 6 to day 14.

    A. Gate settings to measure NP responding and class switch of total GC B cells from day 6 to day 14.

    B-E. Summarizing statistic of the dynamic changes of the percentages of Q1: IgG1⁻NP⁺ (B), Q2: IgG1⁺NP⁺ (C), Q3: IgG1⁻NP⁻ (D), Q4: IgG1⁺NP⁻ (E) GC B cell subsets within total GC B cell populations from IgMwt and IgMg1 mice.

Multiple t test. Bars indicate mean. Each symbol represents sample from one mouse. Data are combined from three independent experiments.

4.2.7 Surface BCR expression levels remain lower at the early stage of GC response in IgMg1 mice

The data presented so far indicates delayed early GC B cell generation after SRBC immunisation (Fig. 4.8), a delay in the shift from NP-specificity during GC B cell response (Fig. 4.12, 4.17), and an increase of IgG1 positive cells at the time when NP-binding cells were expanded (Fig. 4.18). Chapter 3 showed that in IgMg1 B cells IgM expression is reduced by a factor of 2 (Fig. 3.20-23 and 3.27-3.30). It was then interesting to explore whether this suppression of surface IgM expression is preserved after B cell activation and CSR to IgG1. In order to directly compare IgM and IgG1 BCR expression levels in GC B cells, IgM and IgG1 were stained on days 6 and 8 after immunisation with NP-CGG. GC B cells were identified similar to the gating scheme shown in Fig. 4.17.

As observed before, there was an increase in the percentage of Ig class switched cells with fewer IgM expressing cells in IgMg1 mice on day 8 after immunisation (Fig. 4.19, 4.20). Surface IgM expression was 30% lower on GC B cells from IgMg1 mice (Fig. 4.21A and B). This difference is less than that on non-activated naïve B cells (Fig. 3.22). The same reduction was seen on NP-specific IgMg1 GC B cells on day 6 (Fig. 4.22A, B). After class switch to IgG1, the difference in BCR expression became smaller, with B cells of IgMg1 mice expressing on average 16% less IgG1 than GC B cells from IgMwt mice, 6 days after immunisation (Fig. 4.21C, 4.22C). Eight days after immunisation, however, the expression of IgG1 in IgMg1 derived total GC B

cells was now the same as WT counterparts (Fig. 4.21C), and higher when only NP-specific GC B cells were gated (4.22C).
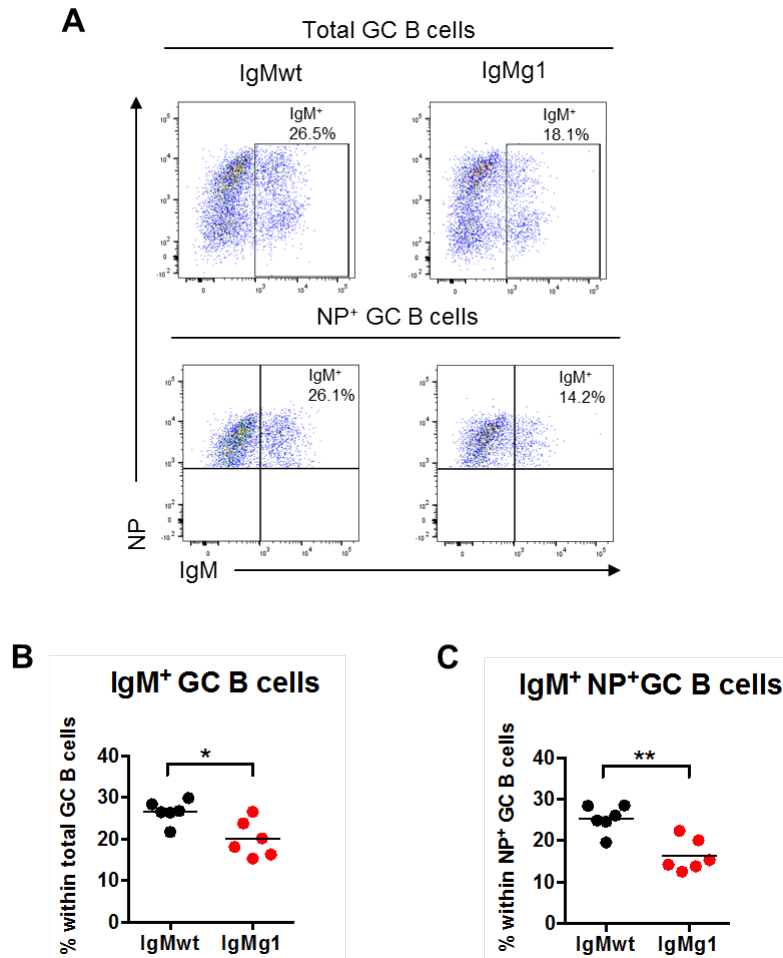
Figure 4.19: Decreased IgM$^+$ GC B cells in IgMg1 mice after 6 days of NP-CGG immunisation.

Mice are immunised with 20 μg alum precipitated NP-CGG on plantar surface of foot, heat-inactivated *Bordetella pertussis* (BP) as adjuvant. After immunisation, popliteal LNs are collected day 6.
- A. Gate settings for IgM$^+$ total GC B cells and NP$^+$ GC B cells after 6 days of NP-CGG immunisation.
- B. Percentages of IgM$^+$ total GC B cell subsets.
- C. Percentages of IgM$^+$ NP-specific GC B cell subsets.

$*p < 0.05$; $**p < 0.01$; multiple t test. Bars indicate mean. Each symbol represents sample from one mouse. Data are representative from two independent experiments.
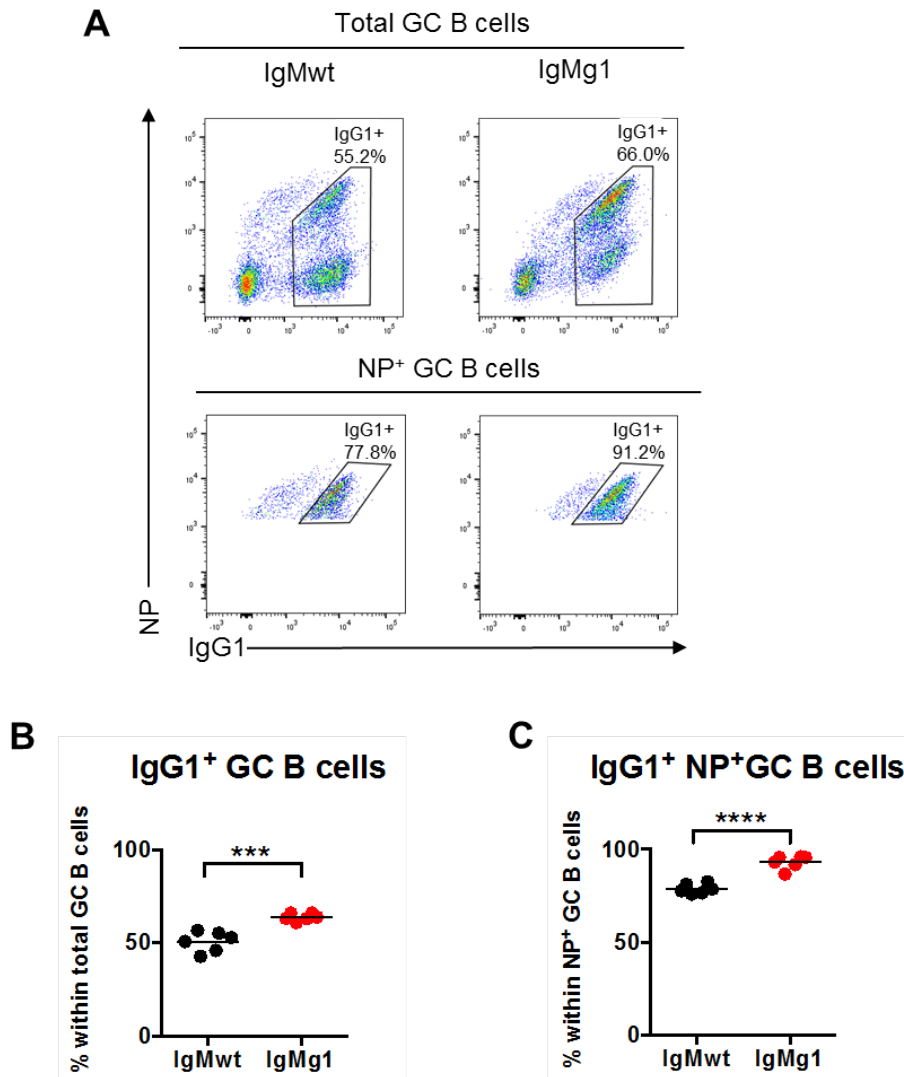
Figure 4.20: Increased IgG1 switching in total and NP$^+$ GC B cells in IgMg1 mice after 8 days of NP-CGG immunisation.

Mice are immunised with 20 µg alum precipitated NP-CGG on plantar surface of foot, heat-inactivated *Bordetella pertussis* (BP) as adjuvant. After immunisation, popliteal LNs are collected day 8.

A. Gate settings for IgG1$^+$ total GC B cells and NP$^+$ GC B cells after 8 days of NP-CGG immunisation.
B. Percentages of IgG1$^+$ total GC B cell subsets.
C. Percentages of IgG1$^+$ NP-specific GC B cell subsets.

***p < 0.001; ****p < 0.0001; multiple t test. Bars indicate mean. Each symbol represents sample from one mouse. Data are representative from two independent experiments.

As NP-PE was used to detect antigen-specific B cells, it was also possible to measure the MFI of NP-PE binding in IgM or IgG1 expressing GC B cells (Fig. 4.23). The ratio between NP-staining intensity and MFI of BCR expression can be used as a measure of BCR affinity (Shimizu, Oda et al. 2003). This showed that, while the amount of NP-binding by GC B cells followed a similar trend to the IgM or IgG1 BCR expression levels (Fig. 4.23B and C), there were subtle differences. On day 6 there was an increased ratio of NP/IgM and NP/IgG1 in GC B cells from IgMg1 mice, indicating that IgMg1 B cells recruited into the early GC response have higher affinity for NP than IgMwt B cells. This changed at day 8 after immunisation, when NP was less efficiently bound by IgG1-expressing B cells from IgMg1 mice than by those from IgMwt mice.

This indicates that IgMg1 B cells are less efficiently recruited in the GC response, as reflected in the higher BCR affinity necessary to enter a GC at the early stages of GC differentiation on day 6. Interestingly, this is also the time when apoptosis levels were increased in IgMg1 GC B cells (Fig. 4.12C). Affinity maturation is delayed, however, in IgMg1 B cells, shown by the lower NP/IgG1 expression ratio on day 8 (Fig. 4.23E). This may be the reason for the delayed expansion of NP-binding GC B cells (Fig. 4.12B) and the delayed switch in antigen-specificity of GCs in IgMg1 mice (Fig. 4.13 and 4.17).

In order to further test this, NP-specific serum antibody affinities were measured 8 days after immunisation. This did not show a significant change in serum IgG1

affinity (Fig. 4.23F). This is perhaps not surprising, as it should take several days to generate plasma cell output from the GC and to observe a significant change serum affinity. Serum antibody affinity measurements later in the response are necessary to address this.
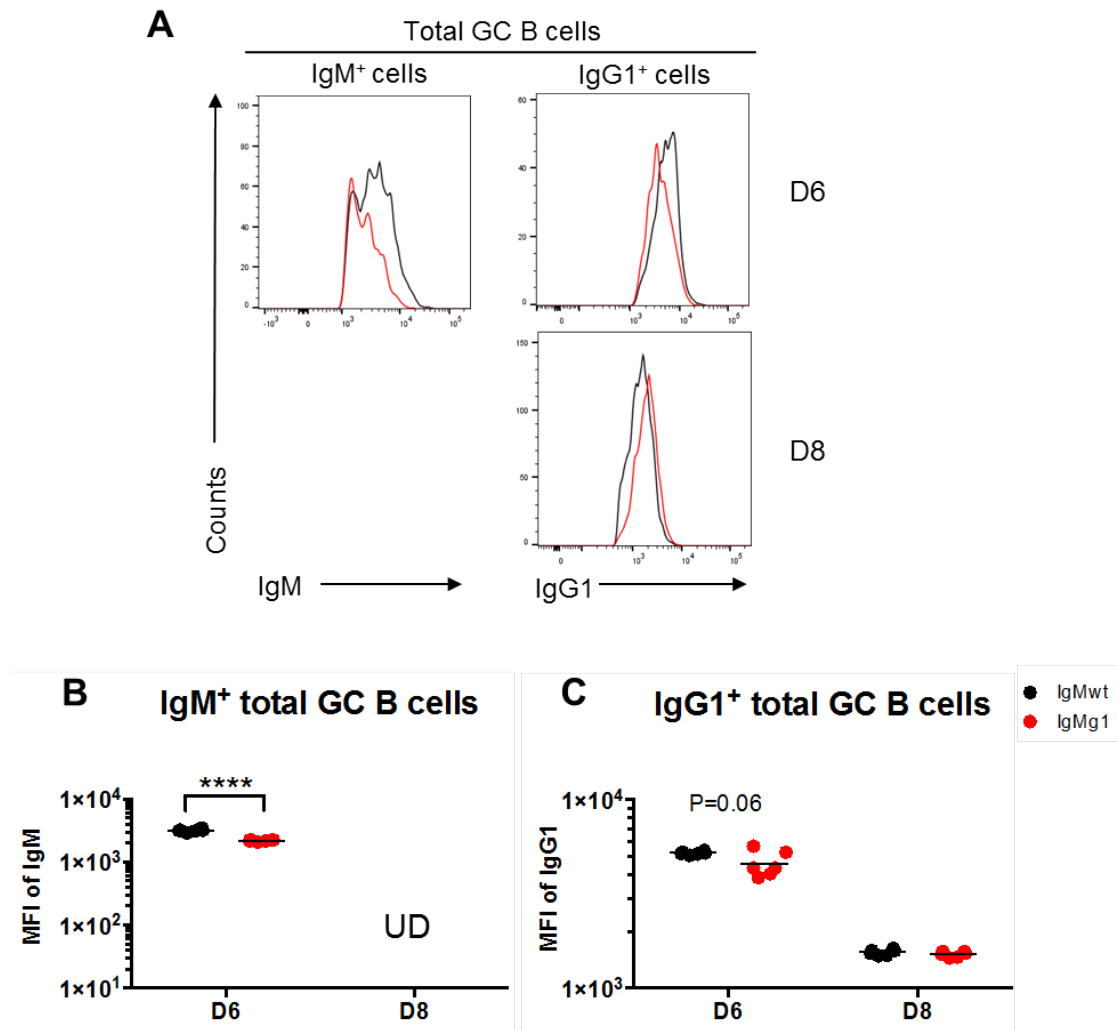
Figure 4.21: Loss of mIgM on IgM$^+$ total GC B cells in IgMg1 mice day 6 after immunisation.

Mice are immunised with 20 μg alum precipitated NP-CGG on plantar surface of foot, heat-inactivated *Bordetella pertussis* (BP) as adjuvant. After immunisation, popliteal LNs are collected on day 6 and day 8. Gates are the same as showed in Fig. 4.20 and 4.21.

    A. Overlays of mIgG1 and mIgM expression levels on total GC B cells.

    B. MFI of mIgM on total GC B cells and compared between IgMwt and IgMg1 mice.

    C. MFI of mIgG1 on total GC B cells and compared between IgMwt and IgMg1 mice.

****p < 0.0001; multiple t test. Bars indicate mean. Each symbol represents sample from one mouse. Data are combined from two independent experiments. UD: Undetected.
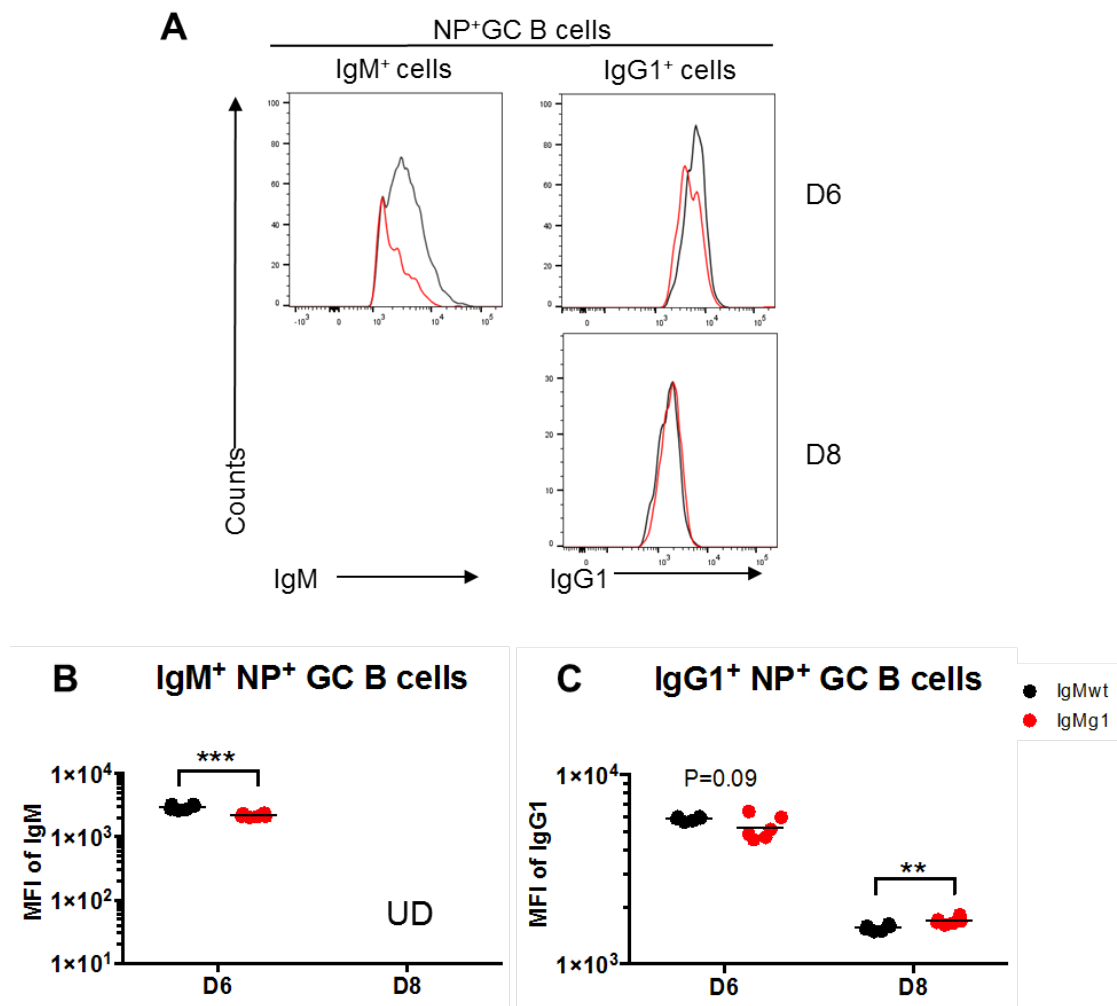
Figure 4.22: Loss of mIgM and increased mIgG1 on NP⁺ GC B cells in IgMg1 mice after immunisation.

Mice are immunised with 20 µg alum precipitated NP-CGG on plantar surface of foot, heat-inactivated Bordetella pertussis (BP) as adjuvant. After immunisation, popliteal LNs are collected on day 6 and day 8. Gates are the same as showed in Fig. 4.20 and 4.21.

A. Overlays of mIgG1 and mIgM expression levels on NP-specific GC B cells.
B. MFI of mIgM on NP-specific GC B cells and compared between IgMwt and IgMg1 mice.
C. MFI of mIgG1 on NP-specific GC B cells and compared between IgMwt and IgMg1 mice.

**p < 0.01; ***p < 0.001; multiple t test. Bars indicate mean. Each symbol represents sample from one mouse. Data are representative from two independent experiments. UD: Undetected.
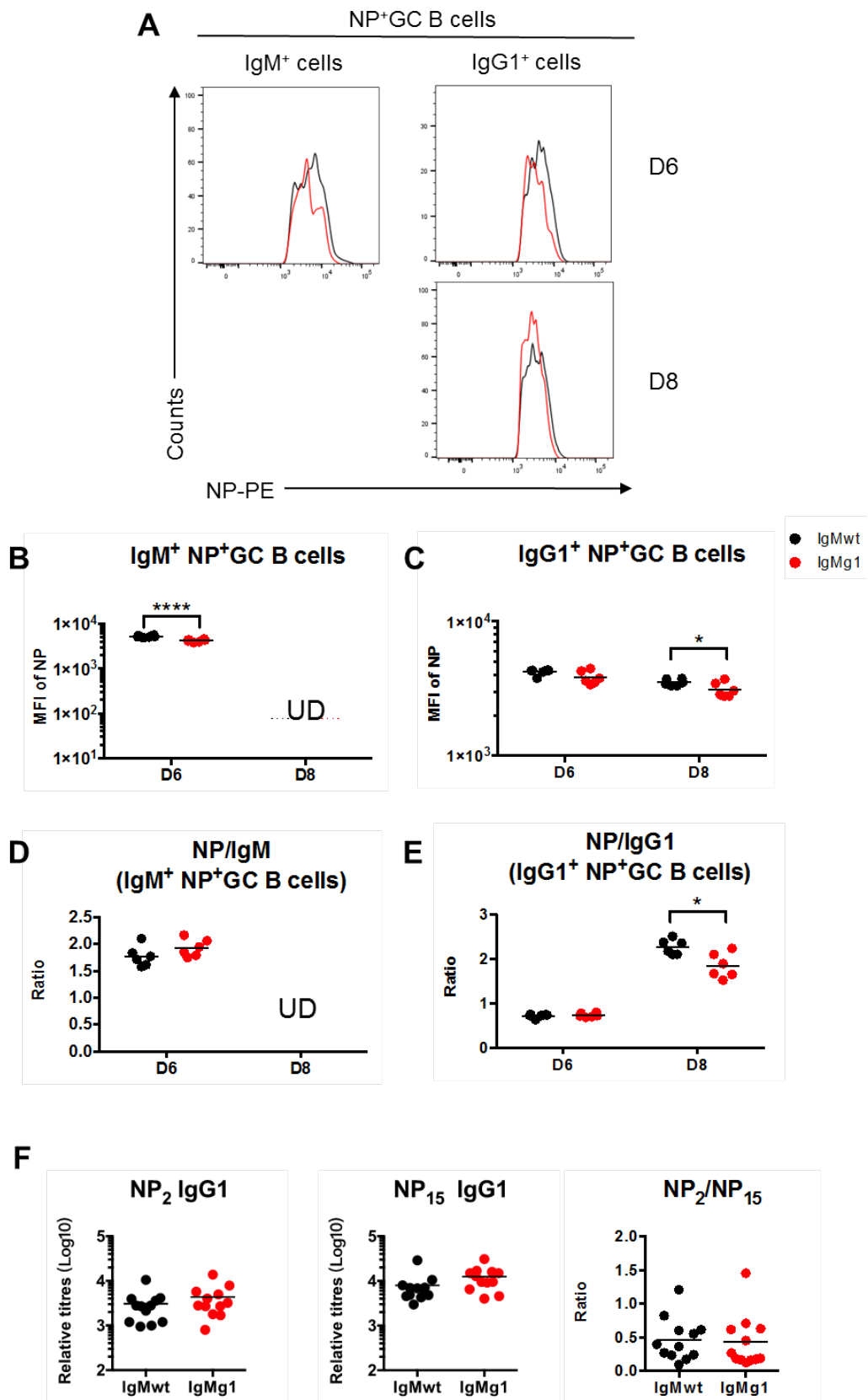
Figure 4.23: Lower affinity for NP on IgG1$^+$ GC B cells 8 days after immunisation in IgMg1 mice.

Data are from the same experiment in Fig. 4.19 – 4.22, gates are set as shown in Fig. 4.20 and Fig. 4.21.

   A. Overlays of NP-binding on both IgM$^+$ and IgG1$^+$ NP-specific GC B cells after 6 days and 8 days of immunisation.
   B. MFI of NP-binding on IgM$^+$ NP$^+$GC B cells and compared between IgMwt and IgMg1 mice.
   C. MFI of NP-binding on IgG1$^+$ NP$^+$GC B cells and compared between IgMwt and IgMg1 mice
   D. Ratio of NP-PE MFI to IgM MFI showing the relative NP-binding ability (affinity) of IgM.
   E. Ratio of NP-PE MFI to IgG1 MFI showing the relative NP-binding ability (affinity) of IgG1.
   F. Relative titers of NP specific high affinity (NP2) and low affinity (NP15) antibodies. Affinity of NP antibody in both IgMwt and IgMg1 mice on day 8 after immunisation. Affinity is calculated as the ratio of relative titers of NP2 to relative titers of NP15 in each sample.

*p < 0.05; ****p < 0.0001; multiple t test. Bars indicate mean. Each symbol represents sample from one mouse. Data are representative from two independent experiments. UD: Undetected.

4.2.8 Repressed BCR signalling in IgMg1 mice during T-D immune responses

The last section showed that the inhibition of BCR expression is gradually lost in GC B cells of IgMg1 mice. In order to test whether the inhibition of BCR signalling seen in naïve IgMg1 B cells (Fig. 3.26) is also lost during GC differentiation, Nur77-GFP expression was used as a surrogate read-out for the intensity of BCR signalling (Zikherman, Parameswaran et al. 2012). IgMwt and IgMg1 mice were immunised with NP-CGG and Nur77-GFP expression measured in the popliteal lymph nodes 8 days after immunisation. B cells were gated into B220$^+$CD138$^-$CD38$^+$Fas$^-$ NP-binding or -nonbinding follicular B cells and NP-binding or non-binding CD138$^-$CD38^{low} Fas$^+$ GC B cells (Fig. 4.24). As shown in chapter 3 (Fig. 3.26), non-activated splenic follicular B cells from IgMg1 mice show slightly lower Nur77-GFP expression than counterpart B cells from IgMwt mice, signalling of NP-nonspecific non-GC B cells in IgMg1 B cells was substantially lower than that in IgMwt B cells (Fig. 4.25A). More than 95% of these NP-nonspecific non-GC follicular B cells should be naive and not been activated by antigen. The GFP expression of these cells was higher than that of GC B cells, which should all have been activated by antigens (Fig. 4.25B, C). This is consistent with previous observations showing that BCR signalling is shortcut in GC B cells, as shown by PhosFlow (Khalil, Cambier et al. 2012) and in GFP-Nur77 reporter mice (Mueller, Matloubian et al. 2015). Despite being low, Nur77-GFP expression was still marginally lower in GC B cells from IgMg1 than from IgMwt mice (Fig. 4.25B, C). While NP-binding MBCs showed higher Nur77-GFP expression again, IgMg1 derived MBCs continued to express lower levels of Nur77-GFP than in IgMwt derived MBCs (Fig. 4.25D). This shows a continuous reduction

of BCR signalling, reflected by lower Nur77-GFP expression, in non-activated Fo B cells, activated GC B cells and differentiated MBCs in IgMg1 mice.

The majority of GC B cells and MBCs have switched to IgG and lost the IgMg1 BCR on day 8 after immunisation. In order to test whether reduction in BCR signalling in IgMg1 B cells is lost after class switch recombination, Nur77-GFP expression was compared between IgM expressing and Ig class switched B cells. GC B cells were gated on whether they were binding the hapten NP or not, followed by gating on expression of IgM or IgG1 (Fig. 4.26A). This showed that IgG1 switching led to a general repression of Nur77-GFP expression in GC B cells, whether they were from IgMwt or IgMg1 mice, and regardless of their specificities (Fig. 4.26 B-D). Comparing side by side Nur77-GFP expression in GC B cells from IgMwt and IgMg1 mice showed that Nur77-GFP expression was clearly suppressed in IgM expressing GC B cells of IgMg1 origin (Fig. 4.27A, B), whereas this difference disappeared once the cells had switched to IgG1 (Fig. 4.27C, D).

When NP-specific B220$^+$CD138$^-$CD38^{high} non-GC B cells were gated (Fig 4.28A), most of them being antigen-experienced memory B cells (Conter, Song et al. 2014), there was no reduction in Nur77 in IgG1$^+$ memory B cells as was observed in total GC B-cells (Fig 4.26C). While IgM and IgG1 expressing MBCs from IgMwt showed the same levels of Nur77 expression, IgG1-switched memory B cells from IgMg1 mice had significantly increased Nur77 expression (Fig. 4.28B). Remarkably, IgMg1 derived memory B cells expressed considerably less Nur77-GFP than memory B cells

of IgMwt origin, even if they had switched to IgG1 (Fig. 4.28B). This indicates that there is a continued rewiring of BCR signalling in IgMg1 derived anergic B cells that continues to affect memory B cells even if they have switched to IgG.

In summary, the experiment confirms that GC B cells undergo a phase of reduced BCR signalling (Khalil, Cambier et al. 2012, Mueller, Matloubian et al. 2015). IgG1 switched GC B cells show a stronger suppression of Nur77 expression than non-switched GC B cells. Once B cells differentiate into memory B cells, IgG1 provides a stronger signal than IgM, as expected (Waisman, Kraus et al. 2007, Weston-Bell, Forconi et al. 2014). Memory B cells from IgMg1 mice show a continued anergic footprint with repressed BCR signalling, even if the IgMg1 chimeric BCR is not expressed any longer. These conclusions should be confirmed by re-challenge studies and observation of BCR signalling after antigen-receptor stimulation *in vitro*.
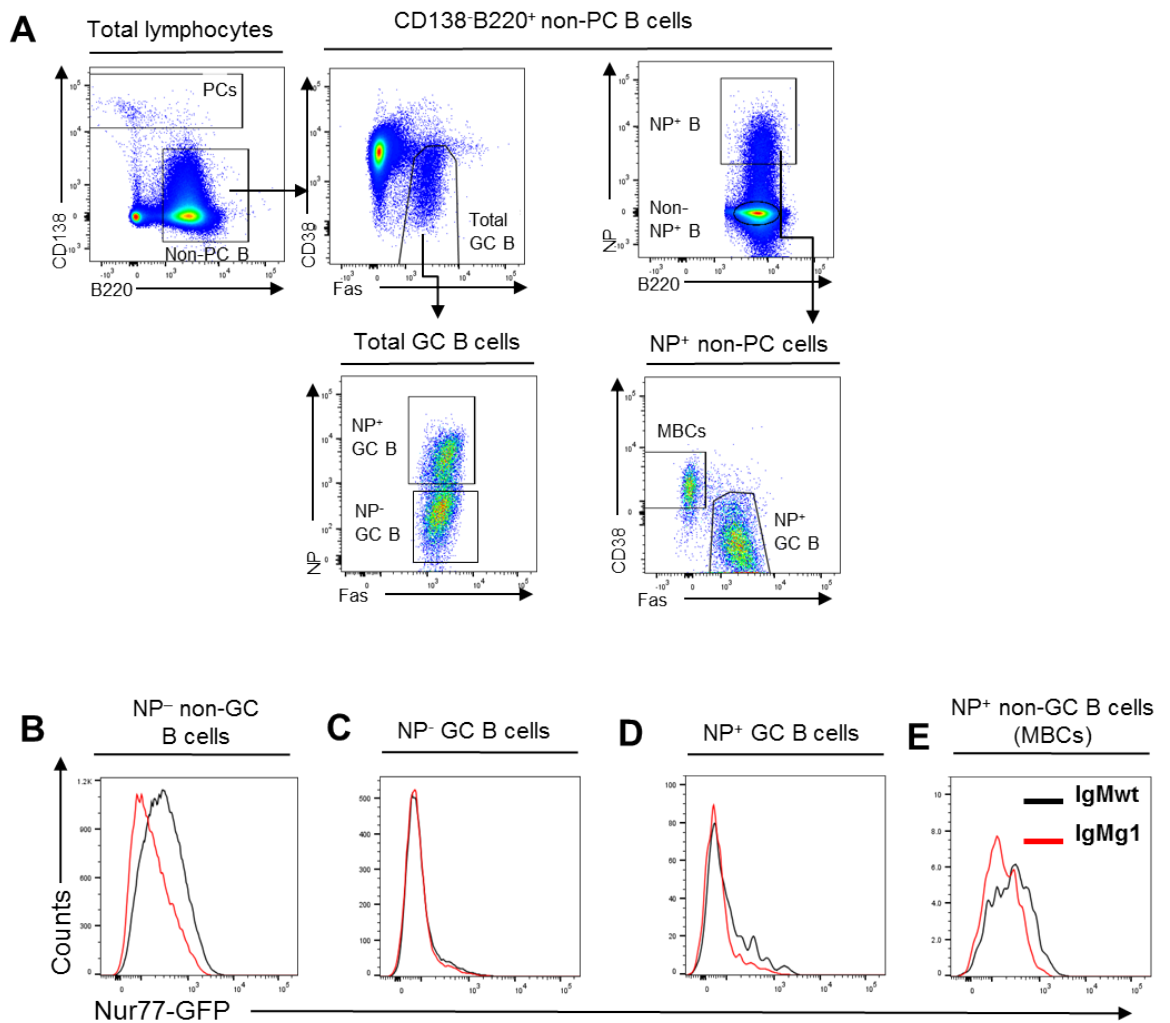
Figure 4.24: Nur77-GFP expression in the T-D immune response.

Both Nur77-GFP IgMwt and IgMg1 mice are immunised with 20 µg heat-inactivated *Bordetella pertussis* (BP) into plantar surface of foot. Popliteal LNs are collected 8 days after immunisation.

    A. Gates for different B cell populations assessed during T-D immune response. B-E. Overlays of Nur77-GFP expression levels in different B cell populations from both IgMwt (black) and IgMg1 (red) mice.
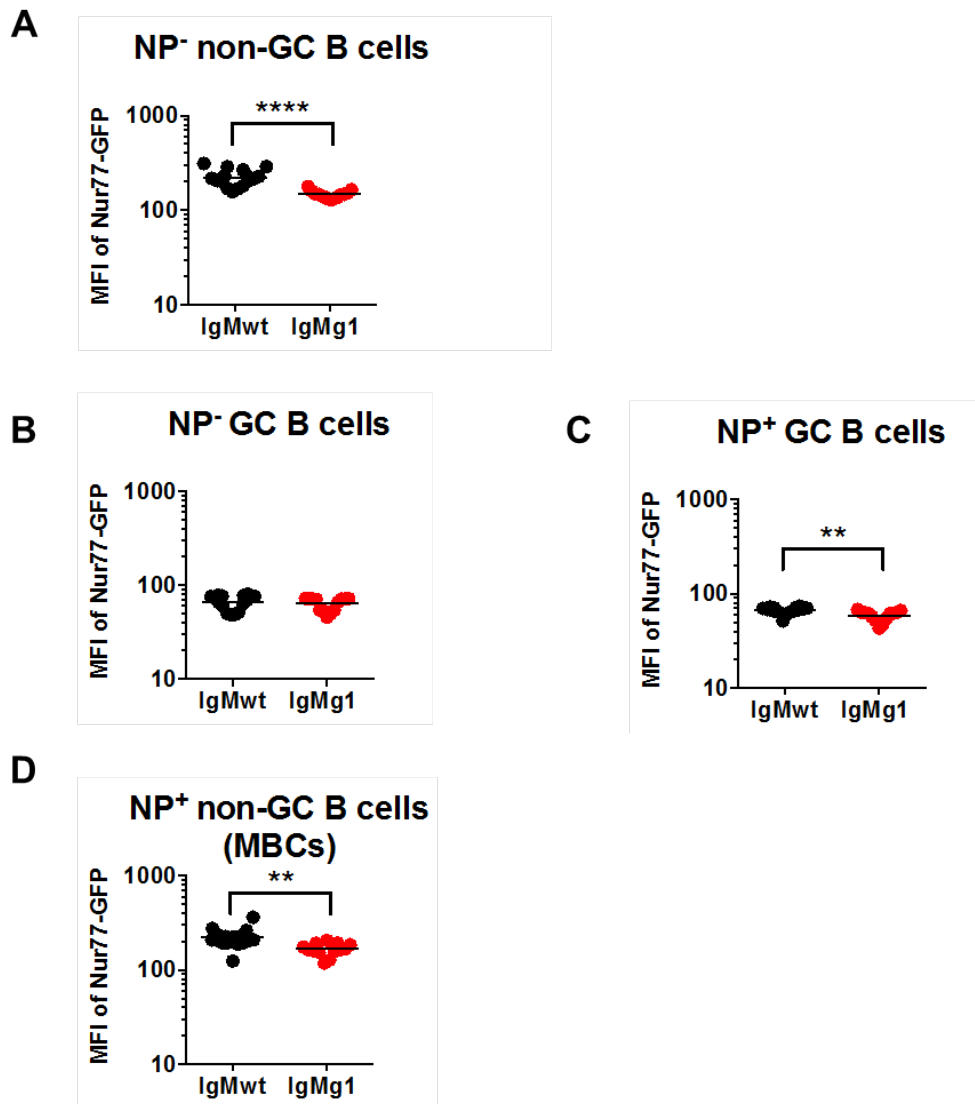
Figure 4.25: Lower Nur77-GFP expressions in different B cell populations from IgMg1 mice during T-D immune response.

Both Nur77-GFP and IgMg1 Nur77-GFP mice are immunised with 20 µg alum precipitated NP-CGG on plantar surface of foot, heat-inactivated *Bordetella pertussis* (BP) as adjuvant. After immunisation, popliteal LNs are collected on day 8.
A-D. Statistical analysis of Nur77-GFP expression levels within different B cell populations during T-D immune response.
$**p < 0.01$; $****p < 0.0001$; multiple t test. Bars indicate mean. Each symbol represents sample from one mouse. Data are combined from two independent experiments.

A

Total GC B

IgMwt
NP+ 23.6%
NP- 76.4%

IgMg1
NP+ 37.3%
NP- 62.7%

NP

Fas

NP+ total GC B

IgMwt
IgG1+ 81.3%
IgM+ 10.9%

IgMg1
IgG1+ 90.5%
IgM+ 4.64%

IgG1

IgM

NP- total GC B

IgMwt
IgG1+ 48.5%
IgM+ 21.1%

IgMg1
IgG1+ 50.5%
IgM+ 14.8%

IgG1

IgM

B

Total GC B cells

NP-   NP+

IgMwt   IgM
IgMg1   IgG1

Counts

Nur77-GFP

C NP− total GC B

● IgM+ GC B
● IgG1+ GC B

MFI of Nur77

100

10

****   ****

IgM+ IgG1+   IgM+ IgG1+
WT   IgMg1

D NP+ total GC B

MFI of Nur77

100

10

****   ****

IgM+ IgG1+   IgM+ IgG1+
WT   IgMg1
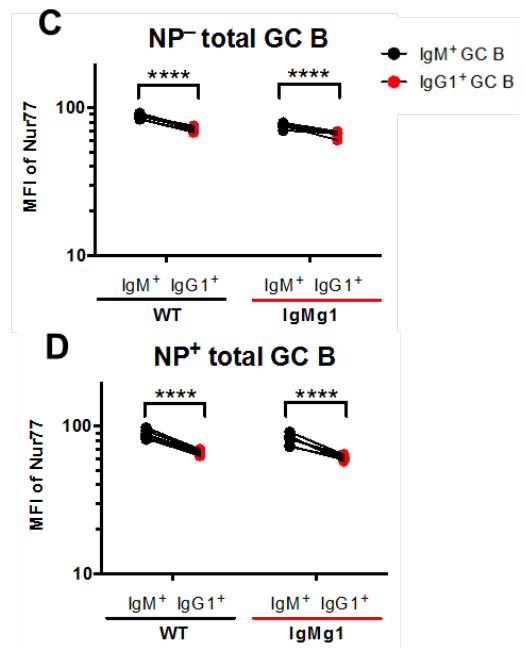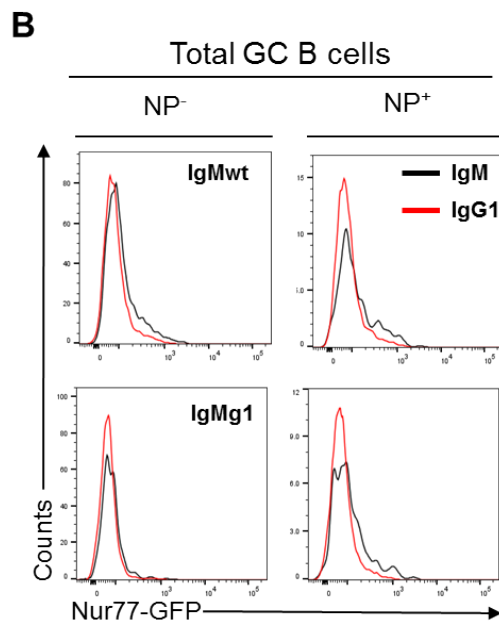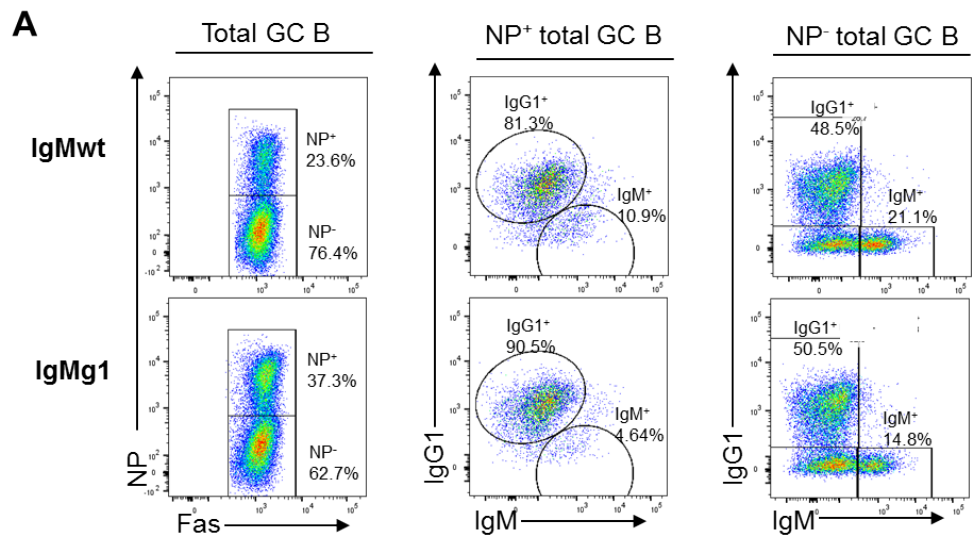
Figure 4.26: IgG1$^+$ GC B cells transduce lower down-stream BCR signalling than IgM$^+$ GC B cells.

Both Nur77 IgMwt and IgMg1 mice are immunised with 20 μg alum precipitated NP-CGG on plantar surface of foot, heat-inactivated *Bordetella pertussis* (BP) as adjuvant. After immunisation, popliteal LNs are collected on day 8.

    A. Gates for NP-specific and NP-non-specific total GC B cell populations, and IgM$^+$, IgG1$^+$ subsets within each population after 8 days of immunisation.

    B. Overlays of Nur77-GFP expression levels in NP-specific and NP-non-specific total GC B cells after 8 days of immunisation.

    C. MFI of Nur77-GFP expression levels in NP-non-specific total GC B cells and compared between IgM$^+$ GC B cells and IgG1$^+$ GC B cells.

    D. MFI of Nur77-GFP expression levels in NP-specific total GC B cells and compared between IgM$^+$ GC B cells and IgG1$^+$ GC B cells

****$p < 0.0001$; multiple t test. Each symbol represents sample from one mouse. Data are representative from two independent experiments.
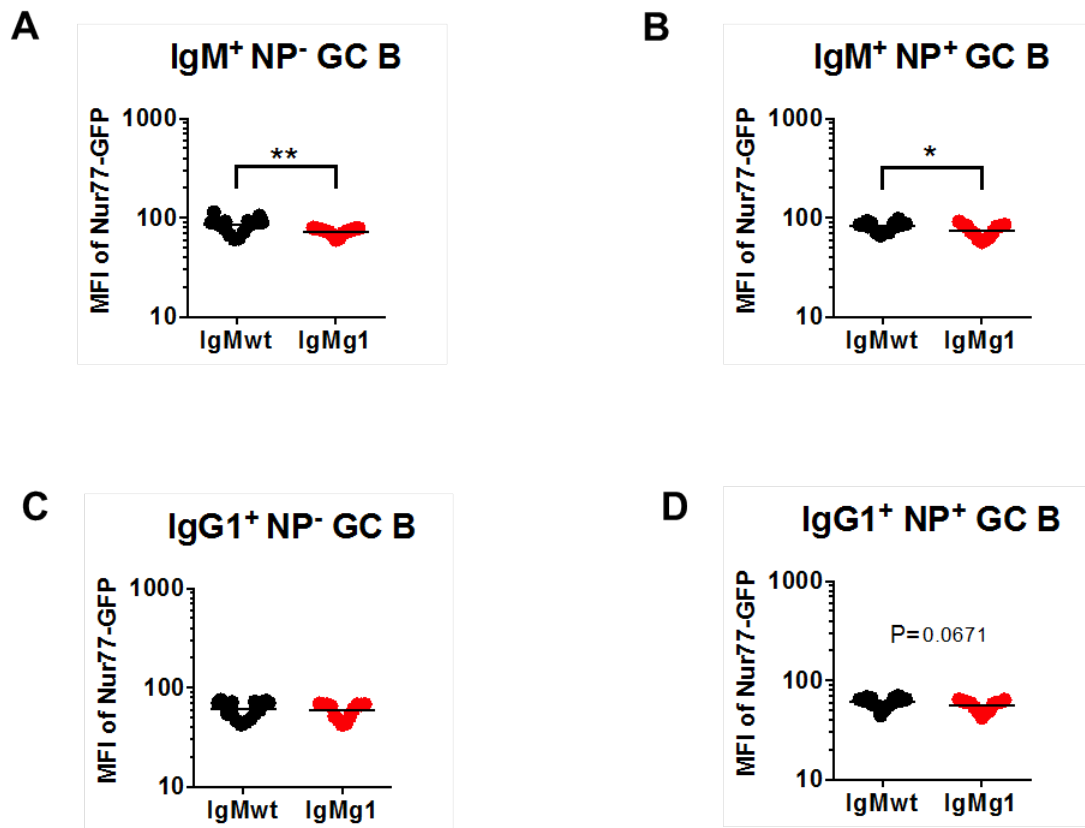
Figure 4.27: The suppression of BCR signalling is retained in IgM$^+$ GC B cells from IgMg1 mice.

Both Nur77-GFP IgMwt and IgMg1 mice are immunised with 20 μg alum precipitated NP-CGG on plantar surface of foot, heat-inactivated *Bordetella pertussis* (BP) as adjuvant. After immunisation, popliteal LNs are collected on day 8. Gates for NP-specific and NP-non-specific total GC B cell populations, and IgM$^+$, IgG1$^+$, IgM$^-$ IgG1$^-$ subsets within each population are shown in Fig. 4.27A.

- A. MFI of Nur77-GFP expression levels in IgM$^+$ NP-non-specific total GC B cells.
- B. MFI of Nur77-GFP expression levels in IgM$^+$ NP-specific total GC B cells.
- C. MFI of Nur77-GFP expression levels in IgG1$^+$ NP-non-specific total GC B cells.
- D. MFI of Nur77-GFP expression levels in IgG1$^+$ NP-specific total GC B cells.

*p < 0.05; **p < 0.01; multiple t test. Bars indicate mean. Each symbol represents sample from one mouse. Data are combined from two independent experiments
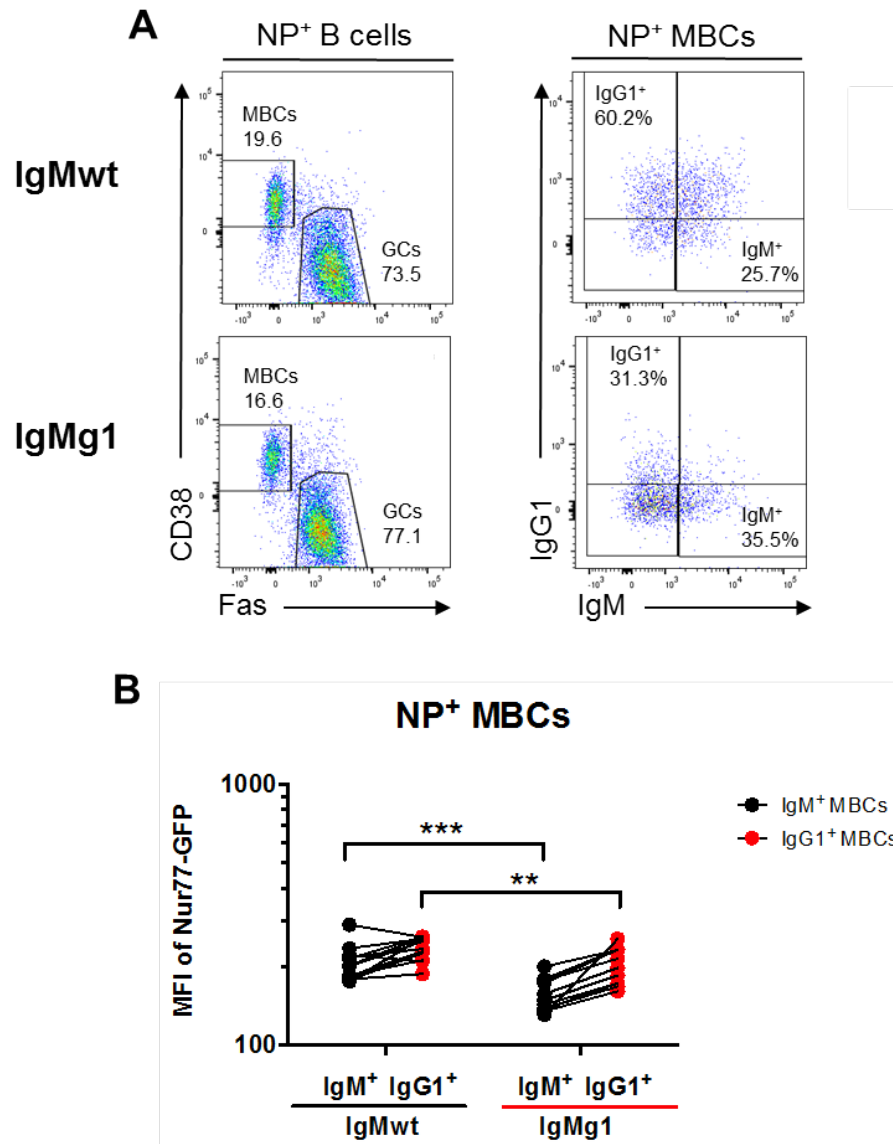
Figure 4.28: Continued repressed BCR signalling in IgG1-switched MBCs from IgMg1 mice.

Both Nur77-GFP and IgMg1 Nur77-GFP mice are immunised with 20 μg alum precipitated NP-CGG on plantar surface of foot, heat-inactivated *Bordetella pertussis* (BP) as adjuvant. After immunisation, popliteal LNs are collected on day 6 and day 8.

A. Gates for IgG1$^+$ and IgM$^-$ NP-specific MBCs after 8 days of immunisation.
B. MFI of Nur77-GFP expression levels in IgM$^+$ and IgG1$^+$ NP-specific MBCs, and compared between IgMwt and IgMg1 mice.

**p < 0.01; **p < 0.001; ****p < 0.0001; unpaired t test between IgMwt and IgMg1. Paired T test between IgM$^+$ and IgG1$^+$ MBCs from the same mouse. Each symbol represents sample from one mouse. Data are combined from two independent experiments.

4.2.9 Increased Tfh cell differentiation in the presence of IgMg1 B cells

The previous sections showed a B cell intrinsic mechanism that confers a reduction in BCR signalling in non-switched and switched B cells from IgMg1 mice. However, the general changes of population sizes in IgMwt/IgMg1 bone marrow chimeras (Fig 4.16) indicate that there are also some general environmental changes in the presence of IgMg1 B cells. In order to test which non-B cell intrinsic factor might be responsible, Tfh cell numbers were assessed over time after immunisation with NP-CGG.

Two main functional T cell populations were tested in IgMwt and IgMg1 homozygous mice: $CD3^+CD4^+CD62L^-CD44^+$ cells as activated $CD4^+$ T cell, and $CD3^+CD4^+CD62L^-CD44^+CXCR5^+PD-1^+$ cell as Tfh cells (Fig. 4.29A). This showed that the proportions of total activated T cells in the two groups were quite similar during the whole time course (Fig. 4.29B). Testing the proportion of these activated T cells differentiating into Tfh cells showed a significantly larger fraction of activated T cells had differentiated into Tfh cells in IgMg1 mice compared to IgMwt mice from day 6 to day 14 after immunisation (Fig. 4.29C). In-line with this, there was a trend towards higher Tfh cell percentages within total $CD4^+$ T cells from day 6 after immunisation in IgMg1 mice (Fig. 4.29D).

Tfh cell differentiation was also tested in IgMwt and IgMg1 B cell bone marrow chimeric mice after immunisation with NP-CGG on the rear feet (Fig. 3.15). Tfh cells

were gated 8 days after immunisation (Fig. 4.30A). As in homozygous mice, similar percentages of activated T cells developed in IgMwt/IgMwt and IgMwt/IgMg1 chimeras (Fig. 4.30B), suggesting that the presence of IgMg1 B cells did not affect general T cell activation. However, IgMwt/IgMg1 chimeras had significantly higher proportions of Tfh cells within activated T cells than IgMwt/wt chimeras (Fig. 4.30C). Tfh cells also accounted for higher percentages within total CD4$^+$ T cells (Fig. 4.29D). Taken together these data suggest that IgMg1 B cells can promote Tfh cell differentiation, which may generate an environment where B cell activation is increased, whether B cells are IgMwt or IgMg1 derived.

A

CD3⁺CD4⁺ T cells

CD62L⁻CD44⁺ activated T cells

IgMwt

IgMg1

CXCR5 isotype

TfH 39.4%

TfH 52.4%

CD62L⁻CD44⁺ Activated T cells

CD62L⁻CD44⁺ activated T cells

PD-1

CXCR5

CD62L

CD44

PD-1

CXCR5

B CD62L⁻CD44⁺ activated T cells

% within T cells

D4 D5 D6 D8 D14

C TfH cells

IgMg1
IgMwt

% within CD62L⁻CD44⁺ activedT cells

P=0.005 P=0.024 P=0.002

D4 D5 D6 D8 D14

D TfH cells

IgMg1
IgMwt

% within T cells

P=0.027

D4 D5 D6 D8 D14

209

Figure 4.29: Biased Tfh cell differentiation during T-D immune response in IgMg1 mice.

WT and IgMg1 mice were immunised with 20 µg alum precipitated NP-CGG on plantar surface of foot, heat-inactivated *Bordetella pertussis* (BP) as adjuvant. Popliteal LNs were collected 4, 5, 6, 8 and 14 days after immunisation.

A. Gate setting for $CD3^+CD4^+CD62L^-CD44^+CXCR5^+PD-1^+$ Tfh cells. CXCR5 isotype control has been used for the quality control.
B. Percentages of $CD3^+CD4^+CD62L^-CD44^+$ active T cells.
C. Percentages of Tfh cells within active T cells.
D. Percentages of Tfh cells within CD4+ T cells.

Multiple t test. Bars and whiskers indicate mean ± SD. D4 and D5 data are from one experiment, with a total number of 4 mice. D6 and D8 data are from three independent experiments, with a total number of 12 mice. D14 data are from two independent experiments, with a total number of 8 mice.
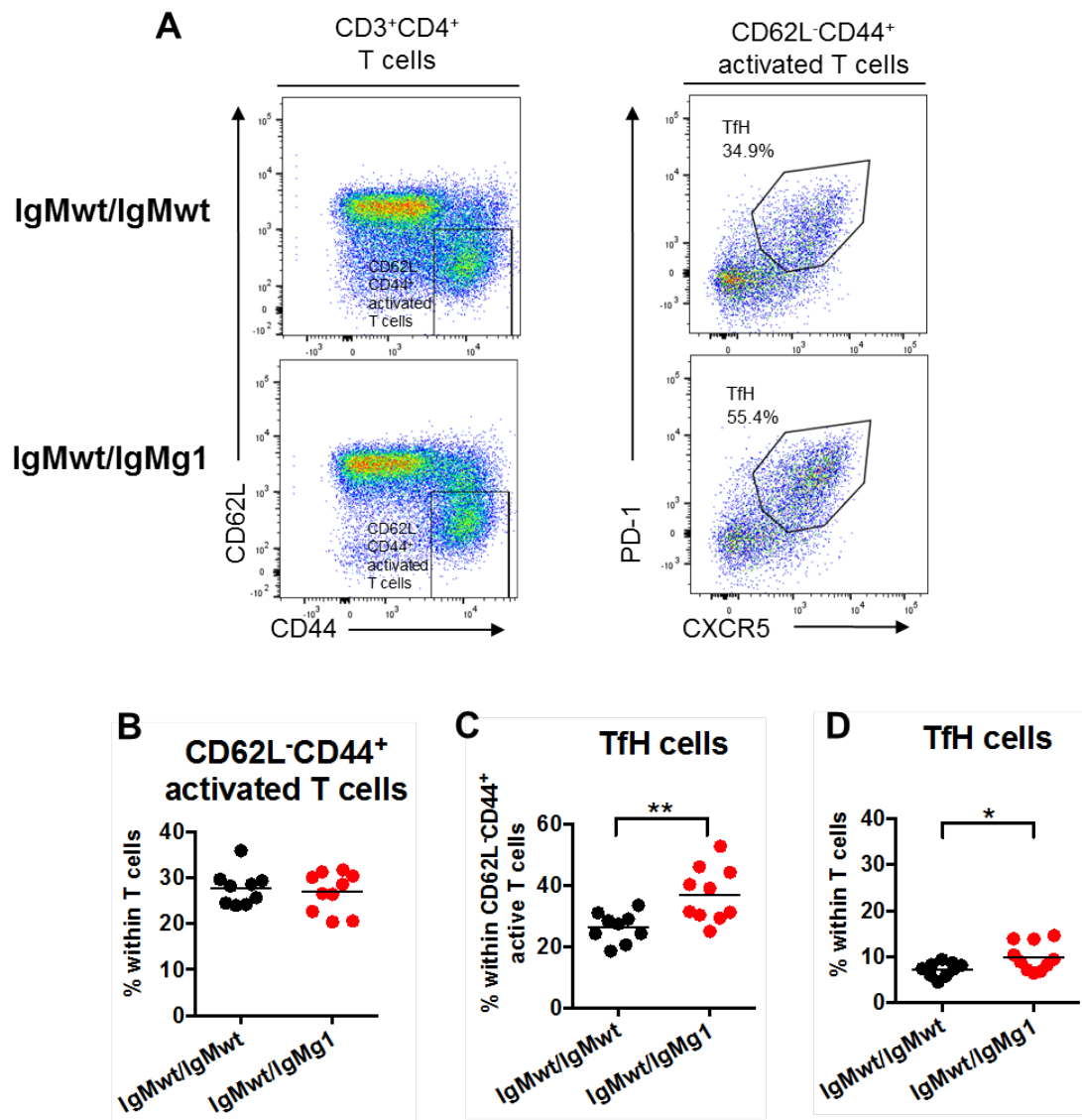
Figure 4.30: Biased Tfh cell differentiation during T-D immune response in IgMg1 bone marrow chimeras.

IgMwt/IgMwt and IgMwt/IgMg1 chimeric mice were immunised with 20 µg alum precipitated NP-CGG on plantar surface of foot, heat-inactivated *Bordetella pertussis* (BP) as adjuvant. Popliteal LNs were collected 8 days after immunisation.

- A. Gate setting for $CD3^+CD4^+CD62L^-CD44^+CXCR5^+PD-1^+$ Tfh cells.
- B. Percentages of $CD3^+CD4^+CD62L^-CD44^+$ active T cells.
- C. Percentages of Tfh cells within active T cells.
- D. Percentages of Tfh cells within CD4+ T cells.

$*p < 0.05$; $**p < 0.01$; unpaired Student t test. Bars indicate mean. Each symbol represents sample from one mouse. Data are combined from two independent experiments.

4.2.10 Presence of auto-immune antibodies in aged IgMg1 mice
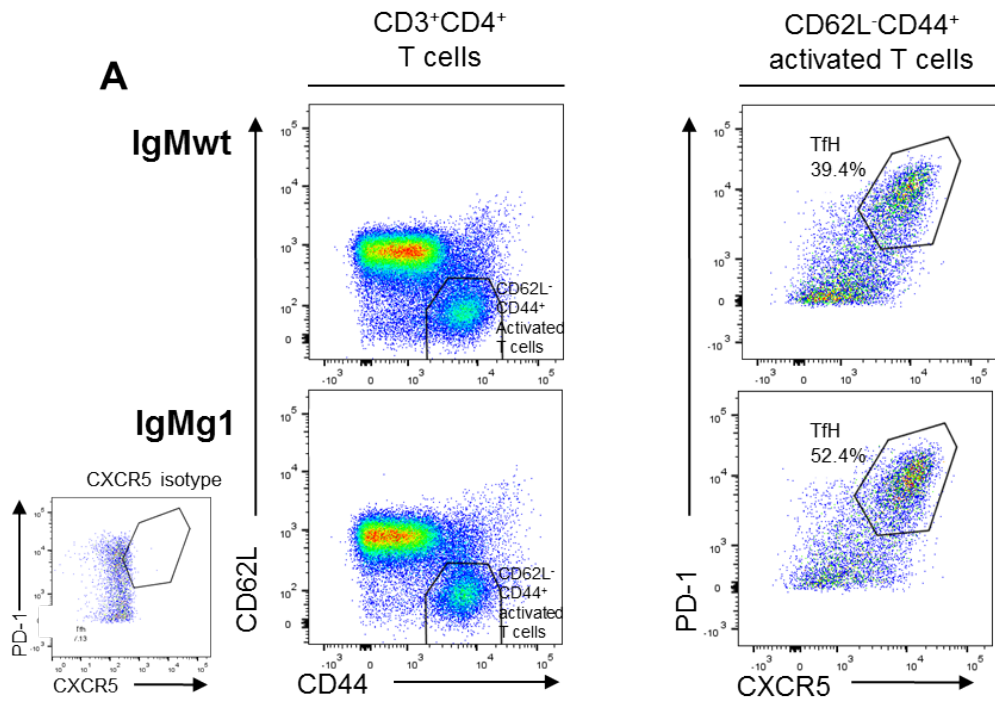
B cell anergy is reversible (Gauld, Benschop et al. 2005, Getahun, Beavers et al. 2016). Breakage of tolerance, development of auto-antibodies, and overt auto-immunity has been observed in different animal models of B cell anergy during ageing (Hibbs, Tarlinton et al. 1995, Getahun, Beavers et al. 2016). Not only in mice, but also in healthy humans and non-human primates, has the production of auto-antibodies been observed to increase with ageing (Rowley, Buchanan et al. 1968, Attanasio, Brasky et al. 2001). In order to test whether or not auto-antibodies develop during ageing in the IgMg1 mouse model, serum samples were harvested from young (8 weeks) or old aged mice (6-month or 1 year) and applied to rat tissue slides to detect crossreactive autoantibodies. Each spot on these auto-immune slides is pre-coated with sections of rat liver, gut, stomach, and kidney. These slides allow the detection of anti-nuclear antibody (ANA), anti-smooth muscle antibody (ASMA), anti-mitochondrial antibody (AMA) and different liver and kidney-specific auto-antibody patterns. Slides were incubated with serum overnight and screened next day by an experienced clinical immunologist (Dr. Abid Karim, Clinical Immunology Service, UoB Medical School).

After incubation of slides with serum samples from young IgMwt and IgMg1 mice, one in four slides from both IgMwt and from IgMg1 mice showed weak non-typical binding of serum antibody to membranes or gastric parietal cells (Fig. 4.31A, B and C). The majority of aged IgMwt mice showed no specific serum antibody binding to

the tissue arrays, or only non-specific binding at the edge of tissue sections (Fig. 4.32A). Two of eight aged IgMwt mice showed specific anti-smooth muscle antibody (ASMA) staining (Fig. 4.32C and D). Aged IgMg1 mice, on the contrary, showed clear diverse auto-immune antibody binding patterns (Fig. 4.32B and D). There were at least four different auto-antibody patterns: anti-nuclear antibody (ANA), anti-kidney antibody, ASMA, and anti-kidney-liver microsome (KLM) antibody (Fig. 4.32B and D). 87.5% of IgMg1 serum samples displayed the presence of auto-antibodies, which was more than three times higher than wildtype (Fig. 4.32C).

To explore whether production of autoantibody in aged mice is due to a break of tolerance during ageing or due to a change of VDJ repertoire and a higher occurrence of B cells with auto-reactive BCRs emerging from the bone marrow in IgMg1 mice, B cells of young IgMg1 mice were cloned to test their autoreactive potential. Single follicular B cells were sorted from spleens of non-immunised young IgMwt and IgMg1 mice and seeded onto CD40L, BAFF, and IL-21 expressing fibroblastic feeder cells to generate single cell derived plasma cell colonies. Cells were cultured in microtitre plates for 10 days, and cell culture medium was not changed in the last 48 h to enrich for secreted antibodies. At the end of culture, microtitre plates were screened for the presence of large plasma cell colonies. Supernatants from these wells were harvested and tested for the presence of autoantibodies.

Supernatants from all B cell colonies were applied to auto-immune slides and screened for the presence of tissue specific auto-antibody patterns. Among the 76

samples tested of each IgMwt and IgMg1 B cells, the frequency of auto-reactivity was quite low, with 1 in 76 from IgMwt and 2 in 76 from IgMg1 testing positive for autoantibody (Fig. 4.33B). While the one positive IgMwt sample showed a strong anti-mitochondrial antibody staining pattern (AMA), the two positive IgMg1 samples showed a very weak anti-kidney autoantibody pattern (Fig. 4.33A). These results suggest that the BCR repertoire emerging from bone marrow in young IgMg1 mice is not more prone to be auto-reactive than that of IgMwt mice. It does not exclude that the breach of tolerance observed in aged mice is due to impaired negative selection during B cell development, and further experiments studying the autoreactivity of the naïve B cell repertoire emerging from bone marrow in aged IgMwt and IgMg1 mice should be performed to answer this.

A negative control

B IgMwt 8 weeks   IgMg1 8 weeks

Membrane-binding   Gastric parietal cell binding

C Young WT   Young IgMg1

Negative / membrane binding   Negative / gastric parietal cell binding

N=4   N=4
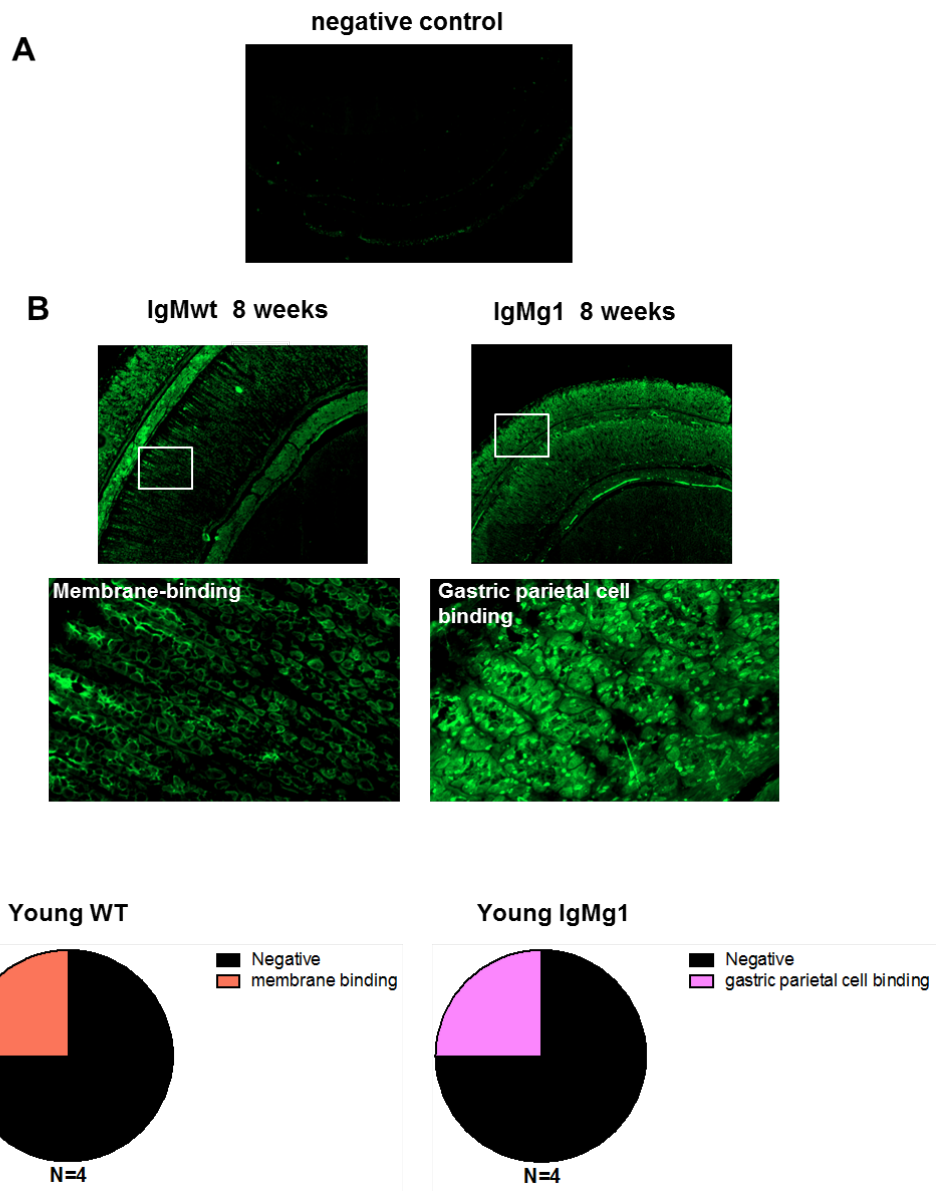
Figure 4.31: Auto-reactive B cells have not been detected to increase in serum samples from young IgMg1 mice.

Serum samples have been collected from both young (8 weeks) IgMwt and IgMg1 mice. 50 µl net sera is added to each spot on the auto-immune slide, incubated at 4 ˚C, overnight. Auto-antibodies are detected by FITC conjugated anti-mouse IgG1 antibody.

- A. Representative image from negative control incubated spots.
- B. Positive images from both IgMwt and IgMg1 serum samples incubated spots.
- C. Pie charts to summarize results from auto-immune slides. Total number of sample, the diversity of auto-immune patterns and frequency of auto-immune patterns have been displayed.

215

A PBS negative control   C57BL/6 IgMwt Female 1Y

B Mg1/g1 Female 6M   Mg1/wt Female 1Y   Mg1/wt Male 1Y   Mg1/wt Male 1Y

ANA   Anti-Kidney   KLM   ASMA

C Aged mice serum

auto-immune
Negative

Sample number

WT   IgMg1

D Aged WT   Aged IgMg1

Negative
ASMA

Negative
ASMA
ANA
Anti-Kidney
KLM

N=8   N=8
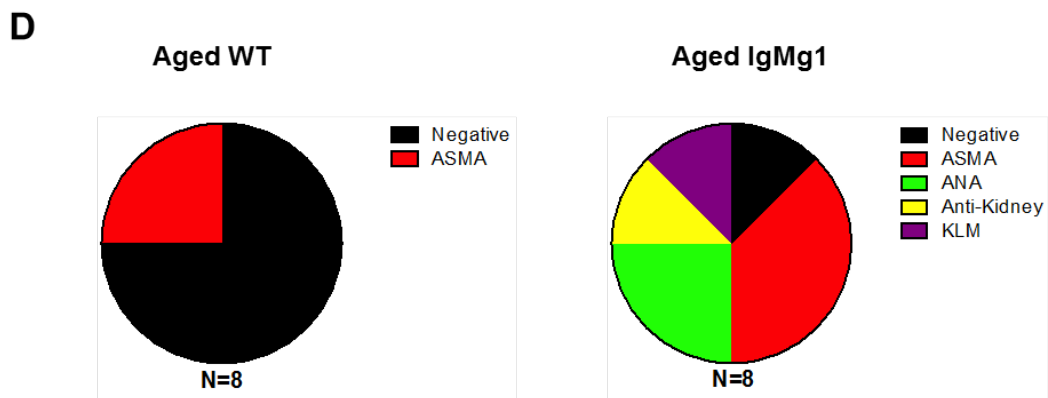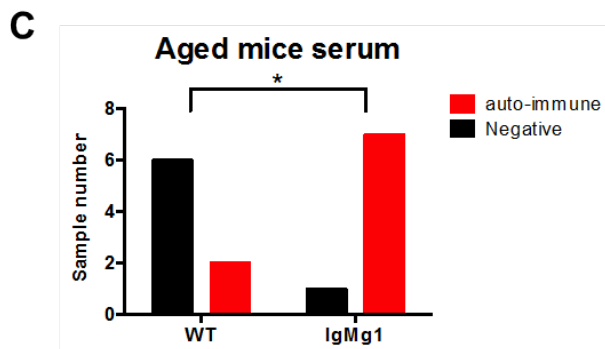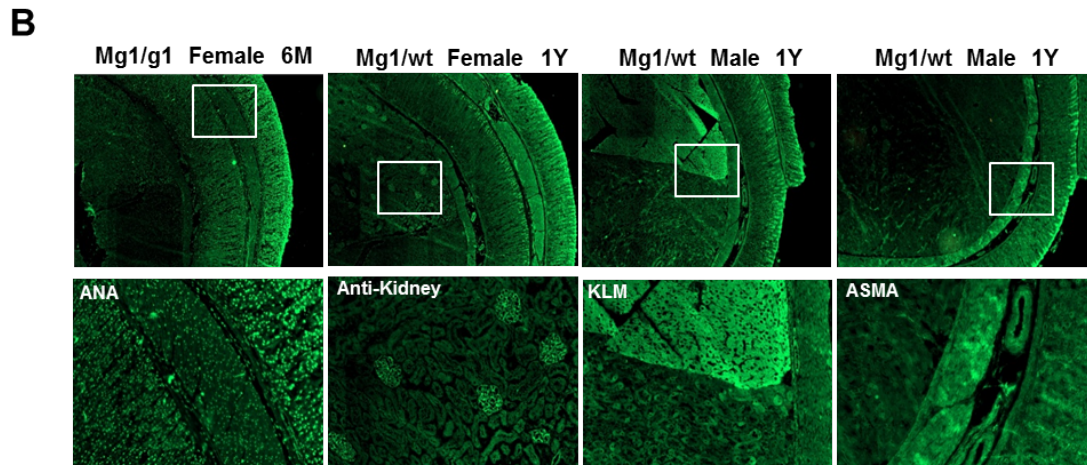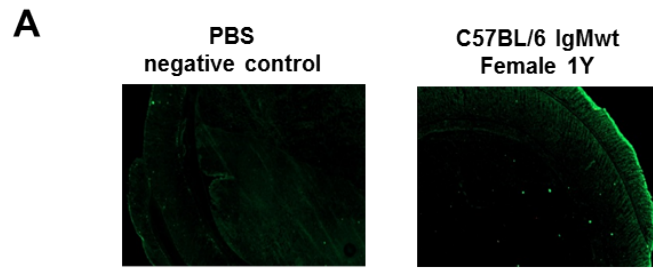
Figure 4.32: The presence of diverse auto-antibodies in IgMg1 mice aged more than 6 months.

Serum samples have been collected from both IgMwt and IgMg1 mice aged more than 6 months. Add 50 µl net sera to each spot on the auto-immune slides, incubated at 4 ˚C, overnight. Auto-antibodies are detected by FITC conjugated anti-mouse IgG1 antibody.

A. Representative image from PBS and IgMwt serum sample incubated spots.
B. Representative images of IgMg1 serum samples incubated spots.
C. Summarizing statistic of samples displaying auto-immune patterns and not displaying auto-immune patterns (negative). Compared between groups.
D. Pie charts to summarize results from auto-immune slides. Total number of sample, the diversity of auto-immune patterns and frequency of auto-immune patterns have been displayed.

*$p < 0.05$; Fishser's exact test. Histogram indicates the exact sample numbers. Data are combined from two independent experiments.

A

IgMwt   IgMg1

AMA   Anti-Kidney

B

Single cell culture

ns

auto-immune
Negative
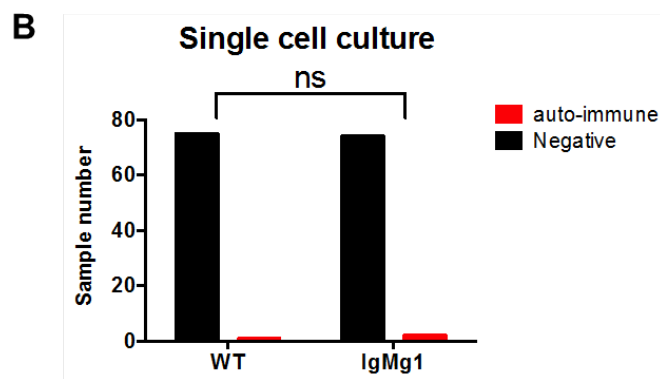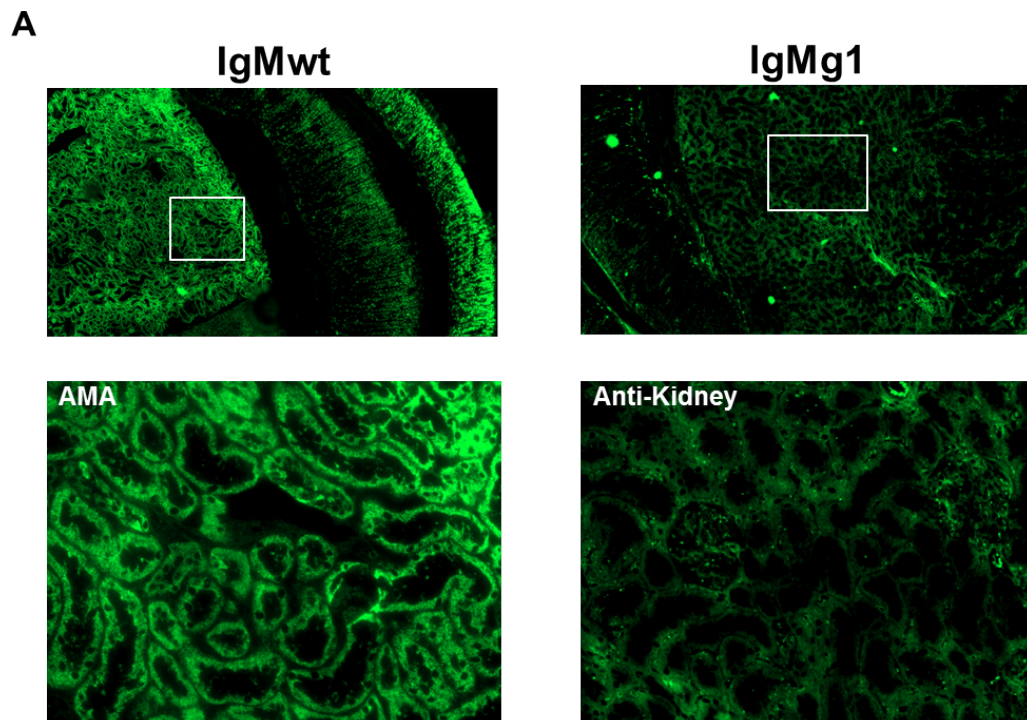
Figure 4.33: Auto-reactive B cells have not been detected to increase in the follicular B cell pool of young IgMg1 mice.

A. Positive images of autoimmune tissue slides incubated with supernatants from single cell cultures of IgMwt and IgMg1 follicular B cells. Single cell culture system is used to induce single sorted follicular B cells into plasma cell colonies. Supernatant of each plasma cell colony have been harvested, added to auto-immune slides and assessed for auto-immune staining.
B. Summary of single cell culture results.

ns, not significant; Fishser's exact test. Histogram indicates the exact sample numbers. Data are combined from three independent experiments in B.

4.3 Discussion

4.3.1 IgMg1 B cells are permanently programmed to be anergic

After 8 days of NP-CGG immunisation, in local responding LNs, there is a pronounced reduction of Nur77-GFP expression in naïve follicular B cells and a continuous significant reduction in IgM$^+$ non-switched GC B cells in IgMg1 mice. However, IgG1-switched GC B cells in IgMg1 mice seem to have similar Nur77-GFP expression levels as IgMwt-derived IgG1$^+$ GC B cells. This does not necessarily indicate a recovery of BCR signalling after B cells switched to IgG1 in IgMg1 mice. Nur77-GFP expression is severely suppressed in GC B cells (Mueller, Matloubian et al. 2015, Gitlin, von Boehmer et al. 2016) and small differences in BCR signalling in IgG1$^+$ GC B cells of IgMg1 mice may be just undetectable using this method. In IgG1-switched MBCs, however, signalling transduced from IgG1 increases and is therefore readily detectable. This shows that Nur77-GFP expression level in IgG1$^+$ MBCs from IgMg1 mice is still substantially lower than their WT counterparts. Taken together, these findings demonstrate that IgMg1 B cells maintain a continued anergic footprint with repressed BCR signalling even after activation, loss of IgM expression, and differentiation into MBCs.

Cell differentiation and the maintenance of cells in a specific state normally require genetic reprogramming, such as epigenetic modification. The maintenance of an anergic pattern in B cells is reported to depend upon continuous signalling from BCR/self-antigen ligation. This anergic state can be reversed after BCRs are freed

from contact with self-antigens (Goodnow, Brink et al. 1991, Gauld, Benschop et al. 2005). These studies led to the assumption that B cell anergy is not a genetically programmed process, and the non-responsive state of these cells is just due to chronic BCR activation and signalling (Goodnow, Brink et al. 1991, Cambier, Gauld et al. 2007). Nevertheless, in these studies, the ability of anergic B cells to respond is not completely reversed after occupied BCRs are freed from self-antigens. After culturing Ars-specific anergic B cells with Ars-tyrosine to free their BCRs from self-antigen binding, these recovered B cells can respond to BCR stimulation but still generate much lower down-stream signalling after activation (Gauld, Benschop et al. 2005). HEL-specific anergic B cells from the MD4 × ML5 mouse model need around 48 hours to regain responsiveness when transferred to a self-antigen free environment and the immune response after activation remains lower afterwards (Goodnow, Brink et al. 1991). These studies show that following recovery from self-antigen binding, these B cells become less tolerized, and can partially respond to self-antigen, but are still in a repressed state. Thus the maintenance of an anergic state is not solely determined by constant BCR/self-antigen ligation, permanent genetic programming is likely to be involved as well.

In the IgMg1 mouse model, additional signalling from the IgG1 cytoplasmic tail is likely to mimic the continuous BCR/self-antigen ligation signalling and induce IgMg1 B cells into an anergic state. Consistent with findings above, the results shown here demonstrate that the maintenance of an anergic pattern in IgMg1 B cells is not solely dependent on the presence of extra signalling from the IgG1 cytoplasmic region.

Despite recovery of surface IgG1 expression level in IgG switched GC B cells and MBCs in IgMg1 mice, BCR signalling reflected by Nur77-GFP expression remains repressed. IgG1$^+$ MBCs have lost the extra signalling from chimeric IgMg1, but the anergic pattern is maintained. This suggests that a combination of constant BCR/antigen ligation and genetic re-programming is involved in the maintenance of this anergic state in IgMg1 B cells.

4.3.2 Continuous repression of BCR signalling in GC B cells from IgMg1 mice might affect GC B cell selection

There was a significantly higher proliferation rate of GC B cells in IgMg1 mice on day 8 after immunisation with NP-CGG, and the proportion of apoptotic GC B cells was significantly higher on day 6 and slightly higher on days 8 and 14. Throughout the GC reaction, GC B cells are selected for different fate decisions, such as survival, differentiation, or death. The different proliferation and apoptosis rates observed in IgMwt and IgMg1 GC B cells reflect an altered balance of fate decisions they experience during GC reactions.

BCR signalling has been reported to be necessary for the effective expression of c-Myc in GC B cells (Luo, Weisel et al. 2018). As discussed above, BCR signalling in activated NP$^+$ GC B cells from IgMg1 mice is continuously repressed throughout the T-D response. Dampened BCR signalling in GC B cells of IgMg1 mice may lead to lower c-Myc expression and result in enhanced apoptosis during the early GC response in IgMg1 mice. Despite BCR signalling remaining repressed on day 8 after

immunization, we observed a higher proliferation rate of GC B cells in IgMg1 mice at this later stage. The strength of T cell help correlates with the GC B cell proliferation rate (Gitlin, Mayer et al. 2015). As our results showed there were higher numbers of Tfh cells on day 8 after immunisation in IgMg1 mice, it is possible that by day 8 IgMg1 GC B cells receive more help from Tfh cells to proliferate faster. More experiments are probably needed to reveal the detailed mechanisms on how the changed BCR and co-stimulation signalling affect IgMg1 GC B cell selections during GC response.

By studying the dynamic process of the GC response, we noticed there is a rapid shift in antigen specificity following immunisation with hapten-carrier protein conjugates (NP-CGG). Tracking of the constant decline of the fraction of NP specific GC B cells in IgMwt mice after immunisation showed that there are significantly higher percentages of NP-specific GC B cells in IgMg1 mice at day 8 after immunisation, i.e. there was a delayed shift in GC B cell specificity from NP to other specificities. The dynamic process of the GC response is regulated by GC intrinsic selection, combined with immigration, emigration, proliferation, and apoptosis. Firstly, the delayed shift in antigen-specificity could be explained by reduced immigration. There is a remarkable repression of BCR signalling in naïve follicular B cells of local responding LNs from IgMg1 mice, which can make these B cells less likely to respond to low-affinity epitope leading to a reduction in GC recruitment, and a longer-lasting response to NP. Secondly, despite the slightly higher affinity observed in non-switched IgMg1 expressing GC B cells at earlier stages of the GC response, IgG1 switched GC B cells

in IgMg1 mice display lower affinity on day 8 after immunisation. This indicates a slower affinity maturation process in the GCs of IgMg1 mice. This reduced affinity maturation could affect the total GC response by limiting emigration of NP-specific cells from the GC, and slowing down recruitment of new Fo B cells which are specific for low-affinity, non-NP-specific epitopes. More experiments are needed to explore the link between lower BCR signalling strength of GC B cells and slower affinity maturation of the GC response in IgMg1 mice.

4.3.3 T cells serve as a peripheral check point to regulate peripheral anergic B cell activation and differentiation

By employing the IgMg1 mouse model, we were able to investigate polyclonal anergic B cells fate decisions in different immune responses. Anergic IgMg1 B cells respond with a significantly lower efficiency to TI-II antigen NP-Ficoll than WT B cells, with an impaired ability to generate NP^+ B cells and NP^+ plasma cells. This observation was compatible with reduced activated BCR signalling in anergic B cells (Goodnow, Crosbie et al. 1988), since NP-Ficoll activates B cells through their BCR only, without co-stimulation signalling from T cells (Inman 1975). The decrease of MZ B cells in IgMg1 mice can to some extent affect T-I immune response as well, as MZ B cells have been reported to be the dominant cell population that respond to T-I antigen stimulation (Martin, Oliver et al. 2001). However, when responding to NP-CGG, a T-dependent antigen, B cells in IgMg1 mice were equally effective to respond compared to their WT counterparts. The opposite results of T-D and T-I immune responses imply that T cells can serve as a checkpoint to control the activation of

anergic B cells in the periphery. BCR signalling in anergic B cells is suppressed which prevents non-specific activation, and it is only with corresponding secondary T cell help, that these cells can be fully activated and effectively involved in the immune response. This observation is compatible with previous studies showing that the CD40-dependent activation pathway is intact in anergic B cells (Cooke, Heath et al. 1994, Eris, Basten et al. 1994) and that silenced auto-reactive B cells can be induced into a GC B cell fate after receiving cognate help from T cells (Fulcher, Lyons et al. 1996, Sabouri, Schofield et al. 2014, Burnett, Langley et al. 2018).

Previous studies have shown that the maintenance of Tfh cells in GCs requires constant signalling from cognate B cells (Coffey, Alabyev et al. 2009, Kerfoot, Yaari et al. 2011, Baumjohann, Preite et al. 2013), indicating that the interactions between Tfh cells and B cells are reciprocal during GC reactions. Results from our study show biased Tfh cell differentiation in the presence of IgMg1 B cells, from either homozygous IgMg1 mice or IgMg1/IgMwt bone marrow chimeras, and that there are significantly more Tfh cells on day 8 after immunisation in IgMg1 mice. These results suggest that IgMg1 B cells can possibly provide enhanced signalling to cognate T cells, which may potentially affect activated T cell differentiation and promote the generation of Tfh cells. Despite the impairment of BCR signalling in anergic B cells, these cells can continuously present self-antigens to T cells (Eris, Basten et al. 1994). Auto-reactive B cells are also shown to trigger auto-immune disease by presenting self-antigen to T cells and activating them (Dai, Carayanniotis et al. 2005, Giles, Kashgarian et al. 2015, Giles, Neves et al. 2017). Altogether this suggests that the

antigen presentation capability of either anergic or auto-reactive B cells might be enhanced, thus they may be able to provide stronger co-stimulation signalling to cognate T cells. During TD immune response, there are significantly higher percentages of class-switched GC B cells in IgMg1 mice on day 6 after immunisation, which points to a potential effect of an increased Tfh population, as the CD40L co-stimulation signal provided by Tfh cells plays a crucial role to mediate immunoglobulin class-switch recombination (Banchereau and Rousset 1991, Kawabe, Naka et al. 1994, Xu, Foy et al. 1994). Detailed mechanisms of the interactions between anergic IgMg1 B cells and Tfh cells during GC response should be further studied.

Chapter 5 . Conclusions

Anergic B cells are defined as B cells which lose the ability or have reduced ability to be activated through BCR ligation. In contrast, hyper-activated B cells display enhanced BCR down-stream signalling, including stronger calcium influx and enhanced phosphorylation of JNK, which leads to higher activation and proliferation rates after stimulation through BCRs (O'Keefe, Williams et al. 1996, Chan, Lowell et al. 1998, Cornall, Cyster et al. 1998). These two contrasting response states after BCR ligation clearly define two different types of B cells.

In this study, the cytoplasmic domain of IgM BCR was replaced with that from IgG1. However, instead of generating hyper-activated BCR signalling as hypothesised, the dominant mature B cell population, recirculating Fo B cells, display comparable tonic BCR signalling to IgMwt B cells. Only MZ B cells clearly display a hyper-activated tonic state. Despite this, after activation through BCR stimulation, both immature and mature B cells in IgMg1 mice transduce a reduced downstream signal (Fig.5.1), which resembles the defining feature of B cell anergy (Goodnow, Crosbie et al. 1988, Cambier, Gauld et al. 2007). During NP-Ficoll mediated TI-II immune response, IgMg1 mice generate very few NP$^+$ B cells and significantly less NP-specific plasma cells than IgMwt mice, confirming that the chimeric IgMg1 BCR is less efficient at activating IgMg1 B cells by direct BCR ligation. Besides reduced BCR signalling, surface IgM expression was reduced by at least 50% from immature B cell stage of IgMg1 mice and on all subsequent B cell differentiation stages (Fig.5.1). This is

consistent with the observation that surface IgM down-regulated in most mouse models of B cell anergy (Cambier, Gauld et al. 2007, Duty, Szodoray et al. 2009). Together, these data suggest IgMg1 B cells are induced into an anergic state.

B cell anergy is induced in negative developmental check points during B cell development by increased BCR signalling if BCRs ligate with self-antigen (Brink and Phan 2018). In the IgMg1 model, extra signalling from the IgG1 cytoplasmic tail possibly mimics the weak to medium BCR activation signalling from BCR ligation with self-antigen. Results from Nur77-GFP reporter mice confirm that chimeric IgMg1 BCR is intrinsically able to transduce a stronger down-stream tonic signal during immature and BM transitional B cell stages. In the following transitional and Fo B cell populations in the spleens, however, signalling has been adjusted and becomes comparable to IgMwt B cells. The attenuation of Nur77-GFP is only observed during BM development, and immature IgMg1 B cells already display features of anergy, such as: down-regulation of surface IgM and low-responsiveness after BCR ligation. Therefore, it seems that anergy induction in IgMg1 B cells is induced at the transition into immature B cell stage (Fig. 5.1). The attenuation of tonic BCR signalling, reflected by Nur77-GFP expression, during IgMg1 B cell development can be achieved through two possible mechanisms. Firstly, increased negative selection that IgMg1 B cells experience during bone marrow development may have selected B cells with lower BCR signalling strength. Alternatively, hyperactive BCR signalling from BCR/self-ligand binding is likely to induced a state of anergy, during this stage.

This observation seems contradictory to what is found in the knock-in mouse strain (MG2) expressing IgM-G1 BCR-recognizing HEL (Horikawa, Martin et al. 2007). IgM-G1 BCR in this model is also a chimeric BCR which contains IgM extra-cellular domain followed with IgG1 transmembrane and cytoplasmic regions (Pogue and Goodnow 2000). Here IgM-G1 induces exaggerated calcium influx after activation and does not display any immune tolerance inductions. This discrepancy could be explained by the different BCR repertoires in these two mouse models. While in our model, the normal germline V-D-J repertoire is retained to allow random rearrangement and generation of B cells with a polyclonal BCR repertoire, in the MG2 model there is only one monoclonal BCR specific for a single foreign protein. HEL, the foreign antigen, is not displayed in bone marrow or the periphery and does not induce negative selection during bone marrow B cell development. Thus the chance for HEL-specific IgM-G1 B cells to experience negative selection during development is considerably lower than that of the polyclonal IgMg1 B cells of the mouse model presented here. Another significant difference between both models is that the HEL-specific IgM-G1 chimeric BCR contains both transmembrane and cytoplasmic regions from IgG1, whereas the chimeric BCR in our model used in this study only has the replacement of the IgM cytoplasmic region with that of IgG1. The difference in transmembrane regions of these two chimeric BCRs could well affect their BCR signalling strength as well.

The Germinal Centre is the antigen-induced environment where affinity maturation takes place. Rather than being a random process, this directed evolution of B cell receptor affinities is regulated by complex selection processes. Although BCR signalling is dampened (Khalil, Cambier et al. 2012), it is required for and involved in selection within GC reactions. The BCR-SYK-PI3K-AKT signalling pathway selectively inactivates Foxo1 in GC B cells and allows for the expression of c-Myc to maintain GC B cells in LZ (Luo, Weisel et al. 2018). Despite the fact that the impact of BCR signalling strength on GC selection remains elusive, the selections of GC B cells are affected by the BCR isotype they express. For example, IgE[+] GC B cells are mainly localised in the DZ, where they are disfavoured and prone to be induced into apoptosis (Yang, Sullivan et al. 2012, He, Meyer-Hermann et al. 2013). As different BCR isotypes can lead to different down-stream signalling (Weston-Bell, Forconi et al. 2014), these studies suggest a potential effect of different BCR signalling strength on GC B cell fate.

Anergic B cells display repressed BCR signalling after activation, but still are capable of joining the GC response (Fulcher, Lyons et al. 1996, Sabouri, Schofield et al. 2014, Burnett, Langley et al. 2018). Furthermore, studies from the Goodnow group promoted the idea of clonal redemption of anergic B cells during GC reactions, which involved more complicated selection within the GC, including affinity maturation toward foreign antigen and loss of affinity towards self-antigens (Sabouri, Schofield et al. 2014, Burnett, Langley et al. 2018). However, we have yet to understand if the

changed BCR signalling in anergic B cells would affect their selection during GC reactions.

Results of this study show that the tolerized state of anergic B cells is not broken for at least 8 days after they were activated by immunisation. This anergic pattern was maintained even when they were activated and differentiated into GC B cells and MBCs, reflected by constantly repressed BCR signalling and the down-regulation of surface BCRs in GC B cells in IgMg1 mice during the early GC response (Fig. 5.2). GC B cells derived from anergic B cells still maintain the anergic feature of reduced BCR signalling, which makes it possible that this changed BCR signalling could potentially affect GC selections.

Selection within the GC leads to the fate decisions of GC B cells to either live, proliferate, or undergo cell death (Mesin, Ersching et al. 2016). IgMg1 B cells had a significantly higher apoptosis rate on day 6, but an enhanced proliferation rate on day 8 after immunisation with NP-CGG, indicating that during the early GC response IgMg1 GC B cells experienced different selection pressures compared to their WT counterparts. This could be a result of continuous anergic BCR signalling in early IgMg1 GC B cells. Another piece of evidence, indicating altered selection pressure, comes from the delayed specificity shift within the total GC response in IgMg1 B cells, showing that IgMg1 GC B cells had a longer-lasting response to the initially dominant immunogenic epitope, NP (Fig. 5.2). The proportion, proliferation and survival of different antigen-specific populations in the GC response are regulated by

positive selection inducing proliferation and/or differentiation events. It is, therefore, likely that changed population dynamics seen in IgMg1 GCs reflect changed selection efficiency during the early stages of the GC response. However, the detailed mechanism behind how anergic BCR signalling impacts GC B cell selection still waits to be answered.

IgMg1 chimeric BCR not only affected B cell development and induced them into an anergic state, but also altered T cell differentiation during a T-D immune response. The presence of anergic IgMg1 B cells induces a bias towards Tfh cell differentiation (Fig. 5.2). In the current T cell centric model, Tfh cells are described as the providers of selection or regulation for GC B cells (Batista and Neuberger 2000, Allen, Okada et al. 2007, Schwickert, Victora et al. 2011, Gitlin, Mayer et al. 2015). However, other studies showed that the initiation of Tfh cell differentiation and the maintenance of Tfh cell phenotype in the GC require sustained signalling from cognate B cells (Coffey, Alabyev et al. 2009, Kerfoot, Yaari et al. 2011, Baumjohann, Preite et al. 2013). Further, it has been shown that T cell immune responses can be regulated by B cells, such as regulatory B cells (Khan, Hams et al. 2015). Together, these studies indicate that anergic IgMg1 B cells might potentially affect the generation or maintenance of Tfh cells in the GC micro-environment. One possible mechanism could be that these anergic IgMg1 B cells can express cytokines to regulate micro-environments around them, which could potentially affect activated T cell differentiation, as described previously for regulatory B cells (Tian, Zekzer et al. 2001, Carter, Rosser et al. 2012, Shen, Roch et al. 2014). Another possibility is that these

anergic IgMg1 B cells can better present pMHCII and provide stronger co-stimulation signalling to T cells and directly promote the differentiation of Tfh. This hypothesis is based on previous observations showing anergic B cells can constantly present self-antigens to T cells (Eris, Basten et al. 1994), and auto-reactive B cells can trigger auto-immune diseases by presenting self-antigen to T cells and activating them (Dai, Carayanniotis et al. 2005, Giles, Kashgarian et al. 2015, Giles, Neves et al. 2017). The potential regulatory roles of anergic IgMg1 B cells on the differentiation of Tfh cells should be further tested. Possible mechanisms of anergic B cells regulating Tfh differentiation may help to gain more insights into T-B interaction and the regulation of the GC response.
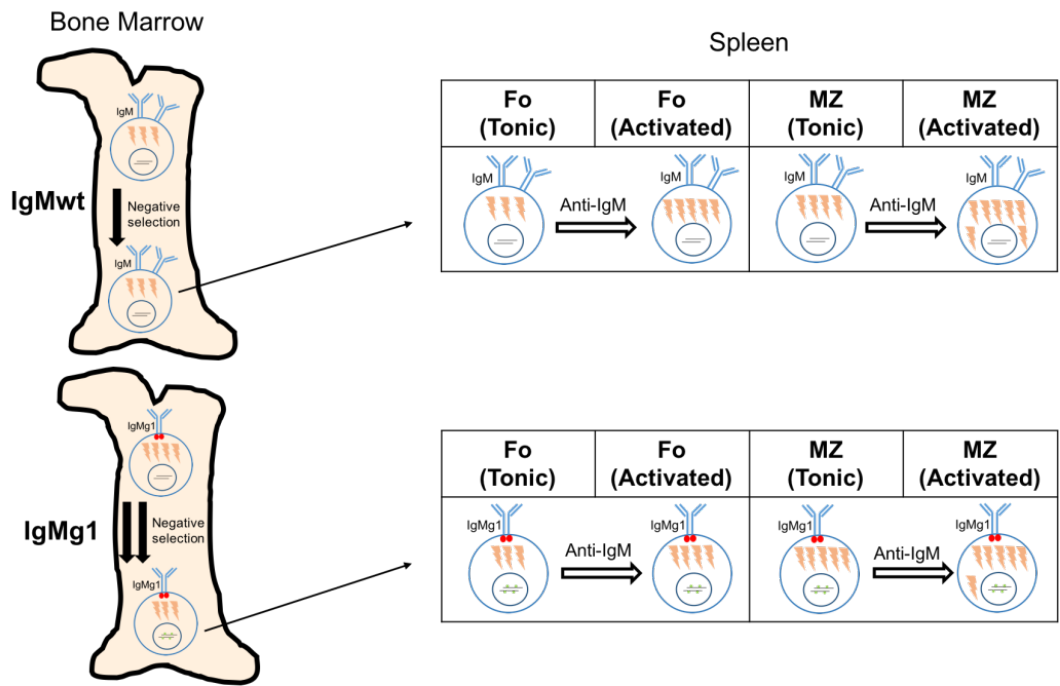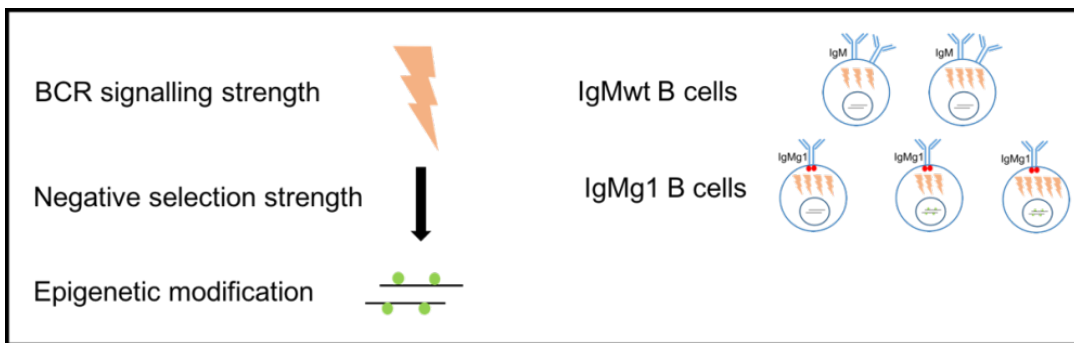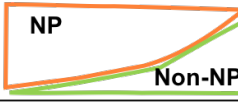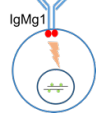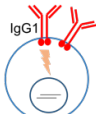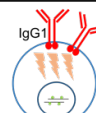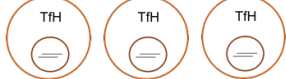
Figure 5.1: Graphic representation of anergy induction and anergic features in IgMg1 mice.

Chimeric IgMg1 BCR is down-regulated from immature B cell stage. However, it is still able to transduce stronger BCR signalling in immature and transitional B cells during BM stage. This hyper-activate tonic signalling makes IgMg1 B cells experience enhanced negative selection, which results in repressed tonic BCR signalling and epigenetic reprogramming. During peripheral stage, all B cell populations in IgMg1 mice maintain this modification and display an anergic pattern, displaying reduced activated BCR signalling after BCR ligation and down-regulation of surface IgM.

	IgMwt	IgMg1
Specificity shift in GC	NP / Non-NP	NP / Non-NP
IgM⁺ GC B cells	IgM	IgMg1
IgG1⁺ GC B cells	IgG1	IgG1
IgG1⁺ MBCs	IgG1	IgG1
Tfh	TfH TfH	TfH TfH TfH

Legend:
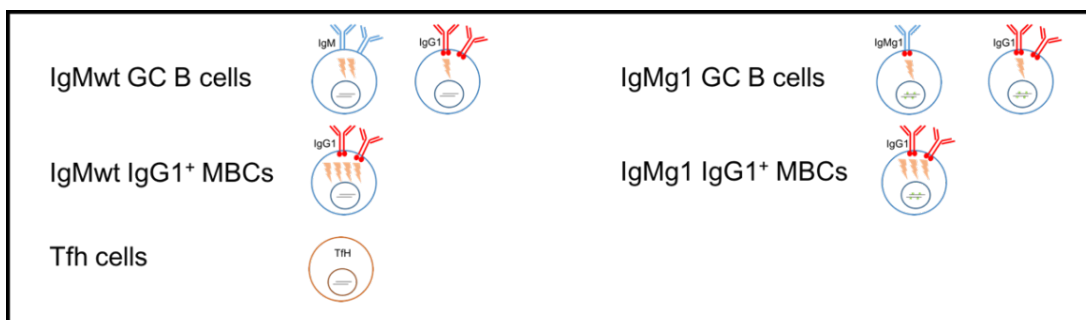
Figure 5.2: Graphic representation of the summary of the T-D immune response towards NP-CGG in IgMwt and IgMg1 mice.

During the T-D immune response, the shift in specificity in the GC B cell response away from the initial NP-specificity is delayed in IgMg1 mice, resulting in longer-lasting responses to NP. In non-switched IgMg1 GC B cells, the suppression of BCR signalling and down-regulation of surface IgM remains. BCR signalling is repressed in all GC B cells, in especially in switched IgG1⁺ GC B cells in both IgMwt and IgMg1 mice. After output from GCs, MBCs (switched to IgG1) regain stronger BCR signalling, however, BCR signalling remains lower in IgMg1 derived MBCs than in those from IgMwt mice. There is a higher proportion of Tfh cells and a higher percentage of switched GC B cells during GC reactions in IgMg1 mice, which could be due to increased stimulation or antigen-presentation from IgMg1 B cells.

Chapter 6 . References

Adolfsson, J., O. J. Borge, D. Bryder, K. Theilgaard-Monch, I. Astrand-Grundstrom, E. Sitnicka, Y. Sasaki and S. E. Jacobsen (2001). "Upregulation of Flt3 expression within the bone marrow Lin(-)Sca1(+)c-kit(+) stem cell compartment is accompanied by loss of self-renewal capacity." Immunity **15**(4): 659-669.

Allen, C. D., K. M. Ansel, C. Low, R. Lesley, H. Tamamura, N. Fujii and J. G. Cyster (2004). "Germinal center dark and light zone organization is mediated by CXCR4 and CXCR5." Nat Immunol **5**(9): 943-952.

Allen, C. D., T. Okada, H. L. Tang and J. G. Cyster (2007). "Imaging of germinal center selection events during affinity maturation." Science **315**(5811): 528-531.

Allman, D., R. C. Lindsley, W. DeMuth, K. Rudd, S. A. Shinton and R. R. Hardy (2001). "Resolution of three nonproliferative immature splenic B cell subsets reveals multiple selection points during peripheral B cell maturation." J Immunol **167**(12): 6834-6840.

Amsbaugh, D. F., C. T. Hansen, B. Prescott, P. W. Stashak, D. R. Barthold and P. J. Baker (1972). "Genetic control of the antibody response to type 3 pneumococcal polysaccharide in mice. I. Evidence that an X-linked gene plays a decisive role in determining responsiveness." J Exp Med **136**(4): 931-949.

Armitage, R. J., B. M. Macduff, M. K. Spriggs and W. C. Fanslow (1993). "Human B cell proliferation and Ig secretion induced by recombinant CD40 ligand are modulated by soluble cytokines." J Immunol **150**(9): 3671-3680.

Arnon, T. I., R. M. Horton, I. L. Grigorova and J. G. Cyster (2013). "Visualization of splenic marginal zone B-cell shuttling and follicular B-cell egress." Nature **493**(7434): 684-688.

Attanasio, R., K. M. Brasky, S. H. Robbins, L. Jayashankar, R. J. Nash and T. M. Butler (2001). "Age-related autoantibody production in a nonhuman primate model." Clin Exp Immunol **123**(3): 361-365.

Azuma, T., N. Sakato and H. Fujio (1987). "Maturation of the immune response to (4-hydroxy-3-nitrophenyl)-acetyl (NP) haptens in C57BL/6 mice." Mol Immunol **24**(3): 287-296.

Balazs, M., F. Martin, T. Zhou and J. Kearney (2002). "Blood dendritic cells interact with splenic marginal zone B cells to initiate T-independent immune responses." Immunity **17**(3): 341-352.

Banchereau, J. and F. Rousset (1991). "Growing human B lymphocytes in the CD40 system." Nature **353**(6345): 678-679.

Bannard, O., R. M. Horton, C. D. Allen, J. An, T. Nagasawa and J. G. Cyster (2013). "Germinal center centroblasts transition to a centrocyte phenotype according to a timed program and depend on the dark zone for effective selection." Immunity **39**(5): 912-924.

Bannish, G., E. M. Fuentes-Panana, J. C. Cambier, W. S. Pear and J. G. Monroe (2001). "Ligand-independent signaling functions for the B lymphocyte antigen receptor and their role in positive selection during B lymphopoiesis." J Exp Med **194**(11): 1583-1596.

Bartlett, R. C., T. S. Kohan and C. Rutz (1979). "Comparative costs of microbial identification employing conventional and prepackaged commercial systems." Am J Clin Pathol **71**(2): 194-200.

Batista, F. D. and N. E. Harwood (2009). "The who, how and where of antigen presentation to B cells." Nat Rev Immunol **9**(1): 15-27.

Batista, F. D. and M. S. Neuberger (2000). "B cells extract and present immobilized antigen: implications for affinity discrimination." EMBO J **19**(4): 513-520.

Baumgarth, N. (2016). "B-1 Cell Heterogeneity and the Regulation of Natural and Antigen-Induced IgM Production." Front Immunol **7**: 324.

Baumjohann, D., S. Preite, A. Reboldi, F. Ronchi, K. M. Ansel, A. Lanzavecchia and F. Sallusto (2013). "Persistent antigen and germinal center B cells sustain T follicular helper cell responses and phenotype." Immunity **38**(3): 596-605.

Bekeredjian-Ding, I. and G. Jego (2009). "Toll-like receptors--sentries in the B-cell response." Immunology **128**(3): 311-323.

Bengten, E., M. Wilson, N. Miller, L. W. Clem, L. Pilstrom and G. W. Warr (2000). "Immunoglobulin isotypes: structure, function, and genetics." Curr Top Microbiol Immunol **248**: 189-219.

Benschop, R. J., K. Aviszus, X. Zhang, T. Manser, J. C. Cambier and L. J. Wysocki (2001). "Activation and anergy in bone marrow B cells of a novel immunoglobulin transgenic mouse that is both hapten specific and autoreactive." Immunity **14**(1): 33-43.

Borrero, M. and S. H. Clarke (2002). "Low-affinity anti-Smith antigen B cells are regulated by anergy as opposed to developmental arrest or differentiation to B-1." J Immunol **168**(1): 13-21.

Brink, R. and T. G. Phan (2018). "Self-Reactive B Cells in the Germinal Center Reaction." Annu Rev Immunol **36**: 339-357.

Burnett, D. L., D. B. Langley, P. Schofield, J. R. Hermes, T. D. Chan, J. Jackson, K. Bourne, J. H. Reed, K. Patterson, B. T. Porebski, R. Brink, D. Christ and C. C. Goodnow (2018). "Germinal center antibody mutation trajectories are determined by rapid self/foreign discrimination." Science **360**(6385): 223-226.

Cambier, J. C., S. B. Gauld, K. T. Merrell and B. J. Vilen (2007). "B-cell anergy: from transgenic models to naturally occurring anergic B cells?" Nat Rev Immunol **7**(8): 633-643.

Campbell, K. S. and J. C. Cambier (1990). "B lymphocyte antigen receptors (mIg) are non-covalently associated with a disulfide linked, inducibly phosphorylated glycoprotein complex." EMBO J **9**(2): 441-448.

Cappione, A., 3rd, J. H. Anolik, A. Pugh-Bernard, J. Barnard, P. Dutcher, G. Silverman and I. Sanz (2005). "Germinal center exclusion of autoreactive B cells is defective in human systemic lupus erythematosus." J Clin Invest **115**(11): 3205-3216.

Cariappa, A., C. Chase, H. Liu, P. Russell and S. Pillai (2007). "Naive recirculating B cells mature simultaneously in the spleen and bone marrow." Blood **109**(6): 2339-2345.

Cariappa, A., H. Takematsu, H. Liu, S. Diaz, K. Haider, C. Boboila, G. Kalloo, M. Connole, H. N. Shi, N. Varki, A. Varki and S. Pillai (2009). "B cell antigen receptor signal strength and peripheral B cell development are regulated by a 9-O-acetyl sialic acid esterase." J Exp Med **206**(1): 125-138.

Cariappa, A., M. Tang, C. Parng, E. Nebelitskiy, M. Carroll, K. Georgopoulos and S. Pillai (2001). "The follicular versus marginal zone B lymphocyte cell fate decision is regulated by Aiolos, Btk, and CD21." Immunity **14**(5): 603-615.

Carsetti, R., G. Kohler and M. C. Lamers (1995). "Transitional B cells are the target of negative selection in the B cell compartment." J Exp Med **181**(6): 2129-2140.

Carter, N. A., E. C. Rosser and C. Mauri (2012). "Interleukin-10 produced by B cells is crucial for the suppression of Th17/Th1 responses, induction of T regulatory type 1 cells and reduction of collagen-induced arthritis." Arthritis Res Ther **14**(1): R32.

Cascalho, M., A. Ma, S. Lee, L. Masat and M. Wabl (1996). "A quasi-monoclonal mouse." Science **272**(5268): 1649-1652.

Chan, O. and M. J. Shlomchik (1998). "A new role for B cells in systemic autoimmunity: B cells promote spontaneous T cell activation in MRL-lpr/lpr mice." J Immunol **160**(1): 51-59.

Chan, T. D., K. Wood, J. R. Hermes, D. Butt, C. J. Jolly, A. Basten and R. Brink (2012). "Elimination of germinal-center-derived self-reactive B cells is governed by the location and concentration of self-antigen." Immunity **37**(5): 893-904.

Chan, V. W., C. A. Lowell and A. L. DeFranco (1998). "Defective negative regulation of antigen receptor signaling in Lyn-deficient B lymphocytes." Curr Biol **8**(10): 545-553.

Chaudhuri, J. and F. W. Alt (2004). "Class-switch recombination: interplay of transcription, DNA deamination and DNA repair." Nat Rev Immunol **4**(7): 541-552.

Cinamon, G., M. Matloubian, M. J. Lesneski, Y. Xu, C. Low, T. Lu, R. L. Proia and J. G. Cyster (2004). "Sphingosine 1-phosphate receptor 1 promotes B cell localization in the splenic marginal zone." Nat Immunol **5**(7): 713-720.

Coffey, F., B. Alabyev and T. Manser (2009). "Initial clonal expansion of germinal center B cells takes place at the perimeter of follicles." Immunity **30**(4): 599-609.

Conter, L. J., E. Song, M. J. Shlomchik and M. M. Tomayko (2014). "CD73 expression is dynamically regulated in the germinal center and bone marrow plasma cells are diminished in its absence." PLoS One **9**(3): e92009.

Cooke, M. P., A. W. Heath, K. M. Shokat, Y. Zeng, F. D. Finkelman, P. S. Linsley, M. Howard and C. C. Goodnow (1994). "Immunoglobulin signal transduction guides the specificity of B cell-T cell interactions and is blocked in tolerant self-reactive B cells." J Exp Med **179**(2): 425-438.

Cornall, R. J., J. G. Cyster, M. L. Hibbs, A. R. Dunn, K. L. Otipoby, E. A. Clark and C. C. Goodnow (1998). "Polygenic autoimmune traits: Lyn, CD22, and SHP-1 are limiting elements of a biochemical pathway regulating BCR signaling and selection." Immunity **8**(4): 497-508.

Culton, D. A., B. P. O'Conner, K. L. Conway, R. Diz, J. Rutan, B. J. Vilen and S. H. Clarke (2006). "Early preplasma cells define a tolerance checkpoint for autoreactive B cells." J Immunol **176**(2): 790-802.

Cyster, J. G., K. M. Ansel, K. Reif, E. H. Ekland, P. L. Hyman, H. L. Tang, S. A. Luther and V. N. Ngo (2000). "Follicular stromal cells and lymphocyte homing to follicles." Immunol Rev **176**: 181-193.

Cyster, J. G. and C. C. Goodnow (1995). "Antigen-induced exclusion from follicles and anergy are separate and complementary processes that influence peripheral B cell fate." Immunity **3**(6): 691-701.

Cyster, J. G. and C. C. Goodnow (1995). "Pertussis toxin inhibits migration of B and T lymphocytes into splenic white pulp cords." J Exp Med **182**(2): 581-586.

Cyster, J. G., S. B. Hartley and C. C. Goodnow (1994). "Competition for follicular niches excludes self-reactive cells from the recirculating B-cell repertoire." Nature **371**(6496): 389-395.

Dai, Y. D., G. Carayanniotis and E. Sercarz (2005). "Antigen processing by autoreactive B cells promotes determinant spreading." Cell Mol Immunol **2**(3): 169-175.

De Silva, N. S. and U. Klein (2015). "Dynamics of B cells in germinal centres." Nat Rev Immunol **15**(3): 137-148.

de Vinuesa, C. G., M. C. Cook, J. Ball, M. Drew, Y. Sunners, M. Cascalho, M. Wabl, G. G. Klaus and I. C. MacLennan (2000). "Germinal centers without T cells." J Exp Med **191**(3): 485-494.

Dogan, I., B. Bertocci, V. Vilmont, F. Delbos, J. Megret, S. Storck, C. A. Reynaud and J. C. Weill (2009). "Multiple layers of B cell memory with different effector functions." Nat Immunol **10**(12): 1292-1299.

Dugas, B., N. Paul-Eugene, E. Genot, J. M. Mencia-Huerta, P. Braquet and J. P. Kolb (1991). "Effect of bacterial toxins on human B cell activation. II. Mitogenic activity of the B subunit of cholera toxin." Eur J Immunol **21**(2): 495-500.

Duty, J. A., P. Szodoray, N. Y. Zheng, K. A. Koelsch, Q. Zhang, M. Swiatkowski, M. Mathias, L. Garman, C. Helms, B. Nakken, K. Smith, A. D. Farris and P. C. Wilson (2009). "Functional anergy in a subpopulation of naive B cells from healthy humans that express autoreactive immunoglobulin receptors." J Exp Med **206**(1): 139-151.

Enders, A., A. Short, L. A. Miosge, H. Bergmann, Y. Sontani, E. M. Bertram, B. Whittle, B. Balakishnan, K. Yoshida, G. Sjollema, M. A. Field, T. D. Andrews, H. Hagiwara and C. C. Goodnow (2014). "Zinc-finger protein ZFP318 is essential for expression of IgD, the alternatively spliced Igh product made by mature B lymphocytes." Proc Natl Acad Sci U S A **111**(12): 4513-4518.

Engels, N., L. M. Konig, C. Heemann, J. Lutz, T. Tsubata, S. Griep, V. Schrader and J. Wienands (2009). "Recruitment of the cytoplasmic adaptor Grb2 to surface IgG and IgE provides antigen receptor-intrinsic costimulation to class-switched B cells." Nat Immunol **10**(9): 1018-1025.

Erikson, J., M. Z. Radic, S. A. Camper, R. R. Hardy, C. Carmack and M. Weigert (1991). "Expression of anti-DNA immunoglobulin transgenes in non-autoimmune mice." Nature **349**(6307): 331-334.

Eris, J. M., A. Basten, R. Brink, K. Doherty, M. R. Kehry and P. D. Hodgkin (1994). "Anergic self-reactive B cells present self antigen and respond normally to CD40-

dependent T-cell signals but are defective in antigen-receptor-mediated functions." Proc Natl Acad Sci U S A **91**(10): 4392-4396.

Feldmann, M. and A. Easten (1971). "The relationship between antigenic structure and the requirement for thymus-derived cells in the immune response." J Exp Med **134**(1): 103-119.

Fillatreau, S. (2015). "Regulatory plasma cells." Curr Opin Pharmacol **23**: 1-5.

Forster, R., A. E. Mattis, E. Kremmer, E. Wolf, G. Brem and M. Lipp (1996). "A putative chemokine receptor, BLR1, directs B cell migration to defined lymphoid organs and specific anatomic compartments of the spleen." Cell **87**(6): 1037-1047.

Forster, R., A. Schubel, D. Breitfeld, E. Kremmer, I. Renner-Muller, E. Wolf and M. Lipp (1999). "CCR7 coordinates the primary immune response by establishing functional microenvironments in secondary lymphoid organs." Cell **99**(1): 23-33.

Forster, R., A. Schubel, D. Breitfeld, E. Kremmer, I. Renner-Muller, E. Wolf and M. Lipp (2016). "Pillars Article: CCR7 Coordinates the Primary Immune Response by Establishing Functional Microenvironments in Secondary Lymphoid Organs. Cell. 1999. 99: 23-33." J Immunol **196**(1): 5-15.

Fu, C., C. W. Turck, T. Kurosaki and A. C. Chan (1998). "BLNK: a central linker protein in B cell activation." Immunity **9**(1): 93-103.

Fuentes-Panana, E. M., G. Bannish, D. van der Voort, L. B. King and J. G. Monroe (2005). "Ig alpha/Ig beta complexes generate signals for B cell development independent of selective plasma membrane compartmentalization." J Immunol **174**(3): 1245-1252.

Fulcher, D. A. and A. Basten (1994). "Reduced life span of anergic self-reactive B cells in a double-transgenic model." J Exp Med **179**(1): 125-134.

Fulcher, D. A., A. B. Lyons, S. L. Korn, M. C. Cook, C. Koleda, C. Parish, B. Fazekas de St Groth and A. Basten (1996). "The fate of self-reactive B cells depends primarily on the degree of antigen receptor engagement and availability of T cell help." J Exp Med **183**(5): 2313-2328.

Gabriel, D. V. and C. N. Michel (2012). "Germinal Centers." Immunology **30**(1): 429-457.

Gagro, A., K. M. Toellner, G. Grafton, D. Servis, S. Branica, V. Radojcic, E. Kosor, M. Hrabak and J. Gordon (2003). "Naive and memory B cells respond differentially to T-dependent signaling but display an equal potential for differentiation toward the centroblast-restricted CD77/globotriaosylceramide phenotype." Eur J Immunol **33**(7): 1889-1898.

Garcia De Vinuesa, C., A. Gulbranson-Judge, M. Khan, P. O'Leary, M. Cascalho, M. Wabl, G. G. Klaus, M. J. Owen and I. C. MacLennan (1999). "Dendritic cells associated with plasmablast survival." Eur J Immunol **29**(11): 3712-3721.

Garcia de Vinuesa, C., P. O'Leary, D. M. Sze, K. M. Toellner and I. C. MacLennan (1999). "T-independent type 2 antigens induce B cell proliferation in multiple splenic sites, but exponential growth is confined to extrafollicular foci." Eur J Immunol **29**(4): 1314-1323.

Garside, P., E. Ingulli, R. R. Merica, J. G. Johnson, R. J. Noelle and M. K. Jenkins (1998). "Visualization of specific B and T lymphocyte interactions in the lymph node." Science **281**(5373): 96-99.

Gauld, S. B., R. J. Benschop, K. T. Merrell and J. C. Cambier (2005). "Maintenance of B cell anergy requires constant antigen receptor occupancy and signaling." Nat Immunol **6**(11): 1160-1167.

Gay, D., T. Saunders, S. Camper and M. Weigert (1993). "Receptor editing: an approach by autoreactive B cells to escape tolerance." J Exp Med **177**(4): 999-1008.

Gerner, M. Y., K. A. Casey, W. Kastenmuller and R. N. Germain (2017). "Dendritic cell and antigen dispersal landscapes regulate T cell immunity." J Exp Med **214**(10): 3105-3122.

Getahun, A., N. A. Beavers, S. R. Larson, M. J. Shlomchik and J. C. Cambier (2016). "Continuous inhibitory signaling by both SHP-1 and SHIP-1 pathways is required to maintain unresponsiveness of anergic B cells." J Exp Med **213**(5): 751-769.

Gibb, D. R., M. El Shikh, D. J. Kang, W. J. Rowe, R. El Sayed, J. Cichy, H. Yagita, J. G. Tew, P. J. Dempsey, H. C. Crawford and D. H. Conrad (2010). "ADAM10 is essential for Notch2-dependent marginal zone B cell development and CD23 cleavage in vivo." J Exp Med **207**(3): 623-635.

Giles, J. R., M. Kashgarian, P. A. Koni and M. J. Shlomchik (2015). "B Cell-Specific MHC Class II Deletion Reveals Multiple Nonredundant Roles for B Cell Antigen Presentation in Murine Lupus." J Immunol **195**(6): 2571-2579.

Giles, J. R., A. T. Neves, A. Marshak-Rothstein and M. J. Shlomchik (2017). "Autoreactive helper T cells alleviate the need for intrinsic TLR signaling in autoreactive B cell activation." JCI Insight **2**(4): e90870.

Gitlin, A. D., C. T. Mayer, T. Y. Oliveira, Z. Shulman, M. J. Jones, A. Koren and M. C. Nussenzweig (2015). "HUMORAL IMMUNITY. T cell help controls the speed of the cell cycle in germinal center B cells." Science **349**(6248): 643-646.

Gitlin, A. D., Z. Shulman and M. C. Nussenzweig (2014). "Clonal selection in the germinal centre by regulated proliferation and hypermutation." Nature **509**(7502): 637-640.

Gitlin, A. D., L. von Boehmer, A. Gazumyan, Z. Shulman, T. Y. Oliveira and M. C. Nussenzweig (2016). "Independent Roles of Switching and Hypermutation in the Development and Persistence of B Lymphocyte Memory." Immunity **44**(4): 769-781.

Glynne, R., G. Ghandour, J. Rayner, D. H. Mack and C. C. Goodnow (2000). "B-lymphocyte quiescence, tolerance and activation as viewed by global gene expression profiling on microarrays." Immunol Rev **176**: 216-246.

Gold, M. R., L. Matsuuchi, R. B. Kelly and A. L. DeFranco (1991). "Tyrosine phosphorylation of components of the B-cell antigen receptors following receptor crosslinking." Proc Natl Acad Sci U S A **88**(8): 3436-3440.

Good, K. L., D. T. Avery and S. G. Tangye (2009). "Resting human memory B cells are intrinsically programmed for enhanced survival and responsiveness to diverse stimuli compared to naive B cells." J Immunol **182**(2): 890-901.

Goodnow, C. C. (1992). "Transgenic mice and analysis of B-cell tolerance." Annu Rev Immunol **10**: 489-518.

Goodnow, C. C., R. Brink and E. Adams (1991). "Breakdown of self-tolerance in anergic B lymphocytes." Nature **352**(6335): 532-536.

Goodnow, C. C., J. Crosbie, S. Adelstein, T. B. Lavoie, S. J. Smith-Gill, R. A. Brink, H. Pritchard-Briscoe, J. S. Wotherspoon, R. H. Loblay, K. Raphael and et al. (1988). "Altered immunoglobulin expression and functional silencing of self-reactive B lymphocytes in transgenic mice." Nature **334**(6184): 676-682.

Goodnow, C. C., J. Crosbie, H. Jorgensen, R. A. Brink and A. Basten (1989). "Induction of self-tolerance in mature peripheral B lymphocytes." Nature **342**(6248): 385-391.

Grandien, A., R. Fucs, A. Nobrega, J. Andersson and A. Coutinho (1994). "Negative selection of multireactive B cell clones in normal adult mice." Eur J Immunol **24**(6): 1345-1352.

Gristick, H. B., L. von Boehmer, A. P. West, Jr., M. Schamber, A. Gazumyan, J. Golijanin, M. S. Seaman, G. Fatkenheuer, F. Klein, M. C. Nussenzweig and P. J. Bjorkman (2016). "Natively glycosylated HIV-1 Env structure reveals new mode for antibody recognition of the CD4-binding site." Nat Struct Mol Biol **23**(10): 906-915.

Guo, B., T. T. Su and D. J. Rawlings (2004). "Protein kinase C family functions in B-cell activation." Curr Opin Immunol **16**(3): 367-373.

Hammad, H., M. Vanderkerken, P. Pouliot, K. Deswarte, W. Toussaint, K. Vergote, L. Vandersarren, S. Janssens, I. Ramou, S. N. Savvides, J. J. Haigh, R. Hendriks, M. Kopf, K. Craessaerts, B. de Strooper, J. F. Kearney, D. H. Conrad and B. N. Lambrecht (2017). "Transitional B cells commit to marginal zone B cell fate by Taok3-mediated surface expression of ADAM10." Nat Immunol 18(3): 313-320.

Hauser, A. E., T. Junt, T. R. Mempel, M. W. Sneddon, S. H. Kleinstein, S. E. Henrickson, U. H. von Andrian, M. J. Shlomchik and A. M. Haberman (2007). "Definition of germinal-center B cell migration in vivo reveals predominant intrazonal circulation patterns." Immunity 26(5): 655-667.

He, J. S., M. Meyer-Hermann, D. Xiangying, L. Y. Zuan, L. A. Jones, L. Ramakrishna, V. C. de Vries, J. Dolpady, H. Aina, S. Joseph, S. Narayanan, S. Subramaniam, M. Puthia, G. Wong, H. Xiong, M. Poidinger, J. F. Urban, J. J. Lafaille and M. A. Curotto de Lafaille (2013). "The distinctive germinal center phase of IgE+ B lymphocytes limits their contribution to the classical memory response." J Exp Med 210(12): 2755-2771.

Hibbs, M. L., D. M. Tarlinton, J. Armes, D. Grail, G. Hodgson, R. Maglitto, S. A. Stacker and A. R. Dunn (1995). "Multiple defects in the immune system of Lyn-deficient mice, culminating in autoimmune disease." Cell 83(2): 301-311.

Hobeika, E., P. C. Maity and H. Jumaa (2016). "Control of B Cell Responsiveness by Isotype and Structural Elements of the Antigen Receptor." Trends Immunol 37(5): 310-320.

Hogan, P. G., R. S. Lewis and A. Rao (2010). "Molecular basis of calcium signaling in lymphocytes: STIM and ORAI." Annu Rev Immunol 28: 491-533.

Hollenbaugh, D., L. S. Grosmaire, C. D. Kullas, N. J. Chalupny, S. Braesch-Andersen, R. J. Noelle, I. Stamenkovic, J. A. Ledbetter and A. Aruffo (1992). "The human T cell antigen gp39, a member of the TNF gene family, is a ligand for the CD40 receptor: expression of a soluble form of gp39 with B cell co-stimulatory activity." EMBO J 11(12): 4313-4321.

Hombach, J., T. Tsubata, L. Leclercq, H. Stappert and M. Reth (1990). "Molecular components of the B-cell antigen receptor complex of the IgM class." Nature 343(6260): 760-762.

Hong, S., Z. Zhang, H. Liu, M. Tian, X. Zhu, Z. Zhang, W. Wang, X. Zhou, F. Zhang, Q. Ge, B. Zhu, H. Tang, Z. Hua and B. Hou (2018). "B Cells Are the Dominant Antigen-Presenting Cells that Activate Naive CD4(+) T Cells upon Immunization with a Virus-Derived Nanoparticle Antigen." Immunity 49(4): 695-708 e694.

Horikawa, K., S. W. Martin, S. L. Pogue, K. Silver, K. Peng, K. Takatsu and C. C. Goodnow (2007). "Enhancement and suppression of signaling by the conserved tail of IgG memory-type B cell antigen receptors." J Exp Med **204**(4): 759-769.

Imanishi, T. and O. Makela (1974). "Inheritance of antibody specificity. I. Anti-(4-hydroxy-3-nitrophenyl)acetyl of the mouse primary response." J Exp Med **140**(6): 1498-1510.

Inman, J. K. (1975). "Thymus-independent antigens: the preparation of covalent, hapten-ficoll conjugates." J Immunol **114**(2 Pt 1): 704-709.

Jacob, J., R. Kassir and G. Kelsoe (1991). "In situ studies of the primary immune response to (4-hydroxy-3-nitrophenyl)acetyl. I. The architecture and dynamics of responding cell populations." J Exp Med **173**(5): 1165-1175.

Jacobi, A. M. and B. Diamond (2005). "Balancing diversity and tolerance: lessons from patients with systemic lupus erythematosus." J Exp Med **202**(3): 341-344.

Johnson, S. A., C. M. Pleiman, L. Pao, J. Schneringer, K. Hippen and J. C. Cambier (1995). "Phosphorylated immunoreceptor signaling motifs (ITAMs) exhibit unique abilities to bind and activate Lyn and Syk tyrosine kinases." J Immunol **155**(10): 4596-4603.

Kabak, S., B. J. Skaggs, M. R. Gold, M. Affolter, K. L. West, M. S. Foster, K. Siemasko, A. C. Chan, R. Aebersold and M. R. Clark (2002). "The direct recruitment of BLNK to immunoglobulin alpha couples the B-cell antigen receptor to distal signaling pathways." Mol Cell Biol **22**(8): 2524-2535.

Karasuyama, H., A. Rolink and F. Melchers (1996). "Surrogate light chain in B cell development." Adv Immunol **63**: 1-41.

Karasuyama, H., A. Rolink, Y. Shinkai, F. Young, F. W. Alt and F. Melchers (1994). "The expression of Vpre-B/lambda 5 surrogate light chain in early bone marrow precursor B cells of normal and B cell-deficient mutant mice." Cell **77**(1): 133-143.

Katakai, T., H. Suto, M. Sugai, H. Gonda, A. Togawa, S. Suematsu, Y. Ebisuno, K. Katagiri, T. Kinashi and A. Shimizu (2008). "Organizer-like reticular stromal cell layer common to adult secondary lymphoid organs." J Immunol **181**(9): 6189-6200.

Kawabe, T., T. Naka, K. Yoshida, T. Tanaka, H. Fujiwara, S. Suematsu, N. Yoshida, T. Kishimoto and H. Kikutani (1994). "The immune responses in CD40-deficient mice: impaired immunoglobulin class switching and germinal center formation." Immunity **1**(3): 167-178.

Kepler, T. B. and A. S. Perelson (1993). "Cyclic re-entry of germinal center B cells and the efficiency of affinity maturation." Immunol Today **14**(8): 412-415.

Kerfoot, S. M., G. Yaari, J. R. Patel, K. L. Johnson, D. G. Gonzalez, S. H. Kleinstein and A. M. Haberman (2011). "Germinal center B cell and T follicular helper cell development initiates in the interfollicular zone." Immunity **34**(6): 947-960.

Khalil, A. M., J. C. Cambier and M. J. Shlomchik (2012). "B cell receptor signal transduction in the GC is short-circuited by high phosphatase activity." Science **336**(6085): 1178-1181.

Khan, A. R., E. Hams, A. Floudas, T. Sparwasser, C. T. Weaver and P. G. Fallon (2015). "PD-L1hi B cells are critical regulators of humoral immunity." Nat Commun **6**: 5997.

Klein, U., S. Casola, G. Cattoretti, Q. Shen, M. Lia, T. Mo, T. Ludwig, K. Rajewsky and R. Dalla-Favera (2006). "Transcription factor IRF4 controls plasma cell differentiation and class-switch recombination." Nat Immunol **7**(7): 773-782.

Klein, U. and R. Dalla-Favera (2008). "Germinal centres: role in B-cell physiology and malignancy." Nat Rev Immunol **8**(1): 22-33.

Knutson, M. and M. Wessling-Resnick (2003). "Iron metabolism in the reticuloendothelial system." Crit Rev Biochem Mol Biol **38**(1): 61-88.

Kondo, M., I. L. Weissman and K. Akashi (1997). "Identification of clonogenic common lymphoid progenitors in mouse bone marrow." Cell **91**(5): 661-672.

Kranich, J. and N. J. Krautler (2016). "How Follicular Dendritic Cells Shape the B-Cell Antigenome." Front Immunol **7**: 225.

Kuraoka, M., A. G. Schmidt, T. Nojima, F. Feng, A. Watanabe, D. Kitamura, S. C. Harrison, T. B. Kepler and G. Kelsoe (2016). "Complex Antigens Drive Permissive Clonal Selection in Germinal Centers." Immunity **44**(3): 542-552.

Kurosaki, T., S. A. Johnson, L. Pao, K. Sada, H. Yamamura and J. C. Cambier (1995). "Role of the Syk autophosphorylation site and SH2 domains in B cell antigen receptor signaling." J Exp Med **182**(6): 1815-1823.

Kurosaki, T., K. Kometani and W. Ise (2015). "Memory B cells." Nat Rev Immunol **15**(3): 149-159.

Lane, P., T. Brocker, S. Hubele, E. Padovan, A. Lanzavecchia and F. McConnell (1993). "Soluble CD40 ligand can replace the normal T cell-derived CD40 ligand signal to B cells in T cell-dependent activation." J Exp Med **177**(4): 1209-1213.

Lassila, O., O. Vainio and P. Matzinger (1988). "Can B cells turn on virgin T cells?" Nature **334**(6179): 253-255.

Lentz, V. M. and T. Manser (2001). "Cutting edge: germinal centers can be induced in the absence of T cells." <u>J Immunol</u> **167**(1): 15-20.

Lin, Y. C., S. Jhunjhunwala, C. Benner, S. Heinz, E. Welinder, R. Mansson, M. Sigvardsson, J. Hagman, C. A. Espinoza, J. Dutkowski, T. Ideker, C. K. Glass and C. Murre (2010). "A global network of transcription factors, involving E2A, EBF1 and Foxo1, that orchestrates B cell fate." <u>Nat Immunol</u> **11**(7): 635-643.

Lindsley, R. C., M. Thomas, B. Srivastava and D. Allman (2007). "Generation of peripheral B cells occurs via two spatially and temporally distinct pathways." <u>Blood</u> **109**(6): 2521-2528.

Liu, Y. J., J. Zhang, P. J. Lane, E. Y. Chan and I. C. MacLennan (1991). "Sites of specific B cell activation in primary and secondary responses to T cell-dependent and T cell-independent antigens." <u>Eur J Immunol</u> **21**(12): 2951-2962.

Loder, F., B. Mutschler, R. J. Ray, C. J. Paige, P. Sideras, R. Torres, M. C. Lamers and R. Carsetti (1999). "B cell development in the spleen takes place in discrete steps and is determined by the quality of B cell receptor-derived signals." <u>J Exp Med</u> **190**(1): 75-89.

Luo, W., F. Weisel and M. J. Shlomchik (2018). "B Cell Receptor and CD40 Signaling Are Rewired for Synergistic Induction of the c-Myc Transcription Factor in Germinal Center B Cells." <u>Immunity</u> **48**(2): 313-326 e315.

MacDonald, I. C., D. M. Ragan, E. E. Schmidt and A. C. Groom (1987). "Kinetics of red blood cell passage through interendothelial slits into venous sinuses in rat spleen, analyzed by in vivo microscopy." <u>Microvasc Res</u> **33**(1): 118-134.

Mackay, F., P. Schneider, P. Rennert and J. Browning (2003). "BAFF AND APRIL: a tutorial on B cell survival." <u>Annu Rev Immunol</u> **21**: 231-264.

MacLennan, I. C. (1994). "Germinal centers." <u>Annu Rev Immunol</u> **12**: 117-139.

MacLennan, I. C., A. Gulbranson-Judge, K. M. Toellner, M. Casamayor-Palleja, E. Chan, D. M. Sze, S. A. Luther and H. A. Orbea (1997). "The changing preference of T and B cells for partners as T-dependent antibody responses develop." <u>Immunol Rev</u> **156**: 53-66.

MacLennan, I. C., Y. J. Liu, S. Oldfield, J. Zhang and P. J. Lane (1990). "The evolution of B-cell clones." <u>Curr Top Microbiol Immunol</u> **159**: 37-63.

MacLennan, I. C., K. M. Toellner, A. F. Cunningham, K. Serre, D. M. Sze, E. Zuniga, M. C. Cook and C. G. Vinuesa (2003). "Extrafollicular antibody responses." <u>Immunol Rev</u> **194**: 8-18.

Maeda, A., A. M. Scharenberg, S. Tsukada, J. B. Bolen, J. P. Kinet and T. Kurosaki (1999). "Paired immunoglobulin-like receptor B (PIR-B) inhibits BCR-induced activation of Syk and Btk by SHP-1." Oncogene **18**(14): 2291-2297.

Makowska, A., N. N. Faizunnessa, P. Anderson, T. Midtvedt and S. Cardell (1999). "CD1high B cells: a population of mixed origin." Eur J Immunol **29**(10): 3285-3294.

Mandik-Nayak, L., A. Bui, H. Noorchashm, A. Eaton and J. Erikson (1997). "Regulation of anti-double-stranded DNA B cells in nonautoimmune mice: localization to the T-B interface of the splenic follicle." J Exp Med **186**(8): 1257-1267.

Mandik-Nayak, L., S. Seo, A. Eaton-Bassiri, D. Allman, R. R. Hardy and J. Erikson (2000). "Functional consequences of the developmental arrest and follicular exclusion of anti-double-stranded DNA B cells." J Immunol **164**(3): 1161-1168.

Marshall, J. L., Y. Zhang, L. Pallan, M. C. Hsu, M. Khan, A. F. Cunningham, I. C. MacLennan and K. M. Toellner (2011). "Early B blasts acquire a capacity for Ig class switch recombination that is lost as they become plasmablasts." Eur J Immunol **41**(12): 3506-3512.

Martin, F., A. M. Oliver and J. F. Kearney (2001). "Marginal zone and B1 B cells unite in the early response against T-independent blood-borne particulate antigens." Immunity **14**(5): 617-629.

Maruyama, M., K. P. Lam and K. Rajewsky (2000). "Memory B-cell persistence is independent of persisting immunizing antigen." Nature **407**(6804): 636-642.

Mauri, C. and A. Bosma (2012). "Immune regulatory function of B cells." Annu Rev Immunol **30**: 221-241.

McAllister, E. J., J. R. Apgar, C. R. Leung, R. C. Rickert and J. Jellusova (2017). "New Methods To Analyze B Cell Immune Responses to Thymus-Dependent Antigen Sheep Red Blood Cells." J Immunol **199**(8): 2998-3003.

McHeyzer-Williams, L. J. and M. G. McHeyzer-Williams (2005). "Antigen-specific memory B cell development." Annu Rev Immunol **23**: 487-513.

McHeyzer-Williams, L. J., P. J. Milpied, S. L. Okitsu and M. G. McHeyzer-Williams (2015). "Class-switched memory B cells remodel BCRs within secondary germinal centers." Nat Immunol **16**(3): 296-305.

Mebius, R. E. and G. Kraal (2005). "Structure and function of the spleen." Nat Rev Immunol **5**(8): 606-616.

Meffre, E. and H. Wardemann (2008). "B-cell tolerance checkpoints in health and autoimmunity." Curr Opin Immunol **20**(6): 632-638.

Melamed, D., R. J. Benschop, J. C. Cambier and D. Nemazee (1998). "Developmental regulation of B lymphocyte immune tolerance compartmentalizes clonal selection from receptor selection." Cell **92**(2): 173-182.

Mempel, T. R., S. E. Henrickson and U. H. Von Andrian (2004). "T-cell priming by dendritic cells in lymph nodes occurs in three distinct phases." Nature **427**(6970): 154-159.

Merrell, K. T., R. J. Benschop, S. B. Gauld, K. Aviszus, D. Decote-Ricardo, L. J. Wysocki and J. C. Cambier (2006). "Identification of anergic B cells within a wild-type repertoire." Immunity **25**(6): 953-962.

Mesin, L., J. Ersching and G. D. Victora (2016). "Germinal Center B Cell Dynamics." Immunity **45**(3): 471-482.

Methot, S. P. and J. M. Di Noia (2017). "Molecular Mechanisms of Somatic Hypermutation and Class Switch Recombination." Adv Immunol **133**: 37-87.

Metzger, H. (1992). "Transmembrane signaling: the joy of aggregation." J Immunol **149**(5): 1477-1487.

Meyer-Hermann, M., E. Mohr, N. Pelletier, Y. Zhang, G. D. Victora and K. M. Toellner (2012). "A theory of germinal center B cell selection, division, and exit." Cell Rep **2**(1): 162-174.

Meyer-Hermann, M. E., P. K. Maini and D. Iber (2006). "An analysis of B cell selection mechanisms in germinal centers." Math Med Biol **23**(3): 255-277.

Minguet, S., E. P. Dopfer and W. W. Schamel (2010). "Low-valency, but not monovalent, antigens trigger the B-cell antigen receptor (BCR)." Int Immunol **22**(3): 205-212.

Mizuno, K., Y. Tagawa, K. Mitomo, Y. Arimura, N. Hatano, T. Katagiri, M. Ogimoto and H. Yakura (2000). "Src homology region 2 (SH2) domain-containing phosphatase-1 dephosphorylates B cell linker protein/SH2 domain leukocyte protein of 65 kDa and selectively regulates c-Jun NH2-terminal kinase activation in B cells." J Immunol **165**(3): 1344-1351.

Monroe, J. G. (2006). "ITAM-mediated tonic signalling through pre-BCR and BCR complexes." Nat Rev Immunol **6**(4): 283-294.

Moran, A. E., K. L. Holzapfel, Y. Xing, N. R. Cunningham, J. S. Maltzman, J. Punt and K. A. Hogquist (2011). "T cell receptor signal strength in Treg and iNKT cell development demonstrated by a novel fluorescent reporter mouse." J Exp Med **208**(6): 1279-1289.

Moran, I., A. Nguyen, W. H. Khoo, D. Butt, K. Bourne, C. Young, J. R. Hermes, M. Biro, G. Gracie, C. S. Ma, C. M. L. Munier, F. Luciani, J. Zaunders, A. Parker, A. D. Kelleher, S. G. Tangye, P. I. Croucher, R. Brink, M. N. Read and T. G. Phan (2018). "Memory B cells are reactivated in subcapsular proliferative foci of lymph nodes." Nat Commun **9**(1): 3372.

Mosier, D. E., J. J. Mond and E. A. Goldings (1977). "The ontogeny of thymic independent antibody responses in vitro in normal mice and mice with an X-linked B cell defect." J Immunol **119**(6): 1874-1878.

Mueller, J., M. Matloubian and J. Zikherman (2015). "Cutting edge: An in vivo reporter reveals active B cell receptor signaling in the germinal center." J Immunol **194**(7): 2993-2997.

Muppidi, J. R., T. I. Arnon, Y. Bronevetsky, N. Veerapen, M. Tanaka, G. S. Besra and J. G. Cyster (2011). "Cannabinoid receptor 2 positions and retains marginal zone B cells within the splenic marginal zone." J Exp Med **208**(10): 1941-1948.

Murphy, K. and C. Weaver (2017). Janeway's Immunology.

Nashar, T. O., H. M. Webb, S. Eaglestone, N. A. Williams and T. R. Hirst (1996). "Potent immunogenicity of the B subunits of Escherichia coli heat-labile enterotoxin: receptor binding is essential and induces differential modulation of lymphocyte subsets." Proc Natl Acad Sci U S A **93**(1): 226-230.

Nguyen, K. A., L. Mandik, A. Bui, J. Kavaler, A. Norvell, J. G. Monroe, J. H. Roark and J. Erikson (1997). "Characterization of anti-single-stranded DNA B cells in a non-autoimmune background." J Immunol **159**(6): 2633-2644.

Nguyen, T. T., K. Klasener, C. Zurn, P. A. Castillo, I. Brust-Mascher, D. M. Imai, C. L. Bevins, C. Reardon, M. Reth and N. Baumgarth (2017). "The IgM receptor FcmuR limits tonic BCR signaling by regulating expression of the IgM BCR." Nat Immunol **18**(3): 321-333.

Nieuwenhuis, P. and W. L. Ford (1976). "Comparative migration of B- and T-Lymphocytes in the rat spleen and lymph nodes." Cell Immunol **23**(2): 254-267.

Niiro, H. and E. A. Clark (2002). "Regulation of B-cell fate by antigen-receptor signals." Nat Rev Immunol **2**(12): 945-956.

Noelle, R. J. and E. C. Snow (1990). "Cognate interactions between helper T cells and B cells." Immunol Today **11**(10): 361-368.

Noorchashm, H., A. Bui, H. L. Li, A. Eaton, L. Mandik-Nayak, C. Sokol, K. M. Potts, E. Pure and J. Erikson (1999). "Characterization of anergic anti-DNA B cells: B cell

anergy is a T cell-independent and potentially reversible process." Int Immunol **11**(5): 765-776.

Noviski, M., J. L. Mueller, A. Satterthwaite, L. A. Garrett-Sinha, F. Brombacher and J. Zikherman (2018). "IgM and IgD B cell receptors differentially respond to endogenous antigens and control B cell fate." Elife **7**.

Nowosad, C. R., K. M. Spillane and P. Tolar (2016). "Germinal center B cells recognize antigen through a specialized immune synapse architecture." Nat Immunol **17**(7): 870-877.

Nutt, S. L., B. Heavey, A. G. Rolink and M. Busslinger (1999). "Commitment to the B-lymphoid lineage depends on the transcription factor Pax5." Nature **401**(6753): 556-562.

O'Keefe, T. L., G. T. Williams, S. L. Davies and M. S. Neuberger (1996). "Hyperresponsive B cells in CD22-deficient mice." Science **274**(5288): 798-801.

O'Neill, S. K., A. Getahun, S. B. Gauld, K. T. Merrell, I. Tamir, M. J. Smith, J. M. Dal Porto, Q. Z. Li and J. C. Cambier (2011). "Monophosphorylation of CD79a and CD79b ITAM motifs initiates a SHIP-1 phosphatase-mediated inhibitory signaling cascade required for B cell anergy." Immunity **35**(5): 746-756.

Obukhanych, T. V. and M. C. Nussenzweig (2006). "T-independent type II immune responses generate memory B cells." J Exp Med **203**(2): 305-310.

Okada, T. and J. G. Cyster (2007). "CC chemokine receptor 7 contributes to Gi-dependent T cell motility in the lymph node." J Immunol **178**(5): 2973-2978.

Okada, T., V. N. Ngo, E. H. Ekland, R. Forster, M. Lipp, D. R. Littman and J. G. Cyster (2002). "Chemokine requirements for B cell entry to lymph nodes and Peyer's patches." J Exp Med **196**(1): 65-75.

Oliver, A. M., F. Martin, G. L. Gartland, R. H. Carter and J. F. Kearney (1997). "Marginal zone B cells exhibit unique activation, proliferative and immunoglobulin secretory responses." Eur J Immunol **27**(9): 2366-2374.

Oliver, A. M., F. Martin and J. F. Kearney (1999). "IgMhighCD21high lymphocytes enriched in the splenic marginal zone generate effector cells more rapidly than the bulk of follicular B cells." J Immunol **162**(12): 7198-7207.

Oprea, M. and A. S. Perelson (1997). "Somatic mutation leads to efficient affinity maturation when centrocytes recycle back to centroblasts." J Immunol **158**(11): 5155-5162.

Overton, W. R. (1988). "Modified histogram subtraction technique for analysis of flow cytometry data." Cytometry **9**(6): 619-626.

Paus, D., T. G. Phan, T. D. Chan, S. Gardam, A. Basten and R. Brink (2006). "Antigen recognition strength regulates the choice between extrafollicular plasma cell and germinal center B cell differentiation." J Exp Med **203**(4): 1081-1091.

Pelanda, R. and R. M. Torres (2012). "Central B-cell tolerance: where selection begins." Cold Spring Harb Perspect Biol **4**(4): a007146.

Phujomjai, Y., A. Somdee and T. Somdee (2016). "Biodegradation of microcystin [Dha(7)]MC-LR by a novel microcystin-degrading bacterium in an internal airlift loop bioreactor." Water Sci Technol **73**(2): 267-274.

Pillai, S. and A. Cariappa (2009). "The follicular versus marginal zone B lymphocyte cell fate decision." Nat Rev Immunol **9**(11): 767-777.

Pillai, S., A. Cariappa and S. T. Moran (2005). "Marginal zone B cells." Annu Rev Immunol **23**: 161-196.

Pinschewer, D. D., M. Perez, E. Jeetendra, T. Bachi, E. Horvath, H. Hengartner, M. A. Whitt, J. C. de la Torre and R. M. Zinkernagel (2004). "Kinetics of protective antibodies are determined by the viral surface antigen." J Clin Invest **114**(7): 988-993.

Pogue, S. L. and C. C. Goodnow (2000). "Gene dose-dependent maturation and receptor editing of B cells expressing immunoglobulin (Ig)G1 or IgM/IgG1 tail antigen receptors." J Exp Med **191**(6): 1031-1044.

Prak, E. L., M. Trounstine, D. Huszar and M. Weigert (1994). "Light chain editing in kappa-deficient animals: a potential mechanism of B cell tolerance." J Exp Med **180**(5): 1805-1815.

Prak, E. L. and M. Weigert (1995). "Light chain replacement: a new model for antibody gene rearrangement." J Exp Med **182**(2): 541-548.

Pugh-Bernard, A. E., G. J. Silverman, A. J. Cappione, M. E. Villano, D. H. Ryan, R. A. Insel and I. Sanz (2001). "Regulation of inherently autoreactive VH4-34 B cells in the maintenance of human B cell tolerance." J Clin Invest **108**(7): 1061-1070.

Ransom, J. T., L. K. Harris and J. C. Cambier (1986). "Anti-Ig induces release of inositol 1,4,5-trisphosphate, which mediates mobilization of intracellular Ca++ stores in B lymphocytes." J Immunol **137**(2): 708-714.

Reed, J. H., J. Jackson, D. Christ and C. C. Goodnow (2016). "Clonal redemption of autoantibodies by somatic hypermutation away from self-reactivity during human immunization." J Exp Med **213**(7): 1255-1265.

Reif, K., E. H. Ekland, L. Ohl, H. Nakano, M. Lipp, R. Forster and J. G. Cyster (2002). "Balanced responsiveness to chemoattractants from adjacent zones determines B-cell position." Nature **416**(6876): 94-99.

Reth, M., G. J. Hammerling and K. Rajewsky (1978). "Analysis of the repertoire of anti-NP antibodies in C57BL/6 mice by cell fusion. I. Characterization of antibody families in the primary and hyperimmune response." Eur J Immunol **8**(6): 393-400.

Roark, J. H., S. H. Park, J. Jayawardena, U. Kavita, M. Shannon and A. Bendelac (1998). "CD1.1 expression by mouse antigen-presenting cells and marginal zone B cells." J Immunol **160**(7): 3121-3127.

Rojas, M., C. Hulbert and J. W. Thomas (2001). "Anergy and not clonal ignorance determines the fate of B cells that recognize a physiological autoantigen." J Immunol **166**(5): 3194-3200.

Rolli, V., M. Gallwitz, T. Wossning, A. Flemming, W. W. Schamel, C. Zurn and M. Reth (2002). "Amplification of B cell antigen receptor signaling by a Syk/ITAM positive feedback loop." Mol Cell **10**(5): 1057-1069.

Roose, J. P., M. Mollenauer, M. Ho, T. Kurosaki and A. Weiss (2007). "Unusual interplay of two types of Ras activators, RasGRP and SOS, establishes sensitive and robust Ras activation in lymphocytes." Mol Cell Biol **27**(7): 2732-2745.

Rowley, M. J., H. Buchanan and I. R. Mackay (1968). "Reciprocal change with age in antibody to extrinsic and intrinsic antigens." Lancet **2**(7558): 24-26.

Rowley, R. B., A. L. Burkhardt, H. G. Chao, G. R. Matsueda and J. B. Bolen (1995). "Syk protein-tyrosine kinase is regulated by tyrosine-phosphorylated Ig alpha/Ig beta immunoreceptor tyrosine activation motif binding and autophosphorylation." J Biol Chem **270**(19): 11590-11594.

Russell, D. M., Z. Dembic, G. Morahan, J. F. Miller, K. Burki and D. Nemazee (1991). "Peripheral deletion of self-reactive B cells." Nature **354**(6351): 308-311.

Sabouri, Z., P. Schofield, K. Horikawa, E. Spierings, D. Kipling, K. L. Randall, D. Langley, B. Roome, R. Vazquez-Lombardi, R. Rouet, J. Hermes, T. D. Chan, R. Brink, D. K. Dunn-Walters, D. Christ and C. C. Goodnow (2014). "Redemption of autoantibodies on anergic B cells by variable-region glycosylation and mutation away from self-reactivity." Proc Natl Acad Sci U S A **111**(25): E2567-2575.

Saijo, K., C. Schmedt, I. H. Su, H. Karasuyama, C. A. Lowell, M. Reth, T. Adachi, A. Patke, A. Santana and A. Tarakhovsky (2003). "Essential role of Src-family protein tyrosine kinases in NF-kappaB activation during B cell development." Nat Immunol **4**(3): 274-279.

Samardzic, T., D. Marinkovic, C. P. Danzer, J. Gerlach, L. Nitschke and T. Wirth (2002). "Reduction of marginal zone B cells in CD22-deficient mice." Eur J Immunol **32**(2): 561-567.

Santulli-Marotto, S., M. W. Retter, R. Gee, M. J. Mamula and S. H. Clarke (1998). "Autoreactive B cell regulation: peripheral induction of developmental arrest by lupus-associated autoantigens." Immunity **8**(2): 209-219.

Scherer, E. M., M. B. Zwick, L. Teyton and D. R. Burton (2007). "Difficulties in eliciting broadly neutralizing anti-HIV antibodies are not explained by cardiolipin autoreactivity." AIDS **21**(16): 2131-2139.

Scholz, J. L., J. E. Crowley, M. M. Tomayko, N. Steinel, P. J. O'Neill, W. J. Quinn, 3rd, R. Goenka, J. P. Miller, Y. H. Cho, V. Long, C. Ward, T. S. Migone, M. J. Shlomchik and M. P. Cancro (2008). "BLyS inhibition eliminates primary B cells but leaves natural and acquired humoral immunity intact." Proc Natl Acad Sci U S A **105**(40): 15517-15522.

Schwickert, T. A., R. L. Lindquist, G. Shakhar, G. Livshits, D. Skokos, M. H. Kosco-Vilbois, M. L. Dustin and M. C. Nussenzweig (2007). "In vivo imaging of germinal centres reveals a dynamic open structure." Nature **446**(7131): 83-87.

Schwickert, T. A., G. D. Victora, D. R. Fooksman, A. O. Kamphorst, M. R. Mugnier, A. D. Gitlin, M. L. Dustin and M. C. Nussenzweig (2011). "A dynamic T cell-limited checkpoint regulates affinity-dependent B cell entry into the germinal center." J Exp Med **208**(6): 1243-1252.

Shen, P., T. Roch, V. Lampropoulou, R. A. O'Connor, U. Stervbo, E. Hilgenberg, S. Ries, V. D. Dang, Y. Jaimes, C. Daridon, R. Li, L. Jouneau, P. Boudinot, S. Wilantri, I. Sakwa, Y. Miyazaki, M. D. Leech, R. C. McPherson, S. Wirtz, M. Neurath, K. Hoehlig, E. Meinl, A. Grutzkau, J. R. Grun, K. Horn, A. A. Kuhl, T. Dorner, A. Bar-Or, S. H. E. Kaufmann, S. M. Anderton and S. Fillatreau (2014). "IL-35-producing B cells are critical regulators of immunity during autoimmune and infectious diseases." Nature **507**(7492): 366-370.

Shimizu, T., M. Oda and T. Azuma (2003). "Estimation of the relative affinity of B cell receptor by flow cytometry." J Immunol Methods **276**(1-2): 33-44.

Shinnakasu, R., T. Inoue, K. Kometani, S. Moriyama, Y. Adachi, M. Nakayama, Y. Takahashi, H. Fukuyama, T. Okada and T. Kurosaki (2016). "Regulated selection of germinal-center cells into the memory B cell compartment." Nat Immunol **17**(7): 861-869.

Shlomchik, M. J. (2008). "Sites and stages of autoreactive B cell activation and regulation." Immunity **28**(1): 18-28.

Shlomchik, M. J. and F. Weisel (2012). "Germinal center selection and the development of memory B and plasma cells." Immunol Rev **247**(1): 52-63.

Smith, M. J., T. A. Packard, S. K. O'Neill, C. J. Henry Dunand, M. Huang, L. Fitzgerald-Miller, D. Stowell, R. M. Hinman, P. C. Wilson, P. A. Gottlieb and J. C. Cambier (2015). "Loss of anergic B cells in prediabetic and new-onset type 1 diabetic patients." Diabetes **64**(5): 1703-1712.

Sobacchi, C., V. Marrella, F. Rucci, P. Vezzoni and A. Villa (2006). "RAG-dependent primary immunodeficiencies." Hum Mutat **27**(12): 1174-1184.

Sonoda, E., Y. Pewzner-Jung, S. Schwers, S. Taki, S. Jung, D. Eilat and K. Rajewsky (1997). "B cell development under the condition of allelic inclusion." Immunity **6**(3): 225-233.

Stein, H., A. Bonk, G. Tolksdorf, K. Lennert, H. Rodt and J. Gerdes (1980). "Immunohistologic analysis of the organization of normal lymphoid tissue and non-Hodgkin's lymphomas." J Histochem Cytochem **28**(8): 746-760.

Stein, K. E. (1992). "Thymus-independent and thymus-dependent responses to polysaccharide antigens." J Infect Dis **165 Suppl 1**: S49-52.

Steiniger, B., L. Ruttinger and P. J. Barth (2003). "The three-dimensional structure of human splenic white pulp compartments." J Histochem Cytochem **51**(5): 655-664.

Stevenson, F. K., G. J. Smith, J. North, T. J. Hamblin and M. J. Glennie (1989). "Identification of normal B-cell counterparts of neoplastic cells which secrete cold agglutinins of anti-I and anti-i specificity." Br J Haematol **72**(1): 9-15.

Stewart, I., D. Radtke, B. Phillips, S. J. McGowan and O. Bannard (2018). "Germinal Center B Cells Replace Their Antigen Receptors in Dark Zones and Fail Light Zone Entry when Immunoglobulin Gene Mutations are Damaging." Immunity **49**(3): 477-489 e477.

Su, T. T., B. Guo, Y. Kawakami, K. Sommer, K. Chae, L. A. Humphries, R. M. Kato, S. Kang, L. Patrone, R. Wall, M. Teitell, M. Leitges, T. Kawakami and D. J. Rawlings (2002). "PKC-beta controls I kappa B kinase lipid raft recruitment and activation in response to BCR signaling." Nat Immunol **3**(8): 780-786.

Szakal, A. K., J. K. Taylor, J. P. Smith, M. H. Kosco, G. F. Burton and J. J. Tew (1990). "Kinetics of germinal center development in lymph nodes of young and aging immune mice." Anat Rec **227**(4): 475-485.

Sze, D. M., K. M. Toellner, C. Garcia de Vinuesa, D. R. Taylor and I. C. MacLennan (2000). "Intrinsic constraint on plasmablast growth and extrinsic limits of plasma cell survival." J Exp Med **192**(6): 813-821.

Takahashi, Y., H. Ohta and T. Takemori (2001). "Fas is required for clonal selection in germinal centers and the subsequent establishment of the memory B cell repertoire." Immunity **14**(2): 181-192.

Tian, J., D. Zekzer, L. Hanssen, Y. Lu, A. Olcott and D. L. Kaufman (2001). "Lipopolysaccharide-activated B cells down-regulate Th1 immunity and prevent autoimmune diabetes in nonobese diabetic mice." J Immunol **167**(2): 1081-1089.

Tiegs, S. L., D. M. Russell and D. Nemazee (1993). "Receptor editing in self-reactive bone marrow B cells." J Exp Med **177**(4): 1009-1020.

Toellner, K. M., A. Gulbranson-Judge, D. R. Taylor, D. M. Sze and I. C. MacLennan (1996). "Immunoglobulin switch transcript production in vivo related to the site and time of antigen-specific B cell activation." J Exp Med **183**(5): 2303-2312.

Toellner, K. M., S. A. Luther, D. M. Sze, R. K. Choy, D. R. Taylor, I. C. MacLennan and H. Acha-Orbea (1998). "T helper 1 (Th1) and Th2 characteristics start to develop during T cell priming and are associated with an immediate ability to induce immunoglobulin class switching." J Exp Med **187**(8): 1193-1204.

Toellner, K. M., D. M. Sze and Y. Zhang (2018). "What Are the Primary Limitations in B-Cell Affinity Maturation, and How Much Affinity Maturation Can We Drive with Vaccination? A Role for Antibody Feedback." Cold Spring Harb Perspect Biol **10**(5).

Tsiantoulas, D., M. Kiss, B. Bartolini-Gritti, A. Bergthaler, Z. Mallat, H. Jumaa and C. J. Binder (2017). "Secreted IgM deficiency leads to increased BCR signaling that results in abnormal splenic B cell development." Sci Rep **7**(1): 3540.

Tze, L. E., B. R. Schram, K. P. Lam, K. A. Hogquist, K. L. Hippen, J. Liu, S. A. Shinton, K. L. Otipoby, P. R. Rodine, A. L. Vegoe, M. Kraus, R. R. Hardy, M. S. Schlissel, K. Rajewsky and T. W. Behrens (2005). "Basal immunoglobulin signaling actively maintains developmental stage in immature B cells." PLoS Biol **3**(3): e82.

Van den Eertwegh, A. J., R. J. Noelle, M. Roy, D. M. Shepherd, A. Aruffo, J. A. Ledbetter, W. J. Boersma and E. Claassen (1993). "In vivo CD40-gp39 interactions are essential for thymus-dependent humoral immunity. I. In vivo expression of CD40 ligand, cytokines, and antibody production delineates sites of cognate T-B cell interactions." J Exp Med **178**(5): 1555-1565.

Victora, G. D. and M. C. Nussenzweig (2012). "Germinal centers." Annu Rev Immunol **30**: 429-457.

Victora, G. D., T. A. Schwickert, D. R. Fooksman, A. O. Kamphorst, M. Meyer-Hermann, M. L. Dustin and M. C. Nussenzweig (2010). "Germinal center dynamics

revealed by multiphoton microscopy with a photoactivatable fluorescent reporter." Cell **143**(4): 592-605.

Waisman, A., M. Kraus, J. Seagal, S. Ghosh, D. Melamed, J. Song, Y. Sasaki, S. Classen, C. Lutz, F. Brombacher, L. Nitschke and K. Rajewsky (2007). "IgG1 B cell receptor signaling is inhibited by CD22 and promotes the development of B cells whose survival is less dependent on Ig alpha/beta." J Exp Med **204**(4): 747-758.

Wardemann, H., S. Yurasov, A. Schaefer, J. W. Young, E. Meffre and M. C. Nussenzweig (2003). "Predominant autoantibody production by early human B cell precursors." Science **301**(5638): 1374-1377.

Weston-Bell, N. J., F. Forconi, H. C. Kluin-Nelemans and S. S. Sahota (2014). "Variant B cell receptor isotype functions differ in hairy cell leukemia with mutated BRAF and IGHV genes." PLoS One **9**(1): e86556.

Willard-Mack, C. L. (2006). "Normal structure, function, and histology of lymph nodes." Toxicol Pathol **34**(5): 409-424.

Williams, J. M., R. H. Bonami, C. Hulbert and J. W. Thomas (2015). "Reversing Tolerance in Isotype Switch-Competent Anti-Insulin B Lymphocytes." J Immunol **195**(3): 853-864.

Winoto, A. and D. R. Littman (2002). "Nuclear hormone receptors in T lymphocytes." Cell **109 Suppl**: S57-66.

Xu, J., T. M. Foy, J. D. Laman, E. A. Elliott, J. J. Dunn, T. J. Waldschmidt, J. Elsemore, R. J. Noelle and R. A. Flavell (1994). "Mice deficient for the CD40 ligand." Immunity **1**(5): 423-431.

Yang, J. and M. Reth (2010). "Oligomeric organization of the B-cell antigen receptor on resting cells." Nature **467**(7314): 465-469.

Yang, Z., B. M. Sullivan and C. D. Allen (2012). "Fluorescent in vivo detection reveals that IgE(+) B cells are restrained by an intrinsic cell fate predisposition." Immunity **36**(5): 857-872.

Yao, X. R., H. Flaswinkel, M. Reth and D. W. Scott (1995). "Immunoreceptor tyrosine-based activation motif is required to signal pathways of receptor-mediated growth arrest and apoptosis in murine B lymphoma cells." J Immunol **155**(2): 652-661.

Yefenof, E., V. M. Sanders, J. W. Uhr and E. S. Vitetta (1986). "In vitro activation of murine antigen-specific memory B cells by a T-dependent antigen." J Immunol **137**(1): 85-90.

Zandvoort, A. and W. Timens (2002). "The dual function of the splenic marginal zone: essential for initiation of anti-TI-2 responses but also vital in the general first-line defense against blood-borne antigens." Clin Exp Immunol **130**(1): 4-11.

Zhang, Y., L. Garcia-Ibanez, G. Brown and K. M. Toellner (2017). "Detecting Gene Expression in Lymphoid Microenvironments by Laser Microdissection and Quantitative RT-PCR." Methods Mol Biol **1623**: 21-36.

Zhang, Y., L. Garcia-Ibanez and K. M. Toellner (2016). "Regulation of germinal center B-cell differentiation." Immunol Rev **270**(1): 8-19.

Zhang, Y., M. Meyer-Hermann, L. A. George, M. T. Figge, M. Khan, M. Goodall, S. P. Young, A. Reynolds, F. Falciani, A. Waisman, C. A. Notley, M. R. Ehrenstein, M. Kosco-Vilbois and K. M. Toellner (2013). "Germinal center B cells govern their own fate via antibody feedback." J Exp Med **210**(3): 457-464.

Zhang, Y., L. Tech, L. A. George, A. Acs, R. E. Durrett, H. Hess, L. S. K. Walker, D. M. Tarlinton, A. L. Fletcher, A. E. Hauser and K. M. Toellner (2018). "Plasma cell output from germinal centers is regulated by signals from Tfh and stromal cells." J Exp Med **215**(4): 1227-1243.

Ziegler, S. F., F. Ramsdell, K. A. Hjerrild, R. J. Armitage, K. H. Grabstein, K. B. Hennen, T. Farrah, W. C. Fanslow, E. M. Shevach and M. R. Alderson (1993). "Molecular characterization of the early activation antigen CD69: a type II membrane glycoprotein related to a family of natural killer cell activation antigens." Eur J Immunol **23**(7): 1643-1648.

Zikherman, J., R. Parameswaran and A. Weiss (2012). "Endogenous antigen tunes the responsiveness of naive B cells but not T cells." Nature **489**(7414): 160-164.

Chapter 7 . Appendices

>Wildtype mouse IgM (partial)
aggggggaggtgaatgctgaggaggaaggctttgagaacctgtggaccactgcctccaccttcatcgtcctcttcctcctga
gcctcttctacagcaccaccgtcaccctgttcaaggtagtgtggttgtggggctgaggacacagggctgggacagggagt
caccagtcctcactgcctctacctctactccctacaagtggacagcaattcacactgtctctgtcacctgcaggtgaaatgact
ctcagcatggaaggacagcagagaccaagagatcctcccacagggacactacctctgggcctgggatacctgactgtat
gactagtaaacttattcttacgtctttcctgtgttgccctccagctttttatctctgagatggtcttctttctagactgaccaaagactt
tttgtcaacttgtacaatctgaagcaatgtctggcccacagacagctgagctgtaaacaaatgtcacatggaaataaatacttt
atcttgtgaactcactttattgtgaaggaatttgttttgtttttcaaacctttcctgcggtgttgacagcccaaggattatctgaata
gagcttaggaactggaaatggaacagtgcagtctgatggtacttaa

>Transgenic mouse IgM (partial)
Aggggggaggtgaatgctgaggaggaaggctttgagaacctgtggaccactgcctccaccttcatcgtcctcttcctcctga
gcctcttctacagcaccaccgtcaccctgttcaaggtagtgtggttgtggggctgaggacacagggctgggacagggagt
caccagtcctcactgcctctacctctactccctacaagtggacagcaattcacactgtctctgtcacctgcaggtgaaatggat
cttctcctcggtggtggagctgaagcagacactggttcctgaatacaagaacatgattgggcaagcaccctgactctcagc
atggaaggacagcagagaccaagagatcctcccacagggacactacctctgggcctgggatacctgactgtatgactagt
aaacttattcttacgtctttcctgtgttgccctccagctttttatctctgagatggtcttctttctagactgaccaaagactttttgtcaa
cttgtacaatctgaagcaatgtctggcccacagacagctgagctgtaaacaaatgtcacatggaaataaatactttatcttgtg
aactcactttattgtgaaggaatttgttttgtttttcaaacctttcctgcggtgttgacagcccaaggattatctgaatagagctta
ggaactggaaatggaacagtgcagtctgatggtacttaa

Red highlighted 75bp is the cDNA sequence encoding for C-terminal cytoplasmic region of IgG1

Genotyping primer sequence:
1. IgM/IgG1: Fwd: 5'- tgcaggtgaaatggatcttctcctc -3'
    Rev: 5' – aaccagagtgctatccattgg – 3'

    Expected PCR product size from transgenic mice: 683bp. Wildtype mice will not give a PCR product.

2. IgM/IgG1: Fwd: 5'- ttcaaggtagtgtggttgtgg -3'
    Rev: 5' – atacagtcaggtatcccagg – 3'

    Expected PCR product size from transgenic mice: 289bp. Expected PCR product size from wildtype mice: 214bp.